i) Design and Synthesis of Butadiene Substrates for Organocatalytic Transformations ii) Synthesis of Functionalized Biaryls and Pyran Derivatives

A thesis submitted by

Ross Brett Driver B.Sc (Hons)

to the

National University of Ireland, Maynooth

For the degree of Doctor of Philosophy

Volume 1 of 1

Based on research carried out in the

Department of Chemistry, Faculty of Science and Engineering,

National University of Ireland, Maynooth

under the supervision and direction of

Dr John C. Stephens

Head of Department - Dr Jennifer McManus

2017

Declaration

This is to clarify that the material presented within this thesis has not been submitted previously for a Degree to this or any other University. All material presented herein, except where acknowledged and cited appropriately, is the work of the author.

_____

Ross Brett Driver

National University of Ireland, Maynooth

2017

Dedication

For my parents Alan and Una.

Acknowledgments

Abbreviations

2,4-DNBA – 2,4-dinitrobenzoic acid

ACA – Asymmetric conjugate addition

APCI – Atmospheric Pressure Chemical Ionization

aq. – Aqueous

Ar – Aryl

ATR – Attenuated total reflection

Bn – Benzyl

Boc – *tert*-Butyloxycarbonyl

DBU - 1,8-diazabicyclo[5.4.0]undec-7-ene

DCM - Dichloromethane

de – Diastereomeric excess

DFT – Density functional theory

DMF - Dimethylformamide

dr – Diastereomeric ratio

DMSO - Dimethylsulfoxide

ee – Enantiomeric excess

eq. – Equivalents

er – Enantiomeric ratio

EDG – Electron-withdrawing group

EWG – Electron-donating group

FDA – Food and Drug Administration

FGI – Functional group interconversion

HFIP – 1,1,1,3,3,3-hexafluoro-2-propanol

HOMO – Highest occupied molecular orbital

HPLC – High performance liquid chromatography

hr – Hour

HWE – Horner-Wadsworth-Emmons

IEDDA – Inverse Electron Demand Diels-Alder

IEDHDA – Inverse Electron Demand Hetero-Diels-Alder

*i*Pr – Isopropyl

LUMO – Lowest occupied molecular orbital

LiHMDS – Lithium hexamethyldisilazane

MeOH – Methanol

NaOEt – Sodium ethoxide

NSFI - N-fluorobenzenesulfonimide

Nu – Nucleophile

OPA – Oxaphosphetane

PCC – Pyrdininium chlorochromate

PE – Petroleum ether

Ph – Phenyl

PMP – *p*-Methoxyphenol

p-TSA – *p*-Tolunesulfonic acid

rt – Room Temperature

sat. – Saturated

TEA – Triethylamine

TFA – Trifluoroacetic acid

THF – Tetrahydrofuran

TS – Transition state

Ts – Tosyl

Ms – Mesyl

CIP – Cahn-Ingold-Prelog

PTC – Phase transfer catalysis

NHC – N-heterocyclic carbene

R_f – Retention factor

DIBAL-H – Diisobutylaluminium hydride

f.v.p – Flash vacuum pyrolysis

MCR – Multi-component reaction

Abstract

This thesis details the exploration of a number of discrete but interlinked projects. 1) The synthesis of 1,3-bis-subsitituted electron-deficient butadiene substrates for the study of vinylogous Michael-type addition chemistry through organocatalytic means. The synthesis of these electron-deficient butadienic systems proved to be quite challenging and required extensive reaction screening in order to access these substrates in synthetically useful scales. A modular approach to diene synthesis was developed in order to gain access to distinct butadiene families through the combination of aryl formyl acrylonitriles and stabilized ylides in a base-free Wittig olefination reaction. The use of the polymerization inhibitor 8-hydroxyquinoline was found to be key to the synthesis of these challenging substrates to prevent the vinyl nitriles from polymerizing. Density Functional Theory (DFT) calculations were also performed on the butadiene substrates in order to develop a better understanding of the conformations and geometries the butadienes adopt, a key part of their potential reactivity. 2) The study of these newly synthesized butadienes in an asymmetric organocatalytic 1,6-conjugate addition/cyclization to yield enantioenriched cyclic hexadienes did not yield the expected products and instead yielded densely functionalized biaryl species which are of some synthetic interest. Our attentions were then turned to the directed synthesis of these biaryls. This was accomplished through the use of stoichiometric quantities of piperidine in order to reduce the potential for polymerization or side-reactions which would consume the starting material. A study into the aromatization of the cyclic hexadienes into the biaryl species was also carried out. A crystal structure of one of the biaryl species **125** was also elucidated which unambiguously confirmed the structure of the biaryls. 3) A key synthetic intermediate in the synthesis of the 1,3-bis-subsitituted butadienes was the aryl formyl acrylonitriles. This class of compounds has been little studied and a number of interesting reactivities that they exhibit were discovered during the attempted syntheses of butadienes. The final part of this thesis details the synthesis of 2-amino-*4H*-pyrans from the conjugate addition of malononitrile to aryl formyl acrylonitriles and the synthesis of 3,4-dihydro-*2H*-pyrans through Inverse Electron Demand Hetero-Diels-Alder (IEDHDA) cycloaddition reactions. An asymmetric variant of the synthesis of 2-amino-*4H*-pyrans was attempted. In depth discussion on the regio- and stereoselectivity of the IEDHDA is also given and supported by detailed NMR analysis.

Table of Contents

1. Chapter 1: Introduction

1.1   Introduction

1.1.1   Chirality and asymmetric synthesis

The natural world is a chiral environment. The homochirality observed in natural products, such as the L amino acids and D sugars, has widespread implications on the structure and function of cellular life on earth.[1] Without rigid stereoregularity, protein folding and ultimately function would be greatly impaired. One could argue that without this stereobias life itself could not have developed on earth, at least not in the form we know today.

Nature has been able to develop and optimize its arsenal of enzymes through natural selection over millions of years. During this time Nature has become an expert at asymmetric synthesis. Enzymes can exhibit complete stereochemical control over the conversion of a substrate to product, however, the rigidity under which they exert this control can also limit substrate scope. This in turn, from a synthetic standpoint, hinders development into new chemical space. The problem of substrate specificity is one that scientists are currently working on through the biochemical method of site-directed mutagenesis.[2]

Chemists, unlike Nature, are relative newcomers to the field of asymmetric synthesis. The property of optical rotation was only first described by Biot in 1815.[3] Some 33 years later, in 1848, the first chiral resolution was achieved by Pasteur, who physically separated the salts of tartaric acids.[4] It was not until the twentieth century that serious consideration was given to the synthesis of optically active compounds predominately through the use of enzymes, the readily available biocatalytic tools of Nature.[5]

The first literature description of an asymmetric synthesis could be claimed in a 1904 report by Marckwald.[6,7] In his report, Marckwald described the brucine catalyzed decarboxylation of 2-ethyl-2-methylmalonic acid to 2-methylbutyric acid, with an observed enrichment of approximately 10 % in the laevorotatory component (Figure 1.1).[6,8] It could be argued that this report represents the first example of enantiotopic discrimination by a small organic molecule and therefore the first non-enzymatic and non-metal catalyzed asymmetric synthesis. In other words, the first asymmetric organocatalytic reaction by today's definitions. As the butyric acid is also a natural product it could also be considered as one of the first asymmetric natural product synthesis. The proposed reaction mechanism for this reaction involves the formation of a brucine salt with the malonic acid, followed by fractional crystallization to yield an enriched mixture of the salts. Pyrolysis of the salt yields the

carboxylate brucine salt, which after neutralization affords the butyric acid with a slight enantioenrichment.
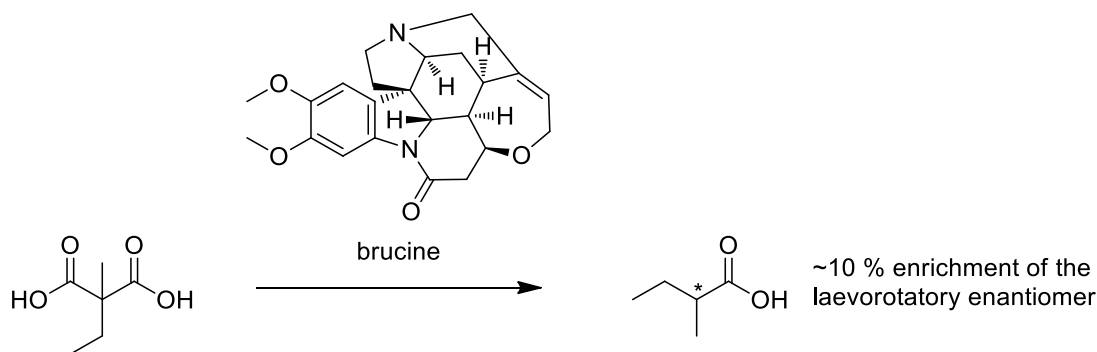
Figure 1.1. The brucine catalysed enantioselective decarboxylation reported by Marckwald.[6]

The importance of this reaction was not clearly evident in 1904. The difficulty in reproducibly measuring enantioenrichment also hindered the study of the synthesis of optically active compounds. It should be noted that at that time ee (enantiomeric excess) was measured using polarimetry, a technique sensitive to changes in concentration and temperature, as well as the presence of chiral contaminants.

Another landmark example of a prochiral substrate being transformed with a degree of enantiocontrol is attributed to the work of Bredig and Fiske in 1913. In their paper entitled "Durch Katalysatoren bewirkte asymmetrische Synthese", which can be translated to "Catalyst induced asymmetric synthesis", they report the asymmetric synthesis of mandelonitrile from benzaldehyde and HCN in the presence of a cinchona alkaloid, quinine, with a modest ee of 8 % (Figure 1.2).[9]
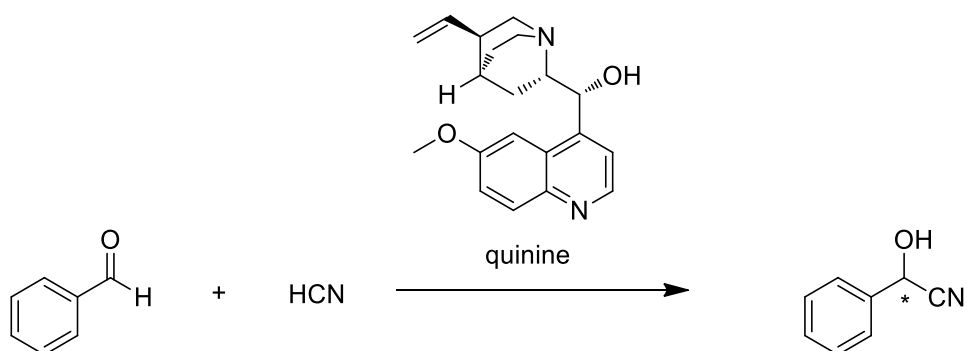
Figure 1.2. Quinine catalyzed enantioselective addition of HCN to benzaldehyde reported by Bredig and Fiske.[9]

Reports describing the synthesis of optically enriched mixtures were dotted throughout the literature over the next number of decades but it wasn't until the 1960's that asymmetric synthesis began to take a prominent position in the interest of chemists. The first truly successful attempts at asymmetric synthesis were taken in the field of organometallic chemistry.

1.1.2   Organometallic asymmetric synthesis

The field of asymmetric organometallic synthesis has its origins in the pioneering work of Nozaki and Noyori.[10] Their 1966 publication on the synthesis of non-racemic cyclopropanes from styrenes and ethyl diazoacetate, in the presences of a Schiff base/Cu[II] complex **1** (Figure 1.3), is a landmark paper in asymmetric synthesis.
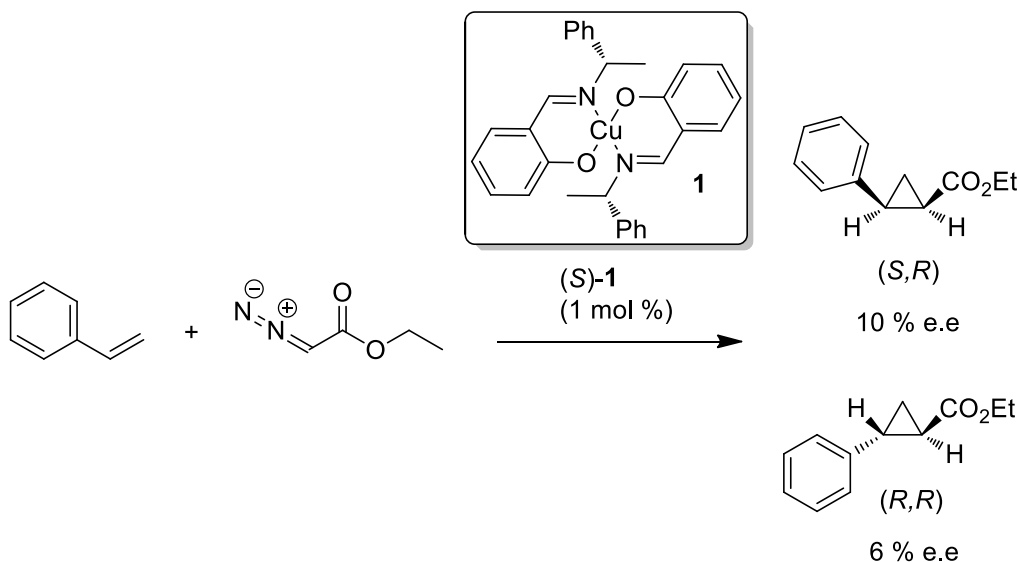
Figure 1.3. The first catalytic asymmetric organometallic reaction.[10]

Although only modest enantiocontrol was achieved, this work sparked interest in the field of asymmetric organometallic transformations and led to explosive growth within the field. Asymmetric organometallic processes dominated the stage of asymmetric synthesis for years to come. Such organometallic process still play an important role in the large scale synthesis of pharmaceuticals, fragrances and argochemicals.[11] Noyori would later go on to develop methods for asymmetric hydrogenation, work for which he would receive a share in the 2001 Nobel Prize in Chemistry. This prize was shared with Knowles and Sharpless, who

also played important roles in the development of asymmetric organometallic transformations.[12]

Great advancements in the synthesis of chiral compounds were made possible through the discoveries made in organometallic transformations in the 20th century. Hand in hand with these progressions came the development of improved methods for the quantification of the constituent stereoisomers. For example, in the late 1970's the use of lanthanide shift reagents and chiral auxiliaries, such as Mosher's acyl halide, became widespread and allowed for the routine determination of enantiomeric excess (ee). Later still, in the 1980's, High Performance Liquid Chromatography (HPLC) using chiral stationary phases became the standard for the separation and quantification of chiral compounds and resulted in the ability to quickly and accurately determine ee's.

1.1.3   Asymmetric organocatalysis

Despite sporadic reports during the late 20th century of asymmetric reactions catalyzed by small organic molecules, none neared the enantiocontrol that asymmetric organometallic chemistry could achieve. As such, much focus was given to the development of novel chiral ligands for use in the booming field of asymmetric organometallic synthesis and transformations catalyzed solely by organic molecules remained understudied.

Some exemplary reports, which hinted at the power of small organic molecules to induce stereocontrol, include the enantioselective addition of MeOH to methyl phenyl ketone by Pracejus in 1960 with a 74 % ee (Figure 1.4).[13]
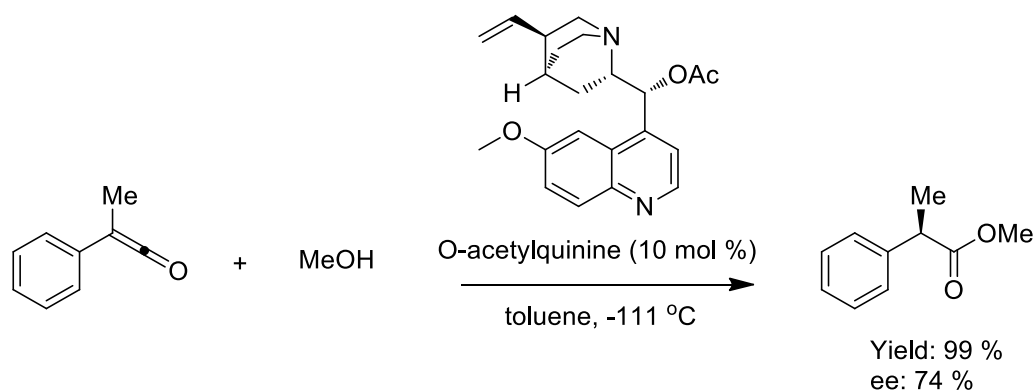
Figure 1.4. Enantioselective addition of MeOH to methyl phenyl ketone reported by Pracejus.[13]

Another example of a cinchona catalyzed transformation can be found in Wynberg's 1975 report of an enantioselective Michael addition. An ee of 76 % was achieved with a low catalytic loading of just 1 mol % (Figure 1.5).[14]
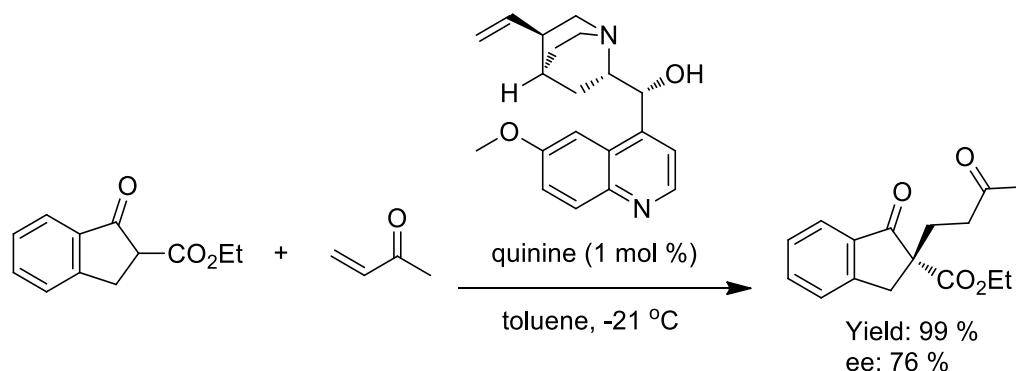
Figure 1.5. Quinine catalyzed enantioselective Michael addition reported by Wynberg.[14]

Perhaps the most well-known early example of an enantioselective reaction, in which the stereocontrol was determined by a small chiral organic molecule, is that of the Hajos-Parrish-Eder-Sauer-Weichart reaction. Developed independently in the 1970's by two industrial groups, Hajos and Parrish at Hoffemann La-Roche and Eder, Sauer and Wiechert working in Schering, it described an L-proline **2** catalyzed intramolecular aldol reaction furnishing the aldol product in quantitative yield and an ee of 93 % (Figure 1.6).[15,16]
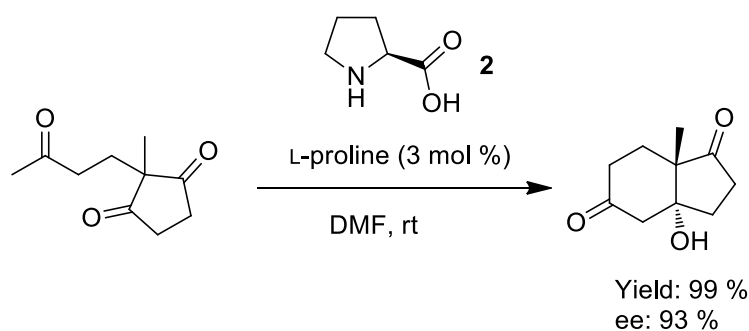
Figure 1.6. The Hajos-Parrish-Eder-Sauer-Wiechert reaction.[15,16]

It was this work by Hajos, Parrish, Eder, Sauer and Wiechert that inspired Barbas *et al.* in their antibody catalyzed variant of the Hajos-Parrish reaction.[17] Barbas *et al.* employed their metal-free approach to yield the Wieland-Miescher ketone, which is a synthetically useful intermediate in the synthesis of a number of natural products, such as sesquiterpenoids, diterpenoids and steroids.[18] In their publication, the authors employed an antibody based

catalyst. The also noted the essential participation of the amino group of a lysine residue on the antibody in the formation of an enamine **3** (Figure 1.7).
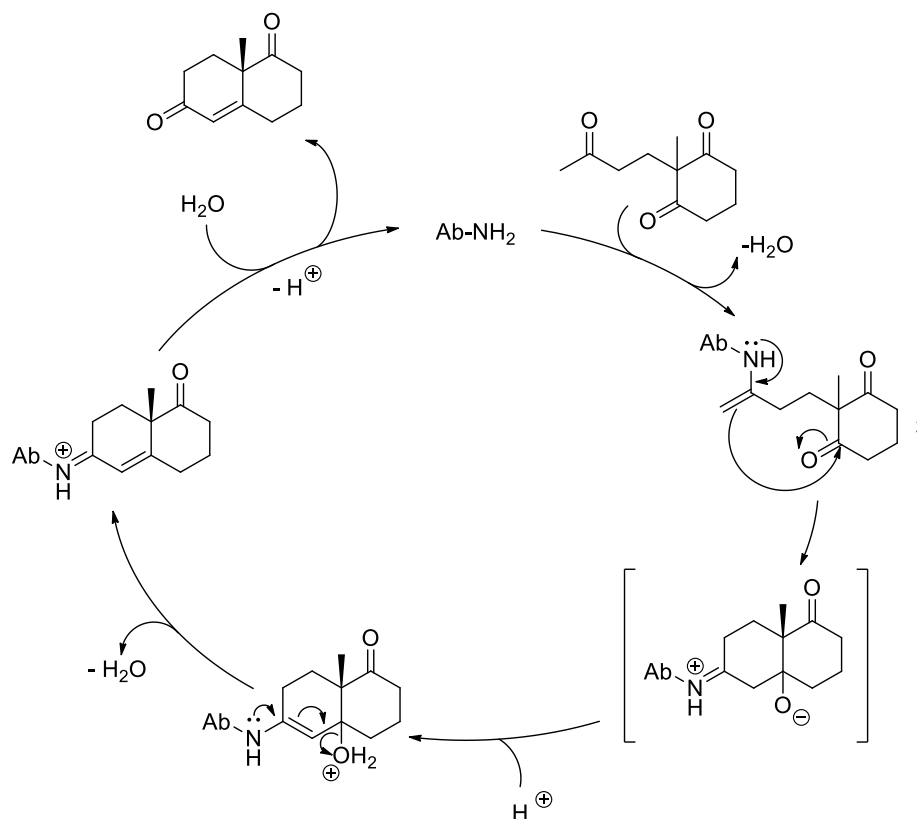
Figure 1.7. The antibody catalyzed intramolecular Robinson annulation reported by Barbas *et al.*[17] Ab = Antibody.

It was their work with the antibody catalyzed Hajos-Parrish reaction that then inspired Barbas, List and Lerner to attempt an intermolecular variant of the reaction, this time returning to the small organic molecule L-proline as the catalyst. In their 2000 publication, Barbas *et al.* reported the intermolecular aldol L-proline **2** catalyzed reaction of acetone with a variety of aldehydes, in some cases achieving high ee's (Figure 1.8).[19]
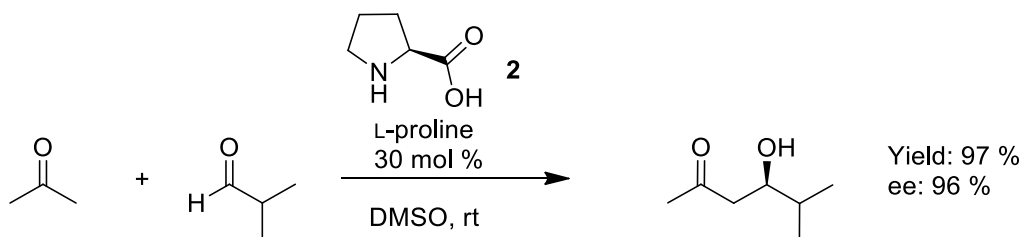
Figure 1.8. The intermolecular proline catalyzed aldol reaction reported by Barbas et al.[19]

In this landmark publication, Barbas *et al.* were the first to suggest that small organic molecules could be used as general catalysts in a variety of enantioselective transformations. They also outlined the importance of the Highest Occupied Molecular Orbital (HOMO) energy raising enamine mode of catalytic activation and listed a number of advantages of catalysis by L-proline. These advantages include:

- Proline is non-toxic, inexpensive and readily available in both enantiomers.

- The reactions could be run at room temperature (rt) in wet solvents and in the absence of an inert atmosphere.

- No prior modification of the carbonyl substrates was required.

- Proline is water-soluble allowing for ease of purification.

Another insight from this publication, which showed the great foresight of Barbas *et al.*, was that they believed that the reaction could be performed on an industrial scale. In fact, L-proline catalysis has been performed on multi-kilogram scale at Schering.[20]

MacMillan *et al.*, also in the year 2000, published a report describing the use of small chiral organic molecules as catalysts in asymmetric synthesis. This report outlined a highly enantioselective Diels-Alder cycloaddition catalyzed by a chiral imidazolidinone catalyst **4** (Figure 1.9).[21] This catalyst operated using a Lowest Unoccupied Molecular Orbital (LUMO) lowering iminium ion as the catalytically active species, a complementary strategy to the HOMO raising enamine mode employed by Barbas *et al.*[19]
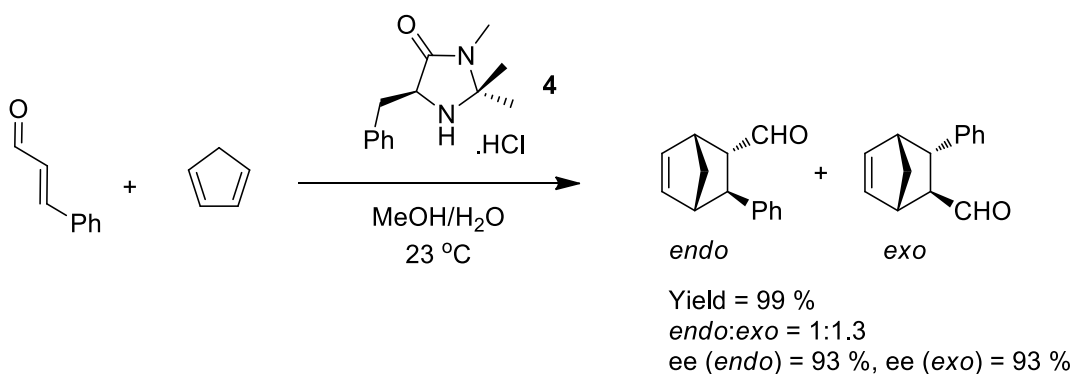
Figure 1.9. MacMillans' report of an imidazolidinone catalyzed Diels-Alder cycloaddition.[21]

This report in particular was pivotal in establishing the field of organocatalysis. Firstly, it gave the field a name, as MacMillan coined the term "organocatalysis", replacing the traditionally

used term "non-metal catalyzed". Secondly, it showed that organocatalysis had the potential to be applied to transformations other than the aldol-type reactions already reported.

The two reports by Barbas *et al.* and MacMillan *et al.* reignited interest in the study of small organic molecule catalysis, a field that had essentially remained hidden in the literature for nearly 100 years. This led to an explosion in the number of publications utilizing organocatalysis and the number of transformations employing it continues to grow today. A SciFinder® search for the term "organocatalysis" yields 14,481 references between the years 2000 and 2017, which is a conservative estimate of the number of publications that utilize organocatalysis. (Search performed on 06-06-2017, using term "organocatalysis") The scope of reactions covered by organocatalytic modes of activation is now vast and continues to grow at an astonishing rate.

To date a number of organocatalytic modes have been described in the literature and they can be broadly divided into two distinct groups, covalent and non-covalent (Table 1.1).

Table 1.1. Organocatalytic modes of activation

Covalent	Non-covalent
Enamine catalysis	Hydrogen-bonding catalysis
Iminium ion catalysis	Ion-pair catalysis
Singly Occupied Molecular Orbital (SOMO) organocatalysis	Phase Transfer Catalysis (PTC)
N-Heterocyclic Carbene (NHC) Catalysis	

Enamine catalysis is the principal mode of catalysis employed in this thesis and as a result, detailed mechanistic discussion will be limited to this mode of catalysis.

1.2   Enamine catalysis

1.2.1   Introduction

The term "enamine" was introduced by Wittig in 1927.[22] The first synthetic report describing the isolation of enamines in the literature is a report by Mannich and Davidsen in 1936.[23] They reported that secondary amines, under dehydrating conditions, underwent condensation with aldehydes and ketones to afford enamine products. Two decades later the nucleophilic properties of enamines were examined in detail by Stork. In his work Stork employed stoichiometric quantities of enamines in α-alkylation and α-acylation reactions of carbonyl compounds.[24,25] This work would later become known as the Stork enamine synthesis (Figure 1.10).
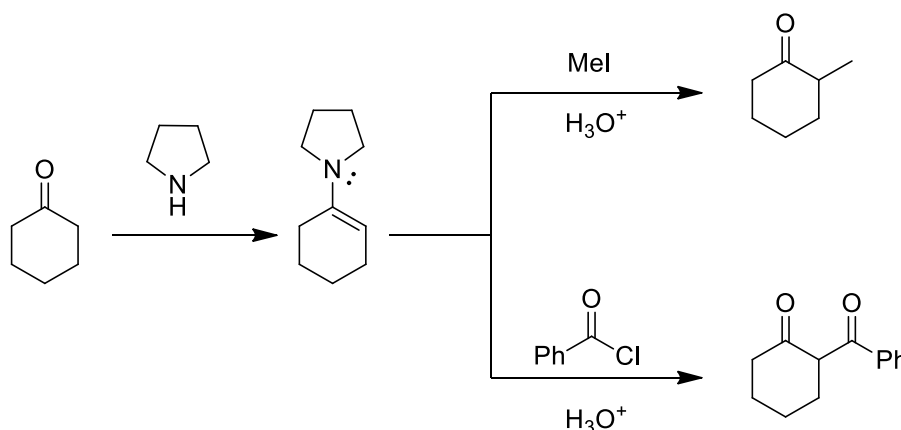
Figure 1.10. Stork enamine alkylation and acylation.

Enamines offered a number of significant advantages over the traditional method for α-alkylation and α-acylation of carbonyl compounds, i.e. over the use of enols or enolates. These advantages include: 1) the use of neutral conditions in the formation of enamines, which allows the use of acid/base sensitive substrates; 2) enamines are more nucleophilic than their enolic counterparts; 3) the secondary amine can be used sub-stoichiometrically; 4) polyalkylation is rarely observed with enamines catalysis; 5) if a chiral secondary amine is used stereocontrol can be exerted over the reaction.

Since the revival of enamine catalysis, brought about by the work of Barbas, List and Lerner in 2000, enamines have shown applicability to a wide variety of transformations including aldol reactions,[19] α-aminations,[26] Mannich reactions,[27] conjugate addition reactions,[28] α-oxygenations[29], and [4 + 2] cycloadditions.[30]

1.2.2 Catalytic cycle

A catalytic cycle describing the reactivity of enamines is outlined in Figure 1.11. Starting from a carbonyl compound (aldehyde or ketone) **5,** condensation with a secondary amine results in the formation of an intermediate LUMO lowered iminium ion **6**. The increased acidity of the α-protons of the iminium species, in comparison to that of the parent carbonyl, allows for facile deprotonation to give the enamine form **7**. In the iminium-enamine equilibrium the nucleophilic enamine is the more thermodynamically stable product and therefore the catalytically active nucleophilic species is the dominant form in the equilibrium. This is in contrast to the keto-enol equilibrium, whereby the non-nucleophilic keto form is usually the thermodynamically more stable form and therefore the dominant component of the equilibrium.

The HOMO raised enamine is now primed for nucleophilic attack on a suitable electrophile **E**. This results in functionalization at the α-position and generation of a new iminium ion intermediate **8**. Iminium **8** then undergoes hydrolysis to yield the α-functionalized carbonyl compound **9,** with concomitant regeneration of the catalyst **10**. The catalyst can then re-enter the cycle to continue product formation.
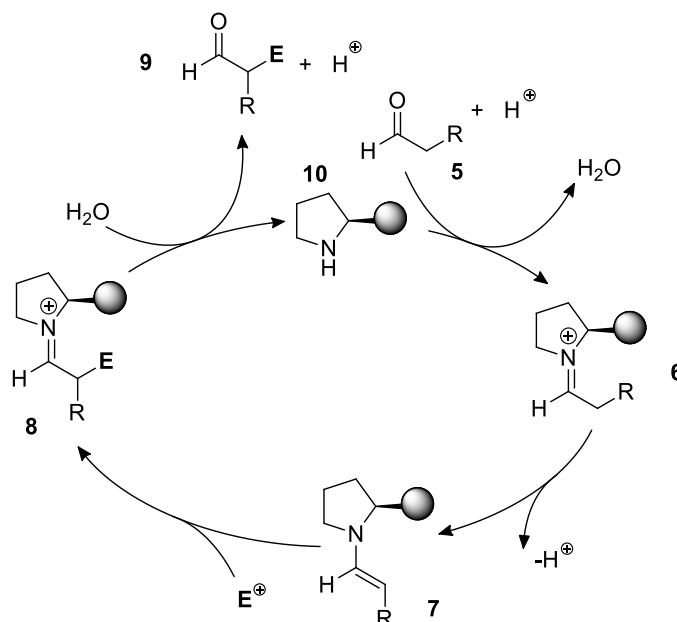
Figure 1.11. The enamine catalytic cycle. Shaded circle represents a stereodirecting group.

If a chiral secondary amine is used then control can be exerted over the three-dimensional approach of the two reactant partners. Therefore the stereochemistry of the reaction

products can be controlled. The types of stereodirecting groups incorporated usually employ either: 1) an electronic interaction, stabilizing the approach of the electrophile to the same face of the catalyst, or 2) steric shielding, which can block approach to one face of the catalyst and so favouring approach from the opposite side.

1.2.3 Catalyst design

As outlined in Section 1.1.3, it was the work of Barbas, List and Lerner that highlighted the utility of enamines in asymmetric organocatalytic transformations. This work was inspired by a class of enzymes known as aldolases, present in both eukaryotic and prokaryotic organisms, and which are known to operate via an enamine mechanism.[31]

Barbas *et al*. took advantage of the known propensity of secondary amines to form enamines when they screened chiral organic catalysts based on the pyrrolidine scaffold.[19] A selection of results from this study is shown below (Table 1.2).
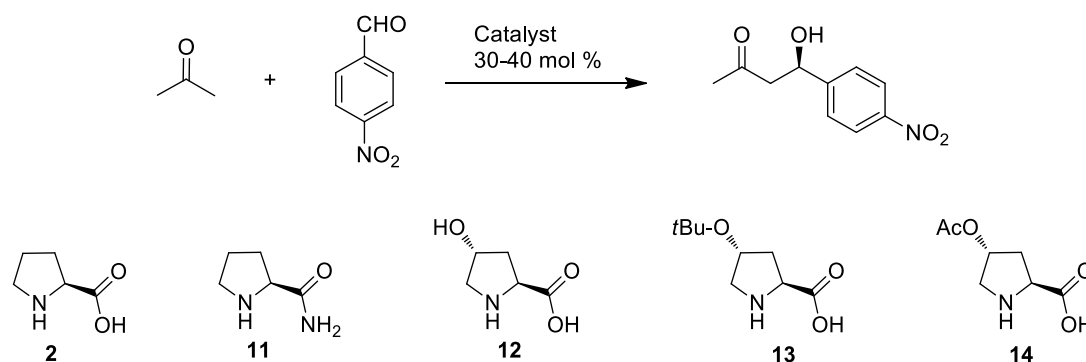
Table 1.2. Selected results from the screening of pyrrolidine based catalysts in an aldol reaction[19]

Entry	Catalyst	Yield	ee
1	**2**	68 %	76 %
2	**11**	< 10 %	n.d
3	**12**	85 %	78 %
4	**13**	> 50 %	62 %
5	**14**	70 %	74 %

As can be seen in Table 1.2, the reactivity and selectivity of the catalysts are highly dependent on their structural features. When comparing entries 1 and 2 (Table 1.2), it is evident that the carboxylic acid moiety plays an important role in L-proline catalyzed aldol reactions.

Despite intense interest and much research in the early years of organocatalysis, no single catalyst scaffold was found at that time that could be applied generally to a number of structurally diverse substrates. This was problematic for experimentalists as it necessitated catalyst structure modification for each new transformation or methodology.

Perhaps the most well know modifications of the pyrrolidine scaffold are that of diarylmethylpyrrolidine **15**, and diarylprolinol **16** and its silyl ether **17** (Figure 1.12).

High reactivity
Low selectivity

Low reactivity
High selectivity

High reactivity
High selectivity
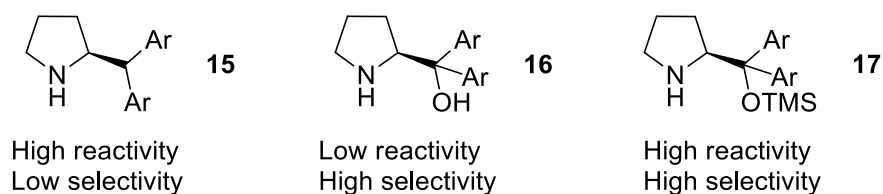
Figure 1.12. Diarylprolinol and related structural modifications.

The diarylmethylpyrrolidine **20** was first investigated by Jørgensen *et al.* in the first organocatalyzed enantioselective Inverse-Electron-Demand Hetero-Diels-Alder (IEDHDA) cycloaddition of aldehydic enamines and enones (Table 1.3).[30]
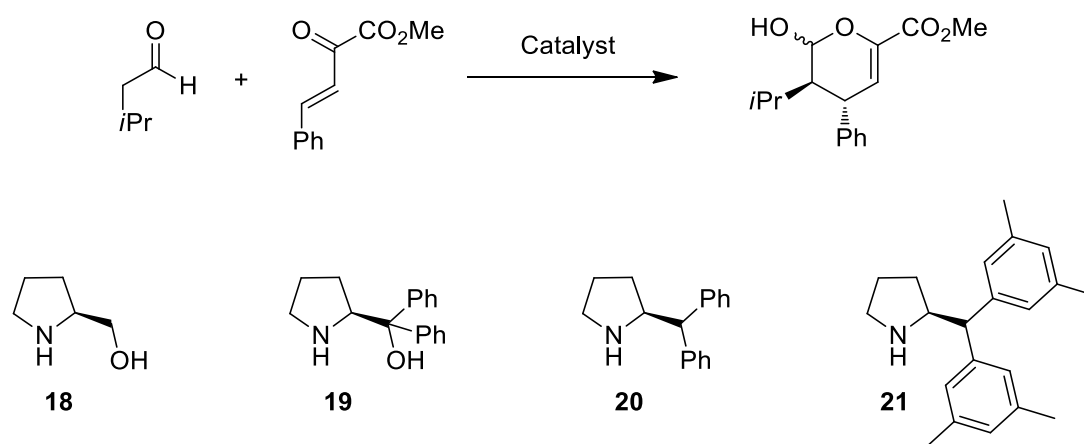
Table 1.3. Selected results of a catalyst screen for the IEDHDA reaction reported by Jørgensen *et al.*[30]

Entry	Catalyst	Solvent	Yield (%)	ee (%)
1	**18**	CH_2Cl_2	54	56
2	**19**	CH_2Cl_2	6	97
3	**20**	CH_2Cl_2	46	88
4	**21**	CH_2Cl_2	71	87

As can be seen in Table 1.3, a strong correlation between catalyst structure and reactivity and stereoselectivity exists. Comparing entries 1 and 2 (Table 1.3) one observes a dramatic drop in reaction yield but a marked increase in stereoselectivity. The cause for this drop in yield of the reaction, whilst using the diarylprolinol catalyst **19**, was found to be a parasitic process sequestering the catalyst and therefore removing the catalytically active species from the reaction mixture.[32] The parasitic process was determined to be the formation of an oxazolidine species **22**, formed via attack of the alcohol on the intermediate iminium ion (Figure 1.13). The formation of the oxazolidine is thermodynamically favoured and as such there is a reduction in the concentration of the catalytically active enamine available to catalyze the reaction, which gives a lower conversion.
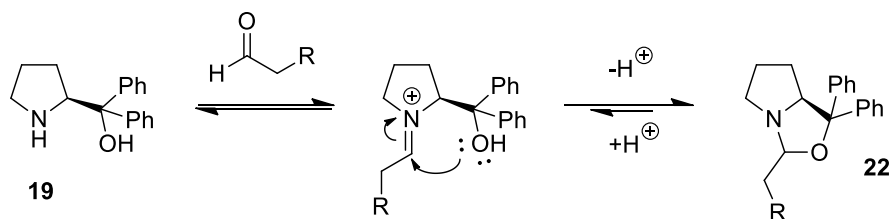
Figure 1.13. Formation of oxazolidine **22** from an intermediate iminium ion.[32]

This problem was overcome with the addition of a silyl protecting group on the hydroxyl group of the diarylprolinol type catalyst. The diarylprolinol silyl ether **23** was found to exhibit high reactivity and selectivity and became the first generally applicable organocatalyst (Figure 1.14).[32]

Ar = 3,5-$(CF_3)_2$-Ph
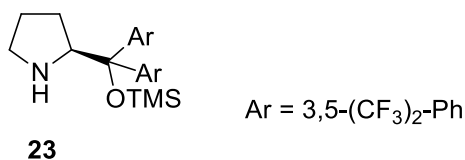
Figure 1.14. The Jørgensen-Hayashi catalyst.

Hayashi *et al.* also worked on the diarylprolinol silyl enol ether catalyst **23** concurrently. They initially demonstrated the applicability of the catalyst to the Michael-type reaction of aldehydes and nitroalkenes.[33] The work by the groups of Jørgensen and Hayashi in the development of the diarylprolinol silyl enol ether catalyst **23** has led to it being colloquially known as the "Jørgensen-Hayashi catalyst".

Pyrrolidine based scaffolds have remained privileged structures in enamine catalysis, as they exhibit an ideal balance between reactivity and stereocontrol. Pyrrolidine enamines are also more nucleophilic than other five and six membered ring N-heterocycles (Figure 1.17). This is due to the higher energy of the HOMO of pyrrolidine derived enamines and an increased electron density at the nucleophilic alkene. The increased electron density is as a result of the delocalization of the enamine nitrogen lone pair, which is aided by increased sp^2 character of the enamine nitrogen atom in the smaller five-membered ring system. This results in the lone pair of the nitrogen occupying an orbital with more unhybridized p orbital character and allows for greater orbital overlap between the orbital containing the nitrogen lone pair and the C=C π-bond. As a result the lone pair can more efficiently delocalise into the π-system of the enamine olefin. Conversely, increasing the sp^3 character of the amine nitrogen leads to increased pyramidalization (sp^3-type geometry) of the amine geometry and

therefore a decrease in the ability of the lone pair to overlap with the π-bond system. The decreased orbital overlap is accompanied by a decrease in the nucleophilicity of the enamine (Figure 1.15).

Figure 1.15. Comparison of lone pair delocalization in five and six-membered ring enamines.
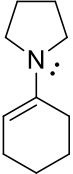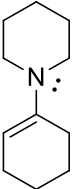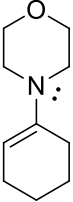
This is exemplified by the fact that cyclic six-membered rings are significantly less nucleophilic than their five-membered ring equivalents, as determined in a study by Mayr *et al.*[34] In this study the authors quenched benzylhydryl cations with enamines and studied the reaction kinetics in order to develop a scale of nucleophilicity (Figure 1.16).
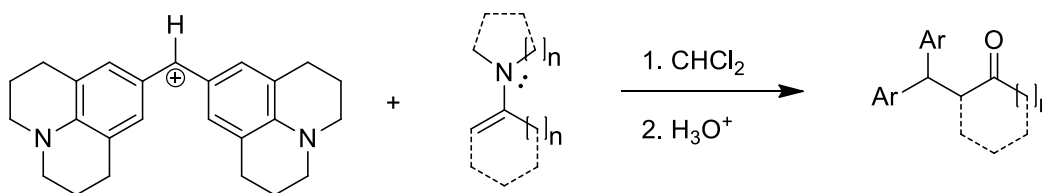
Figure 1.16. The reaction of enamines with benzylhydryl cations studied by Mayr.[34]

Table 1.4, comparing entries 1 and 2 the second-order rate constant of the pyrrolidine derived enamine is an order of magnitude faster than that of the proline derived enamine, an indication of the great nucleophilicity of the 5-membered ring derived enamines. Modification of the cyclic amine can also lead to increased or decreased nucleophilicity as is evidenced by entry 3, a morpholine derived enamine, in which the inductive withdrawal of the electronegative oxygen atom in the ring reduces the electron donating ability of the nitrogen lone pair. This in turn reduces the nucleophilicity of morpholine derived enamines as is seen in the significant reduction to the second-order rate constant of the reaction described in entry 3.

Table 1.4. Selected results from the study by Mayr on enamine nucleophilicty[34]

Entry	Enamine	K_2/M^{-1}s^{-1}
1		4.59×10^4
2		1.41×10^3
3		3.35×10^1

In summary, the increase in sp^3 character of the enamine nitrogen is inversely proportional to the nucleophilicity of the respective enamine (Figure 1.17).
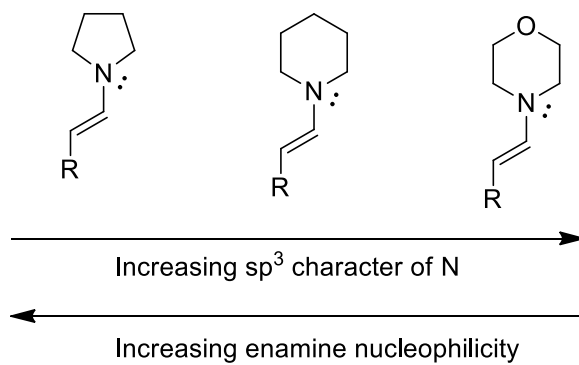
Figure 1.17. Comparison of five and size membered ring heterocycle derived enamines.

1.2.4   Source of stereocontrol

As outlined in Section 1.2.3, catalyst structure is of fundamental importance to catalyst activity, substrate scope and reaction type. Unsurprisingly, the stereocontrolling action of pyrrolidine based organocatalysts is also driven by catalyst structure. The modes of stereocontrol employed in the literature can be broadly divided into two distinct groups: 1) electronic/hydrogen bonding control, and 2) steric shielding (Figure 1.18).[35]
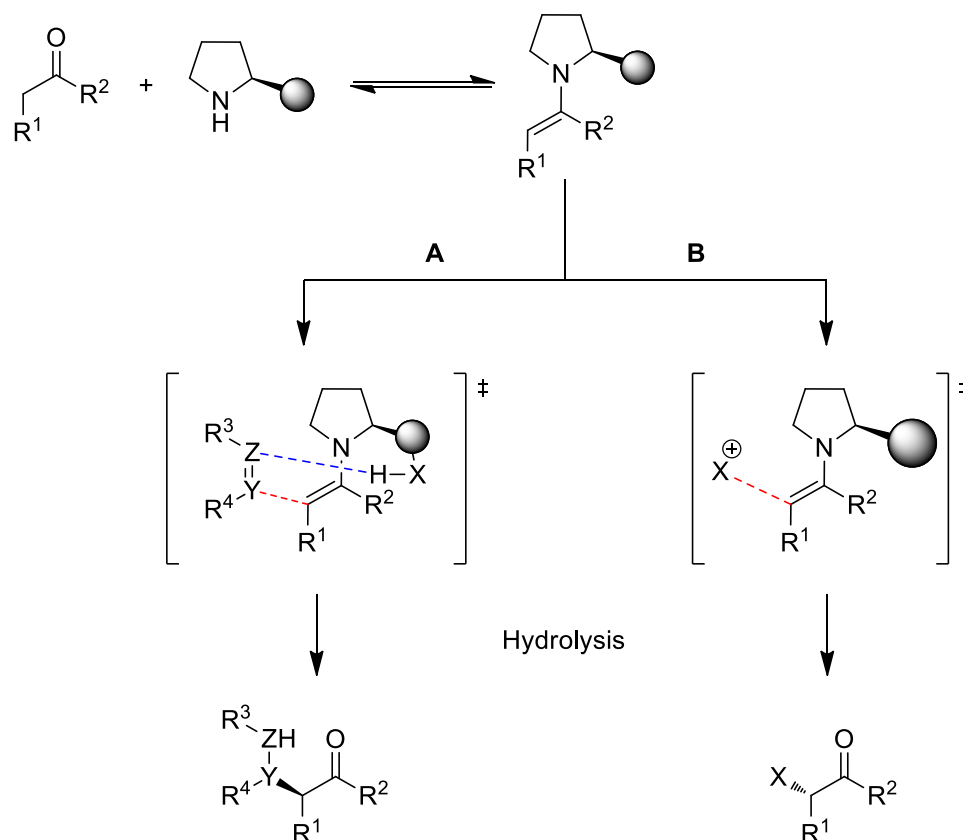
Figure 1.18. Modes of stereocontrol with pyrrolidine based catalysts. **A** = electronic effect/hydrogen bonding control, guides electrophile to top face; **B** = steric shielding control, guides electrophile to bottom face.[35]

Whilst the routes differ in the control of substrate approach, a common feature to both is the initial enamine geometry. Comparing relative ground state energies for the four possible geometries and conformations, *E*-s-*trans*, *E*-s-*cis*, *Z*-s-*trans* and *Z*-s-*cis* the most stable was found to be the *E*-s-*trans* conformation (Figure 1.19).[36]
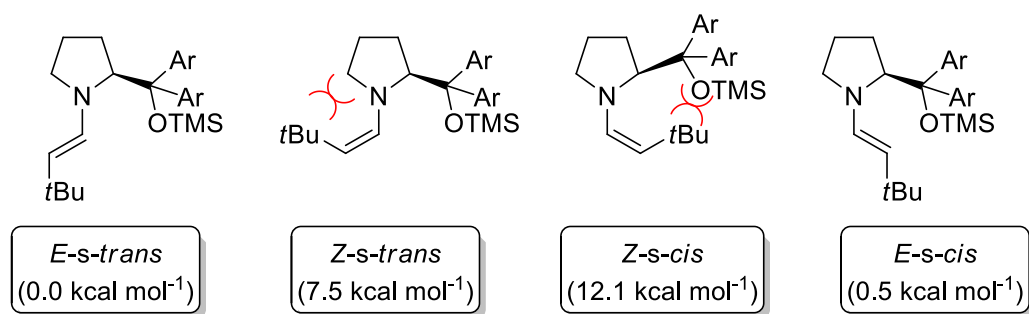
Figure 1.19. Relative energies of different possible enamine conformations, Ar = 3,5-$(CF_3)_2$-Ph.[36]

When the enamine olefin is in the *Z* geometry, there exists a steric clash exists between the substituents and either, the pyrrolidine ring (*Z*-s-*trans*) or the bulky diarylprolinol silyl ether (*Z*-s-*cis*) resulting in higher ground state energies for these conformations. Therefore, it can be considered that these less stable species are less likely to be the major reactive enamine conformation in reactions mixtures.[36]

This finding that the *E*-s-*trans* enamine is the most stable conformation was further supported by the crystal structure analysis of a number of enamines by Seebach *et al.* (Figure 1.20).[37]
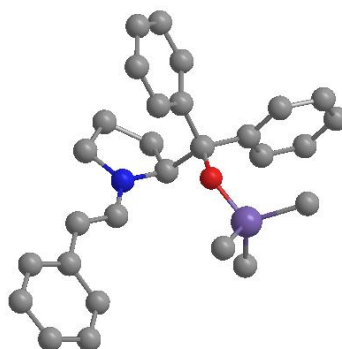
Figure 1.20. Crystal structure CCDC 695934, Seebach 2008, hydrogens omitted for clarity.[37]

Whilst enamines were generally accepted as the reactive intermediates in a number of organocatalytic transformations involving secondary amine catalyst, it was not until as recently as 2010 that an enamine was detected *in-situ* in reaction mixtures. The identification of enamines *in-situ* was hampered by the parasitic formation of the oxazolidine already discussed (Figure 1.13). In their study, the group of Gschwind successfully identified the *E*-s-*trans* enamine as the only observable enamine in self-aldol reaction of propionaldehyde in the presence of 20 mol % L-proline in DMSO-d$_6$.[38]

The two *E*-isomers (s-*cis* and s-*trans*) of the enamine only differ in ground state energy by 0.5 kcal mol^{-1}. This difference does not seem to account for the high stereoselectivities typically observed when using diarylprolinol silyl ether catalysts. To address this incongruity between experimental and theoretical results, Jørgensen *et al.* carried out a theoretical study of a number of possible transition states, using Density Functional Theory (DFT), for the α-fluorination of aldehydes with *N*-fluorobenzenesulfonimide (NFSI) (Figure 1.21).[36]
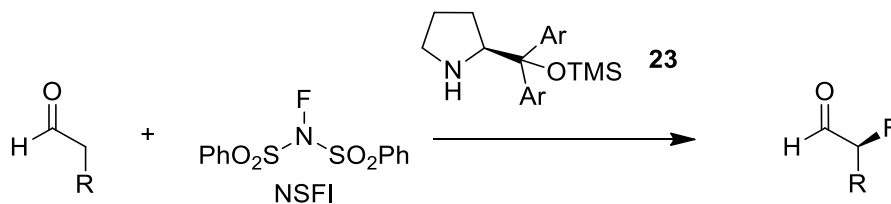
Figure 1.21. Reaction of NSFI with diarylprolinol silyl ether derived aldehydic enamine, Ar = 3,5-(CF$_3$)$_2$-Ph.[36]

The stereochemical outcome of the reaction is determined by the direction of the approach taken by the electrophile as it nears the prochiral sp^2 carbon of the enamine. This leads to eight possible transition states describing the different approaches of the electrophile. Each of the four enamine conformations, outlined in Figure 1.19, can be approached from the top or bottom face (Figure 1.22).
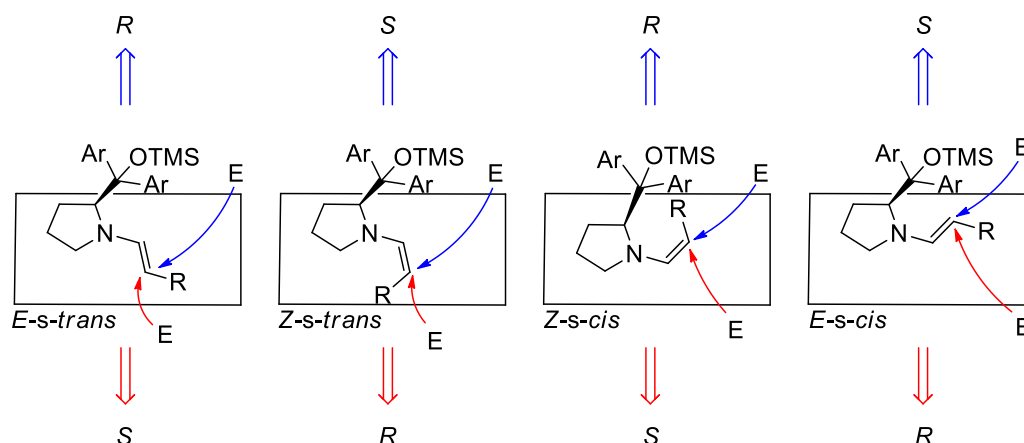
Figure 1.22. Eight possible approaches to the four different enamine intermediates and their stereochemical outcomes, Ar = 3,5-(CF$_3$)$_2$-Ph.[36] Red arrow = approach from bottom face; Blue arrow = approach from top face, E = electrophile.

To avoid confusion when describing heterotopic faces of trigonal atoms the *Re* and *Si* terminology shall be applied. A prochiral trigonal sp^2 hybridized atom shall be designated *Re* when the ligands of the atom appear in a clockwise fashion when assigned priority based on the Cahn-Ingold-Prelog (CIP) system.[39] Similarly a trigonal atom shall be designated *Si* when the ligands of the atoms appear in a counter-clockwise fashion when assigned priority based on the CIP system (Figure 1.23).
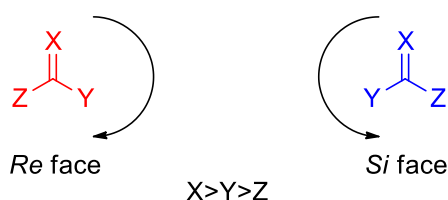
Figure 1.23. Naming conventions for *Re* and *Si* faces of a prochiral trigonal centre.

Jørgensen *et al.* then went on to investigate the free energies of a number of plausible transition states arising from the approach of NSFI on the enamine *Re* and *Si* faces. They found that the lowest energy transition state (Table 1.5) was that of the *Si* face approach, from below, on the lowest energy conformation of the enamine *E*-s-*trans* (**TS1**, Figure 1.24). This results in an *S* configuration at the newly formed stereogenic centre. The transition state closest in energy to **TS1** was found to be **TS3,** which is a result of the *Re* face approach (from below) of the electrophile on the second lowest energy enamine conformation *E*-s-*cis*. This results in an *R* configuration at the newly formed stereogenic centre. The difference in energy between these two transition states was found to be 2.4 kcal mol^{-1}, which may explain the high experimentally observed ee of 97 %.[40]

Table 1.5. Selected results of DFT calculations for transitions states of electrophile approach[36]

TS	E_{elec} [Hartree]	ΔE_{elec} [kcal mol^{-1}]	G [Hartree]	ΔG [kcal mol^{-1}]
1	-4495.64374	0[a]	-4494.95051	0[a]
2	-4495.62701	10.5[a]	-4494.93099	12.2[a]
3	-4495.63998	2.4[a]	-4494.94589	2.9[a]
4	-4496.70807	9.5[a]	-4494.93807	7.8[a]

[a] Energies given relative to lowest energy transition state **1**.
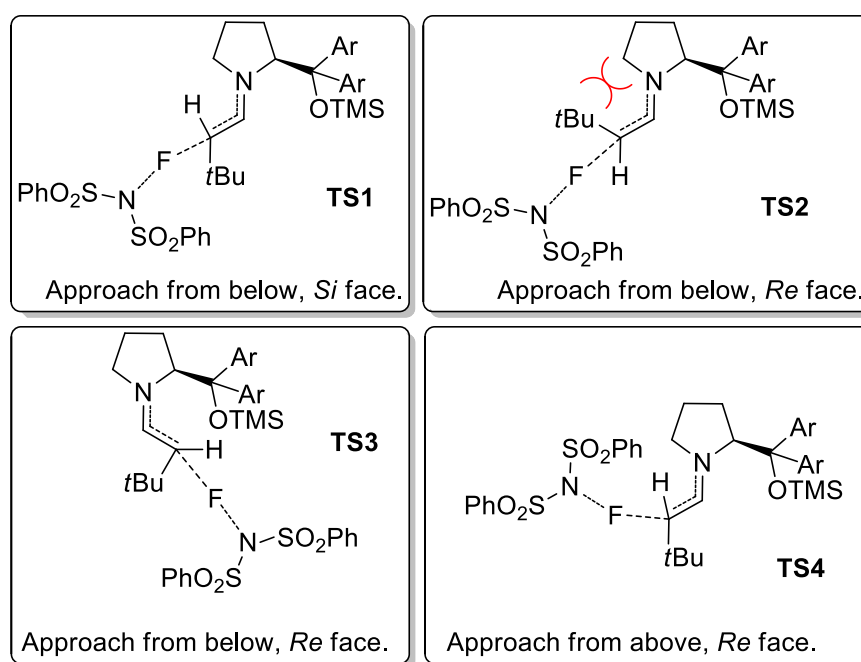
Figure 1.24. Selected transition states of approach of electrophile to enamine.[41]

The authors also investigated the transition state arising from the electrophile approaching the *Re* face (from below) of the less stable *Z-*s*-cis* enamine **TS2.** This transition state was found to be much higher in relative energy, 10.5 kcal mol^{-1}, and as such this transition state was deemed to be much less likely to occur. Another plausible transition state that was investigated was that of the *Re* face approach (from above) on the most stable *E-*s*-trans* enamine, **TS4**. **TS4** was found to be disfavoured by 9.5 kcal mol^{-1}, which was rationalized by the effective shielding of the *Re* face by the large bulky substituent at the 2-position of the pyrrolidine ring.

A different mode of stereocontrol must be considered when the natural amino acid L-proline is used as an organocatalyst. The carboxylic acid moiety can act as a Brønsted acid and can therefore direct suitable substrates towards the face occupied by the carboxylic acid. In this way L-proline can be considered a dual activation catalyst as it activates the nucleophile through the HOMO raising effect of enamine formation as well as simultaneously activating the incoming electrophile through hydrogen bonding, a LUMO lowering effect similar to Lewis acid activation.

A number of transition states for the L-proline catalyzed intermolecular aldol reaction have been proposed to describe the high levels of diastereo- and enantioselectivity observed

experimentally (Figure 1.25). Initially the model proposed by Hajos *et al* did not include an enamine intermediate, instead the authors favoured an "activated" hemiaminal intermediate, which is subsequently attacked by the enol form of the donor carbonyl. This mechanism was questioned quite soon after its proposal and mechanisms, and an enamine intermediate became favoured. Another proposed transition state was that of the Agami group which utilized two L-proline molecules, one to form the enamine and a second to aid in proton transfer (Figure 1.25).[42] This mechanism was supported by a modest non-linear rate effect observed by Agami and co-workers.[43] This however was also later questioned by List and Houk, who suggested that the non-linear effect observed was due to the use of a small sample number, as well as the experimental variance inherent with the use of optical rotation as a means of determining enantiomeric excess.[44] In their own study, aided by advancements in chiral chromatography, Houk and List showed a linear increase in rate with increase in catalyst concentration suggesting the presence of only a single proline molecule in the transition state.[44]

Hajos-Parrish (1971)

Agami (1985)

Houk-List (2002)
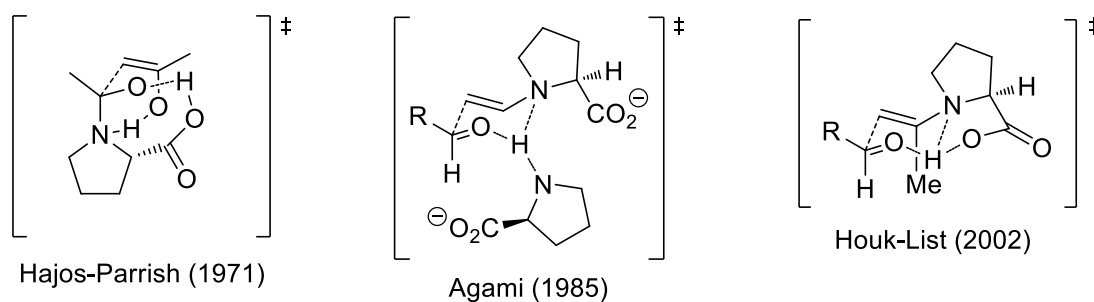
Figure 1.25. Selected transition states proposed for an intermolecular aldol reaction catalyzed by L-proline.[15,19,42]

Arguably, the favoured proposed mechanism is that proposed by Barbas and List[19] in 2000 and further studied extensively by Houk and List (Figure 1.25).[45] In this mechanism the stereochemistry is determined through a Zimmerman-Traxler six-membered ring chair-like model **24** in which the *Re* face of the approaching aldol acceptor is exposed (Figure 1.26).[46]
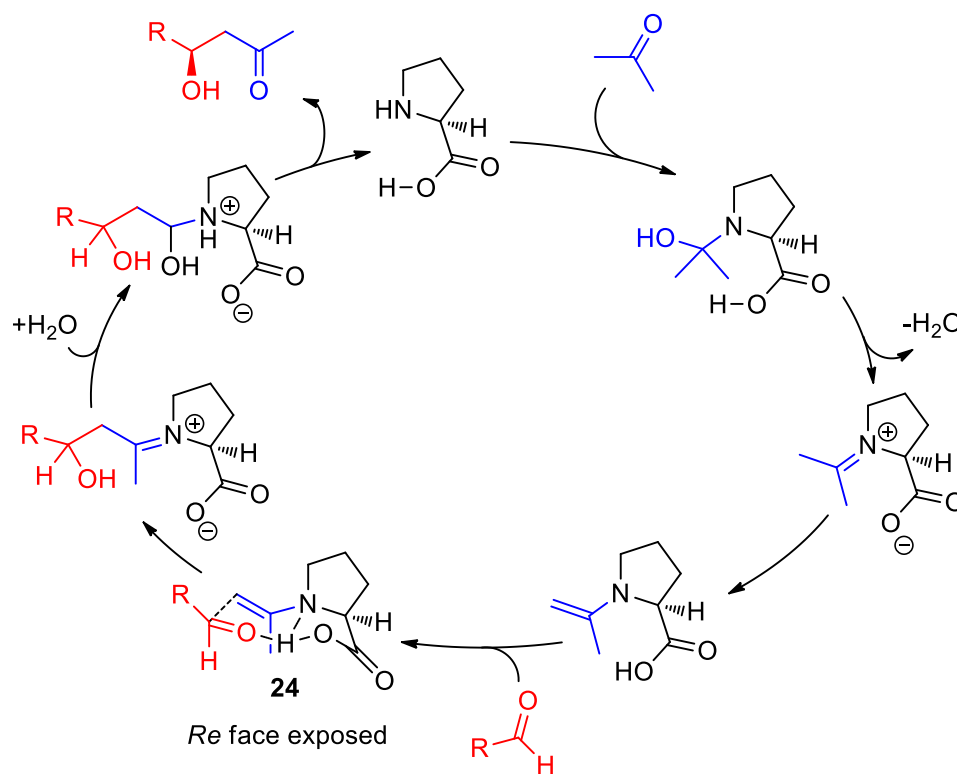
Figure 1.26. Proposed mechanism for the intermolecular aldol reaction invoking the Houk-List transition state.

The fact that this mechanism has remained at the forefront of literature discussion for more than a decade, and has stood up to intense scrutiny from both theoretical and experimental study, is testament to its power in describing the stereochemical outcome of L-proline catalyzed asymmetric reactions.

1.2.5   Reactions employing enamine catalysis

The scope of modern day enamine catalysis is staggering, particularly if one considers its relatively recent revival. From its beginnings in intermolecular aldol reactions,[19] enamine catalysis has found applicability in a large number of transformations. These transformations can be broadly divided into two distinct categories based of the nature of the newly formed bond: 1) C-C bonds and 2) C-X bonds (where X represents a heteroatom). These categories can also be further sub-divided into two reaction types: 1) a substitution-type reaction and 2) an addition-type reaction.

Both reaction types take advantage of the increased nucleophilicity of the enamine olefin, brought about by the HOMO raising property of enamine formation, and differ in the nature of the electrophilic partner.

Examples of substitution-type reactions include, α-amination, α-oxygenation, α-halogenation, α-sulfenylation and α-selenylation reactions (Figure 1.27). Examples of addition-type reactions include enamine additions to polarized π-systems such as nitroso compounds, nitro-olefins, azodicarboxylates and imines (Figure 1.27).
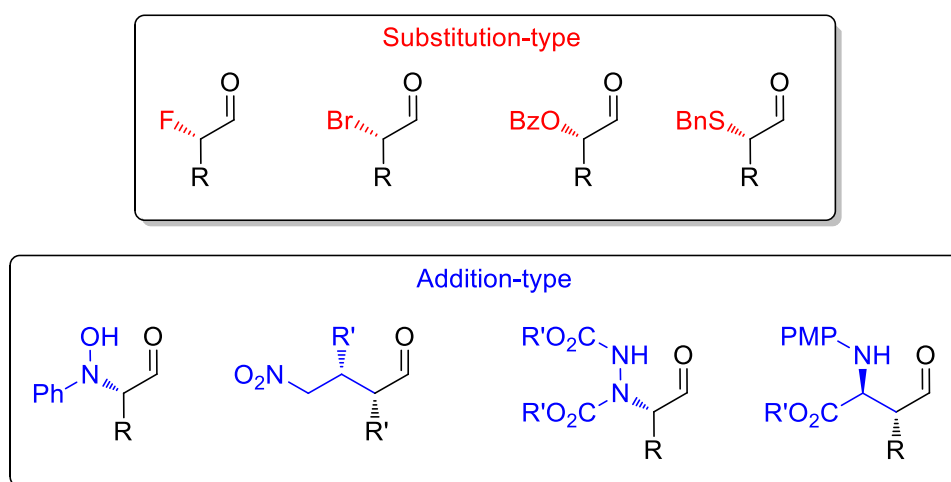
Figure 1.27. Selected examples of enamine catalyzed transformations.

1.2.6   Enamine catalyzed asymmetric conjugate addition reactions

The reaction of ethyl cinnamate and diethyl malonate, in the presence of sodium ethoxide, yields the conjugate addition product **25** (Figure 1.28). This reaction, described by Michael[47]

in 1887, lay the foundation for one of the most studied C-C bond forming reactions, which would later bear the authors' name, the Michael reaction.
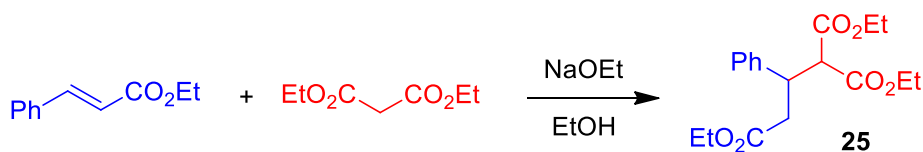
Figure 1.28. The conjugate addition of diethyl malonate to ethyl cinnamate described by Michael.[47]

In modern usage, the definition of a Michael-type reaction has been expanded to include the addition of nearly any nucleophile to an electron-deficient π-system in a 1,4-fashion. To that end, the Michael reaction has been extensively studied and both donor and acceptors have been varied greatly. Typical acceptors include alkenes and alkynes activated by an electron withdrawing group (EWG) such as the nitro, phenylsulfonyl, phosphonate, ester or cyano group. Typical carbon-centred Michael donors include activated methylene compounds such as malonates, as well as enamines and enolates. Hetereoatomic donors include amines, alcohols and thiols to give the aza-, oxo- and thio- variants of the Michael reactions respectively.

The scope and breadth of study on the Michael reaction, under stoichiometric and catalytic conditions, is so vast that it exceeds the limitations of this document. As such, attention will be solely focused on the organocatalytic efforts in the development of this reaction and with a particular emphasis on those reactions invoking an enamine in the activation of the Michael donor.

The Michael reaction represents a powerful method for the construction of C-C and C-X bonds and asymmetric variants of the reaction are extremely useful in the construction of valuable stereochemically enriched materials. With the successes of chiral enamines as carbon-centered nucleophiles in aldol chemistry, pioneered by Barbas *et al.*[19], a natural progression to the application of chiral enamines with other electrophiles was inevitable.

Early examples include the L-proline catalyzed asymmetric Michael addition of unmodified ketones to β-nitrostyrene aldehydes by List *et al.*[28] and the diamine catalyzed addition of aldehydes and ketones to β-nitrostyrene by Alexakis *et al.*[48]
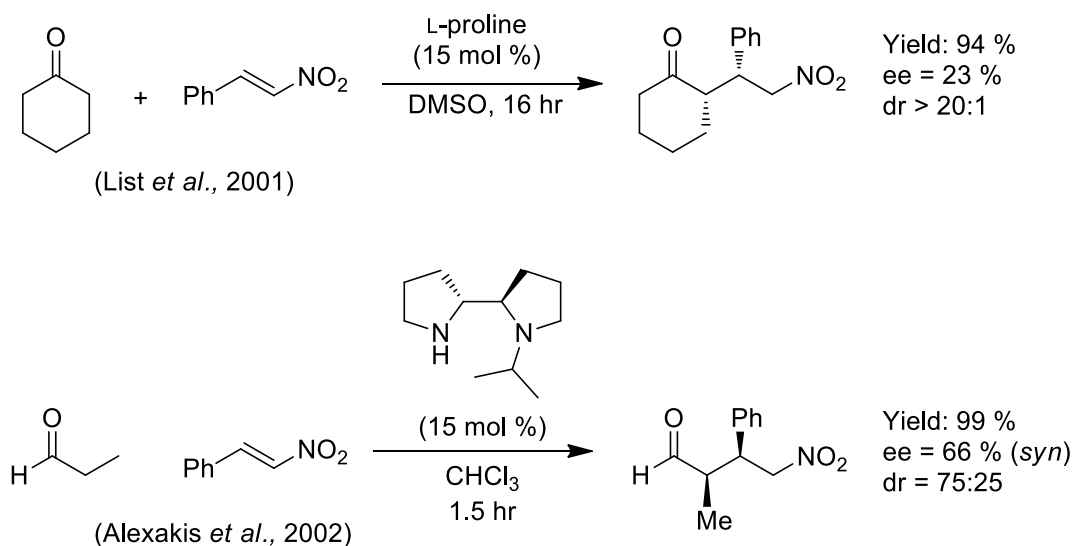
Figure 1.29. Examples of organocatalytic asymmetric conjugate additions (ACA's) by List *et al.*[28] and Alexakis *et al.*[48]

A report by Jørgensen *et al.*, that received widespread attention, described the addition of simple aldehydes to vinyl ketones.[49] The utilization of simple aldehydes over ketones afforded a number of advantages to this methodology: 1) the increased electrophilicity of the aldehydes allowed for more rapid condensation and enhanced reaction rates; 2) the aldehydic hydrogen does not present a steric hindrance and therefore the geometry of the reactive enamine is more heavily weighted towards the more stable *E*-s-*trans* enamine, enhancing enantioselectivities.
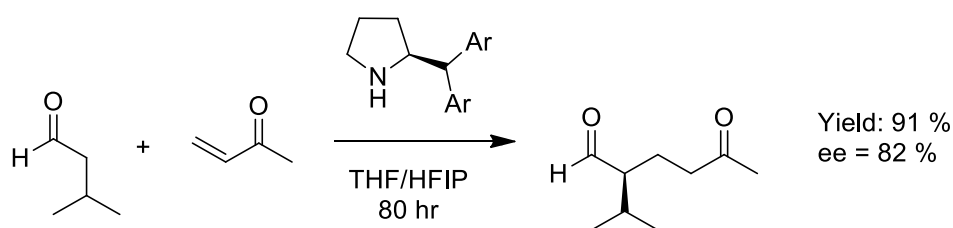
Figure 1.30. Addition of simple aldehydes to vinyl ketones reported by Jørgensen *et al.*[49] THF = Tetrahydrofuran; HFIP = 1,1,1,3,3,3-hexafluoro-2-propanol; Ar = 3,5-dimethylbenzene.

Enamines are less nucleophilic than their enolate counterparts and so there is a necessity for the Michael acceptor to be suitably activated by electron withdrawing groups. These early successes led to an explosion of interest in the expanding the substrate scope of suitable Michael acceptors in enamine catalyzed Asymmetric Conjugate Addition (ACA) reactions.

Some of the more popular substrates to have been developed include doubly activated olefinic systems, are shown in Figure 1.31. Examples include those substituted by

phenylsulfonyl groups (**26** and **27**, Figure 1.31)[50] and the bis-phosphonate substituted olefin (**28**, Figure 1.31)[51]. This is with a view towards incorporating a number of useful functional groups compatible with functional group interconversions (FGI's) for the expedient development of molecular complexity in target molecules.

$$PhO_2S \diagdown \diagup SO_2Ph \qquad PhO_2S \diagdown \diagup SO_2Ph \qquad (EtO)_2OP \diagdown \diagup PO(OEt)_2$$

$$Ph \diagup$$

26   **27**   **28**
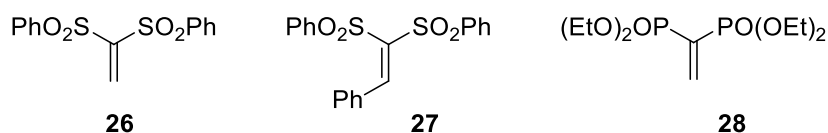
Figure 1.31. Representative Michael acceptors utilized in enamine catalyzed ACA's.

1.2.7   Vinylogous organocatalytic conjugate addition reactions

The propagation of charge delocalisation through conjugated systems has long been known and exploited in the vinylogous reactivity of electron-deficient conjugated systems. Fuson first formulated "the vinylogy principle" in 1934 as a means of formalizing and defining this phenomenon.[52] In his report he described vinylogous reactivity as follows; "When in a compound such as $A-E_1=E_2$ or $A-E_1\equiv E_2$ (where E_1 and E_2 represent non-metallic elements), a structural unit of the type $(-C=C-)_n$ is interposed between A and E_1, the function of E_2 remains qualitatively unchanged, but that of E_1 may be usurped by the carbon atom attached to A.". Fuson also went on to describe a vinylogous series, as one comprised of members such as those outlined above, that differ from each other by one or more vinylene residues and that the members of this series are vinylogs of one another.

Whilst the organocatalytic asymmetric 1,4-conjugate addition has been studied extensively,[53,54] the related vinylogous transformations in comparison have remained underdeveloped. Until recently the challenge of vinylogous conjugate addition chemistry has predominantly been addressed using metal-based catalysis, in particular through the use of complexes of the transition metals copper and rhodium.[55]

This underdevelopment is due, in part, to the added reactivity complications associated with vinylogous series. Of primary concern is the addition of new electrophilic sites on the acceptor. Even expanding the conjugation by only one unit, to yield an $\alpha,\beta,\gamma,\delta$-diunsaturated system, results in an acceptor that could be open to nucleophilic attack at one of three positions (Figure 1.32). Taking the example of a di-unsaturated ketone (Figure 1.32), attack at the 2, 4 or 6 positions results in four possible products. Each of the electrophilic sites

compete with one another and unless product distribution can be controlled, reduces the utility of extended conjugate addition reactions. If a stereoselective process is desired this further complicates matters and the number of potential products increases.
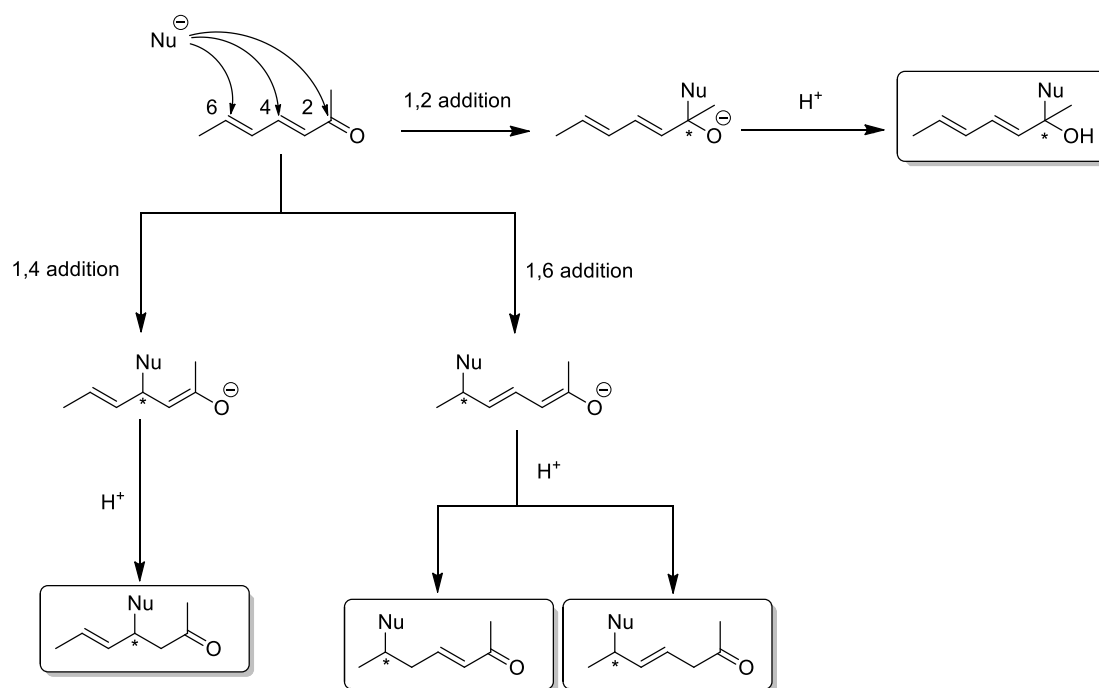
Figure 1.32. The regiochemical and stereochemical concerns of vinylogous reactivity. Nu = nucleophile.

In a 1959 report, Ralls described factors that influence the regioselectivity of the reaction of nucleophiles with conjugated systems, and in particular those that favour 1,6-addition over 1,4-addition.[56] Ralls stated that there are three principal factors governing the regioselectivity of 1,6-additions: 1) steric effects, 2) electronic effects and 3) nature of the incoming nucleophile. These principles have been broadly adhered to in the exploration of vinylogous reactivity and select examples will be highlighted below.

The first literature example of an organocatalytic enantioselective 1,6-conjugate addition was by Jørgensen *et al*.[57] In their report they described the 1,6-conjugate additions of β-ketoesters and glycine imines to electron-deficient δ-unsubstituted dienes. In this instance the authors employed phase transfer catalysis, using the cinchona alkaloids derived catalysts **29** and **30** (Figure 1.33). The reaction stereoselectivity is rationalised through the formation of a tight ion pair between the quaternary ammonium of the cinchona alkaloid and the anions generated from the pronucleophiles. This strong ionic interaction between the

catalyst and nucleophile allows for facial selectivity of the approaching electrophile, and hence affords stereocontrol.
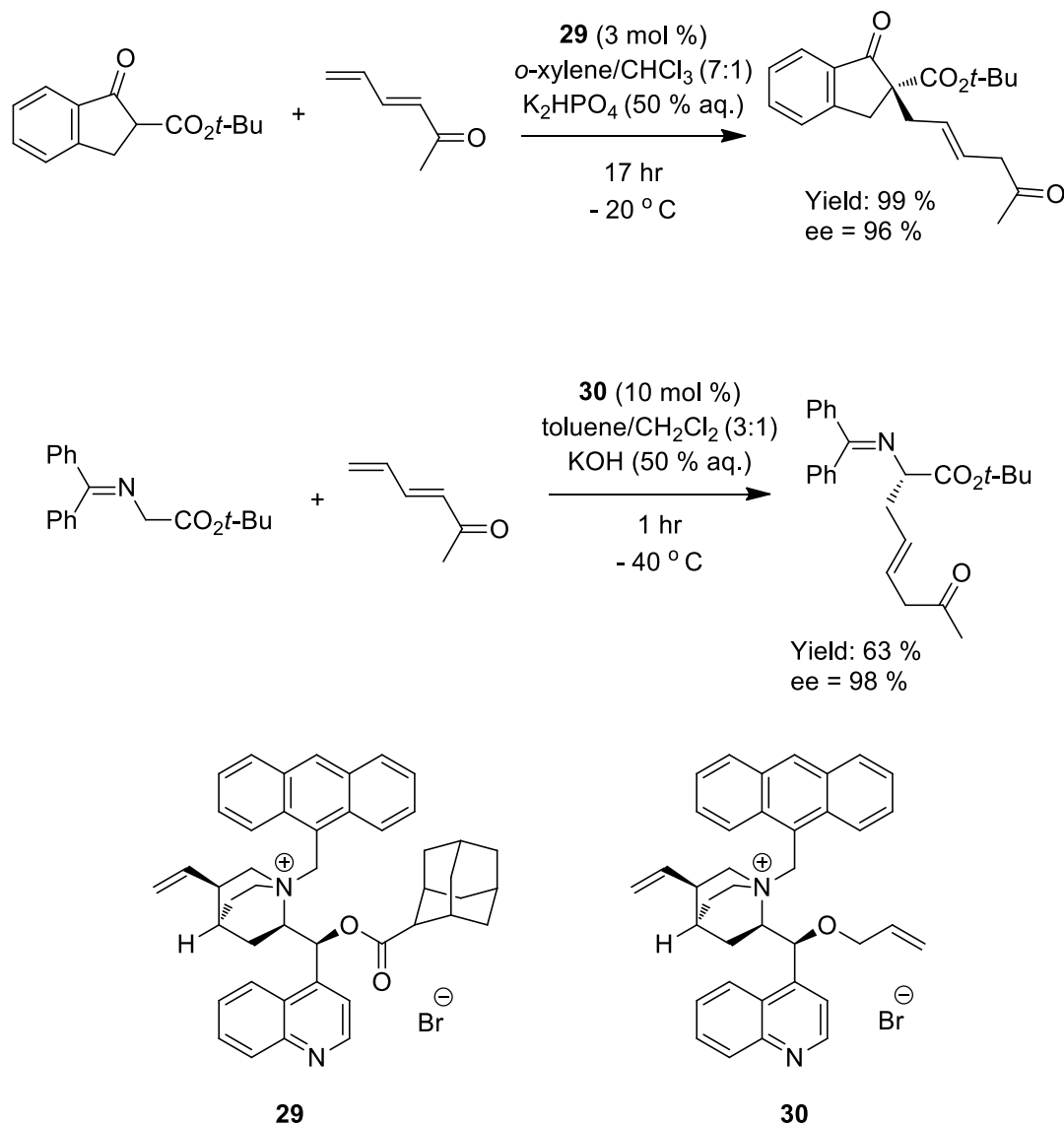
Figure 1.33. The first enantioselective 1,6-conjugate additions reported by Jørgensen *et al.*[57] EWG = CO_2Et, CO_2Me, SO_2Ph.

In this report the authors utilized two of the factors outlined by Ralls in order to favour 1,6-addition over 1,2- or 1,4-addition, namely steric and electronic effects.[56] Sterically, substitution at the δ-position can disfavour 1,6-addition through steric hindrance and so the authors left the δ-position unsubstituted. Electronically, the authors activated the conjugated system through incorporation of an electron withdrawing group into the 1-position of the butadiene. This allows for propagation of the charge delocalization

throughout the π-system which in turn generates polarization of the terminal olefin thereby activating the δ-position (Figure 1.34).
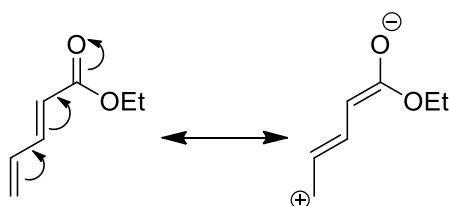
Figure 1.34. Resonance contributors of an EWG substituted dienic system.

1.2.8 Enamine mediated vinylogous ACA reactions

The first enamine mediated 1,6-conjugate addition to electron-deficient dienes was reported by the groups of Stephens and Alexakis in 2011 (Figure 1.35, top).[58] In this instance, the acceptor was dually activated by electron withdrawing phenylsulfonyl groups at the α- and γ-positions. The stereochemical outcome of the reaction was dictated by the nature of the nucleophile, in this case diarylprolinol silyl ether derived aldehydic enamines. This report was later expanded upon in 2013, with an extension of the substrate scope to include bis-ester substituted dienes (Figure 1.35, bottom).[59]
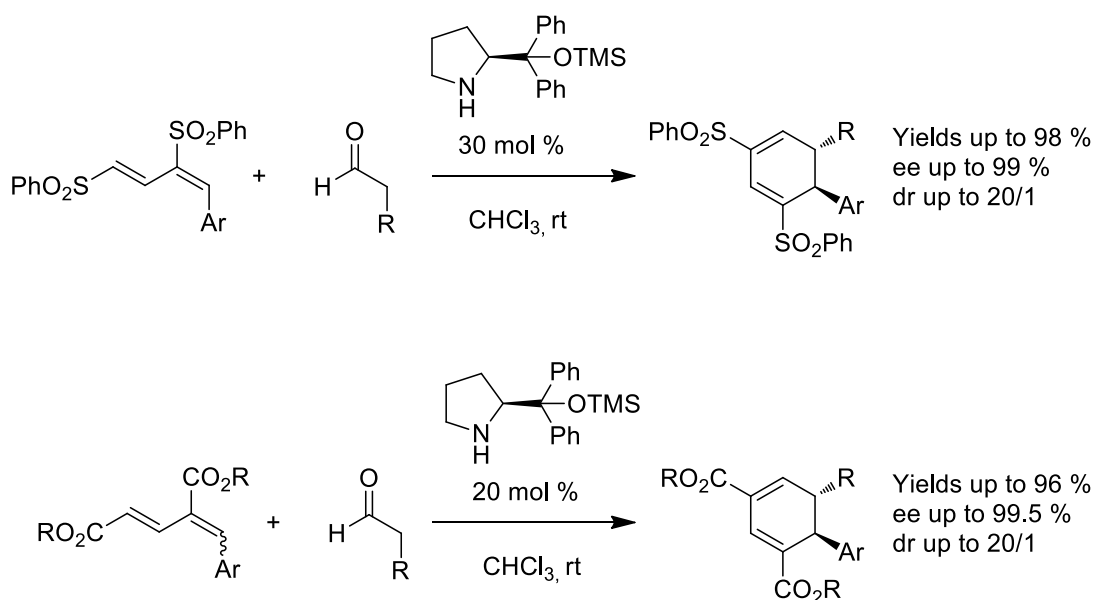
Figure 1.35. Enamine mediated 1,6-conjugate additions reported by Stephens and Alexakis.[58,59] R = alkyl.

Since 2013, there has been limited reports of enamine mediated 1,6-conjugate additions to electron-deficient systems. One, by the Jørgensen group, details the addition of aldehydic enamines to *p*-quinone methides (Figure 1.36).[60]
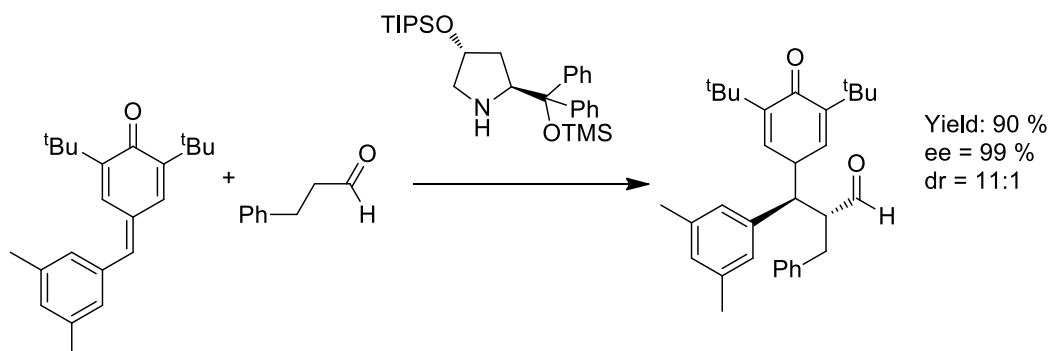
Figure 1.36. The 1,6-conjugate addition of enamines to *p*-quinone methides reported by Jørgensen *et al*.[60]

Although formally neutral *p*-quinone species have a zwitterionic resonance structure which affords *p*-quinone methides increased electrophilicity at the δ-position which in turn favours 1,6-addition.[61]
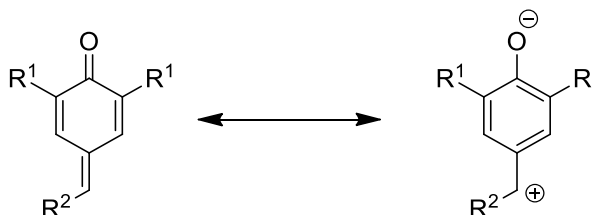
Figure 1.37. Resonance structure of a *p*-quinone methide exemplifying the electrophilicity of the δ-position.

Another report, in 2014, by Ying-Chun Chen *et al*. detailed the use of extended acceptors in conjunction with extended enamines, in this case trienamines, to afford 1,6-addition products in modest yields and with high enantioselectivity utilizing bifunctional thiourea catalyst **31** (Figure 1.38).[62]
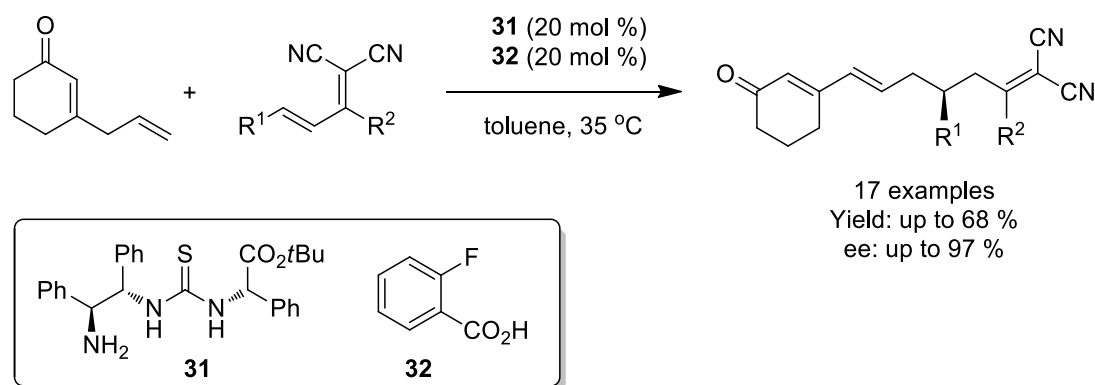
Figure 1.38. Enantioselective 1,6-conjugate addition of trienamines to electron-deficient dienes reported by Ying-Chun Chen *et al.*[62] R[1] and R[2] = aryl (Ar).

In this case the substrate design favours 1,6-addition over 1,4-addition due to the presence of an aryl group at the 4-position, therefore sterically shielding the 4-position and reducing the likelihood of attack at that position. The yields of this reaction were impeded by lack of reactivity (incomplete conversion even after 96 hr) and the formation of a side product **33** formed by a Diels-Alder cycloaddition of the trienamine and the diene (Figure 1.39).
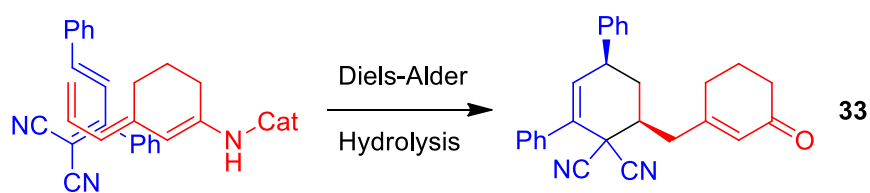
Figure 1.39. Diels-Alder reaction of trienamine and diene. Cat = catalyst structure.

1.2.9   Iminium mediated vinylogous ACA reactions

Other advances in the field of vinylogous conjugate addition have generally been made through the use of the related iminium-ion mode of catalysis.[63] A general catalytic cycle for the formation of an iminium ion is outlined in Figure 1.40. In addition to the enamine mode of activation, secondary amine catalysts have also found prominence in the formation of electrophilic iminium ions which can be intercepted with appropriate nucleophiles to yield addition products.[35] In contrast to enamine activation, iminium ions have a lower LUMO energy making them more susceptible to nucleophilic attack. Condensation of secondary amines with α,β-unsaturated aldehydes leads to an iminium ion **34** primed for attack at the β-position. Protonation of the resulting enamine **35** yields a second iminium ion **36** which

can be hydrolysed to release the β-addition product **37** with concomitant catalyst regeneration.
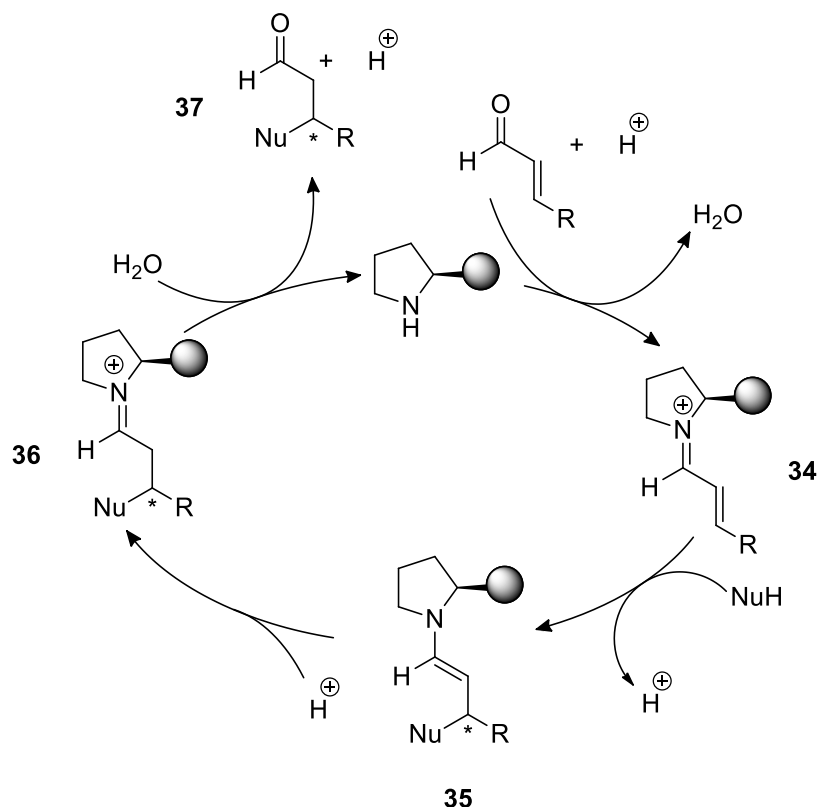
Figure 1.40. Iminium-ion catalytic cycle.

Extension of this methodology to vinylogous iminium ions affords new electrophilic sites on the iminium ion for nucleophilic attack, namely, the δ-position (Figure 1.41).
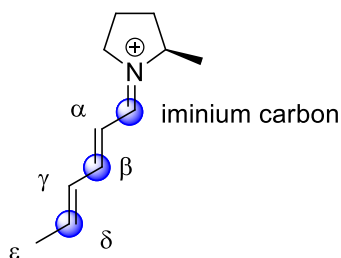
Figure 1.41. Electrophilic sites on a vinylogous iminium ion.

The presence of three electrophilic sites on the iminium ion complicates the regiochemical outcome of addition reactions as outlined in Figure 1.32. Careful tailoring of both the electrophilic and nucleophilic components of the reaction mixture can lead to regioselectivity for the δ-position, yielding 1,6-addition products. In recent years, there have been a number of excellent reports outlining the utility of this methodology with a number

of nucleophiles and electrophiles. Selected examples of these reactions will be highlighted below.

In 2012, Melchiorre *et al.* reported the enantioselective 1,6-conjugate addition of alkyl thiols to cyclic dienones utilizing vinylogous iminium ion activation (Figure 1.42).[64] In this instance, the authors used the primary amine cinchona alkaloid catalyst **38** to form the vinylogous iminium ion in the presence of acid co-catalyst **39**.
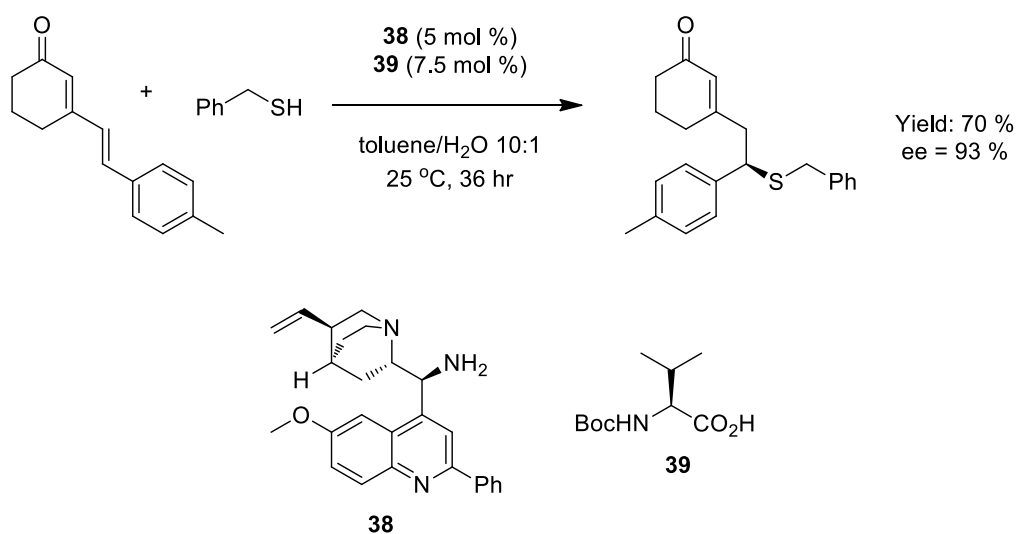
Figure 1.42. Addition of 1,6-conjugate addition of alkyl thiols to cyclic dienones reported by Melchiorre *et al.*[64]

A second report in 2013 by Jørgensen *et al*. highlighted the 1,6-conjugate addition of olefinic lactones with acyclic dienals (Figure 1.43).[65] In this instance the use of the charged nucleophilic dienolate, generated by deprotonation of the olefinic lactone, is thought to be responsible for the regioselectivity of the reaction. The authors postulate that the interaction of the charged iminium ion and the charged dienolate is responsible for the observed 1,6-selectivity of the reaction.
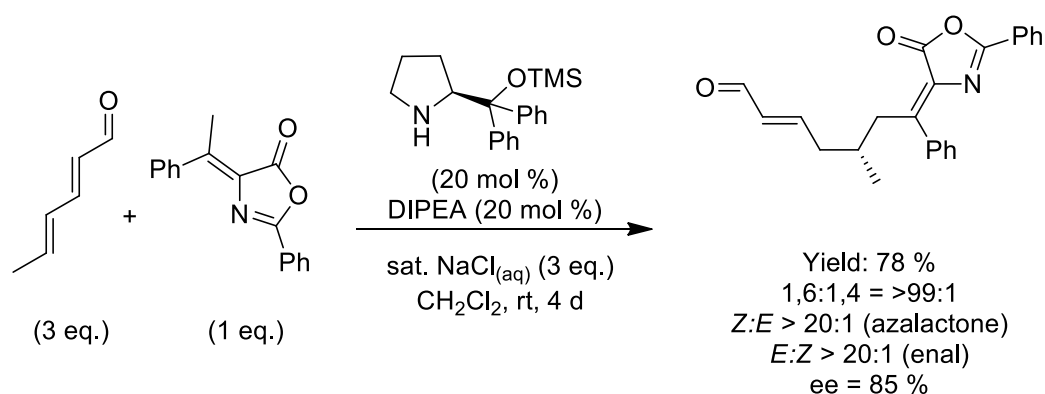
Figure 1.43. 1,6-conjugate addition of olefinic lactones and 2,4-dienals reported by Jørgensen *et al.*[65]

Iminium ion catalysis has proven itself a viable methodology for the stereoselective generation of 1,6-conjugate addition products through the activation of suitable electrophiles. These electrophiles are limited to carbonyl substrates, i.e. those amenable to condensation with secondary amine catalysts in order to form the LUMO lowered iminium ion species. Development of novel conjugated electron-deficient substrates which do not require iminium ion activation in order to achieve 1,6-conjugate additions is of some interest as it would expand on the structures accessible through conjugate addition chemistry. Also, the study of these electron-deficient substrates would also give insight into the propagation of electron-withdrawing capabilities of electron-withdrawing substituents through conjugated systems.

1.3   Conclusion

The field of organocatalysis lay dormant for nearly two centuries despite a number of promising insights into this powerful methodology being scattered throughout the literature. It was not until the year 2000 when a resurgence in interest, thanks to the work of Barbas and MacMillan and others, that organocatalysis was given the opportunity to flourish into a cornerstone of chemical synthesis.

Within 15 short years, asymmetric organocatalysis has firmly established its role as the third arm of asymmetric synthesis, along with organometallic and biocatalytic methods, with a number of large scale pharmaceutical examples. Another testament to the power of organocatalysis is its incorporation into natural products syntheses, such as strychnine[66], a true measure of the utility and applicability of any synthetic methodology.

The current trend of research within organocatalysis lies in a number of avenues: 1) with pushing the boundaries of the already discovered modes of activation to examine their flexibility with diverse substrates, 2) the development of novel substrates in order to open new reaction pathways applicable to known modes, 3) the combination of known modes of catalysis into multicatalytic systems, be it a number of organocatalytic modes or a combination of organocatalytic and organometallic modes, 4) the continual search for new modes of organocatalytic activation that will further broaden this already considerable field.

In conclusion, organocatalysis has shown itself to be an excellent challenger to the already well established field of asymmetric organometallic chemistry in terms of yields and stereoselectivities. Whilst organocatalysis cannot compare with organometallic catalysis in terms of catalyst loading (predominantly due to much higher turn-over numbers of metal-based catalysts), it can offer other significant advantages such as compatibility with air/water and relatively mild reaction conditions, all the while still obtaining high enantioselectivities. In this way, organocatalysis should be considered one of the staple tools that organic chemists draw on in their synthetic planning, and one which can be used in the synthesis of simple and complex compounds of interest.

1.4   Research aims

As already outlined in the preceding sections, a number of modes of organocatalysis have already been detailed in the literature and applied to recognised substrates for conjugate addition and other methodologies. The initial aim of this thesis was to develop novel substrates which could be applied in these modes, namely the synthesis of novel electron-deficient butadienes. Such substrates could be utilized in 1,6-addition chemistry and the extension of known catalytic modes of organocatalysis. During the course of this work into the development of synthetic pathways to these substrates, it became clear that intermediates in their synthesis were also of synthetic interest and presented an opportunity for discovery. Such opportunities lay, not just in their application to organocatalytic methodologies, but also in a number of other reaction types. This resulted in a number of additional aims: 1) the development of a modular route to the synthesis of butadiene scaffolds bearing electron-withdrawing functionalities, 2) the synthesis of functionalised biaryl species via a 1,6-addition-cyclisation-aromtization pathway, 3) the synthesis of 4-*H* aminopyrans exploiting conjugate addition chemistry, and 4) the synthesis of 3,4-dihydro-2*H*-pyrans via an inverse electron demand hetero Diels Alder cycloaddition methodology.

2   Chapter 2: Substrate synthesis

2.1 Introduction

This chapter details the discovery and application of a modular approach towards the synthesis of 1,3-disubstituted butadienes with aryl formyl acrylonitriles as key synthetic intermediates. The butadienes in question bear two electron-withdrawing substituents at the 1- and 3-positions. The families described in this chapter are: 1) the bis-cyano butadienes, substituted with nitrile groups at the 1- and 3-positions; 2) the cyano-ester butadienes, bearing an ester functionality at the 1-position and a nitrile at the 3-position; 3) the cyano-phenylsulfonyl butadienes, bearing a phenyl-sulfonyl group at the 1-position and a nitrile at the 3-position. All of the described 1,3-disubstituted butadienes are electron-poor olefinic systems and are of interest in the exploration of conjugate addition chemistry, in particular vinylic 1,6-conjugate additions. Initial experiments expanding the modular approach to trienic systems are also described, which have potential as substrates for the study of 1,8-conjugate addition reactions.

2.1.1 Vinylogous Michael-type acceptors

As already outlined in Chapter 1, the use of Michael-type acceptors in the stereoselective formation of C-C bonds is an extremely useful transformation in the synthesis of valuable chemical targets. Electron-deficient olefinic systems make ideal substrates for this type of transformation. A number of electron-withdrawing substituents have been successfully utilized in the polarization of mono-olefins through a combination of inductive and mesomeric effects. Such effects activate the β-carbon towards nucleophilic attack where examples of effective electron-withdrawing groups include the nitro group, the nitrile group, and the ester group (Figure 2.1).
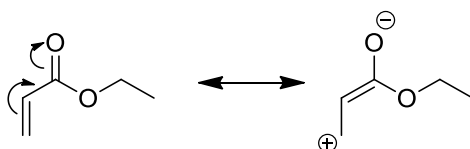
Figure 2.1. Ester substituted olefin polarization through a mesomeric effect.

Extension of these substrates into poly-olefinic systems allows for extended reactivity and investigation of additional electrophilic sites, namely that of the δ- and ζ-carbons in dienic

and trienic substrates respectively (Figure 2.2). The olefinic substrates shown in Figure 2.2 comprise a vinylogous series differing from one another by a vinylene residue (-CH=CH-) as described in 1934 by Fuson.[52]
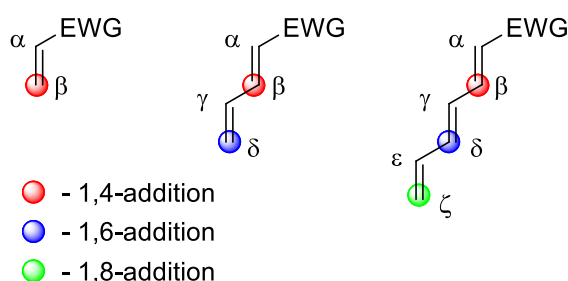
Figure 2.2. Michael-type acceptors

In literature reports utilizing 1-substituted butadienes and hexatrienes as vinylogous conjugate addition substrates, one can see a clear regioselectivity for 1,4-addition, over 1,6- or 1,8-additions. A lack of propagation of the polarization to vinylic positions on the conjugated backbone could be responsible for this observed selectivity towards 1,4-addition. In these cases, one could suggest that the β-carbon experiences the greatest polarization due to its close proximity to the electron-withdrawing substituent. One such report by Alexakis *et al*., which details the addition of aldehydic enamines to nitrodienes, noted the exclusive formation of the 1,4-addition product **40** (Figure 2.3).[67]
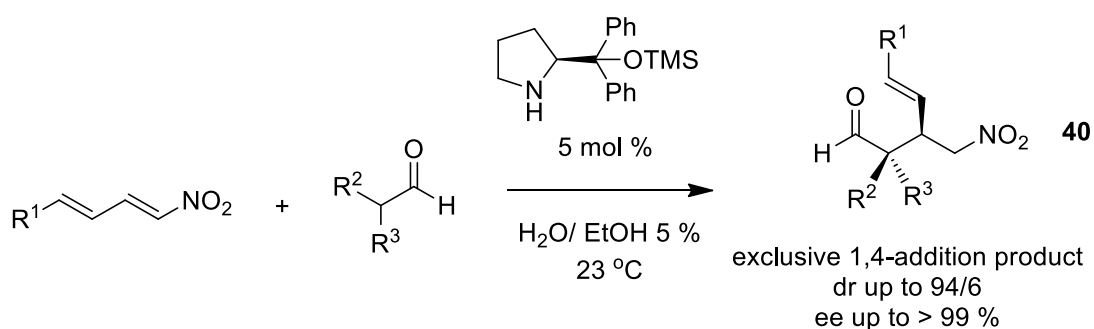
Figure 2.3. The 1,4-conjugate addition of aldehydic enamines to nitro-dienes reported by Alexakis *et al*.[67]

2.1.2   Literature reports of vinylogous Michael-type acceptors

In order to increase reactivity at the δ-position, and therefore increase the likelihood of selectivity for a 1,6-conjugate addition, a number of research groups have developed substrates and catalytic systems that favour such vinylogous additions. A selection of these substrates are shown in Figure 2.4.
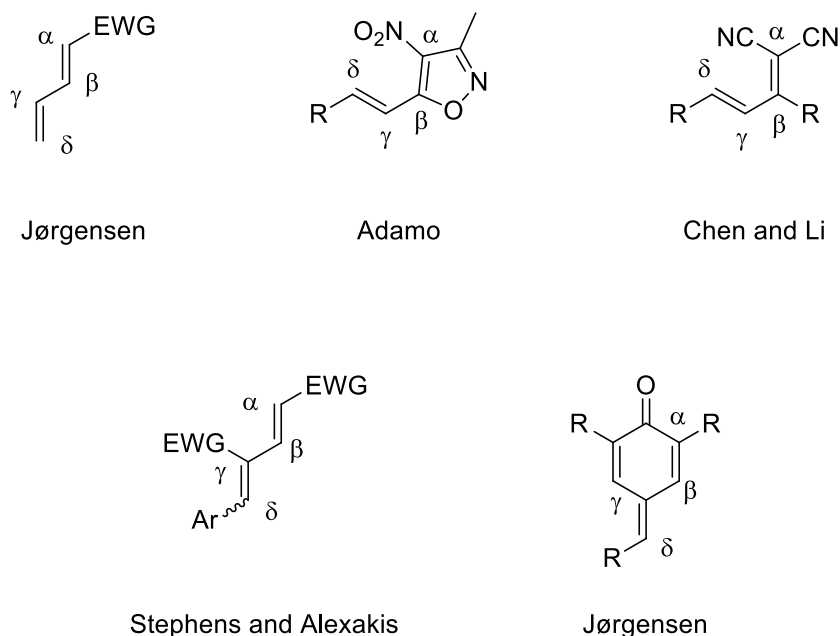
Figure 2.4. A selection of substrates used in organocatalytic vinylogous ACA reactions by the groups of Jørgensen[57], Adamo[68], Stephens and Alexakis,[58,59] Chen and Li.[62]

As described in Section 1.2.7, Jørgensen *et al.* reported an organocatalytic 1,6-conjugate addition of β-ketoesters and glycine imines, under PTC conditions, to electron deficient δ-unsubstituted dienes Figure 1.33.[57] To the best of our knowledge this is the single example of 1-substituted dienes reacting preferentially at the δ-position under organocatalytic conditions.

A method that has seen some success in favouring 1,6-addition is that of sterically hindering the β-position, thereby disfavouring reactivity at this position. This can be seen in the substrates utilized by the groups of Adamo (the β-position is a quaternary carbon and part of an isoxazole ring) and Chen and Li (the β-position is sterically hindered by an aryl or alkyl group) (Figure 2.4).[62,68] In both cases high yielding and selective 1,6-additions were reported.

Previous attempts by our group to utilize sterically hindered nitro substituted butadienes did not yield any 1,6-addition products and further efforts to develop these substrates were not explored (Figure 2.5).[69]
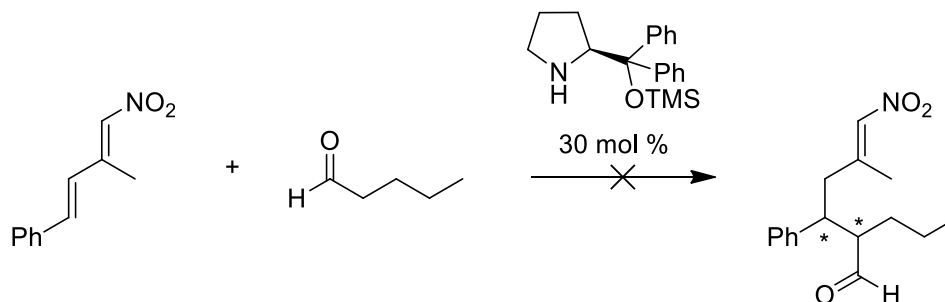
Figure 2.5. Attempted 1,6-conjugate addition to sterically hindered nitro-diene.[69]

Our group, in collaboration with the Alexakis group, have found success through the use of an electronic approach that controls the regioselectivity of the addition reaction. This approach utilized the application of a bis-activation strategy, through the use of 1,3-disubstituted electron deficient dienes, with the possibility of enhanced polarization of the terminal olefin. This allows for increased reactivity at the δ-position, over the β-position, and thereby increasing the likelihood of a successful 1,6-addition (Figure 2.6).
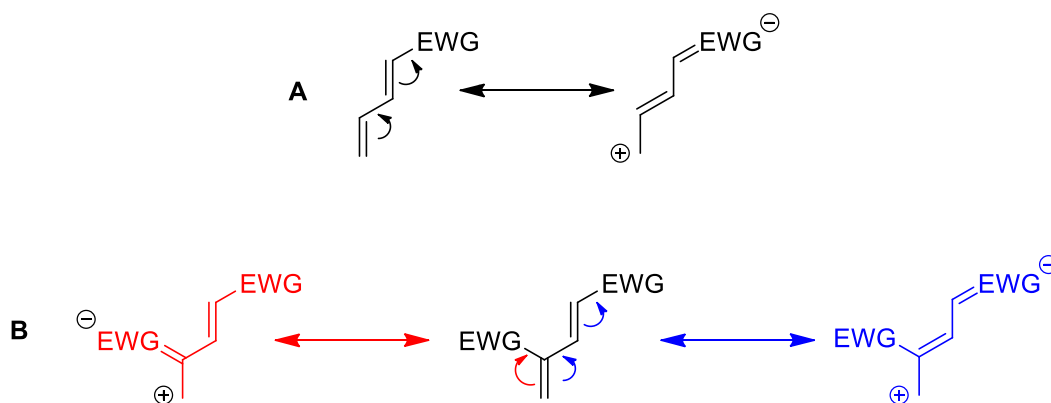
Figure 2.6. Mono- (**A**) vs bis-(**B**) activation of dienic systems.

More recently, Jørgensen *et al.* have also found success using electronic means to control the regiochemical outcome of vinylogous conjugate addition reactions. Their use of *p*-quinone methides resulted in selective 1,6-conjugate additions.[60] As discussed in Section 1.2.8 *p*-quinone methides possess a resonance contributor in which the cyclohexadiene can fully aromatize and induce a formally positive charge on the δ-carbon, activating it towards addition at this position.

2.1.3   1,3-Disubstituted butadienes in the literature

There are a limited number of reports describing butadienes substituted with electron-withdrawing groups at both the 1- and 3-positions. The application of such substrates in further synthetic transformations is even less reported.

Ahn *et al*. have described the synthesis, via flash vacuum pyrolysis (f.v.p), of terminally unsubstituted 1,3-disubstituted butadienes bearing either a nitrile or ester functionality at the 1- and 3-positions (Figure 2.7).[70] Interestingly, the authors note the instability of terminally unsubstituted 1,3-disubstituted butadienes and state that they are prone to polymerization. Flash vacuum pyrolysis utilizes high vacuum conditions to vaporize materials, allowing them to be exposed to high temperatures in the gas phase for controlled time periods. This technique can allow for the formation of products that are thermally unstable at high temperatures, as the residence time in the furnace can be controlled to limit degradation of such products.[71]
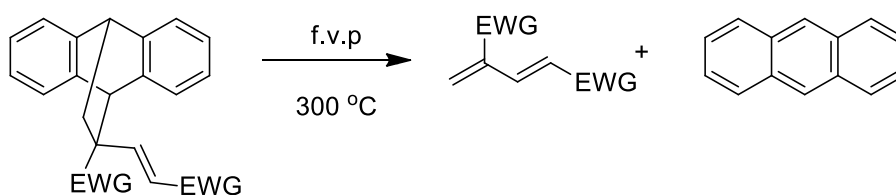
Figure 2.7. Pyrolysis of anthracene adducts to yield bis-substituted butadienes.[70] EWG = CN or CO_2Me.

The authors did not explore the further reactivity of these substrates in subsequent transformations. They did, however, suggest that the polymers formed from the 1,3-disubstituted dienes tended to consist of 1,4-linkages (Figure 2.8).[70]

a) X = Y = CN; b) X = CN, Y = CO_2Me; c) X = Y = CO_2Me
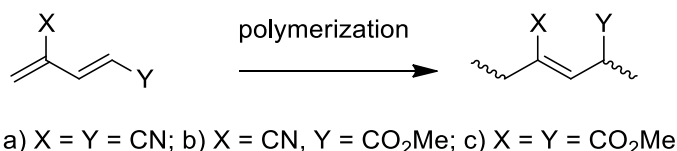
Figure 2.8. Polymerization of 1,3-disubstituted butadienes through 1,4-linkages.[70]

In 1998, Banciu *et al*. reported their findings on the f.v.p of 1,3-bis-cyano butadiene **41**. Banciu *et al.* applied f.v.p conditions to the bis-cyano diene generating electrocyclized products in moderate yields (Figure 2.9).[72] In addition to the electrocyclization product **42**,

small amounts of product **43**, resulting from two [1,5]-H shifts and elimination products **44** and **45**, were also detected. The use of vacuum in f.v.p is again of importance to the success of this methodology as it limits secondary reactions of the bis-cyano butadienes. Such secondary reactions can lead to decomposition/polymerization under regular heating, even at low temperatures. Under f.v.p conditions the pyrolysis still led to a number of products which required multiple purification procedures to yield only milligram quantities. This example highlights some of the challenges associated with the synthesis and purification of conjugated nitrile species.
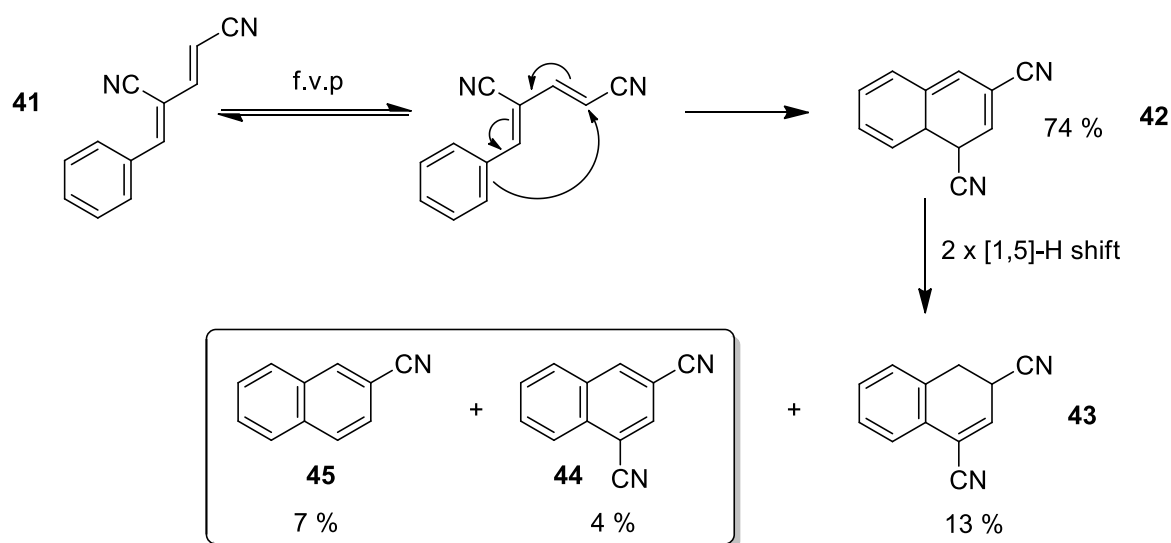
Figure 2.9. The products from the electrocyclization reactions of bis-cyano butadiene **X** under f.v.p conditions.[72]

In 1985, Masuyama *et al.* explored the use of bis-phenylsulfonyl butadienes **46** in reactions with morpholine derived enamines to yield racemic cyclic hexadienes **47** (Figure 2.10).[73] In addition to the hexadiene products **47**, the oxidised aryl products **48**, after treatment with 1,8-diazabicyclo[5.4.0]undec-7-ene (DBU), were also obtained.
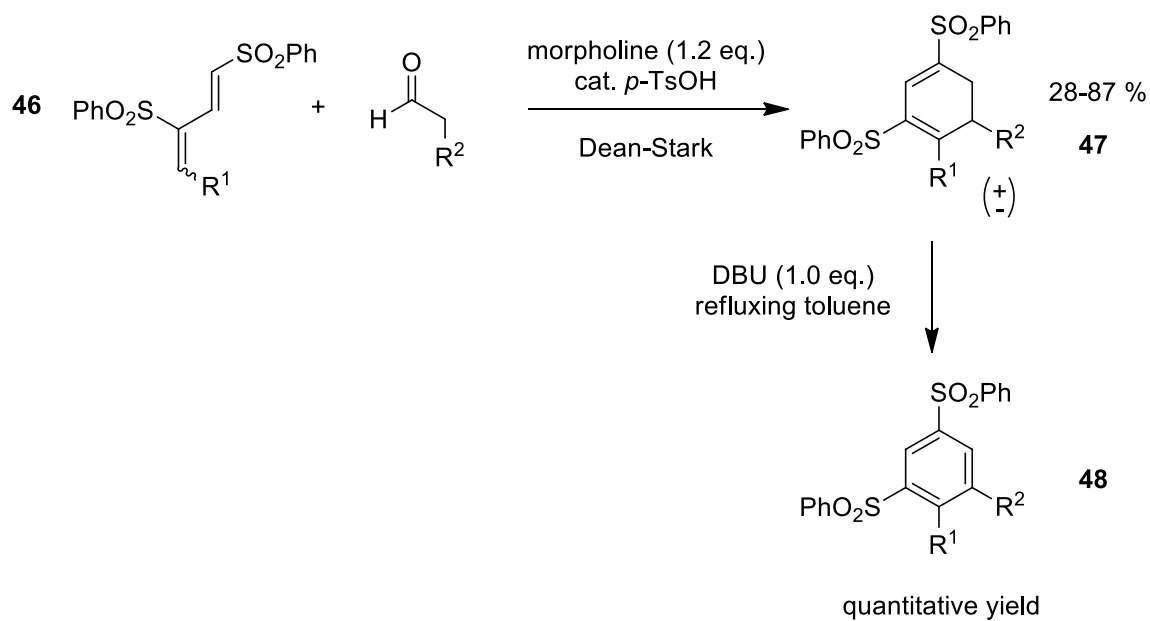
Figure 2.10. Synthesis of racemic cyclic hexadienes and aryl sulfones as described by Masuyama *et al.*[73]

In 1991, Padwa *et al.* utilized a member of the same family of bis-phenylsulfonyl butadienes **49** and the newly described cyano-sulfonyl butadiene **51** in a [4+2] Inverse Electron Demand Hetero-Diels-Alder (IEDHDA) cycloaddition with aryl imines. A subsequent [1,3-H] shift yielded the tetrahydropyridines **50** and **52** (Figure 2.11).[74]
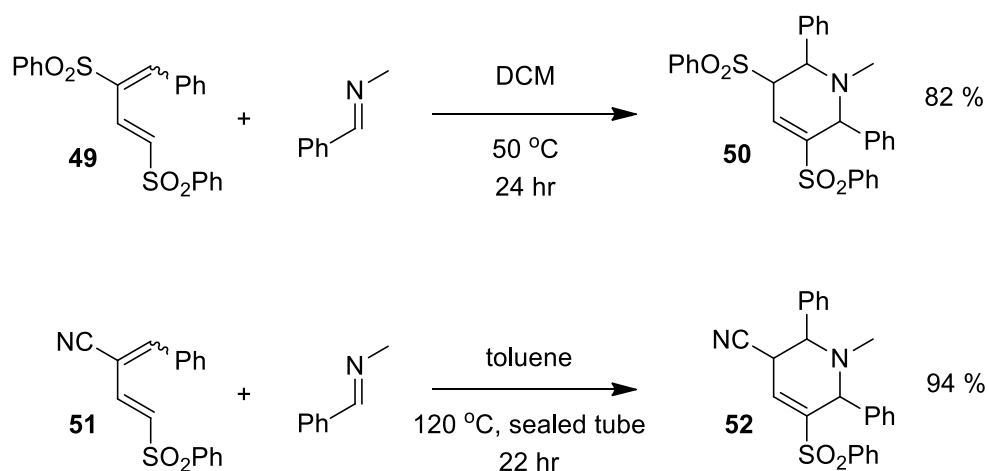
Figure 2.11. Cycloaddition of 1,3-disubstituted butadienes described by Padwa *et al.*[74]

Despite a few reports describing their synthesis, the lack of reports detailing the use of 1,3-disubstituted butadienes as Michael-type acceptors, especially in an asymmetric fashion, led to our interest in the study of this intriguing class of substrates.

2.1.4   Bis-phenylsulfonyl butadienes and bis-ester butadienes

Previous reports from our group have described the synthesis of two distinct families of 1,3-disubstituted butadienes, the bis-phenylsulfonyl and the bis-ester butadienes.[58,59] Both of these families have been utilized by our group as Michael-type acceptors in an asymmetric organocatalytic annulation (1,6-conjugate addition followed by cyclization) reaction to give cyclic hexadienes in high yields and in high enantiopurity (Figure 2.12).
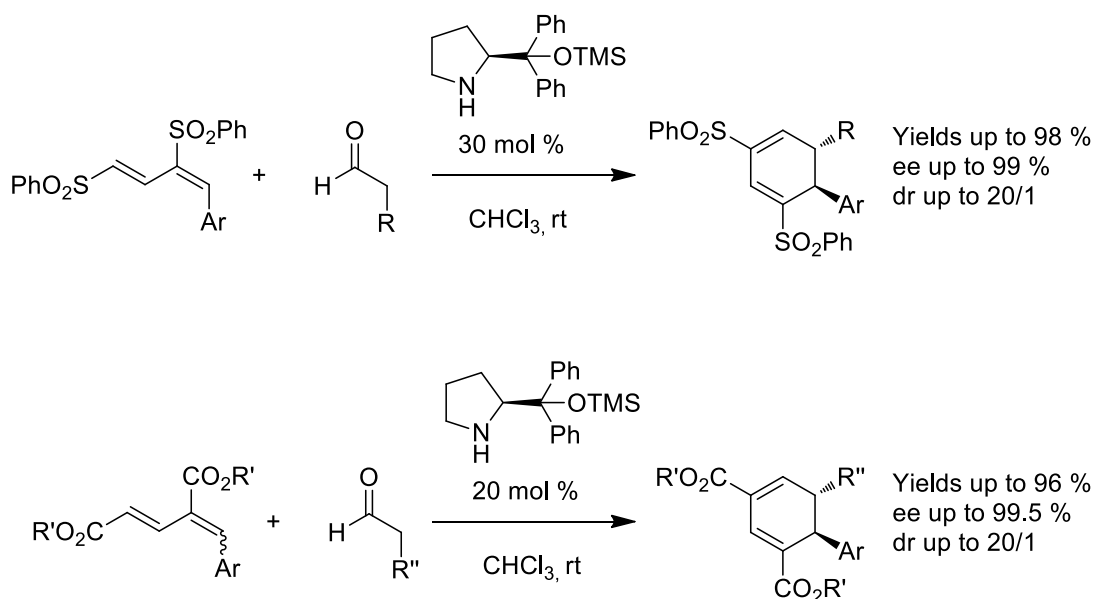
Figure 2.12. Asymmetric organocatalytic [4+2] cycloannulation reaction of 1,3-bis-substituted butadienes.[58,59] R=R''=alkyl.

Access to the bis-phenylsulfonyl and bis-ester butadienes was achieved utilizing similar synthetic routes. Both routes culminate in the condensation of a bis-substituted propene **53** with an aryl aldehyde (Figure 2.13).[58,59]
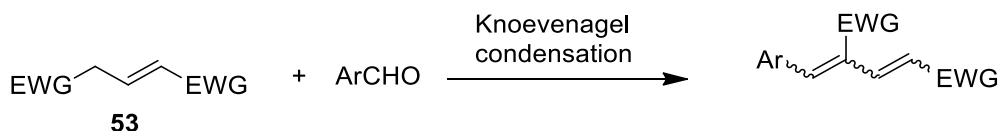
Figure 2.13. Knoevenagel condensation of bis-activated propenes and aryl aldehydes.[58,59]

The bis-phenylsulfonyl propene was synthesized through the bromination of allyl phenyl sulfone and then elimination of HBr to yield the bromo-phenylsulfonyl propene **54**. This

propene was then reacted with sodium salt of benzenesulfinic acid to yield the bis-phenylsulfonyl propene **55** (Figure 2.14).
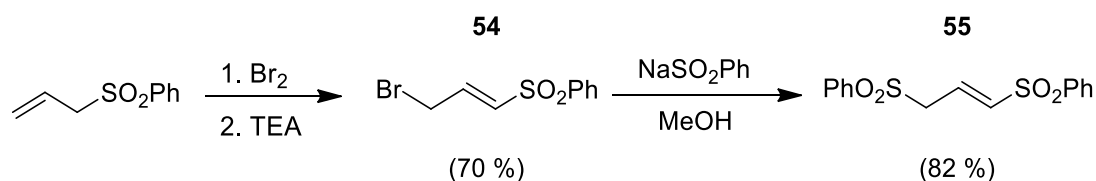
Figure 2.14. Synthesis of bis-phenylsulfonyl propene X reported by Murphy *et al.*[58,69]

As diethyl and dimethyl glutaconate, the bis-ester propene equivalents of **55**, are commercially available this step of the synthesis could be by-passed for the bis-ester butadienes.

All three propenes were then subjected to condensation with aryl aldehydes and under traditional Knoevenagel condensation conditions the butadienes were successfully generated (Figure 2.15).
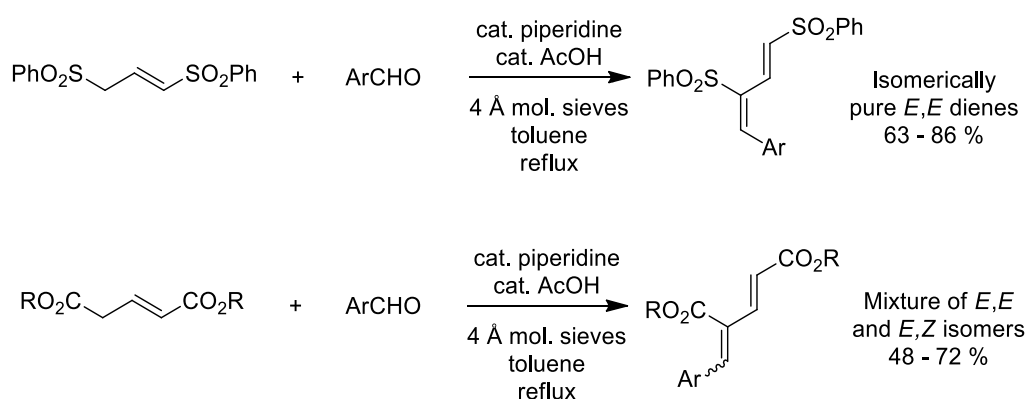
Figure 2.15. Synthesis of 1,3-bis-substituted butadienes.[58,59]

A noteworthy distinction between the two families of butadienes lies in the isomeric ratios of the final isolated dienes. In the case of the bis-phenylsulfonyl butadienes, the dienes were isolated isomerically pure in the *E,E* geometry. This geometry was confirmed by X-ray crystal structure analysis (Figure 2.16).[69]
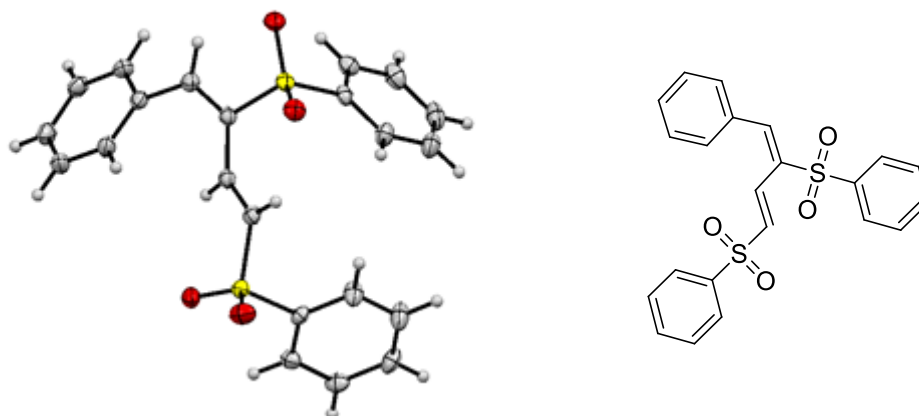
Figure 2.16. X-Ray crystal structure of ((1E,3E)-4-phenylbuta-1,3-diene-1,3-diyldisulfonyl)dibenzene.[69]

The bis-ester butadienes, on the other hand, were isolated as a mixture of *E*,*E* and *E*,*Z* isomers. This isomeric ratio can be calculated by integration of the ^{1}H NMR signals observed for the olefinic protons. For the alpha olefin, these signals appear as two distinct doublets with large J_{trans} coupling constants of 16 Hz each, which is consistent with the assignment of *E* geometry. Two of the possible four diene isomers, the *E*,*E* and the *E*,*Z*, were clearly visible in the ^{1}H NMR spectrum. Neither the *Z*,*E* nor *Z*,*Z* isomer of the butadienes were observed. This is presumably due to the increased stability of *E* olefins over *Z*.

The bis-ester butadienes were applied to the asymmetric organocatalytic annulation reaction as a mixture of isomers. The reaction appears to be a stereoconvergent process with only a single diastereoisomer of the cyclic diene product isolated in each case.

In order to further investigate the reactivity of this intriguing family of di-substituted electrophilic substrates, it is important to expand the family to include different electron-withdrawing substituents and assess their ability to undergo annulation reactions and other related transformations.

2.1.5   Nitriles as electron-withdrawing substituents

Unsaturated nitriles have been described as a recalcitrant class of Michael acceptors.[75] This is in part due to the marked differences in reactivity in comparison to the more typically utilized carbonyl-containing electron withdrawing groups, namely aldehydes, ketones and esters. Conjugate addition of carbon nucleophiles to unsaturated nitriles are complicated by

the apparent inactivity of typical carbon nucleophiles, e.g. Gilman reagents, to react in a conjugate fashion.[75,76] The use of more reactive nucleophiles such as Grignard reagents can lead to 1,2-addition products. Acrylonitrile is an exception to this and displays similar reactivity to other activated ethylenes, such as ethyl acrylate, in conjugate addition chemistry.[75]

Despite these complications, nitriles offer a number of benefits to synthetic chemists and can give access to a number of otherwise difficult to obtain chemical scaffolds. Nitrile groups represent versatile functional groups for further modification and their incorporation into target structures can offer a handle for transformation into a wide number of other functional groups such as aldehydes, amines, and carboxylic acids (Figure 2.17).[77] Therefore, taming the reactivity of unsaturated nitrile systems is of synthetic interest.
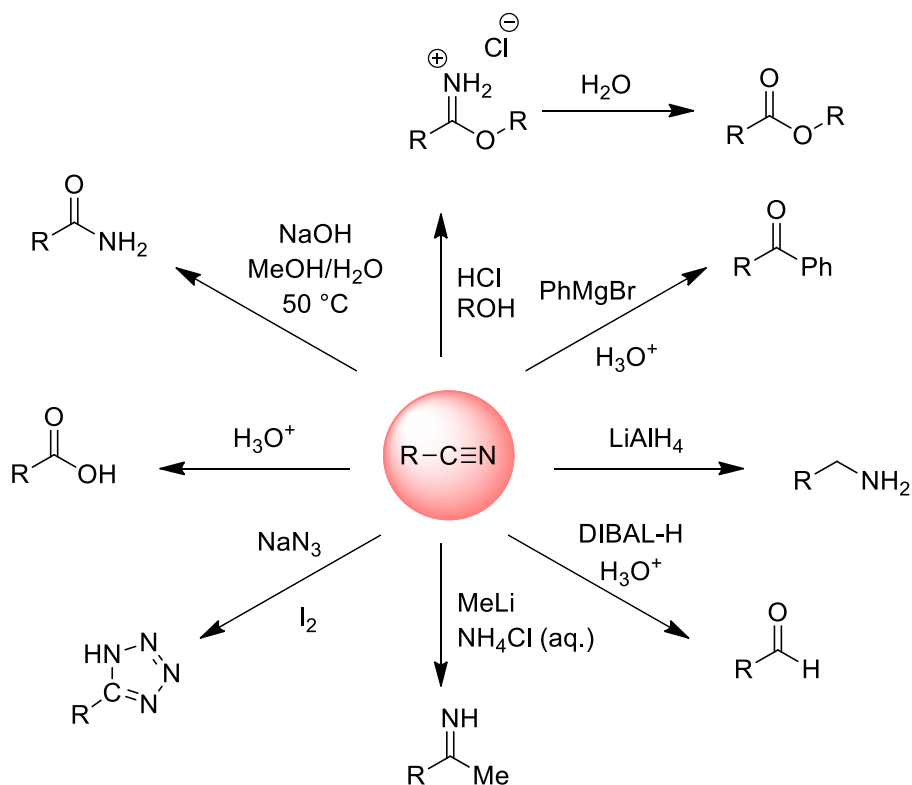
Figure 2.17. Transformations of nitriles into a number of other functional groups.

2.1.6   Target dienes

The families of dienes initially targeted in this project included the bis-cyano diene and the cyano-sulfonyl diene (Figure 2.18). Whilst there is a literature preparation for the synthesis of the bis-cyano diene available it was considered advantageous to improve on the low reported yield of 31 %.[72] Also of interest were other novel mixed diene families, such as the cyano-ester diene (Figure 2.18). All of these butadiene subtrates are of interest in the study of conjugate addition chemistry.
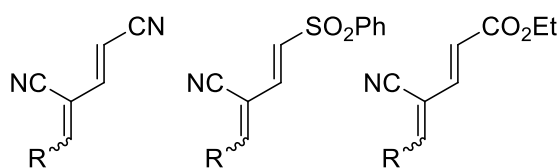
Figure 2.18. Target diene families. R = aryl.

2.2   Results and discussion

2.2.1   Bis-cyano butadienes

The first family of 1,3-disubstituted butadienes we attempted to access was that of the bis-cyano butadienes. Two retrosynthetic analyses are outlined in Figure 2.19. Disconnection **A** results from the disconnection at the terminal olefin, which could be reinstalled through a Knoevenagel-type condensation of the bis-cyano propene **56** and an aryl aldehyde. Disconnection **B** results from a disconnection at the α-olefin, which could be reinstalled via a number of olefination reactions such as a Wittig or Horner-Wittig reaction on the aryl formyl acrylonitrile **57**.
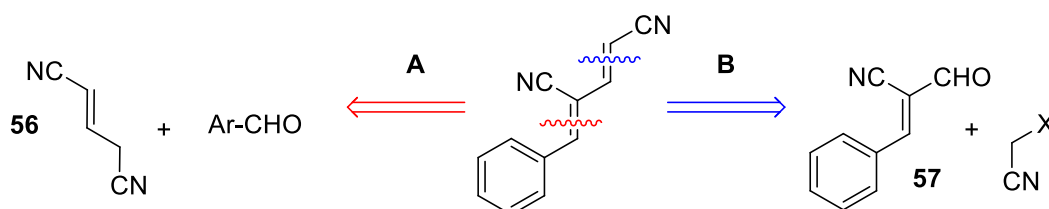
Figure 2.19. Retrosynthetic analyses of bis-cyano butadiene **X**. X = PPh$_3$ or P(OEt)$_3$. **A** = Knoevenagel-type disconnection, **B** = Wittig/Horner-Wittig disconnection.

2.2.2   Previous attempts within the group to access bis-cyano butadienes, a first generation synthetic strategy

Previous members of the group had found success utilizing the Knoevenagel-type condensation route (Figure 2.19, pathway **A**) to access the bis-phenylsulfonyl and bis-ester butadienes.[58,59] Hence, preliminary efforts by previous members of the group to access the bis-cyano butadienes employed the same strategy.[69] The corresponding retrosynthetic pathway to access the bis-cyano butadienes via a bis-cyano propene **56** is shown in Figure 2.20.
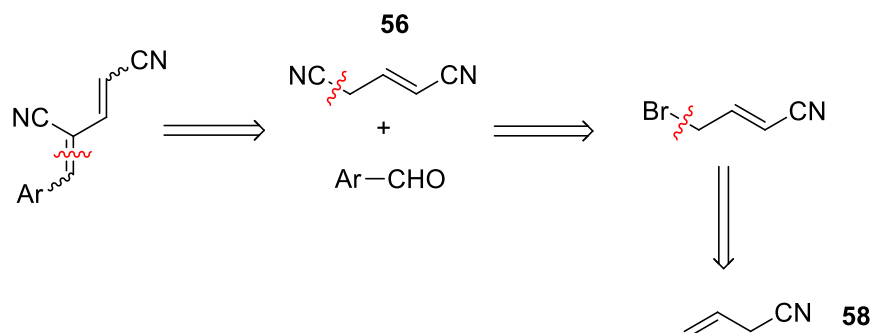
Figure 2.20. Retrosynthetic analysis of bis-cyano butadiene **X**.

This first generation pathway is analogous to the synthetic routes used to access both the bis-phenylsulfonyl and bis-ester butadienes, as reported by our group.[58,59]

This route starts with bromination of commercially available allyl cyanide **58**, followed by elimination to yield the mono-brominated propene **59**, which after S_N2 substitution with a cyanide anion source affords the bis-cyano propene **56** (Figure 2.21). The bis-cyano propene **56** could then undergo simple Knoevenagel-type condensation with a variety of commercially available aryl aldehydes to yield a diverse family of bis-cyano butadienes.
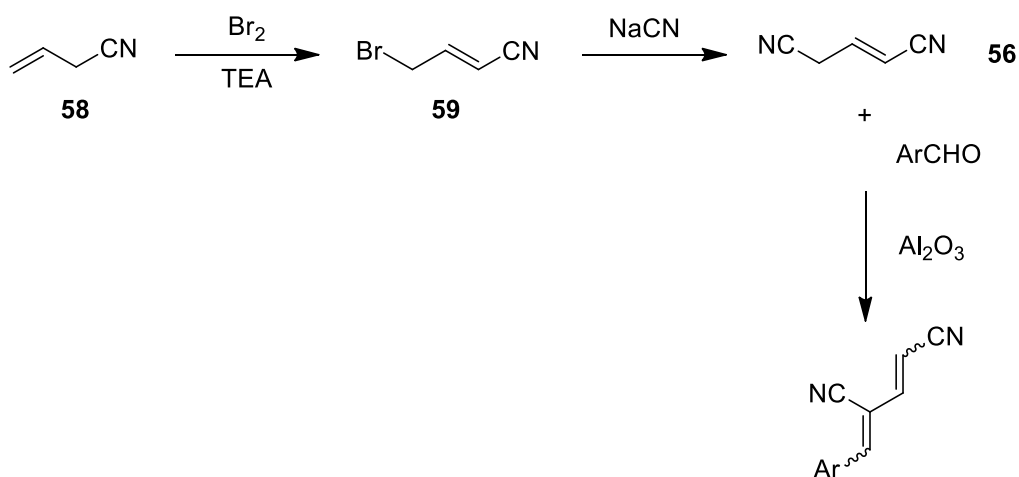
Figure 2.21. Forward synthetic route to bis-cyano butadienes.

Although there is literature precedent using this exact synthetic route to access the bis-cyano butadienes, previous group members encountered significant difficulties while attempting to access the bis-cyano butadiene **41**.[69,72] Firstly, the S_N2 substitution of the bromide invokes the use of metal cyanide salts, which are extremely toxic. Secondly, this substitution was found to be exothermic, raising concerns of temperature control during the reaction. Thirdly,

the bis-cyano propene was found to be thermally unstable and handling at temperatures even modestly above 4 ˚C led to decomposition/polymerization and intractable black residues.

Despite these significant synthetic difficulties the bis-cyano propene was synthesized by a previous group member, albeit in small quantities.[69] The bis-cyano propene was then applied in a Knoevenagel condensation promoted by basic aluminium oxide, which also acts as a desiccant driving the equilibrium towards the product, to yield the bis-cyano butadiene **41** in a low yield of 13 % (Figure 2.22).[69]
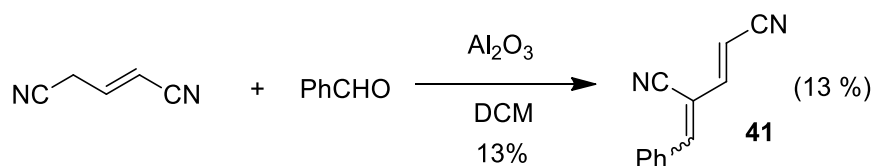
Figure 2.22. Synthesis of phenyl substituted bis-cyano diene **41**.[69]

An alternative route to the bis-cyano butadienes was desired in order to avoid the use of the extremely toxic metal cyanide salts. Furthermore, this first generation synthetic route was not amenable to the production of synthetically useful quantities of the bis-cyano diene **41**.

A number of other routes have been explored by our group, as outlined in Figure 2.23, however difficulties were encountered with each. Route **A** illustrates a Ramberg-Bäcklund synthesis of bis-cyano propene **56**, access to the α-chloro sulfone was the limitation of this pathway. Route **B** illustrates the elimination of either a bromide or mesylate group to form the olefin. Elimination of either leaving group did yield the bis-cyano propene, however once again only in small amounts. Route **C** illustrates an acid catalyzed triple dehydration of the bis-amide alcohol. This route led to the small quantities of the bis-cyano propene but not at synthetically useful scales.
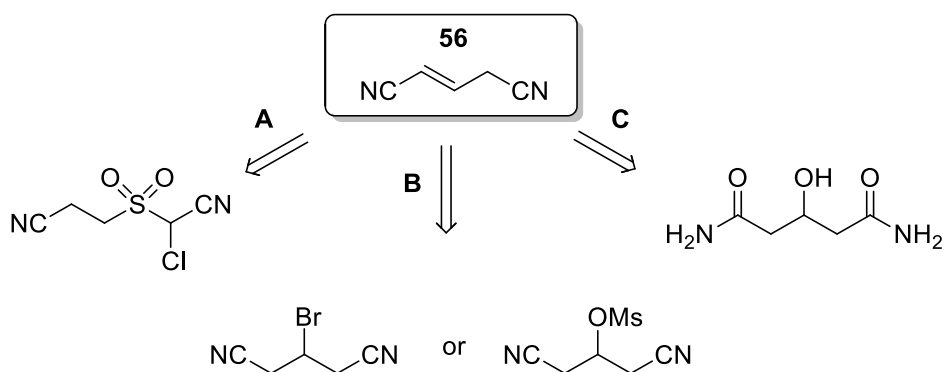
Figure 2.23. A number of routes explored in the synthesis of bis-cyano propene **56**.[69]

2.2.3   Alternative retrosynthetic pathway

The bis-cyano butadienes are clearly challenging synthetic targets and access to them through the use of the bis-cyano propene **56** synthetic intermediate proved unsuccessful. This project takes up from the previous efforts towards the synthesis of the bis-cyano butadiene family. Subsequent efforts saw a return to the retrosynthetic pathways outlined in Figure 2.19. In order to circumvent disconnections leading to the bis-cyano propene **56** we next attempted to access the butadiene backbone through the disconnection of the alpha olefin (Figure 2.19, pathway B).

2.2.3.1   Second generation synthetic strategy – Wittig approach

The second generation retrosynthetic analysis is outlined in Figure 2.24 and this series of disconnections led to readily accessible starting materials. It also avoided any of the other potential drawbacks of the first generation approach, e.g. the use of toxic cyanide salts and the unstable bis-cyano propene intermediate.
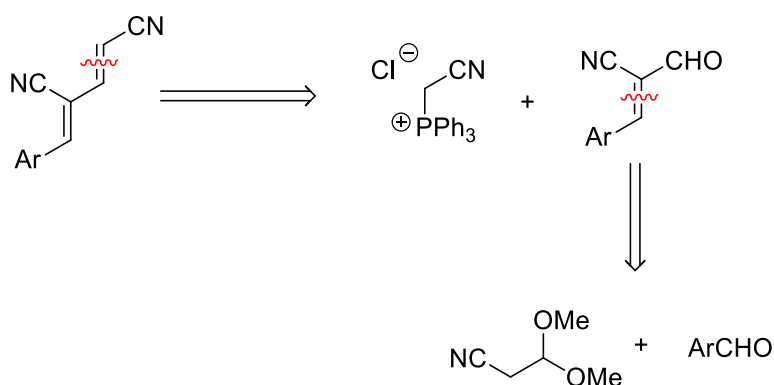
Figure 2.24. Second generation retrosynthetic analysis of bis-cyano butadiene**s**.

This forward synthetic route begins with the Knoevenagel condensation of the commercially available aryl aldehydes with 3,3-dimethoxypropionitrile and a subsequent acetal hydrolysis to give the formyl acrylonitrile. Formyl acrylonitriles of this type have been described in the literature since as early as 1956, with a report by Wasserman *et al*. suggesting that the olefin is in the *Z* geometry. The authors assign the geometry as *Z* by analogy, based on the UV absorptions of related cinnamonitriles.[78] The preferred literature preparation of the phenyl formyl acrylonitrile **57** was first carried out by Elliot *et al*. and the authors have assigned the

resulting geometry as *E* (Figure 2.25).[79] Pleasingly, this synthesis was facile in our hands and yielded the formyl acrylonitrile **57** in 71 % yield. NOE studies suggest that the geometry is indeed *E*, as a NOEDiff experiment showed an apparent enhancement of 8 % of the olefinic ^{1}H signal upon selective irradiation of the aldehydic proton.
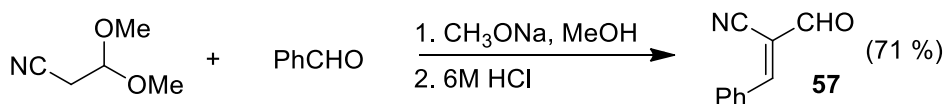
Figure 2.25. Synthesis of formyl acrylonitrile **57**.

With the formyl acrylonitrile in hand, the final olefination reaction was attempted with phosphonium salt **60**, under normal Wittig conditions (Figure 2.26).
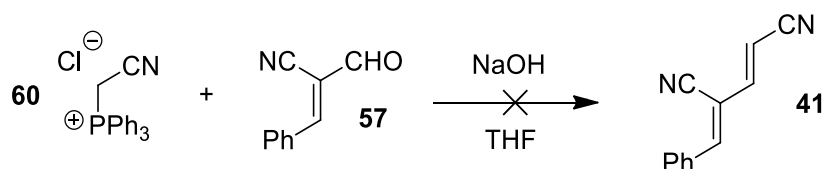
Figure 2.26. Attempted Wittig olefination reaction.

Initial monitoring of the reaction progress by TLC was promising as consumption of the starting formyl acrylonitrile was observed. After a short time, the reaction mixture changed from a clear pale yellow colour to deep red in colour. Disappointingly however, subsequent neutralization and extraction of the reaction mixture yielded a deep red intractable oil, which defied spectroscopic characterization. This result hinted at some instability present in either the formyl acrylonitrile or the bis-cyano butadiene, or potentially both components, under the reaction conditions.

Another possible side reaction, leading to consumption of the starting materials, could be conjugate addition of the ylide to the olefin. Whilst uncommon, there is literature precedent for the conjugate addition of phosphorus ylides to suitably activated olefinic nitriles.[80] The reaction was also cooled to -78 °C in order to promote the kinetic addition of the ylide to the carbonyl carbon, this approach however also resulted in uncharacterizable red oils.

Access to the bis-cyano butadiene did not appear to be forthcoming through the use of this Wittig methodology. However, a number of other olefination reactions could be attempted using the formyl acrylonitrile.

2.2.3.2   Third generation synthetic strategy – Wittig-Horner approach.

The third generation retrosynthetic analysis only differs in the choice of olefination reaction used to install the alpha olefin of the butadiene (Figure 2.27).
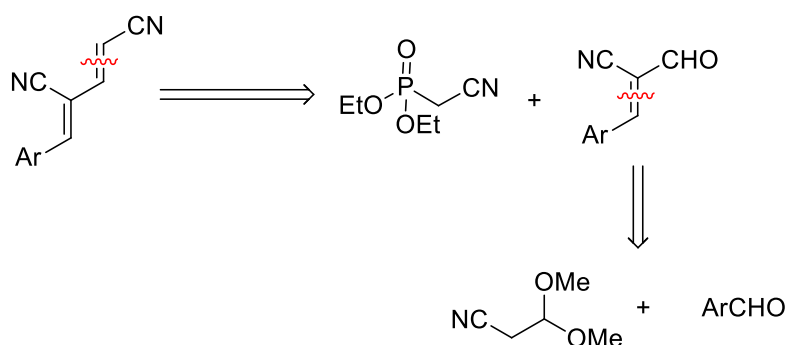
Figure 2.27. Third generation retrosynthetic analysis of bis-cyano butadienes.

In this instance, we chose to employ the Wittig-Horner/Horner-Wadsworth-Emmons reaction to install the alpha olefin (Figure 2.28). We chose this reaction for a number of reasons, firstly, the Wittig-Horner reaction is known to have high *E*-selectivity, easing any potential separation of the stereoisomers formed. Secondly, the use of cryogenic temperatures in the generation of the phosphonate anion would generate conditions favouring the kinetic direct addition of the anion to the electrophilic carbonyl carbon. Additionally, the reaction also has a number of synthetic advantages over the traditional Wittig reaction in that the diethyl (cyanomethyl)phosphonate is commercially available and the resulting lithiated phosphate by-product is readily soluble in water. This would simplify purification of the reaction mixture, something that can be hampered by the presence of the triphenylphosphine oxide by-product generated in the Wittig reaction.
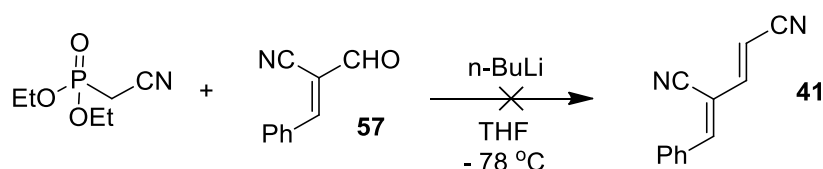
Figure 2.28. Wittig-Horner synthesis of bis-cyano diene **41**.

The formyl acrylonitrile **57** was applied in the Wittig-Horner reaction with (cyanomethyl)phosphonate under typical reaction conditions and screened for equivalents, temperature and solvent. Trace amounts of the product could be observed in the crude reaction mixtures but isolation of the butadiene from the reaction mixture proved extremely difficult, often leading to intractable oils. Even after extensive reaction condition refinement, the yield could not be reliably improved upon and the reactions led to only trace amounts of the product being observed (Table 2.1).

Table 2.1 – Wittig-Horner reaction refinement.

Entry	Aldehyde	Phosphonate	n-BuLi	Solvent	Temp	Time (hrs)	Yield
1	1 eq	1.1 eq	1.1 eq	DME	-50 ˚C	2.5	Intractable oil
2	1 eq	2.2 eq	2.2 eq	DME	-50 ˚C	2.5	Intractable oil
3	1 eq	3.3 eq	3.3 eq	DME	-50 ˚C	2.5	Intractable oil
4*	1 eq	1.4 eq	1.4 eq	DME	-50 ˚C	2	Trace
5	1 eq	1.1 eq	1.1 eq	THF	-78 ˚C	16	Intractable oil
6	1 eq	2.2 eq	2.2 eq	THF	-78 ˚C	16	Trace
7	1 eq	3.3 eq	3.3 eq	THF	-78 ˚C	16	Intractable oil

* TMEDA used as an additive

In an effort to synthesize a more stable bis-cyano butadiene under the reaction conditions, the Horner-Wittig procedure was carried out on the *p*-OMe formyl acrylonitrile **61** (synthesis of which is discussed in Section 2.2.4). We postulated that the mesomeric donation of the

ary ether into the conjugated system would result in a less electrophilic diene and therefore a diene that is less susceptible to degradation under the reaction conditions. Some success was encountered utilizing the *p*-OMe formyl acrylonitrile. The *p*-OMe bis-cyano butadiene **62** could be obtained in a low 10 % yield employing typical Horner-Wittig conditions of n-BuLi in THF (Figure 2.29). Masamune and Roush developed reaction conditions suitable for use with base-sensitive substrates through the use of LiCl as an additive and DBU as the base.[81] The LiCl additive acts in a Lewis-acid fashion to lower the pKa of the α-protons of the phosphonate through the formation of a complex.[81] The increased acidity of the α-protons also allows for milder amine bases to be substituted for the harsher alkyl lithium bases, which could cause degradation of base-sensitive compounds. Pleasingly, when these conditions were applied to the *p*-OMe formyl acrylonitrile **61**, the bis-cyano butadiene **62** was obtained in a 24 % yield (Figure 2.29).
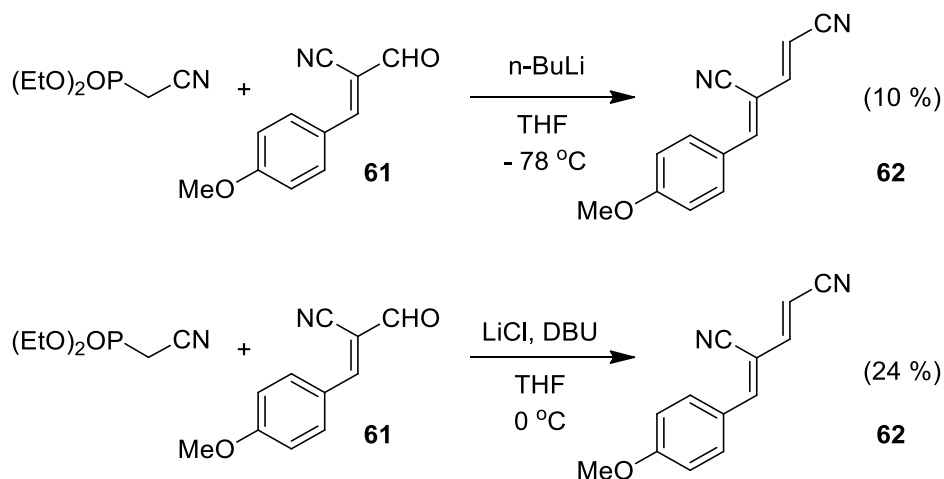
Figure 2.29. Access to the *p*-OMe bis-cyano butadiene **62** through the Horner-Wittig reaction.

A number of observations were made through the extensive screening of reaction parameters. Prolonged reaction times led to the formation of red uncharacterizable oils, as did an increase in the reaction temperature. For the reactions shown in Figure 2.29, the starting formyl acrylonitrile was completely consumed and directly observed to have been transformed into the butadienic product in sub-quantitative yields. This observation, coupled with the observed relative stability of the formyl acrylonitrile, hinted that the instability perhaps lay with the butadiene product under the reaction conditions rather than that of the starting formyl acrylonitrile.

With this success we continued to pursue the HWE methodology further and attempted to access a more stable diene intermediate, which could then be transformed into the bis-cyano

diene product. This led to the synthetic route in Figure 2.30, which begins with an initial HWE reaction to yield the cyano-amide diene **63** followed by the dehydration of the amide to yield the bis-cyano butadiene **41**.
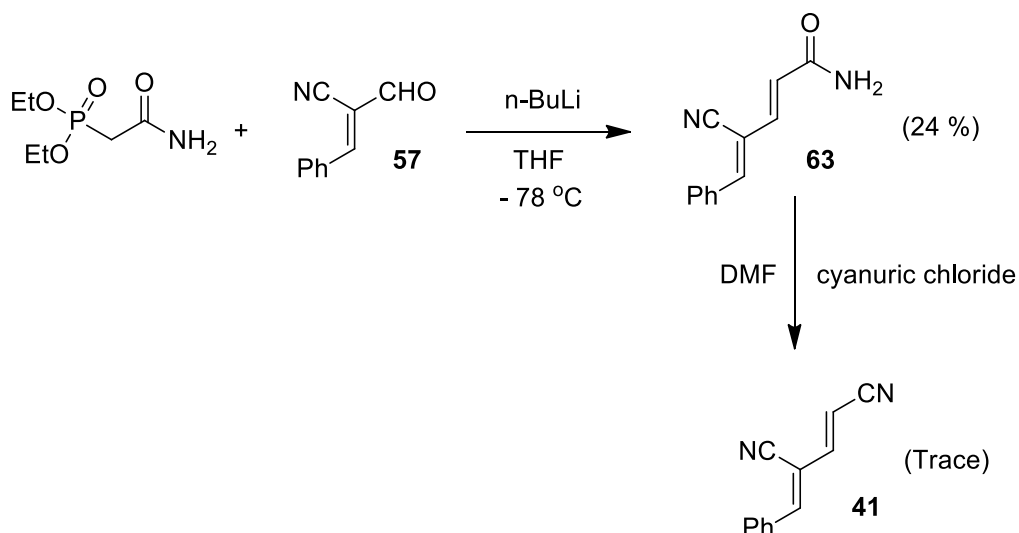
Figure 2.30. Synthetic route to bis-cyano diene **41** utilizing a Horner-Wittig olefination reaction followed by an amide dehydration.

The dehydrating agent, cyanuric chloride, was chosen for its mild reaction conditions, in comparison to traditional dehydration methods, e.g. phosphorous pentoxide or titanium tetrachloride.[82]

The amide containing HWE reagent **64** was synthesized using an Arbuzov reaction, by refluxing neat triethyl phosphite (3 eq.) and 2-chloro-acetamide (1 eq.) at 110 ˚C. Precipitation from DCM/PE gave an off-white solid in an 80 % yield (Figure 2.31).[83]
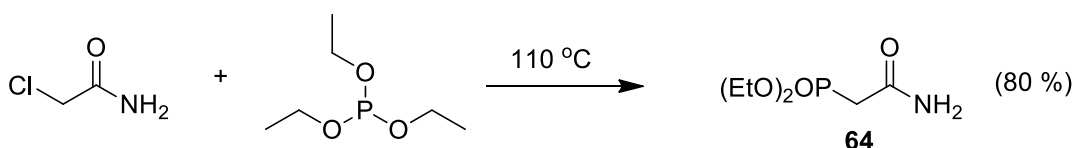
Figure 2.31. Synthesis of amide HWE reagent **64**.

This reagent was then applied in the HWE reaction with phenyl formyl acrylonitrile **57** to yield the cyano amide butadiene product **63** in a 24 **%** yield. With the butadiene **63** in hand we turned our attention to the cyanuric chloride amide dehydration reaction. Pleasingly, the

product bis-cyano butadiene **41** was observed in crude ^{1}H NMR spectra via the characteristic olefinic doublets, with large J_{trans} coupling constants, at 7.14 and 5.91 ppm. Despite this success the purification of the crude reaction mixture proved to be extremely difficult and the bis-cyano diene could not be isolated from the mixture without complete degradation. This degradation appeared to be as a result of the thermal stress applied in the removal of the DMF reaction solvent.

2.2.3.3   Fourth generation synthetic strategy – Peterson olefination

A synthetically useful methodology for the generation of the desired butadienes remained elusive and so we next attempted another of the well know olefination reactions, the Peterson reaction. Retrosynthetic analysis, with the Peterson olefination reaction in mind, gives the familiar formyl acrylonitrile **57** and the commercially available trimethylsilylacetonitrile **65** (Figure 2.32).
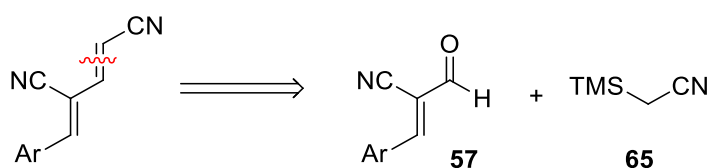
Figure 2.32. Retrosynthetic analysis of bis-cyano butadienes resulting in Peterson olefination starting materials.

The exact mechanism of the Peterson olefination is not very well understood and may be dependent on the reaction conditions as well as the substrates utilized. A step-wise mechanism is outlined in Figure 2.33 and begins with the deprotonation of the alkyl silane **65** followed by direct addition of the carbanion to the carbonyl carbon of the formyl acrylonitrile. Quenching of the resulting anion with H_2O yields the alcohol **66**, which after deprotonation gives the oxyanion **67**. The strong affinity of oxygen for silicon then leads to the transfer of the silyl group to the oxygen and the resulting carbanion **68** can eliminate the silanolate and generate the product diene. Subsequent protonation of the silanolate produces the silanol by-product **69**.[84]
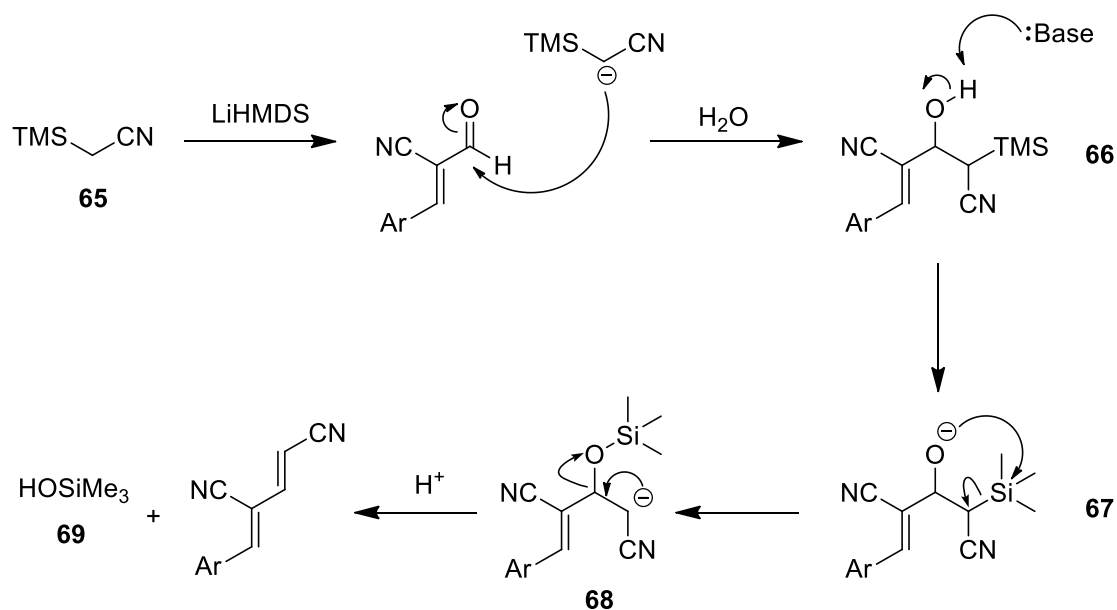
Figure 2.33. Proposed mechanism of the Peterson olefination route to the bis-cyano dienes.[84]

A concerted mechanism can also be used to describe the final steps of the Peterson olefination during which the collapse of a four-membered oxasiletanide intermediate (analogous to the oxaphosphetane intermediate postulated as part of the Wittig reaction) leads to the reaction products.[84] In either case, the step-wise or concerted mechanisms, the formation of the strong silicon-oxygen bond pushes the equilibrium towards the olefin products.

Disappointingly, when the Peterson olefination was attempted it also resulted in the formation of intractable red oils, the composition of which could not be determined spectroscopically (Figure 2.34).
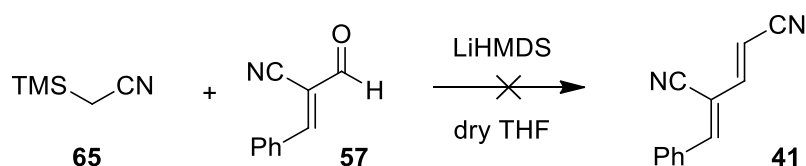
Figure 2.34. Attempted Peterson olefination of α-cyano cinnamaldehyde **57**.

2.2.3.4   Fifth generation synthetic strategy – A return to Wittig Chemistry

A number of insights were gained into the physical and chemical properties of the bis-cyano butadienes through the previous attempts at their synthesis. A noted sensitivity towards basic conditions and temperatures above 40 ˚C was observed. These observations confirmed that the bis-cyano diene substrates were indeed challenging compounds to synthesize and handle, similar to the terminally unsubstituted bis-cyano butadienes reported by Ahn *et al.* (Section 2.1.3).[70] A return to the literature yielded some potential options for limiting exposure of the dienic product to conditions that could lead to decomposition. The first possible contributor to decomposition, that could be easily removed, was the use of stoichiometric or greater quantities of base in the *in-situ* generation of the anionic component employed in the olefin forming reaction. A number of stabilized Wittig-type ylides can be pre-formed and are known to be bench stable. Use of such ylides would remove the need for the presence of a base in the reaction mixture and so protect any base-sensitive starting materials or products. The nitrile moiety is extremely anion stabilizing through conjugation and is an excellent example of a stabilized ylide. As such, the stabilized nitrile ylide **71** was easily prepared from the corresponding chloride salt **70** by washing with 2 M NaOH, followed by drying over Na_2SO_4. Removal of the organic solvent *in vacuo* followed by precipitation from DCM/PE generated an off-white solid in 93 % yield (Figure 1.35). This stabilized ylide was found to be bench stable, once kept in the absence of light, and retained its activity for a number of months.
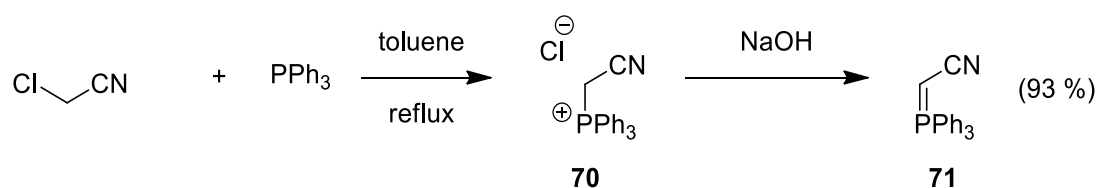
Figure 2.35. Synthesis of nitrile ylide **71**.

The stabilized ylide **71** was then applied in a Wittig reaction with the formyl acrylonitrile **57**. A number of solvents were explored, as was the presence of the additive LiCl (Table 2.2). In all cases a red intractable oil resulted.

Table 2.2. Wittig reaction refinement
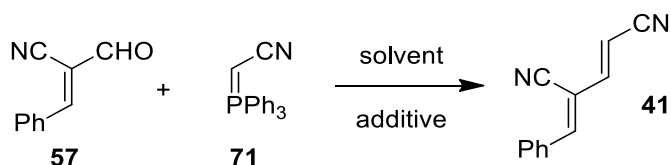
Solvent	Aldehyde	Ylide	Additive	Time	Result
DCM	1 eq	1.1 eq	N/A	16 hr	Red intractable oil
DCM	1 eq	1.1 eq	LiCl (5 eq.)	16 hr	Red intractable oil
Toluene	1 eq	1.1 eq	N/A	16 hr	Red intractable oil
Toluene	1 eq	1.1 eq	LiCl (5 eq.)	16 hr	Red intractable oil
THF	1 eq	1.1 eq	N/A	16 hr	Red intractable oil
THF	1 eq	1.1 eq	LiCl (5 eq.)	16 hr	Red intractable oil

A second consideration was the instability of α,β-unsaturated nitriles species and their reported tendency to polymerize. This instability leads to difficulties in the large scale synthesis and purification α,β-unsaturated nitriles. A number of patents and publications have attempted to offer solutions to deal with this issue and suggest a number of inhibitors to prevent/reduce the polymerization and ease handling.[85] The inhibitor chosen greatly

depends on the proposed mode of polymerization, as α,β-unsaturated nitriles are known to undergo polymerization through both anionic and radical means. The observed polymerization or degradation of the bis-cyano diene occurred under basic conditions and so we postulated that the method of polymerization may be anionic in nature (although radical polymerization cannot be ruled out definitively). As such, we considered 8-hydroxyquinoline (8-HQ) as a polymerization inhibitor as it has been previously shown to act in this manner in the synthesis, purification and storage of unsaturated nitriles (Figure 2.36).[85]
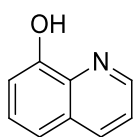
Figure 2.36. 8-Hydroxyquinoline.

An advantage of 8-HQ over other inhibitors is the ease of removal of the inhibitor during purification. We found that a number of methods could be employed to remove the 8-HQ, with recrystallization, a simple 1 M HCl wash and silica gel chromatography as three such examples.

A test reaction was carried out using the newly synthesized stabilized ylide **71** and the phenyl formyl acrylonitrile **57** in the presence of 8-HQ (Figure 2.37). Gratifyingly, the reaction proceeded and after 2 hrs at 120 ˚C there was no indication of the starting formyl acrylonitrile by TLC (stained with DNP). The product butadiene **41** was isolated, by precipitation from DCM/PE following a short silica plug of the reaction mixture, in a 49 % yield and as a single stereoisomer. The presumed geometry of the diene was the *E,Z* geometry due to a large *trans* coupling constant of 16 Hz exhibited by the alpha olefin protons and retained geometry of the formyl acrylonitrile. The *Z,Z* isomer could also be observed in the reaction mixture, however it was not isolated at this time. The stereoisomeric distribution of the product was not found to be reproducible yielding different ratios of the *E,Z* and the *Z,Z* dienes from reaction to reaction. As will be discussed in Chapter 3, the use of stereoisomeric mixtures does not affect the utility of the dienes in further transformations, such as a conjugate addition reaction.
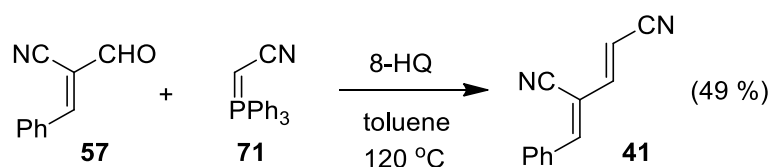
Figure 2.37. Wittig reaction of phenyl formyl acrylonitrile and stabilized ylide.

Although this methodology was a vast improvement on the previous methods there were still some drawback to its employment. The reaction did not proceed to completion at rt in toluene and so the use of elevated temperature (120 ˚C) was required. Using toluene as a solvent also meant that high temperatures were required for its removal, even *in vacuo*. The use of even moderate temperatures during the reaction workup would often lead to degradation of the product, even in the presence of 8-HQ, resulting in the formation of an intractable red oil. As such, to avoid the use of elevated temperatures during solvent removal a solvent exchange process was developed. The solvent exchange was facilitated by the use of a short plug of silica. The reaction mixture in toluene was poured directly onto a dry silica plug and rinsed with PE. The filtrate could then be discarded and the solvent polarity increased to 80:20 PE:EtOAc resulting in product elution. This procedure was advantageous in that the majority of the triphenylphosphine oxide, a by-product of the Wittig reaction, would remain on the silica easing product isolation. Another advantage was the transfer of the product into a lower boiling point solvent, which could be removed *in vacuo* at lower temperatures. This reduced the likelihood that the products would come under any thermal stress during purification. Using this procedure allowed for the isolation and separation of the bis-cyano butadiene **41** into its constituent diastereoisomers in a 40 % yield for the *E,Z* isomer and a 37 % yield for the *Z,Z* isomer.

With the refined reaction conditions and a preferred solvent in hand we could now move to synthesize a bis-cyano diene family. This would first require the expansion of the formyl acrylonitrile partner family.

2.2.3.4.1 Wittig reaction mechanism

As many as eight mechanisms have been proposed for the Wittig reaction since its initial description in 1953 by Wittig and Geissler.[86] The most prominent mechanism described in textbooks invokes betaines as the first intermediate in route to an oxaphosphetane (OPA) intermediate. This mechanism has been utilized to describe the reaction path of the Wittig reaction since the time of the reactions development.[87,88] However, this mechanism cannot be applied to all Wittig reactions as it does not take into account the nature of the ylide and carbonyl compound utilized, and their effect on the mechanism.

The origin of the *E/Z* selectivity in the betaine mechanism originates from the discrepancy in the energies of the proposed transition states leading to the *E* and *Z* olefins. The energy gap between these two transition states is in turn dependent on a number of factors including, 1) nature of the ylide; 2) carbonyl compound utilized; 3) nature of solvent; 4) reaction conditions, i.e. presence of coordinating ions.

With regards to the ylide, the nature of the substituent on the ylide can fall into three distinct sub-groups, namely that of stabilizing, semi-stabilizing and non-stabilizing. Stabilized ylides have substituents that are strongly electron-withdrawing, e.g. $-CO_2Et$ or $-CN$. Ylides that fall into the semi-stabilized group bear substituents such as aryl and alkenyl substituents, which are not as stabilizing as strongly electron-withdrawing groups. Finally, non-stabilized ylides usually bear substituents such as alkyl groups, which cannot stabilize the ylide through either inductive withdrawal or delocalization of the negative charge. Experimentally, stabilized triphenylphosphonium derived ylides show selectivity for *E*-olefin formation whilst non-stabilized ylides show a selectivity for *Z*-olefin formation. Semi-stabilized ylides generate mixtures of *E* and *Z* olefins with low selectivity.[89]

The proposed betaine reaction mechanism for the Wittig reaction can be seen in Figure 2.38.
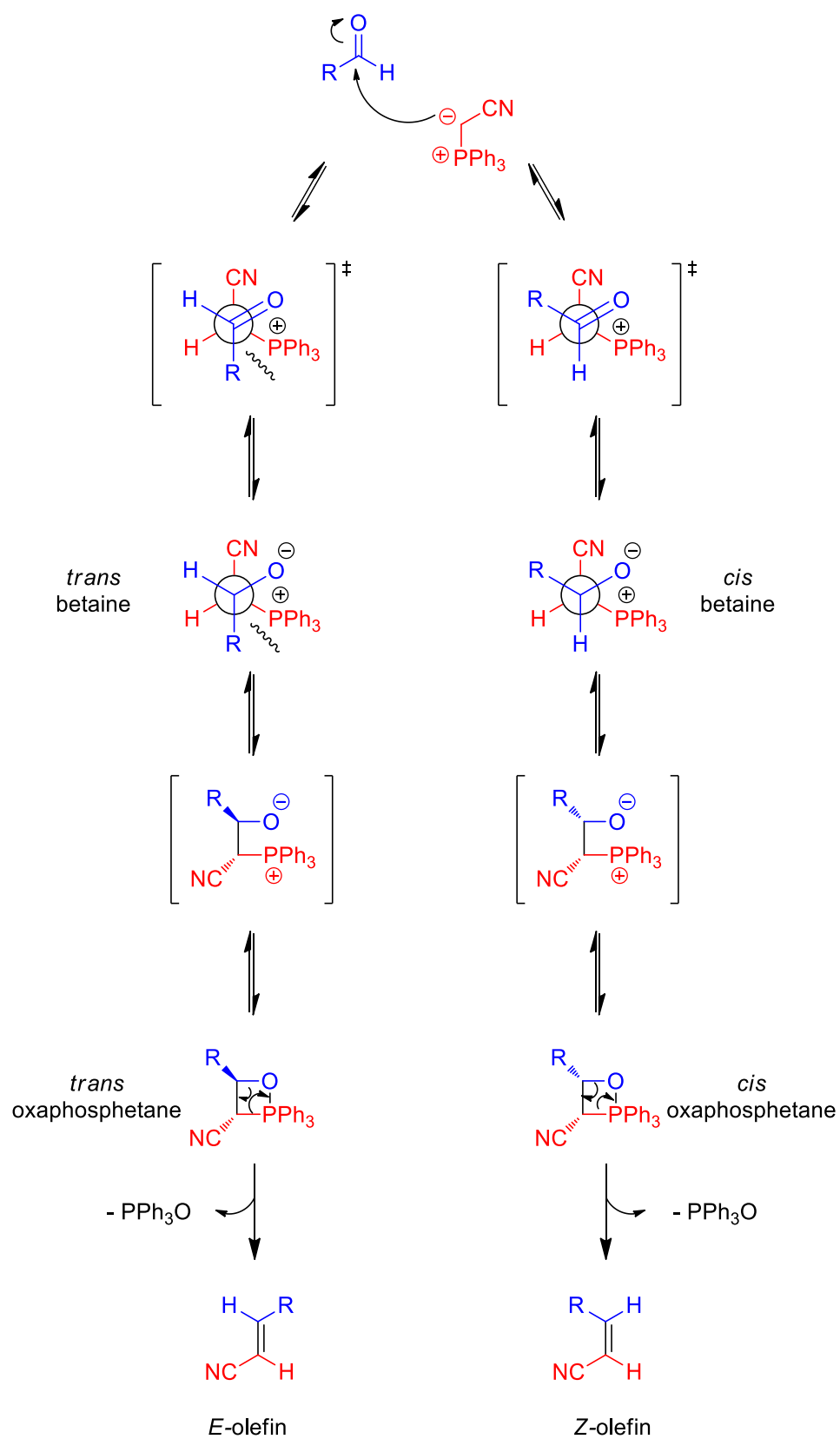
Figure 2.38. Betaine mechanism for the Wittig reaction.

The initial attack of the ylide on the carbonyl can be described as occurring at either the *Re* or *Si* face of the carbonyl compound. This generates diastereoisomeric transition states that lead to the *trans* and *cis* betaines respectively. Depending on the nature of the carbonyl compound, a steric clash may exist between the triphenylphosphonium of the ylide and the R group of the carbonyl compound in the transition state leading to the *trans* betaine. This steric clash could lead to a greater activation energy barrier in the formation of the *trans* betaine compared to the *cis* betaine. Therefore, under irreversible conditions i.e. non-stabilized ylide, the kinetically favoured *cis* betaine could be expected to dominate resulting in generation of the less stable *cis* OPA and ultimately the *Z* olefin. Under reversible conditions, i.e. stabilized ylide, where an equilibrium between the *cis* OPA and the *trans* OPA is established, the thermodynamically favoured *trans* OPA could be expected to dominate and ultimately lead to a preference for the *E* olefin.

Stereospecific s*yn*-periplanar elimination of triphenylphosphine oxide from the OPA leads to either the *E* or *Z* olefins. This step is irreversible and the affinity of phosphorous for oxygen in the formation of the phosphorus-oxygen double bond drives the reaction forward. If the betaine mechanism was correct then theoretically one could predict the Wittig selectivity through careful analysis of the reacting partners, i.e. ylide stability. In practice, the *E/Z* stereoselectivity of each reaction is highly dependent on the unique reactivity of the individual components under the reaction conditions.

The betaine mechanism itself is disputed and under Li-salt free conditions betaine formation has never been observed.[90] Furthermore, OPA formation has been shown to be in fact an irreversible process, and hence a reversible reaction employing a betaine mechanism cannot be used to account for the *E* selectivity observed experimentally when stabilized ylides are utilized.[89]

Recently, Gilheany *et al*. outlined the arguments for eight postulated mechanisms of the Wittig reaction, including the betaine mechanism and their favoured [2+2] cycloaddition mechanism for Li-salt free Wittig reactions.[90] The irreversible [2+2] cycloaddition of the ylide and the carbonyl compound was a mechanism first postulated by Vedejs *et al.* in 1973 (Figure 2.39).[91]
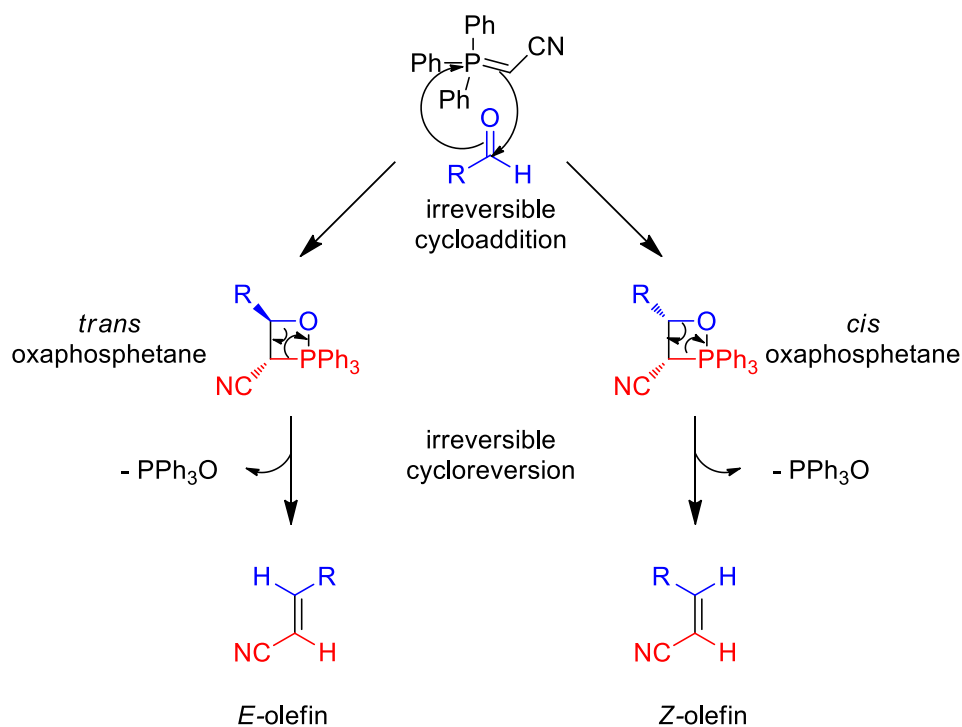
Figure 2.39. [2+2] cycloaddition Wittig reaction mechanism proposed by Vedejs *et al.*[91]

In this proposed mechanism the OPA is the only intermediate in the reaction pathway and it is formed through the irreversible [2+2] cycloaddition of the ylide and carbonyl compound. The second step of this mechanism is the irreversible and stereospecific cycloreversion of the OPA to yield phosphine oxide and alkene, the exact mechanism of this step is still under debate. As the second step is both stereospecific and irreversible, then the irreversible first step can be considered to be the stereodetermining step.

Computational work by Aggarwal *et al*. on the four-membered transition states of the [2+2] cycloaddition of triphenylphosphine derived ylides and aldehydes shed some more light on the stereoselectivity of the Li-salt free Wittig reaction.[89] A selection of their results for computed transition states can be seen in Figure 2.40.
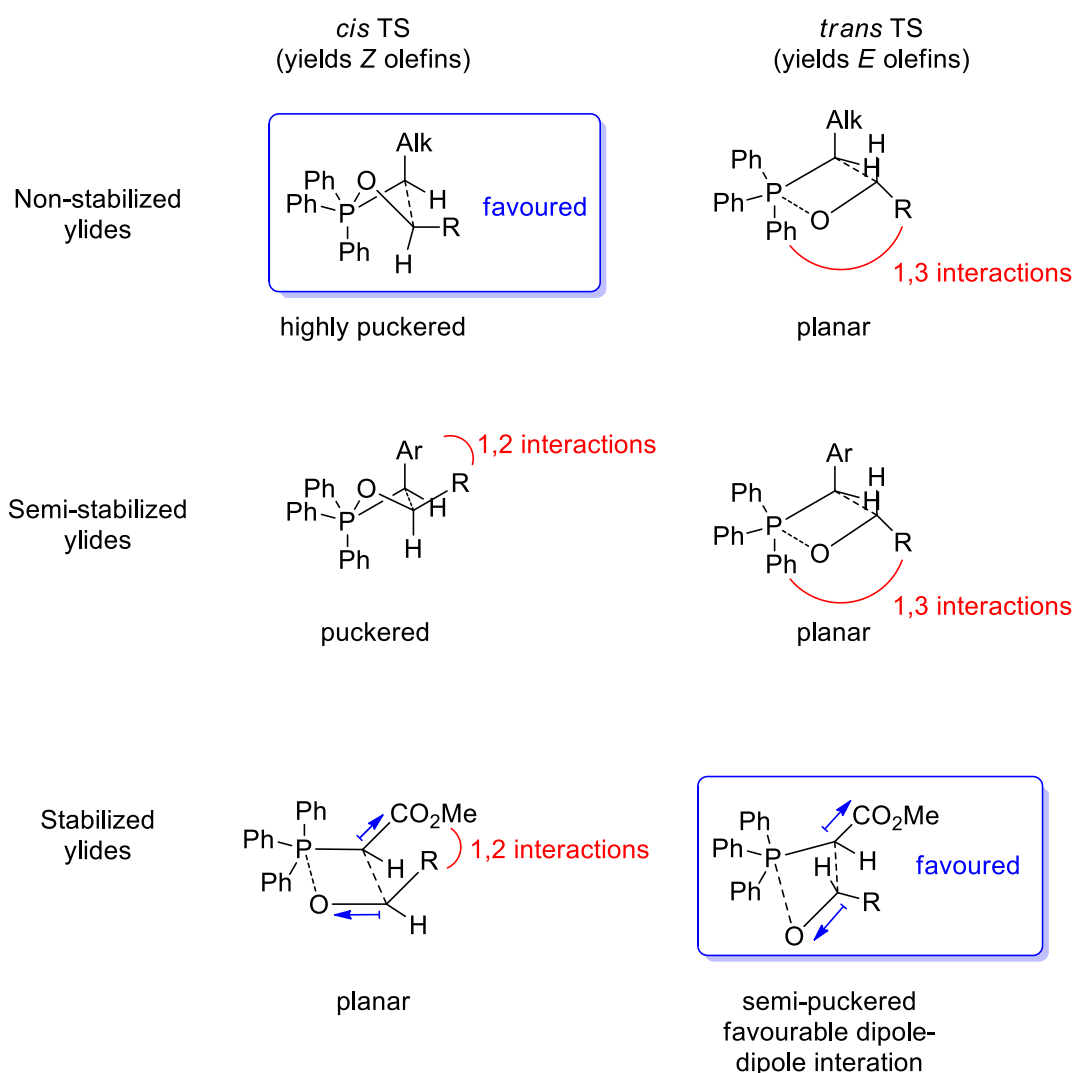
Figure 2.40. Calculated transition states by Aggarwal *et al.* accounting for *E/Z* selectivity of the Wittig reaction through a [2+2] cycloaddition. Blue arrows indicate dipole directionality.[89]

Figure 2.40 details the transition states of triphenylphosphine derived, non-stabilized, semi-stabilized, and stabilized ylides with an aldehyde. In the non-stabilized ylide case, a highly puckered transition states leading to the *cis*-OPA and *Z*-olefin is favoured over the planar transition state leading to the *trans*-OPA and *E*-olefin. This is due to the destabilizing 1,3-interactions between a phenyl substituent on the phosphine and the aldehydic substituent. In the case of the semi-stabilized ylide transition states, there are competing 1,2- and 1,3-interactions in the *cis* and *trans* transition states leading to the *cis*- and *trans*-OPAs respectively. The balance between these two competing destabilizing interactions leads to a discrepancy in the transition states energies leading to both the *cis*-OPA and the *trans*-OPA,

which in turn dictates the stereoisomeric ratio of the olefin products. This is consistent with the observation of low *E/Z* selectivity in the Wittig reaction of semi-stabilized ylides and is highly dependent on the substituents on the phosphorous and the nature of the ylidic substituent. In the final case of stabilized ylides, the semi-puckered transition state leading to the *trans*-OPA and *E*-olefin is favoured over the planar transition state leading to the *cis*-OPA and *Z*-olefin. This is due to a number of factors, namely the destabilizing 1,2-interactions between the ylidic substituent and the aldehydic substituent of the planar transition state, as well as the stabilizing effect of the alignment of the dipoles in the puckered transition state leading to the *trans*-OPA.

In summary, the mechanism for the Li-salt free Wittig reaction consists of an irreversible [2+2] cycloaddition as its first step in which the stereochemistry of the OPA is set. High *E* or *Z* olefin selectivity is due to the competing destabilizing interactions in either planar, puckered or semi-puckered transition states disfavouring either the formation of either the *cis* or *trans* OPAs. The second step of the mechanism is still not entirely understood, however it is known that OPA decomposition to olefin and phosphine oxide occurs stereospecifically.

2.2.4   Synthesis of formyl acrylonitriles

2.2.4.1   Introduction to formyl acrylonitriles

In order to develop a family of bis-cyano butadiene subtrates it was first necessary to expand our library of 3-substituted formyl acrylonitriles. A typical 3-substituted formyl acrylonitrile moiety can be seen in **72**, Figure 2.41. The reactivity of formyl acrylonitriles of type **72** can be compared to that of other electron-deficient olefinic systems, such as acrylonitrile **73** and nitrostyrene **74,** many of which have been extensively utilized in conjugate additions reactions (Figure 2.41).
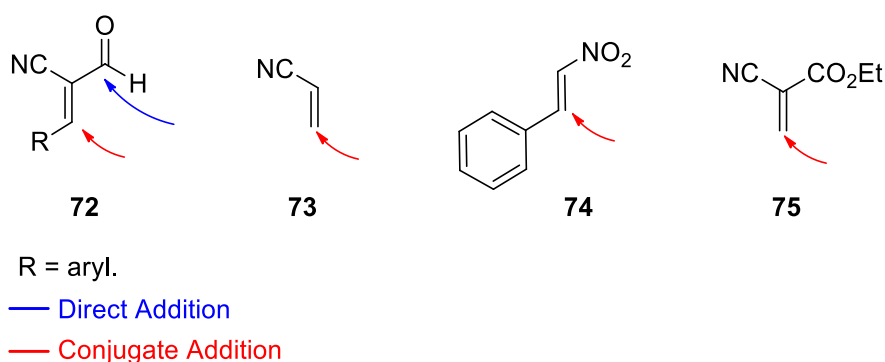
Figure 2.41. Electrophilic sites of selected Michael acceptors.

Despite the structural and electronic similarities between formyl acrylonitriles **72** to acrylonitriles **73** and nitrostyrenes **74,** their synthesis and study of reactivity has been relatively underexplored. In particular, the realm of conjugate addition chemistry to formyl acrylonitriles remains underdeveloped. This lack of exploration may be due to a perceived instability of formyl acrylonitriles. This perceived instability can be understood when one considers how closely related in structure 3-substituted formyl acrylonitriles are to that of the highly reactive ethyl cyano-acrylate **75** (Figure 2.41), the major reactive component of commercial super-glue.

In addition to the possible instability of formyl acrylonitriles, the presence of an additional reactive site, the aldehyde functionality, presents additional complexity through the possibility of direct addition as well as conjugate addition (Figure 2.41). This is another factor to consider when planning reactions utilising formyl acrylonitriles.

The literature has few examples of the synthesis of formyl acrylonitriles and even fewer still of their utilization in further synthetic modifications. The first literature report of phenyl formyl acrylonitrile **73** was in 1956 by Wasserman *et al.* during their studies of the reaction on acrylonitrile with benzaldehyde under cyanoethylation conditions.[78] They reported the formation of four products, **76, 77, 78** and **57** which was the phenyl formyl acrylonitrile and was obtained in only a 2 % yield (Figure 2.42).
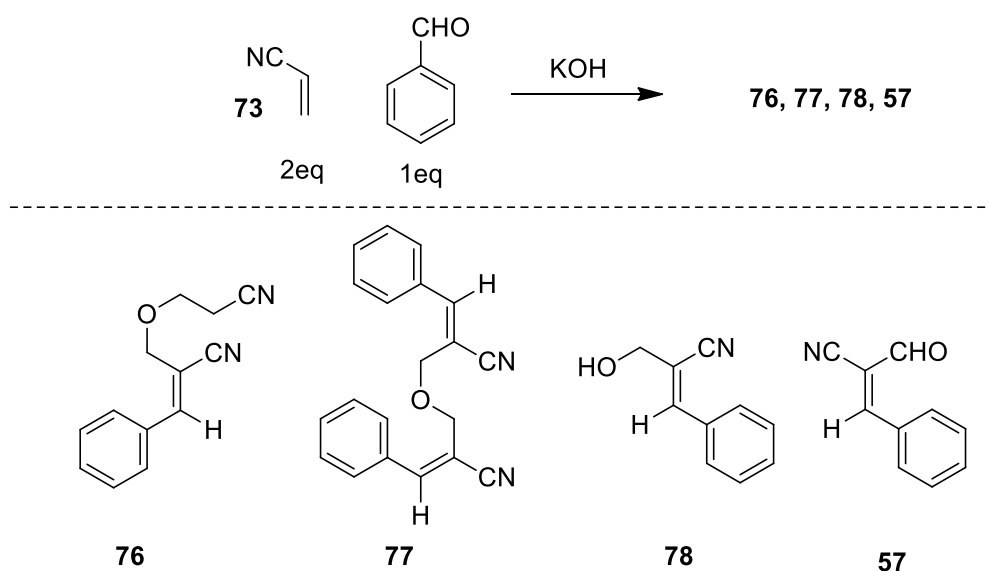
Figure 2.42. Reaction of acrylonitrile with benzaldehyde under cyanoethylation conditions.[78]

The authors confirmed the identity of **57** by independent synthesis using freshly prepared alcohol **79** and MnO_2 (Figure 2.43).
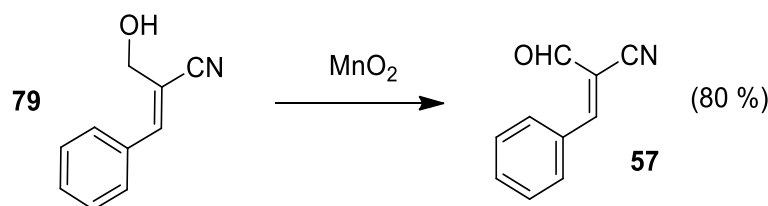
Figure 2.43. Manganese dioxide oxidation of alcohol **80** by Wasserman *et al.*[78]

The authors assigned the geometry of phenyl formyl acrylonitrile **57** as *Z* by comparison of the UV absorption spectra of the three compounds **76,77,78** to the UV absorption of *trans*-cinnamonitrile. However, the assignment of the stereochemistry of the phenyl formyl acrylonitrile **57** as *Z* could be questioned as the authors did not appear to perform UV analysis

on the formyl acrylonitrile **57**. This assignment would also seem to contradict future literature reports of the compound, which all assign the geometry as *E*.[79,92]

Our preferred literature method for the synthesis of formyl acrylonitriles was found to be that reported by Elliott and co-workers.[79] We applied a simple Knoevenagel condensation of aryl aldehyde and commercially available 3,3-dimethoxypropionitrile, in the presence of sodium methoxide, to yield the intermediate acetal. This acetal was not isolated but carried through and deprotected by treatment with 6 M HCl to give the aldehyde **57** in a 71 % yield (Figure 2.44).
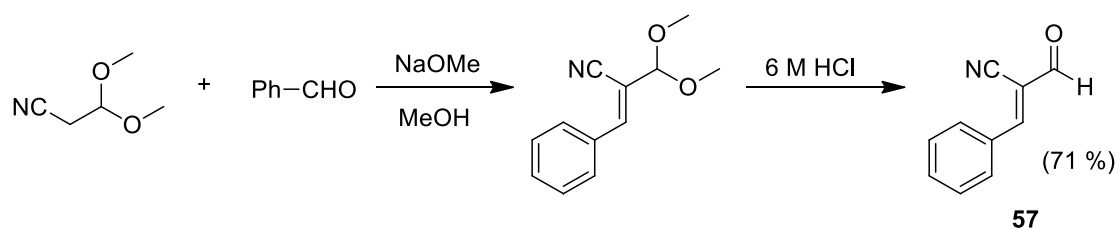
Figure 2.44. Synthesis of formyl acrylonitrile **57**.

Expansion of this methodology to substituted aryl aldehydes led to the synthesis of a number of formyl acrylonitriles as detailed in Table 2.3.
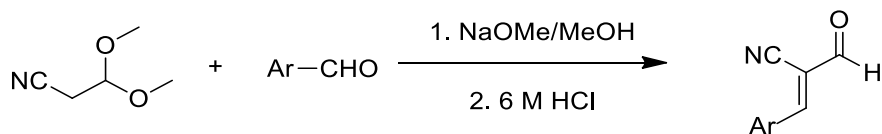
Table 2.3 – Formyl acrylonitrile family.

Ar =					
71 % **(57)**	84 % **(61)**	49 % **(80)**	71 % **(81)**	43 % **(82)**	58 % **(83)**
53 % **(84)**	34 % **(85)**	42 % **(86)**	48 % **(87)**	35 % **(88)**	70 % **(89)**
		51 % **(90)**	60 % **(91)**		

The limitation of this methodology became apparent once attempts were made to expand the scope to that of electron deficient aryl aldehydes. The introduction of substituents with strong inductive withdrawal at the *o/p* position of the aromatic ring resulted in complex mixtures from which no formyl acrylonitrile products could be isolated. This limitation is unfortunate as a butadiene resulting from such an electron poor formyl acrylonitrile would make an interesting substrate for 1,6-conjugate additions. Electron withdrawing groups on the aryl ring would increase the electrophilicity of the δ position of the butadiene carbon backbone, which could help favour 1,6-conjugate addition over 1,4-additon.

A number of electron-withdrawing group substituted benzaldehydes were explored as starting materials for the synthesis of formyl acrylonitriles. These efforts are detailed in Figure 2.45. The failure to generate formyl acrylonitriles bearing electron-withdrawing

substituents on the aromatic ring is presumably due to their enhanced reactivity and hence inherent instability under the basic reaction conditions used to achieve the transformation.
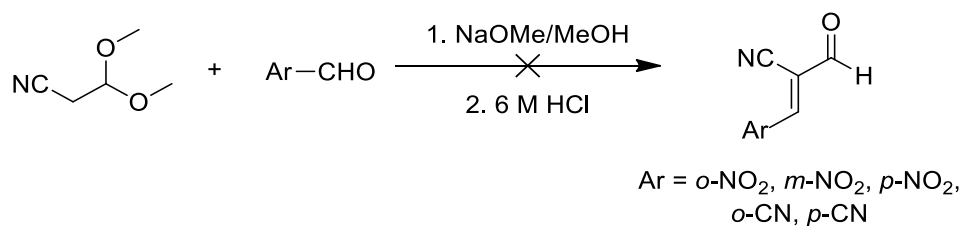
Figure 2.45. Attempted syntheses of electron deficient formyl acrylonitriles.

There are few reports in the literature describing the synthesis of electron deficient 3-substituted formyl acrylonitriles. One publication by Yadav *et al.* suggests that the *p*-NO$_2$ substituted formyl acrylonitrile **93** can be synthesized in a 75 % yield.[93] The authors propose that the transformation of Baylis-Hillman adducts into formyl acrylonitriles can be achieved in the presence of sodium nitrate and the ionic liquid [HMIM]HSO$_4$. Their proposed mechanism for this transformation is shown in Figure 2.46.
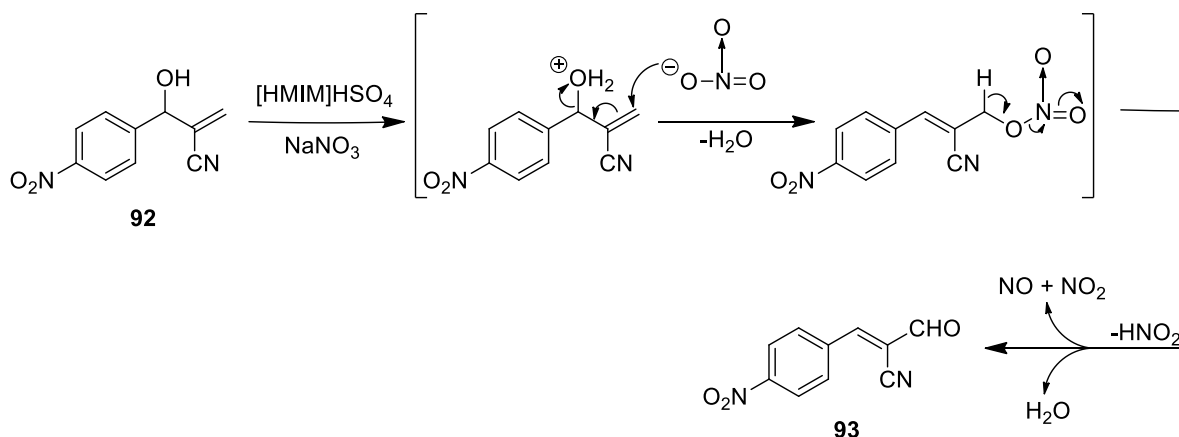
Figure 2.46. Proposed mechanism for the transformation of Baylis-Hillman adducts into formyl acrylonitriles as reported by Yadav *et al.*[93]

We attempted to synthesize *p*-NO$_2$ phenyl formyl acrylonitrile **93** using Yadav's method. The Baylis-Hillman adduct **92** was prepared using literature methods in a yield of 81 %.[94] In our hands, the application of the Baylis-Hillman adduct **92** in the [HMIM]HSO$_4$ and NaNO$_3$ system developed by Yadav *et al.* did not result in conversion of the Baylis-Hillman adducts to formyl acrylonitriles, even after prolonged reaction times (Figure 2.47).
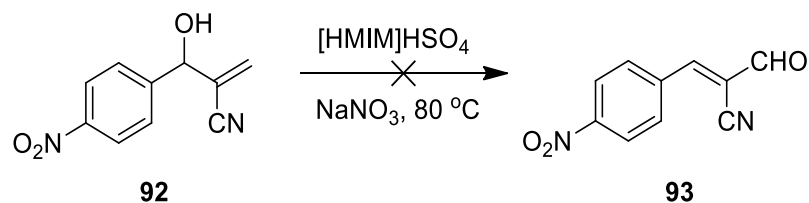
Figure 2.47. Failed conversion of a Baylis-Hillman adduct into a formyl acrylonitrile.

As access to electron-withdrawing group substituted formyl acrylonitriles was not forthcoming, we turned our efforts to the synthesis of butadienes from the formyl acrylonitriles that we had already accessed.

2.2.5   Synthesis of bis-cyano dienes

With a number of formyl acrylonitriles synthesized we could now begin the synthesis of the bis-cyano butadienes. The previously described method utilizing 8-HQ as a polymerization inhibitor was utilized to synthesize a number of different dienes. The reaction conditions and results are outlined in Figure 2.48. The yields reported refer to the isolated yield of the *E,Z* geometry dienes with the exception of the thiophenyl bis-cyano butadiene **95** which was contaminated with 11 % of the *Z,Z* isomer (see experimental detail for more info).
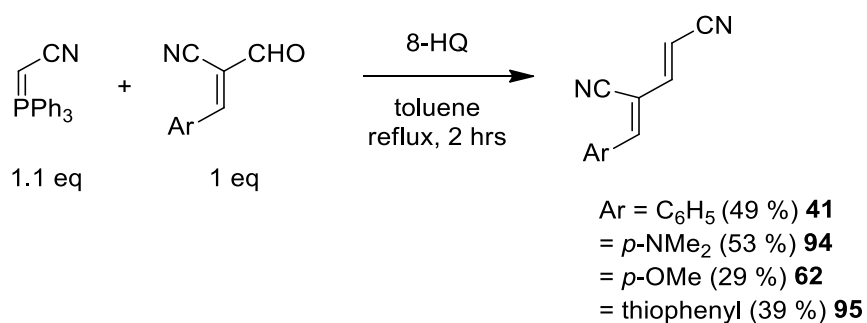
Figure 2.48. Synthesis of bis-cyano butadienes.

2.2.5.1   Spectroscopic characterization

The bis-cyano butadienes were characterized through a combination of ^{1}H NMR and ^{13}C NMR experiments, as well as correlation NMR experiments such as Heteronuclear Multiple Bond

Correlation (HMBC) and Heteronuclear Single Quantum Correlation (HSQC). The structural characterization of phenyl bis-cyano butadiene **41** is outlined below as an example.

The ^{1}H NMR spectrum of phenyl bis-cyano butadiene **41** is relatively simple in that it only contains six signals, all of which appear between 5.80 and 8.00 ppm (Figure 2.49). The most distinctive signals are the two doublets, with coupling constants of *J* = 16.0 Hz, arising from the olefinic protons of the α-olefin. The more deshielded of the doublets appears downfield at 7.14 ppm and can be assigned to the proton on the β-carbon due to the deshielding effect of the nitrile group on the α-carbon. The doublet appearing further upfield at 5.91 ppm arises from the proton on the α-carbon. The large coupling constant of 16.0 Hz indicates that the geometry of the α-olefin is *E*. As such, the protons about this olefin are *anti*-periplanar to one another, which results in the large coupling constant. The singlet appearing at 7.32 ppm arises from the proton on the δ-carbon. The aromatic protons appear as multiplets at 7.52 and 7.89 ppm.
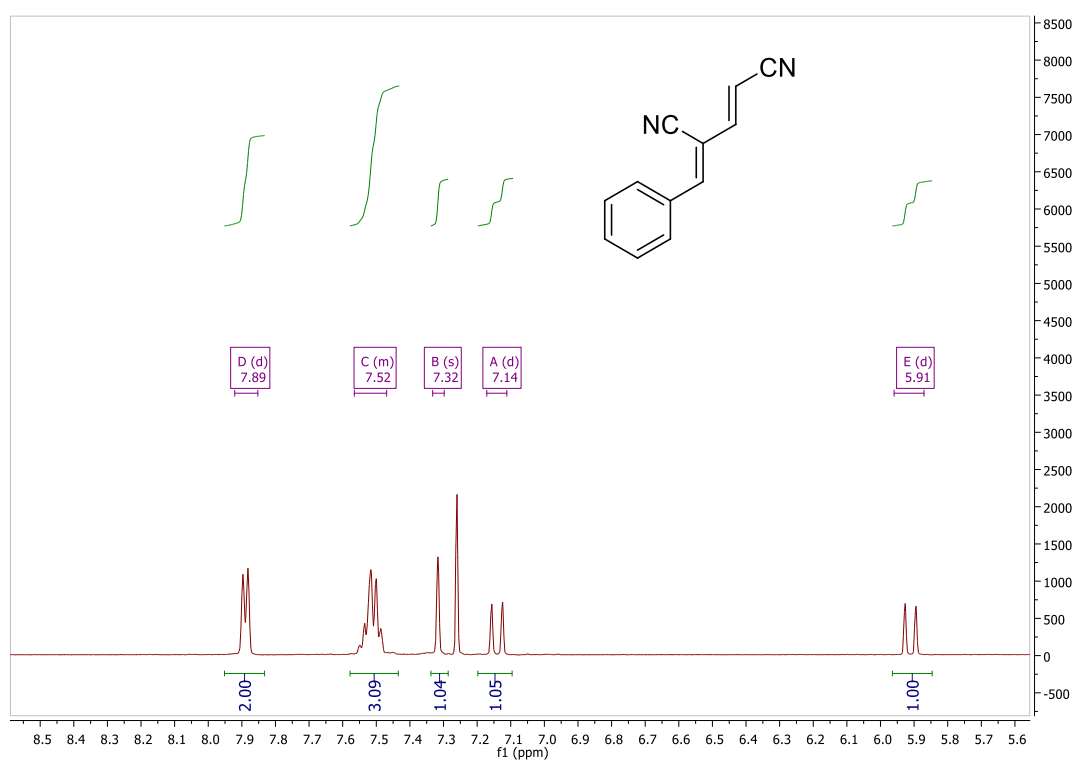
Figure 2.49. Expanded region of the ^{1}H NMR spectrum of bis-cyano butadiene **41**.

The ^{1}H NMR spectral assignment of the bis-cyano butadiene is summarized in Figure 2.50.

E (5.91 ppm, d, 1H)

CN

NC

D (7.89 ppm, d, 2H)

A (7.14 ppm, d, 1H)

C (7.57 - 7.47 ppm, m, 2H)

B (7.32 ppm, s, 1H)

C (7.57 - 7.47 ppm, m, 1H)
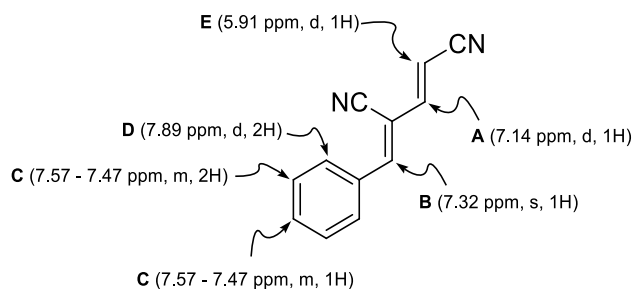
Figure 2.50.^{1}H NMR spectral assignment of bis-cyano butadiene **41**.

With the ^{1}H NMR spectrum assigned, a combination of HSQC and HMBC 2D NMR experiments could be used to assign the ^{13}C NMR spectrum. The ^{13}C NMR signals arising from carbons with protons directly attached to them could be easily assigned through examination of the HSQC spectrum of bis-cyano butadiene **41** (Figure 2.51). This allowed for the straightforward assignment of six of the ^{13}C NMR signals.
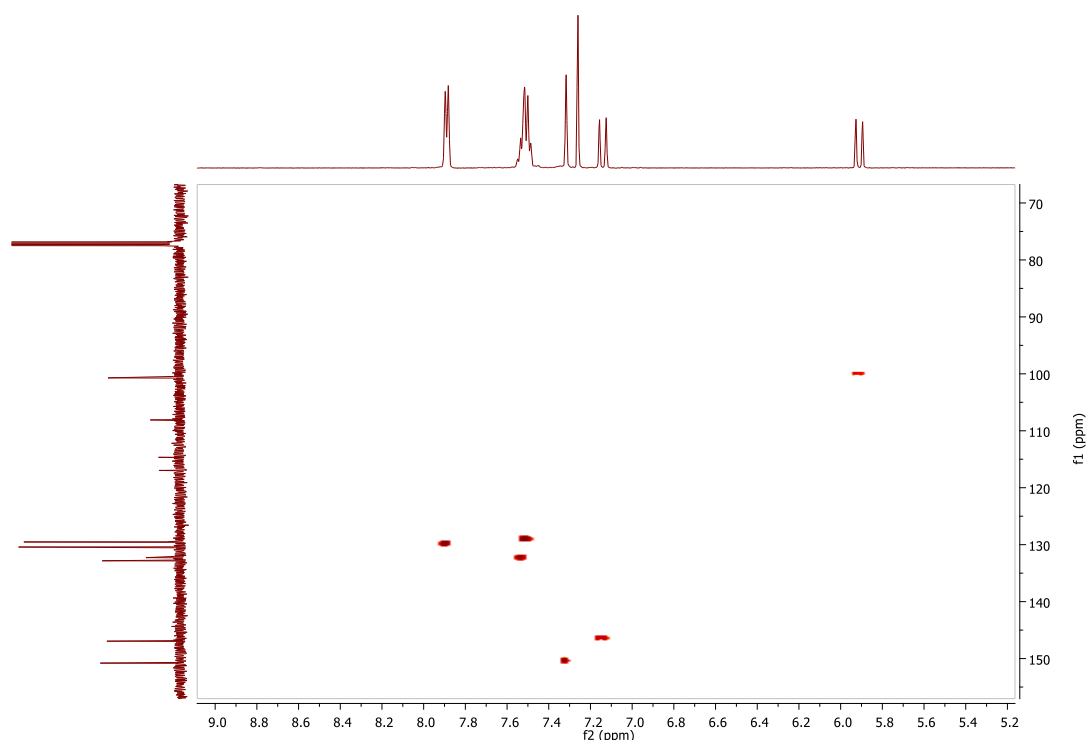
Figure 2.51. HSQC spectrum of bis-cyano butadiene **41**.

The remaining ^{13}C NMR signals were all arising from quaternary carbon signals of bis-cyano butadiene **41**. These four signals arise from the two nitrile quaternary carbons, the quaternary olefin carbon and a quaternary aromatic carbon. These signals could only be clearly assigned through the use of a HMBC experiment, which probes the correlation between proton signals with carbon signals up to 4 bonds away. The HMBC spectrum can be seen in Figure 2.52.
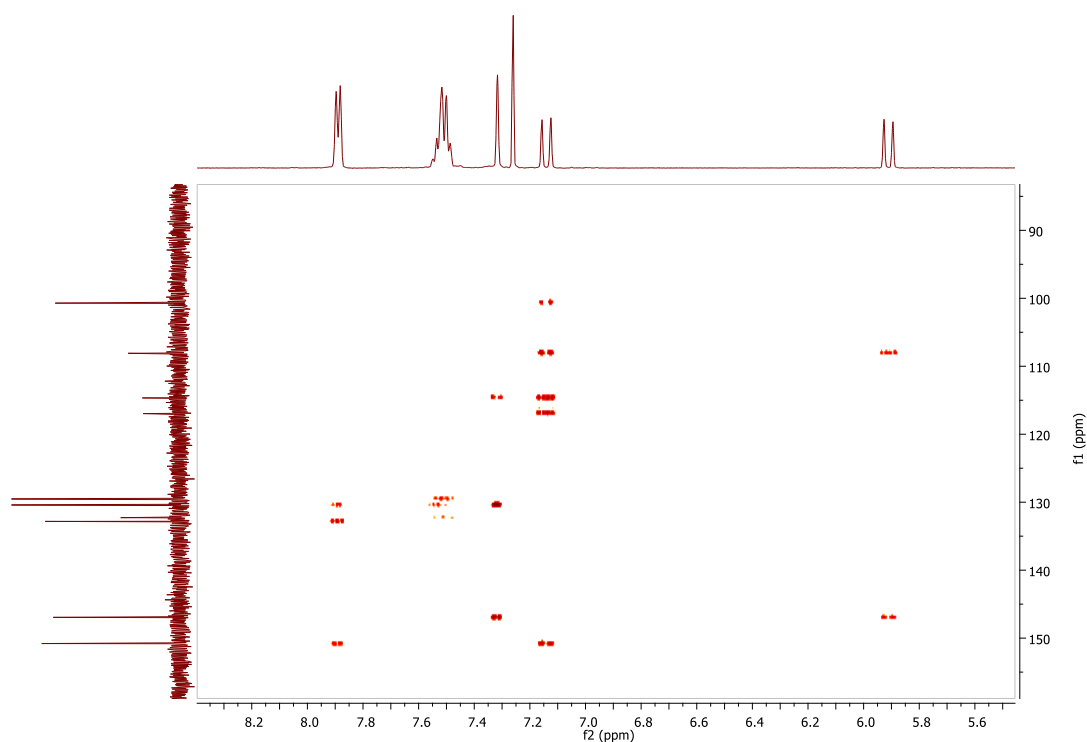
Figure 2.52. HMBC spectrum of bis-cyano butadiene **41**.

In order to first distinguish between the two nitrile quaternary carbon signals it is helpful to examine the correlations arising from the ^{1}H NMR signals of the α-olefin and the ^{1}H NMR signal arising from the proton attached to the δ-carbon (Figure 2.56).
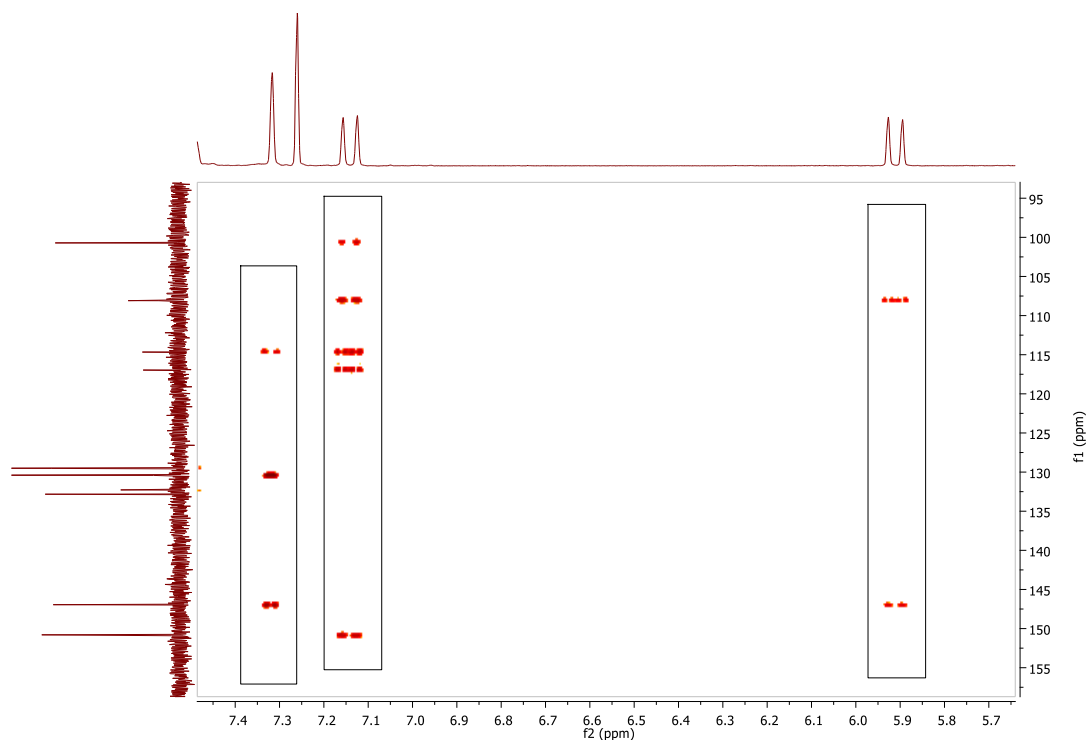
Figure 2.53. Expansion of the HMBC spectrum of bis-cyano butadiene **41**.

As can be seen in Figure 2.53, the ^{1}H NMR signal appearing at 7.14 ppm correlates to five distinct carbon signals, whilst the ^{1}H NMR signal appearing at 5.91 ppm correlates to only two distinct carbon signals. This is due to a peculiarity of the HMBC experiment in that signals arising from three bond correlations appear more intense than those of two bond correlations. Similarly the ^{1}H NMR signal appearing at 7.32 ppm correlates to three distinct carbon signals. These two and three bond relationships for bis-cyano butadiene **41** are shown in Figure 2.54**.**
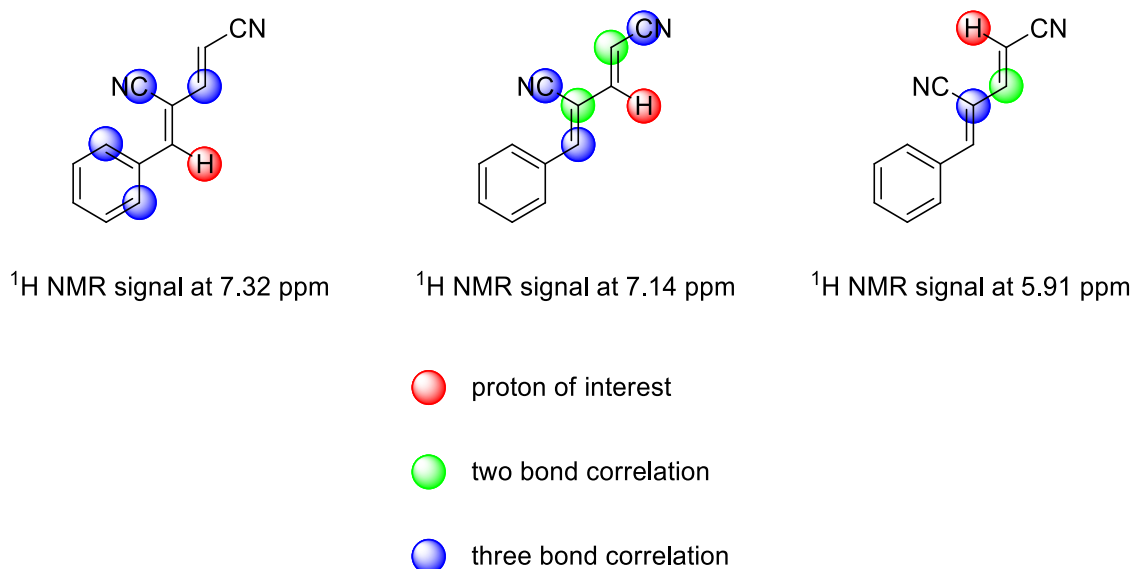
Figure 2.54. HMBC correlations for the protons on the α-olefin.

The ^{1}H NMR signal appearing at 7.14 ppm shows three bond correlations to both the nitrile quaternary carbons, whilst the ^{1}H NMR signal appearing at 5.91 ppm does not show any correlation to the quaternary nitrile carbons. The ^{1}H NMR signal appearing at 7.32 ppm does show a correlation to the quaternary nitrile carbon at 114.7 ppm as it is a three bond correlation. This discrepancy in the number of carbon signals correlating to the proton signals allows for the unambiguous assignment of the nitrile on the α-carbon as the ^{13}C NMR signal appearing at 117.0 ppm and the nitrile on the δ-carbon as the ^{13}C NMR signal appearing at 114.7 ppm. The ^{1}H NMR signal appearing at 7.14 ppm also shows a two bond correlation to the quaternary δ-carbon allowing for its assignment as the ^{13}C NMR signal appearing at 108.1 ppm.

The final signal left to assign is that of the quaternary carbon at the *ipso* position on the phenyl ring. The HMBC correlation which aides in the identification of this signal is the correlation between the protons on the *meta* position of the phenyl ring to the *ipso* carbon, which is a three bond correlation once again. This correlation is shown in Figure 2.55.
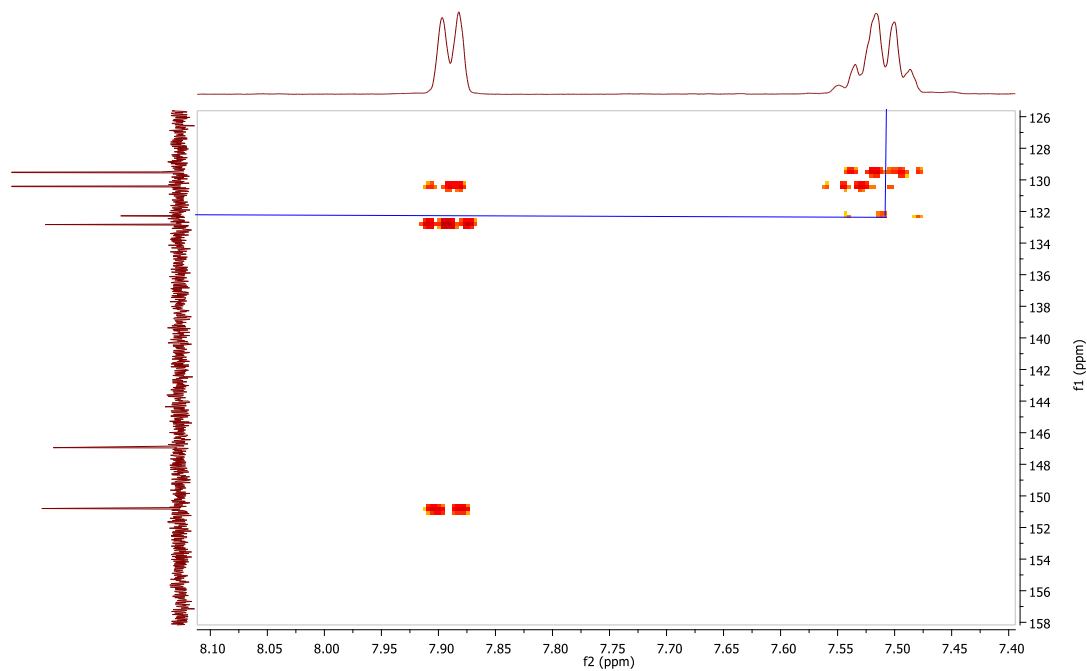
Figure 2.55. Expansion of the HMBC spectrum of bis-cyano butadiene **41**.

Through the combination of the HSQC and HMBC experiments the ^{13}C NMR spectrum of bis-cyano butadiene was unambiguously assigned as summarized in Figure 2.56.
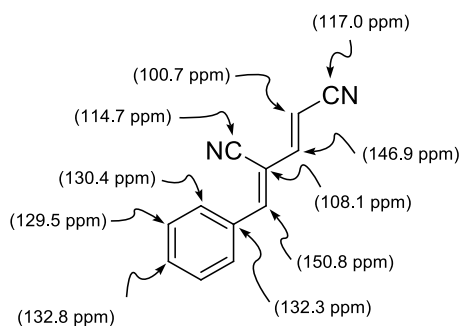
Figure 2.56. ^{13}C NMR spectral assignment of bis-cyano butadiene **41**.

2.2.6   Synthesis of cyano-ester dienes

In conjunction with efforts to access the bis-cyano substituted butadiene family, alternative routes to expand the substrate scope to include mixed butadienes were also explored. One such family of mixed butadienes was that of the cyano ester butadienes. A retrosynthetic analysis of the cyano-ester butadiene **96** is outlined in Figure 2.57. This retrosynthetic approach first leads to the secondary alcohol **97** through hydration of the alpha olefin. The next disconnection leads to the familiar α-cyano cinnamaldehyde **57** and the Reformatsky enolate **98**.
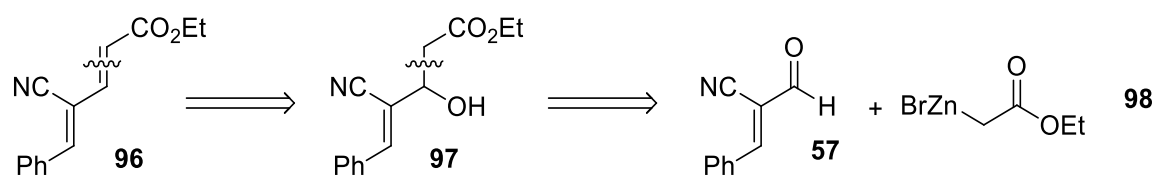
Figure 2.57. Retrosynthetic analysis of cyano-ester butadienes.

The envisaged forward synthetic route (Figure 2.58) would begin with the direct addition of the Reformatsky enolate **98** to the carbonyl carbon on the α-cyano cinnamaldehyde **57** to yield the secondary alcohol **97**. Mesylation or tosylation of the hydroxyl group of **97** would lead to the generation of a substrate **99** amenable to base induced elimination of the mesylate/tosylate group to generate the alpha olefin of the butadiene **96**.
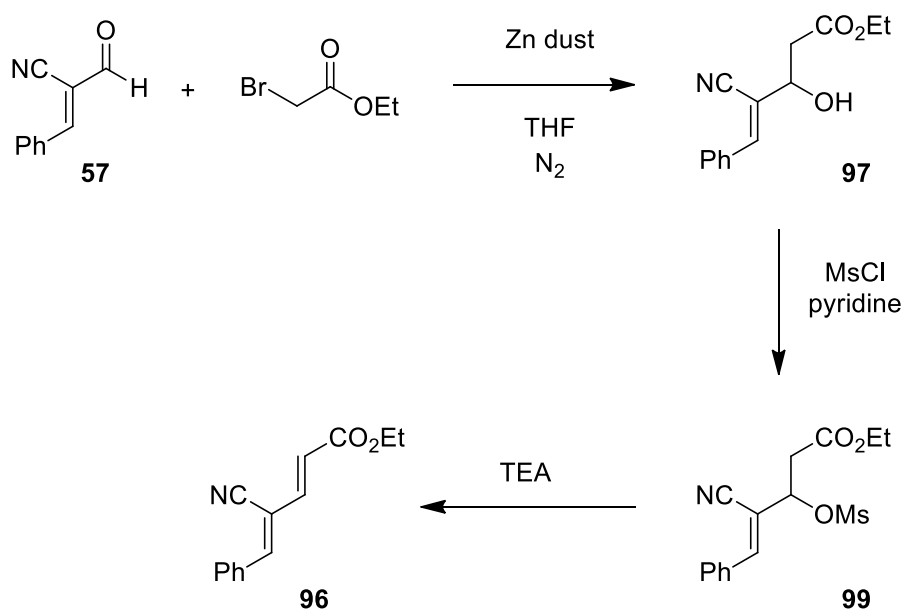
Figure 2.58. Proposed forward synthetic route towards cyano-ester butadienes.

Unfortunately the initial Reformatsky reaction did not yield the product diene **96** (Figure 2.58) and instead resulted in the formation of an intractable red resin, the composition of which could not be identified spectroscopically.

It was during these studies that we found success using 8-HQ as a polymerization inhibitor and base-free Wittig olefination conditions in the synthesis of bis-cyano butadienes, as discussed in Section 2.2.3.4. As a result, we attempted to synthesize the cyano-ester butadienes using this same methodology. This method now represented a versatile modular approach that could be applied to the synthesis of several families of butadienes through the generation and subsequent combination of different ylides and formyl acrylonitriles (Figure 2.59).
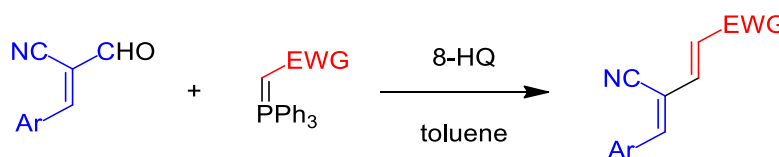
Figure 2.59. Modular synthesis of 1,3-disubstituted butadienes.

The phosphonium bromide salt **100** is readily accessible through S_N2 substitution of ethyl bromoacetate by triphenylphosphine. The bromide salt **100** was washed with 2 M NaOH to liberate the stabilized ylide **101**, which is a bench stable crystalline solid, after recrystallization from DCM/PE (78 **%** yield).
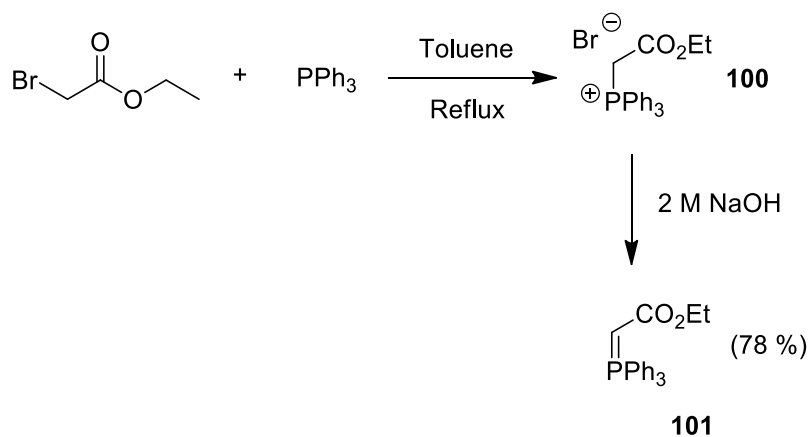
Figure 2.60. Synthesis of ethyl 2-(triphenylphosphoranylidene)acetate **101**.

The ester stabilized ylide **101** was then utilized in a Wittig reaction with formyl acrylonitriles to yield a number of cyano-ester substituted butadienes (Figure 2.61). The reactions, employing 8-HQ as a polymerization inhibitor proceeded to yield a number of cyano-ester butadienes, the yields of which are shown in Figure 2.61. Once again the yields reported are for the *E,Z* stereoisomer. The yields of the cyano-ester butadienes are typically greater than

that of the bis-cyano butadienes, with regards to the isolation of the *E,Z* stereoisomer. This is presumably due an increased preference for the formation of the *E,Z* stereoisomer during the initial [2+2] cycloaddition between the formyl acrylonitrile and the ester ylide. Thus in turn could be explained through a combination of stabilizing interactions in the transition state leading to the *E,Z* stereoisomer and destabilizing effects in the transition state leading to the *Z,Z* stereoisomer.
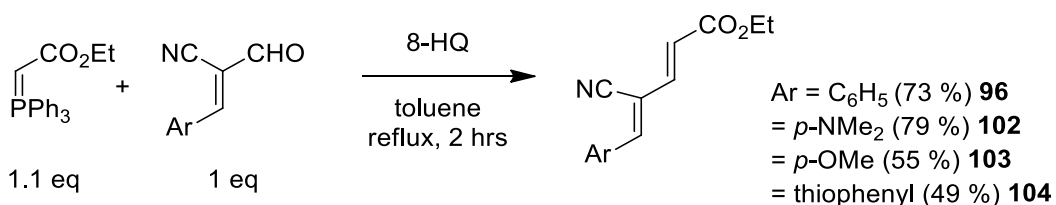
Figure 2.61. Synthesis of cyano-ester butadienes.

2.2.6.1 **Spectroscopic characterization**

In similar fashion to the bis-cyano butadiene family, the cyano-ester butadiene **96** ^{1}H and ^{13}C NMR spectra were unambiguously assigned through the use of 1D and 2D NMR experiments. The ^{1}H NMR spectrum of the cyano-ester butadiene is very similar to that of the bis-cyano butadiene with the addition of the ethyl group signals. Once again, the characteristic olefinic proton signals of the alpha olefin are present with large coupling constants of *J* = 15.4 Hz, indicative of an *E* geometry about that olefin. In this instance there is also the presence of a small allylic coupling of *J* = 0.6 Hz for the olefinic proton on the β-carbon due to ^{4}*J* coupling to the proton on the δ-carbon. The reciprocal coupling cannot be seen in the signal for the proton on the δ-carbon due to the signal appearing as a broad singlet. The signal for the proton on the α-carbon appears more downfield compared to the bis-cyano signal due to its close proximity to the strongly electron-withdrawing carbonyl group. The ^{1}H NMR spectral assignment of the cyano-ester butadiene is summarized in Figure 2.62.
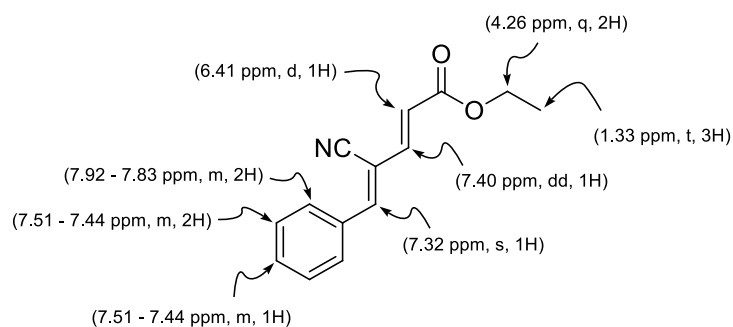
Figure 2.62. ^{1}H NMR spectral assignment of cyano-ester butadiene **96**.

Through a combination of HSQC and HMBC experiments the ^{13}C NMR could be fully assigned and these assignments are summarized in Figure 2.63. A number of signals exhibit similar chemical shifts to signals in the ^{13}C NMR spectrum of bis-cyano butadiene **41**. Similarly to the ^{1}H NMR spectrum the signal for the α-carbon appears significantly more downfield due to its proximity to the electron-withdrawing carbonyl group.
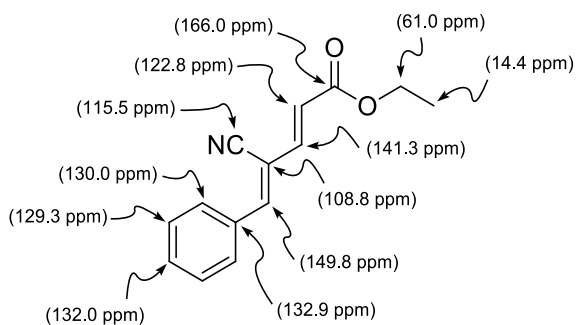
Figure 2.63. ^{13}C NMR spectral assignment of cyano-ester butadiene **96**.

2.2.7   Synthesis of cyano-phenylsulfonyl dienes

In order to further expand the substrate scope of the 1,3-bis-substituted butadienes we also investigated the synthesis of the cyano-sulfonyl butadiene family. In terms of reactivity, we expected this family to lie between that of the already explored bis-phenylsulfonyl butadienes and newly synthesized bis-cyano butadienes. A number of members of this family had already been synthesized by Masuyama *et al.* and applied to an achiral Michael-type addition cyclization reaction with aldehydic enamines.[95] Padwa *et al.* also synthesized the unsubstituted phenyl cyano phenylsufonyl butadiene **105** (the geometry of which was not assigned) and applied it to a [4+2] cycloaddition with aryl imines to yield a tetrahydropyridine product **106** Figure 2.64.[74]
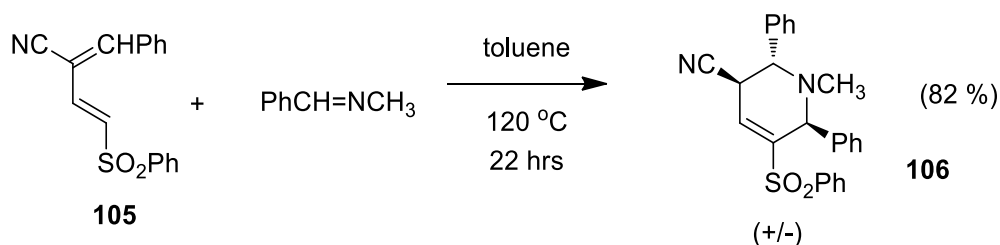
Figure 2.64. [4+2] cycloaddition of cyano-phenylsulfonyl butadiene **105** reported by Padwa *et al.*[74]

The modular approach to butadiene synthesis was attempted to access the cyano-phenylsulfonyl butadienes. The retrosynthetic analysis of the cyano-phenylsulfonyl butadiene family shows that access to the stabilized phenylsulfonyl ylide **107** would be required (Figure 2.65).
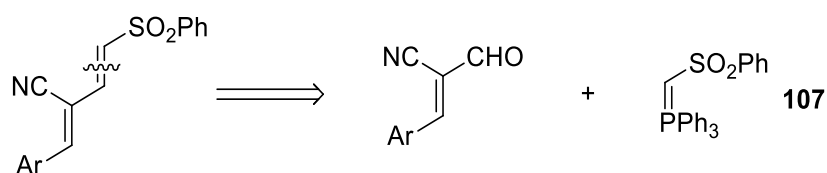
Figure 2.65. Retrosynthetic analysis of cyano-phenylsulfonyl butadienes.

As this ylide should by highly stabilized by the inductive withdrawal of the phenylsulfonyl group, it was reasoned that access to this ylide would be quite facile. Despite a number of attempts to access the phenylsulfonyl ylide, the isolation and purification of the ylide in

synthetically useful quantities proved to be too difficult. The attempted routes utilized to access the phenylsulfonyl ylide **107** are detailed in Figure 2.66.
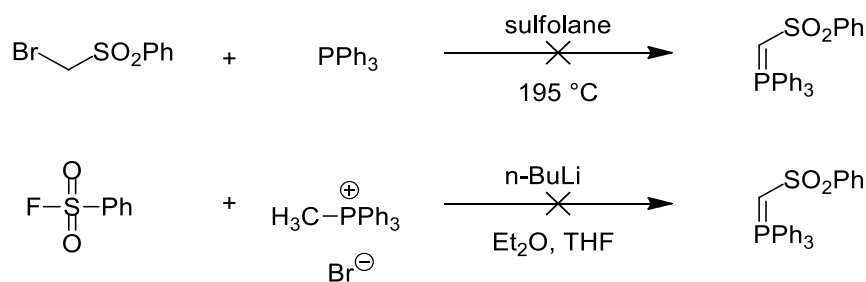
Figure 2.66. Attempted syntheses of phenylsulfonyl ylide **107**.

As attempts to access the phenylsulfonyl ylide **107** were not fruitful, the synthesis of the cyano-phenylsulfonyl butadienes was attempted using the methodology that our group had already employed in the synthesis of the bis-phenylsulfonyl butadienes and the bis-ester butadienes. Bromination and subsequent elimination of allyl cyanide yielded the bromo cyano propene **108**. The propene was then subjected to reaction with the sodium salt of benzenesulfinic acid in refluxing MeOH to generate the cyano phenylsulfonyl propene **109** as a black foul smelling oil in a crude yield 28 % (Figure 2.67). This material was utilized without any further purification.
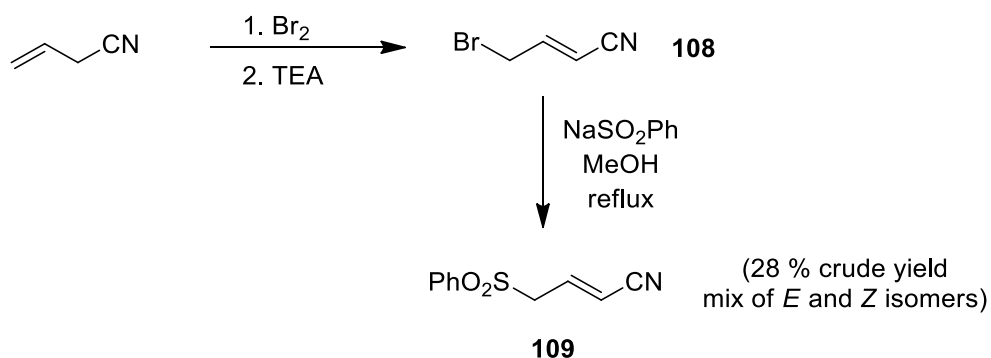
Figure 2.67. Synthesis of cyano phenylsulfonyl propene **109**.

The cyano phenylsulfonyl propene **109** could then be subjected to Knoevenagel condensation with aryl aldehydes using Al_2O_3 as the catalyst to yield the cyano phenylsulfonyl butadienes (Figure 2.68).
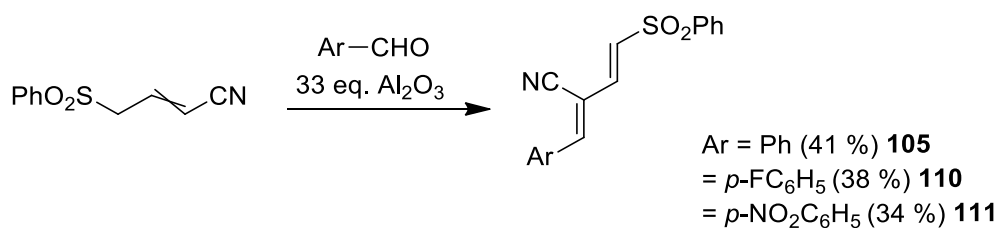
Figure 2.68. Synthesis of the cyano phenylsulfonyl butadienes.

2.2.7.1   Spectroscopic characterization

The ^{1}H and ^{13}C spectra of the cyano-phenylsulfonyl butadiene **105** were unambiguously assigned through the use of 1D and 2D experiments. The geometry of the α-olefin of the cyano phenylsulfonyl butadienes could be assigned as *E* using ^{1}H NMR spectroscopy as the large coupling constant of *J* = 14.9 Hz resulting from the olefinic proton on the α-carbon could be observed. The reciprocal coupling constant for the signal arising from the proton on the β-carbon could not be observed as it overlapped with signals arising from aromatic protons. The geometry of the γ-olefin could not be assigned by ^{1}H NMR as there are no adjacent protons from which useful coupling constants could be gleaned. The ^{1}H NMR spectral assignment of the cyano-phenylsulfonyl butadiene is summarized in Figure 2.69.
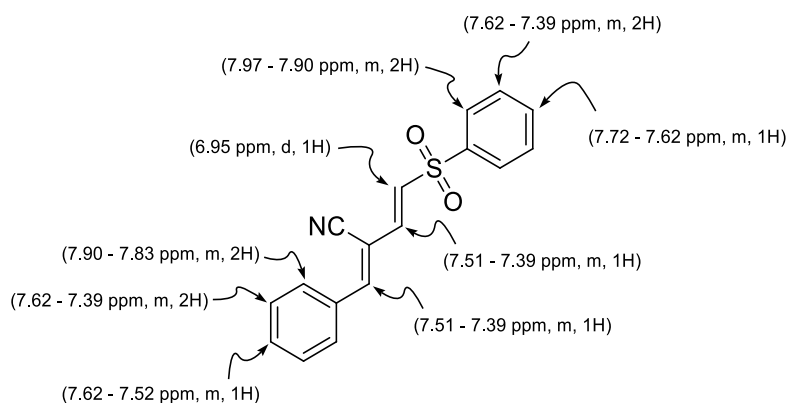
Figure 2.69. ^{1}H NMR spectral assignment of cyano-phenylsulfonyl butadiene **105**.

The ^{13}C NMR spectral assignement of the cyano-phenylsulfonyl butadiene is summarized in Figure 2.70.
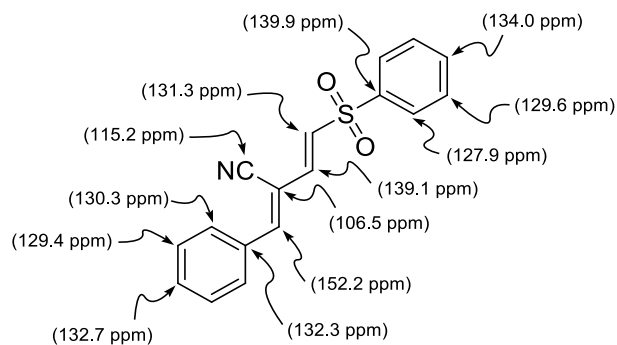
Figure 2.70. ^{13}C NMR spectral assignment of cyano-phenylsulfonyl butadiene **105**.

X-Ray crystallographic analysis was performed on crystals grown of the unsubstituted phenyl cyano phenylsulfonyl butadiene **105** in order to confirm the geometry of both olefins. This led to the assignment of the cyano phenylsulfonyl butadienes as 1*E*,3*Z* (Figure 2.71).
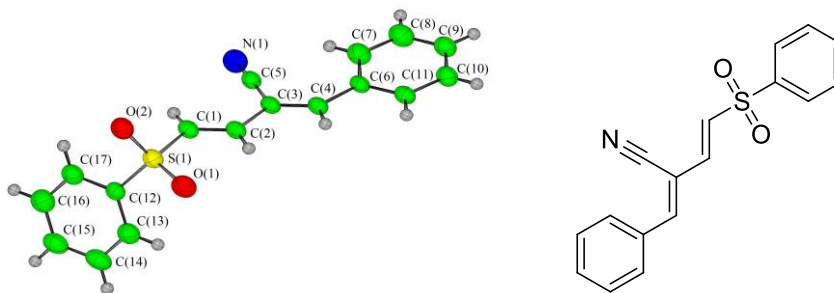
Figure 2.71. X-Ray crystal structure of phenyl cyano phenylsulfonyl butadiene **105**.

2.2.8   Attempted synthesis of γ-ester butadienes

We were also interested in how variations in the electron-withdrawing substituent on the γ-carbon affects the reactivity of the butadienes. To achieve this we explored this synthesis of butadienes with an ester group on the γ-carbon. In theory, the α-carbon could then be adorned with an additional electron-withdrawing group to yield novel families of electron poor bis-substituted butadienes.

A retrosynthetic analysis of γ-ester butadienes can be seen in Figure 2.72. Starting from the butadiene **112**, disconnecting the α-olefin leads to similar synthetic intermediates to those we had already utilized in the synthesis of butadienes and so this seemed like a logical route to pursue. The formyl acrylate **113** represents a challenge as it contains geminal, yet different, carbonyl groups namely the aldehyde and the ester groups. Disconnecting the ester functionality first leads to the bromo-acetal **114**, which after an FGI leads to the bromo-cinnamaldehyde **115**. Bromo-cinnamaldehyde can be readily synthesized from commercially available cinnamaldehyde **116**.
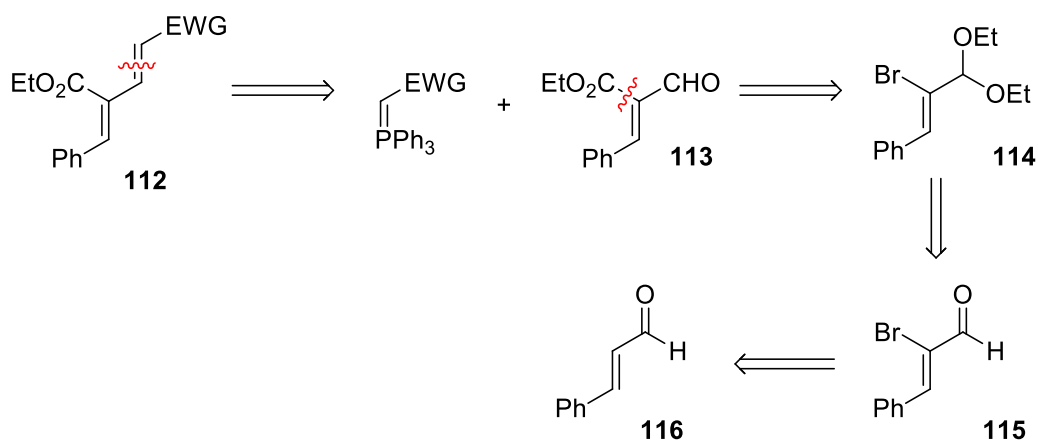
Figure 2.72. Retrosynthetic analysis of 3-ester butadienes **112**.

The forward synthetic route to the γ-ester butadienes is shown in Figure 2.73. Starting from cinnamaldehyde, the bromination and subsequent elimination of HBr yields α-bromocinnamaldehyde **115**. To install the ester functionality we envisaged utilizing Li/Br exchange and quenching with ethyl chloroformate. This transformation requires the use of a strong lithiated base such as n-BuLi and therefore protection of the aldehyde from any direct nucleophilic attack by the base is required.
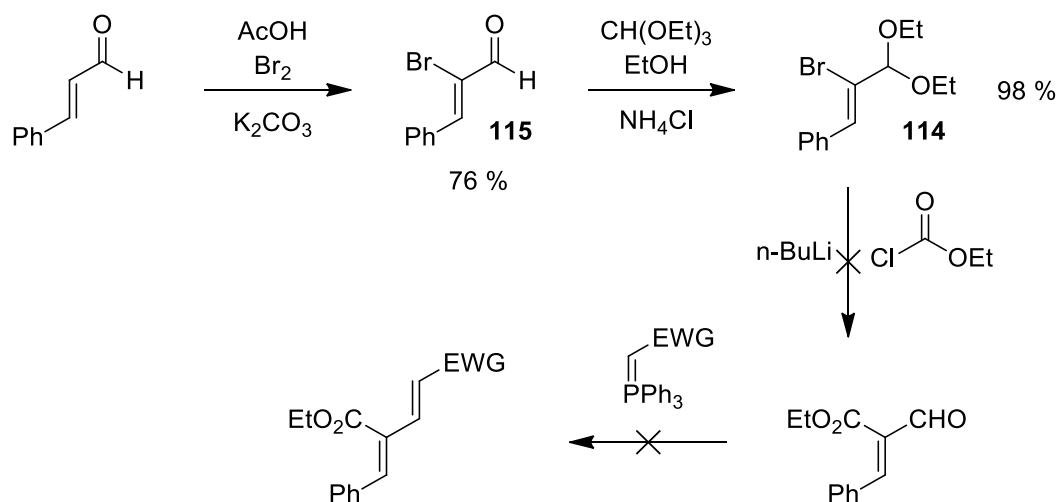
Figure 2.73. Proposed forward synthetic route to 3-ester butadienes.

The acetal protecting group was chosen as it is stable under strongly basic conditions and can be readily removed under acidic conditions at room temperature. Interestingly, the acetal protection of **115** did not proceed to completion under what would be considered normal acetal forming conditions (excess EtOH in the presence of catalytic amounts of *p*-toluenesulfonic acid). Instead, we had to employ the entropically driven acetal formation utilizing triethyl orthoformate in the presence of ammonium chloride. This strategy yielded the α-bromo acetal **114** in near quantitative yield (98 %).

With the α-bromo acetal in hand it was applied to the Li/Br exchange reaction and quenched with ethyl chloroformate. The acetal protecting group was removed as part of the reaction workup. The reaction generated a mixture of cinnamaldehyde, obtained through the protonation of the intermediate lithiated alkene, and the product as a mixture of inseparable isomers and as the minor product as observed by ^{1}H NMR spectroscopy. As a result, the final olefination reaction could not be carried out.

2.2.9   Synthesis of trienes

2.2.9.1   Synthesis of 1,5-bis-cyano hexatriene

We were also interested in whether our methodology could be applied to the synthesis of vinylogous hexatrienic substrates. These substrates would be of interest in the study of 1,8-conjugate addition reactions (Figure 2.75). As with the related 1,6-conjugate addition, limited attention has been given to organocatalytic variants of the synthetically interesting 1,8-conjugate addition. This is presumably due to the compounding regioselectivity issues arising from the introduction of new electrophilic sites on the olefinic backbone. To the best of our knowledge, an organocatalytic 1,8-conjugate addition has not been reported in the literature to date. A number of organometallic efforts have been described utilizing transition metal catalysts and in particular copper catalysis.[96-98]

A recent example of efforts in this area is that of the work of Feringa *et al*. in which they describe the conjugate addition of Grignard reagents to esters and thioesters in the presence of the chiral reversed JosiPhos ligand **117** (Figure 2.74).[96] This report exemplifies the difficulty that still remains in the control of regio- and enantioselectivity of extended conjugate addition reactions as the authors could only achieve both moderate regio- and stereocontrol, as shown in entries 1 and 2 of Figure 2.74.

Figure 2.74. 1,8-conjugate addition reported by Feringa *et al.*[96] X = OEt/Set, R = Me/Et.
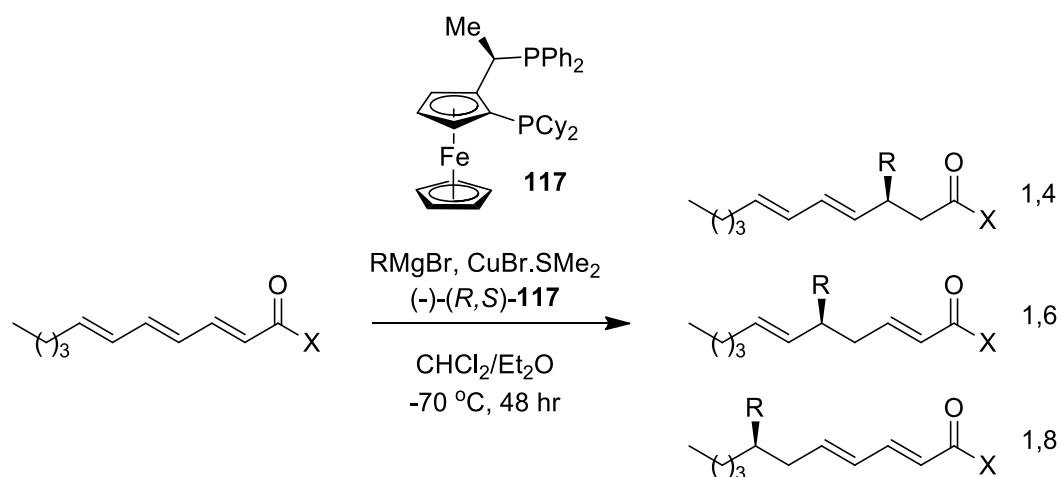
Entry	X	R	cat. (%)	conv. (%)	Yield	1,8:1,6:1,4	ee of 1,8-product
1	OEt	Et	5	>95	47	63:8:2	7
2	Set	Me	7.2	92	63	86:0:14	72

As can be seen in Figure 2.75, the same retrosynthetic analysis can be applied to 1,5-hexatrienic substrates as applied to the butadienic substrates described previously. The installation of the two olefins was planned through the use of stabilized ylides in Wittig olefination reactions starting from the phenyl formyl acrylonitrile **57**.
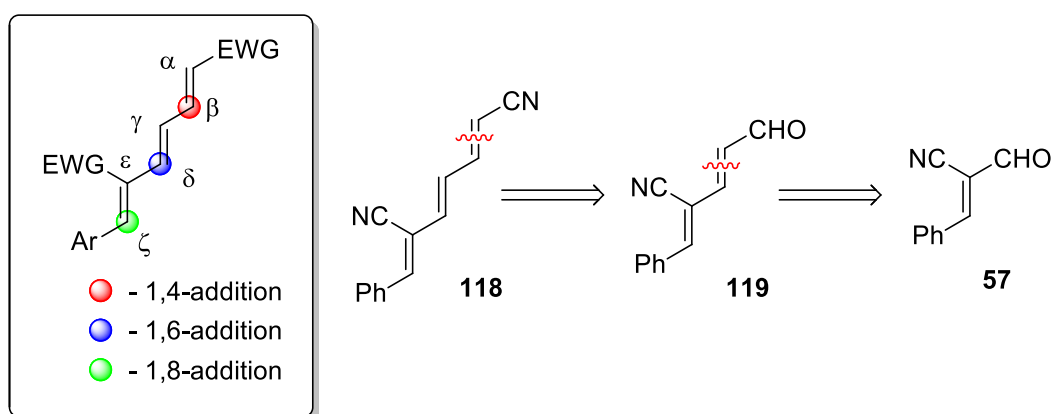
Figure 2.75. Reactivity pattern and retrosynthetic analysis of 1,5-bis-cyano hexatriene **118**.

Applying this in a forward synthetic scheme led to the results outlined in Figure 2.76. The aldehyde ylide **120** was synthesized according to literature procedure in 69 % yield.[99] The intermediate dienal **119** was obtained in low yield (36 %). The dienal **119** could then be applied to a further Wittig olefination with the nitrile ylide **71** already prepared. Whilst the triene **118** could be obtained, it was also in low yield (31 %). In addition to the low yield of the olefination reactions the presence of two isomers of the product triene **118** could be observed by ^{1}H NMR spectroscopy.
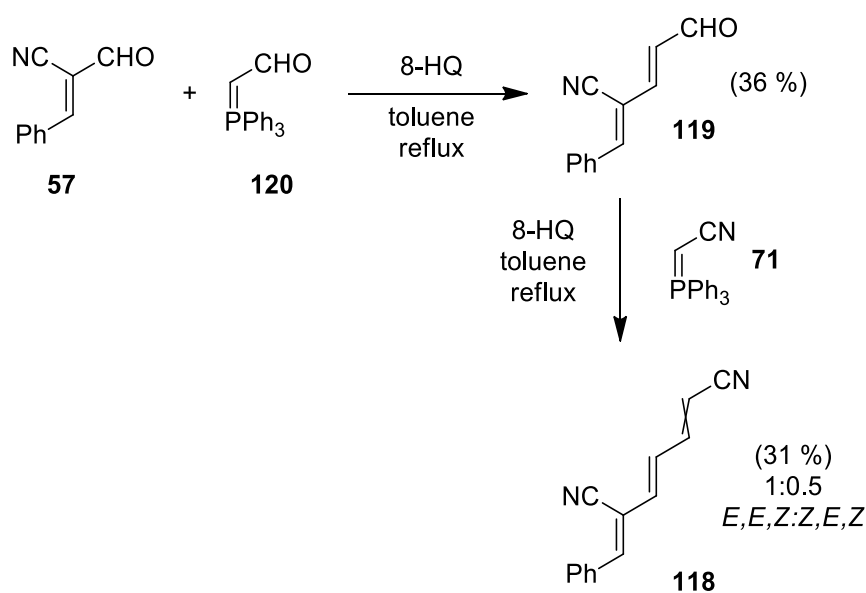
Figure 2.76. Synthesis of 1,5-biscyano hexatriene **118**.

The difficulty in obtaining isomerically pure starting hexatrienic starting materials dissuaded us from exploring these substrates further at this time.

2.2.10   Attempted synthesis of 1,1,3-trisubstituted butadienes

In an attempt to synthesize a 1,1,3-trisubstituted butadiene, which would in theory be more activated that the 1,3-disubstituted butadiene families, we envisaged the retrosynthetic analysis as outlined in Figure 2.77. Through a simple Knoevenagel condensation of formyl acrylonitrile **57** and malononitrile, the alpha olefin could be installed to yield the target butadiene **121**.
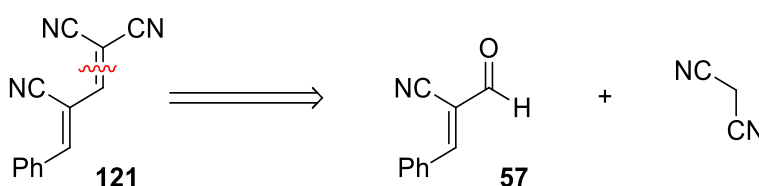
Figure 2.77. Retrosynthetic analysis of 1,1,3-trisubstituted butadiene **121**.

When the forward reaction was attempted, instead of the expected butadiene product **121**, we observed the formation of the 4-H amino pyran **122**, Figure 2.78. Presumably this product is formed through the conjugate addition of the highly stabilized malononitrile anion to the olefin of formyl acrylonitrile. This conjugate addition is then followed by attack of the resulting oxyanion on the nitrile carbon followed by imine/amine tautomerization to yield the 4-*H*-amino-pyran **122**.
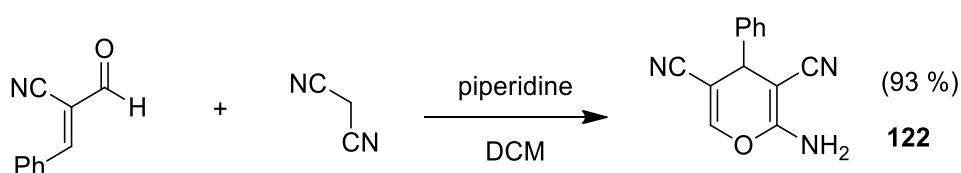
Figure 2.78. Synthesis of 4-*H*-amino-pyran **122**.

Investigations into the reactivity of formyl acrylonitriles in these conjugate addition reactions was continued and will be discussed in more detail in Chapter 4.

2.2.11   Computational studies on butadiene substrates

In order to further develop our understanding of the potential reactivity of the newly synthesized butadienes, we thought it helpful to gain some insight into the stability of different configurations/conformations of the butadiene scaffolds. In order to do this, the ground state energies for four distinct 4-phenyl substituted butadienes was investigated utilizing Density Functional Theory (DFT) at the B3LYP/6-31g(d) level of theory. The butadienes investigated were: 1) the phenyl bis-cyano butadiene **41**; 2) the cyano-ester butadiene **96**; 3) the cyano-phenylsulfonyl butadiene **105**; and 4) the bis-phenylsulfonyl butadiene **123** (Figure 2.79).
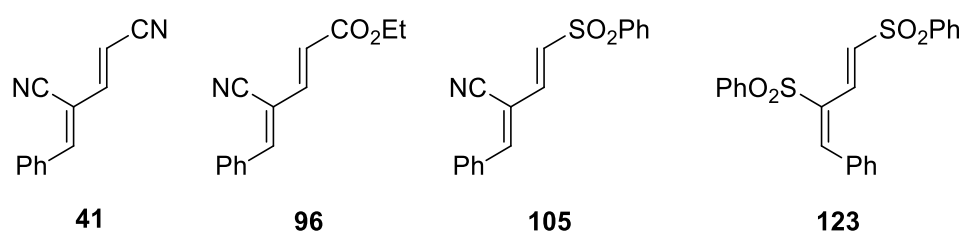
Figure 2.79. Butadienes investigated computationally.

In the case of each butadiene optimized geometries were found for eight possible configurations/conformations and the computed ground state energies of these were calculated. These results could then be compared to experimentally observed trends in the synthesis of the butadienes.

2.2.11.1 Bis-cyano diene (41)

In the case of the pheyl bis-cyano butadiene **41**, as can be seen in Figure 2.80, the *s-trans E,Z* butadiene conformation/configuration was found to have the lowest computed ground state energy. This would be in agreement with what is observed experimentally in that the *E,Z* isomer was the major constituent of crude reaction mixtures. Whilst it was not possible to unambiguously assign the geometry of the γ-olefin of the bis-cyano butadienes through NMR spectroscopy, or X-ray crystallographic analysis, it is a reasonable assumption based on the mechanism of the Wittig reaction (Section 2.2.3.4.1) that the geometry of the formyl acrylonitrile remains unchanged and therefore the geometry of the butadiene can be assigned as *E,Z*. The *s-trans* conformation was found to be 3.6 kcal/mol lower in energy than that of the *s-cis* conformation. This is presumably due to steric clashes arising from the close proximity of substituents on the two olefins.
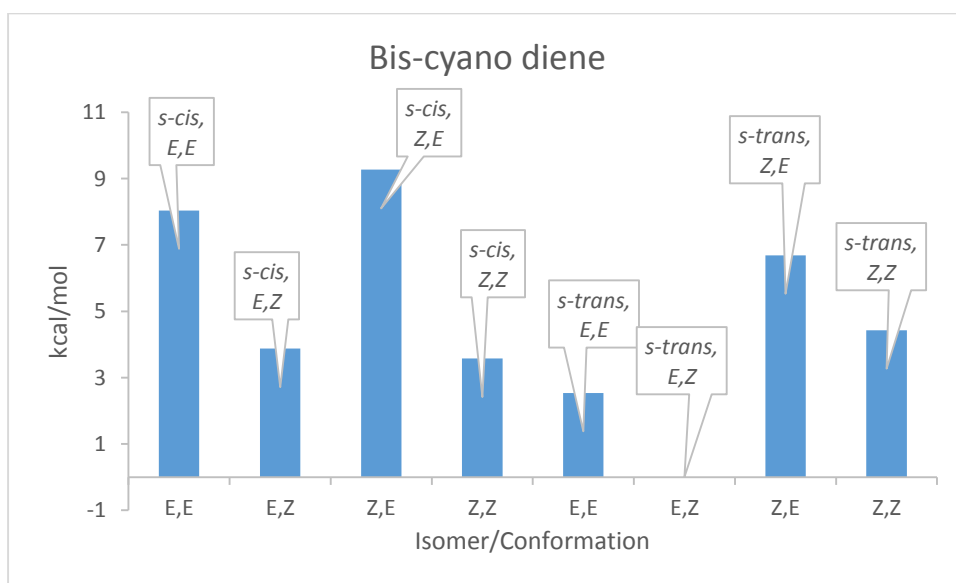
Figure 2.80. Bis-cyano diene conformation/isomer comparison. Energies relative to isomer/conformation with lowest computed ground state energy.

In the case of the other experimentally observed isomer, the *Z,Z* isomer, the *s-cis* conformation was found to have a lower computed ground state energy than that of its *s-trans* counterpart. Relative to the lowest energy configuration/conformation (the *s-trans E,Z* isomer), the *s-cis Z,Z* isomer was found to be 3.6 kcal/mol higher in energy and the *s-trans Z,Z* isomer was found to be 4.4 kcal/mol higher. With only a 0.8 kcal/mol difference in energy

between the *s-cis* and *s-trans* conformation it is difficult to state conclusively which conformation would predominate in solution.

None of the other configurations/conformations of the bis-cyano butadiene were experimentally observed and the computed ground state energies for these other configurations/conformation were all found to be higher in energy than that of the lowest configuration/conformation, the *s-trans E,Z* isomer, Table 2.4. Optimized structures can be found in Appendix 6.1.

Table 2.4 – Relative computed ground state energies for all conformation/isomer combinations

Conformation	Isomer	kcal/mol
s-cis	E,E	8.0
	E,Z	3.9
	Z,E	9.3
	Z,Z	3.6
s-trans	E,E	2.5
	E,Z	0
	Z,E	6.7
	Z,Z	4.4

2.2.11.2 Cyano-ester butadiene (96)

In the case of the cyano-ester butadiene, experimentally once again the *E,Z* isomer was found to be the predominate configuration. Computationally the *s-trans E,Z* isomer was also found to be the lowest energy ground state. The *s-cis Z,E* configuration/conformation was found to be 11.3 kcal/mol higher in energy and therefore it is reasonable to assume that there would be a preference for this conformation of the diene. This high energy difference is presumably due to steric clashes arising from the close proximity of substituents on the two olefins.
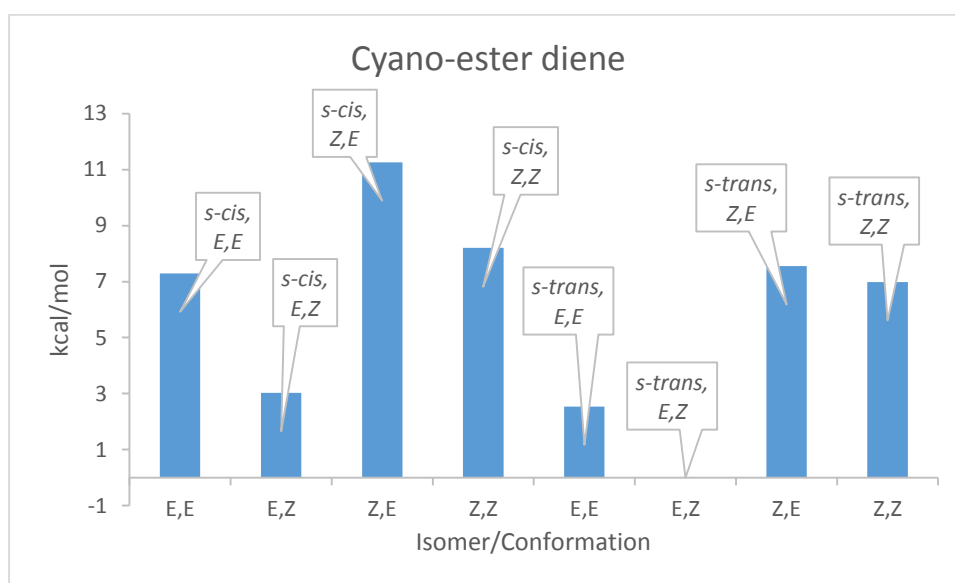
Figure 2.81. Cyano-ester diene conformation/isomer comparison. Energies relative to isomer/conformation with lowest computed ground state energy.

Once again, all other configurations/conformations were found to be higher in energy than that of the *s-trans E,Z* isomer, Table 2.5. Optimized structures can be found in Appendix 6.1.

Table 2.5 Relative computed ground state energies for all conformation/isomer combinations

Conformation	Isomer	kcal/mol
s-cis	E,E	7.3
	E,Z	3.0
	Z,E	11.3
	Z,Z	8.2
s-trans	E,E	2.5
	E,Z	0.0
	Z,E	7.6
	Z,Z	7.0

2.2.11.3 Cyano-phenylsulfonyl diene (105)

In the case of the cyano-phenylsufonyl butadienes, again the *s-trans E,Z* conformation/configuration was found to have the lowest computed ground state energy. In this instance this configuration/conformation could be confirmed by X-ray crystallographic analysis and is therefore unambiguously in agreement with the computational results.
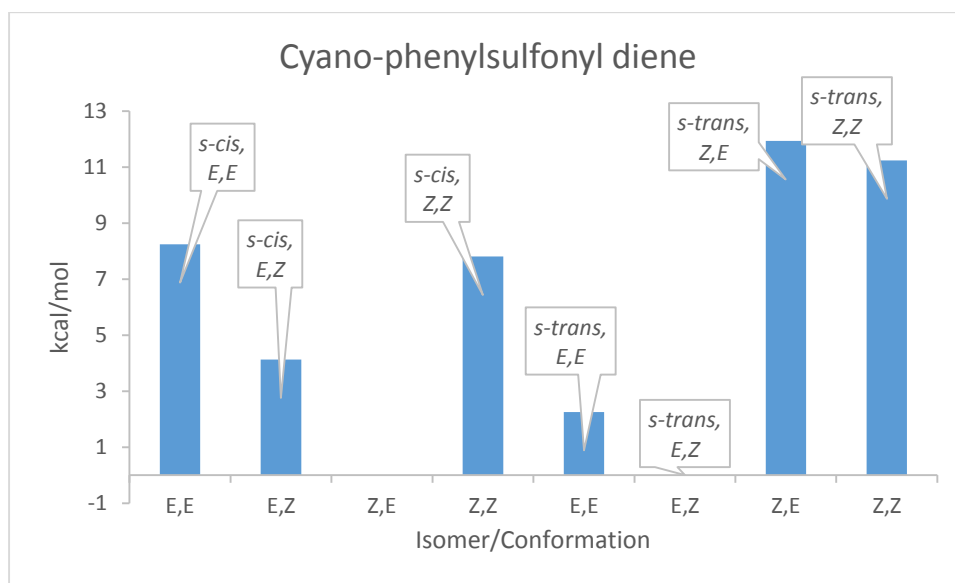
Figure 2.82. Cyano-phenylsulfonyl diene conformation/isomer comparison. Energies relative to isomer/conformation with lowest computed ground state energy.

Interestingly, a computed lowest ground state energy could not be found for the *s-cis Z,E* configuration/conformation, Table 2.6. This is presumably due to the large steric clash between the phenylsulfonyl group, when the α-olefin exhibits a *Z* geometry, with the rest of the butadiene scaffold in the *s-cis* conformation. Optimized structures can be found in Appendix 6.1.

Table 2.6 Relative computed ground state energies for all conformation/isomer combinations

Conformation	Isomer	kcal/mol
s-cis	E,E	8.2
	E,Z	4.1
	Z,E	N/A
	Z,Z	7.8
s-trans	E,E	2.3
	E,Z	0.0
	Z,E	11.9
	Z,Z	11.2

2.2.11.4 Bis-phenylsulfonyl diene (123)

In contrast to the other butadienes investigated, the bis-phenylsulfonyl butadiene was found to have a different lowest energy ground state conformation/configuration, that of the *s-trans E,E* butadiene. This ties in with experimental observations that the *E,E* configuration was the only configuration observed during the studies of the reactions of this butadiene. Furthermore, there is X-ray crystallographic data showing the *E,E* butadiene in a *s-trans* conformation.[69] In this conformation it would be impossible for this butadiene to undergo a concerted Diels-Alder cycloaddition type reaction and if it were to undergo a cycloaddition it would have to occur through some step-wise process. This observation is relevant to mechanistic discussion on the reactions of this butadiene and is discussed in more detail in Chapter 3.
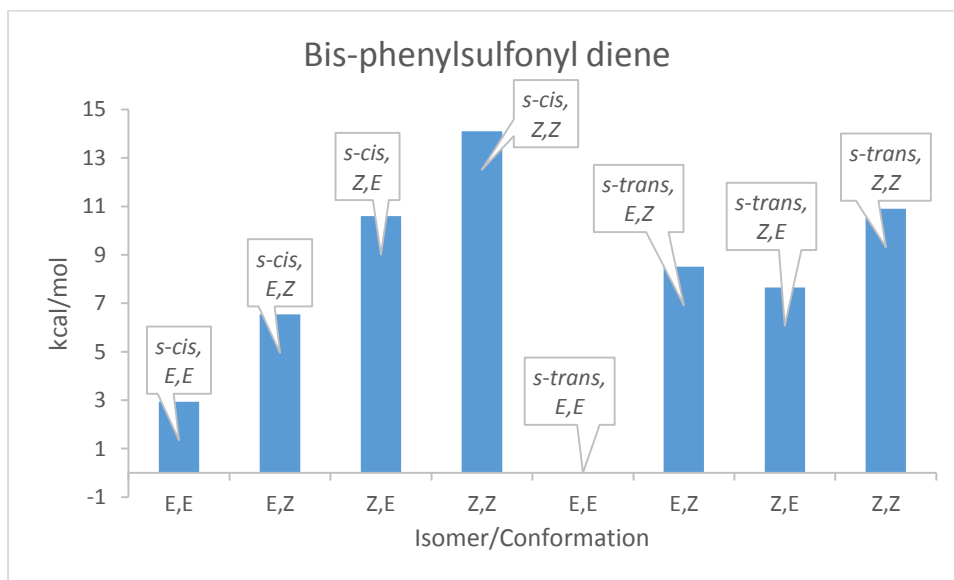
Figure 2.83. Bis-phenylsulfonyl diene conformation/isomer comparison. Energies relative to isomer/conformation with lowest computed ground state energy.

None of the other configurations/conformations of the bis-phenylsulfonyl butadiene were experimentally observed and the computed ground state energies for these other configurations/conformation were all found to be higher in energy than that of the lowest configuration/conformation, the *s-trans E,E* isomer, Table 2.7. Optimized structures can be found in Appendix 6.1.

Table 2.7 Relative computed ground state energies for all conformation/isomer combinations

Conformation	Isomer	kcal/mol
s-cis	E,E	2.9
	E,Z	6.5
	Z,E	10.6
	Z,Z	14.1
s-trans	E,E	0.0
	E,Z	8.5
	Z,E	7.7
	Z,Z	10.9

2.3 Conclusion and future work

In conclusion, access to the bis-cyano butadiene family proved to be exceptionally difficult due to the instability of these highly conjugated nitrile systems. Through extensive reaction screening, a high yielding route employing a base-free Wittig reaction to yield families of bis-cyano and cyano-ester 1,3-butadienes has been developed. Access to these butadienes required the synthesis of a family of substituted formyl acrylonitriles, which are in themselves interesting substrates and will be discussed further in Chapter 4. This approach to diene synthesis represents a modular approach towards the construction of 1,3-disubstituted butadienes depending on the combination of ylide and formyl acrylonitrile utilized.
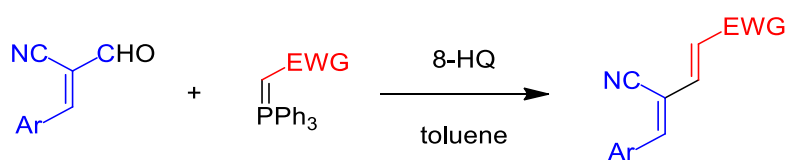
Figure 2.84. Modular synthesis of 1,3-disubstituted butadienes.

Future work includes expansion of this methodology to the formyl acrylonitriles not already explored as well as the synthesis of additional stabilized ylides to give access to new butadiene families.

In addition to the two previous butadiene families, access to the mixed cyano-phenylsulfonyl butadiene family was also achieved utilizing a previously developed Knoevenagel condensation strategy to build the diene backbone. An X-ray structure of one of the members of this butadiene family was obtained unambiguously confirming the olefin geometries as *E,Z.*

Preliminary studies towards the synthesis of 1,5-bis-subtituted hexatrienes as novel substrates for the study of extended conjugate addition chemistry also showed some promise in that the substrates could be accessed. The low yields and the presence of two stereoisomers in the final product have presented challenges yet to be addressed.

Finally, DFT studies were performed on a selection of the diene substrates to determine ground state energies for the possible isomers/conformations and these studies matched experimental observations of the favoured isomers/conformations.

Studies of the reactions of these three intriguing substrates will be discussed in Chapter 3.

3   Chapter 3: Applications of 1,3-bis-substituted butadienes

3.1   Introduction

This chapter describes efforts to explore the synthetic utility of the electron-deficient butadienes, the synthesis of which was discussed in Chapter 2, in a number of synthetic transformations. Preliminary investigations on the asymmetric 1,6-conjugate addition of aldehydic enamines to the bis-cyano butadienes were undertaken by a previous group member and expansion of this methodology to the novel members of this family is of interest. The newly synthesized families of cyano-ester and cyano-phenylsulfonyl electron-deficient butadienes are also potentially applicable to this conjugate addition methodology. All three families also represent substrates of interest in a number of other transformations which utilize their electron-deficient nature such as the Baylis-Hillman reaction, IEDDA cycloadditions and IEDHDA reactions.

3.1.1   Organocatalytic ACA to electron-deficient dienes

With a number of novel electron-deficient butadiene substrates in hand we could now begin investigations into their applicability in asymmetric organocatalytic conjugate addition chemistry. As already discussed in detail in Chapter 1, conjugate addition reactions are amongst some of the most useful synthetic transformations and allow for access to a wide range of synthetically valuable scaffolds. Inspired by the previous successes within our group we initially began with the addition of aldehydic enamines to these novel butadienes.[58,59]

3.1.2   Bis-cyano butadienes as substrates in 1,6-conjugate addition reactions

The first bis-cyano substrate subjected to the 1,6-conjugate addition was the phenyl substituted bis-cyano butadiene **41**. This initial work was carried out by John Murphy utilizing the small amounts of diene accessible through the HWE olefination procedure outlined in Section 2.2.2 .[69] John Murphy employed similar conditions to those that were employed to give bis-phenylsulfonyl and bis-ester cyclic hexadienes in high yields and with a high degree of enantiocontrol (Figure 3.1).[58,59,69]
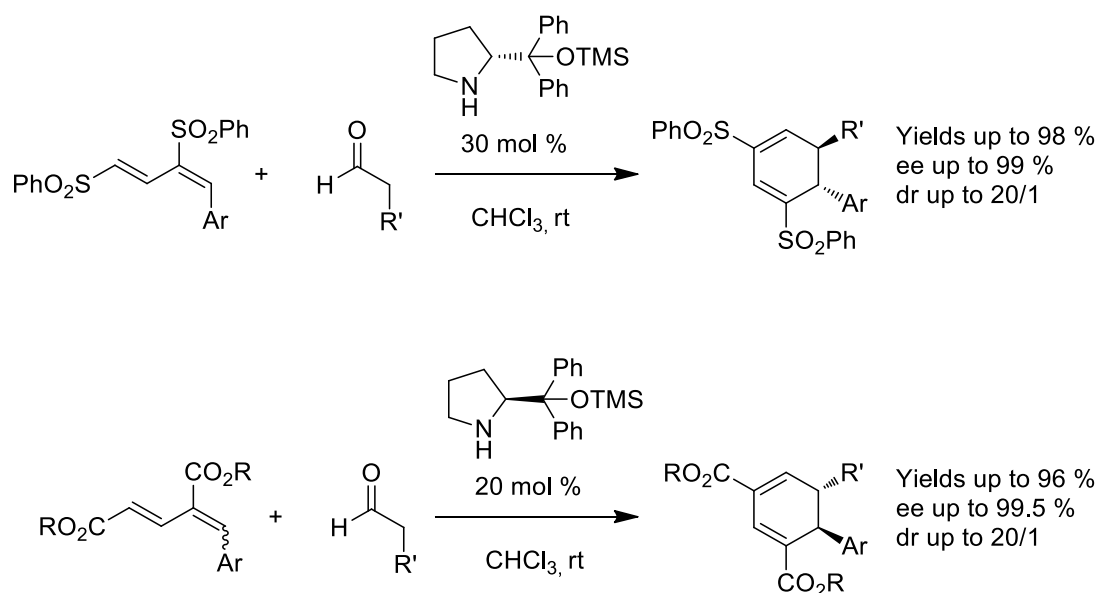
Figure 3.1. The conjugate addition of aldehydic enamines to bis-phenylsulfonyl and bis-ester butadienes reported by Stephens and Alexakis.[58,59]

However, in the case of the bis-cyano butadiene **41** a significantly more complicated reaction occurred and after significant spectroscopic characterization the major side-product was identified as the biaryl **125** (Figure 3.2).[69]
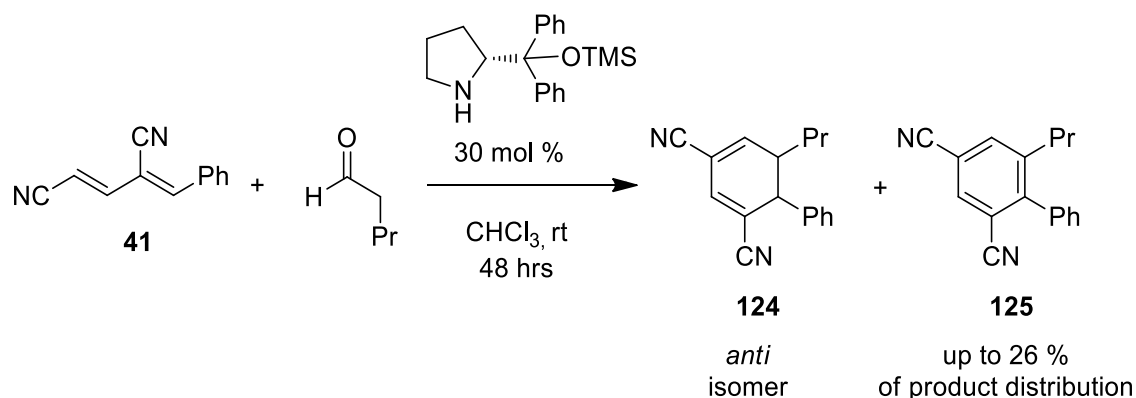
Figure 3.2. Organocatalytic conjugate addition of aldehydic enamines to bis-cyano butadiene **41** to yield the cyclic hexadiene **124** and the aromatized biaryl **125**.[69]

This identification was later confirmed by mass spectrometry. This product is presumably formed through the aromatization of the desired cyclic hexadiene product **124**. The ^{1}H NMR spectra of crude reaction mixtures were complicated by the presence of other side-products,

the identity of which could not be confirmed but could be presumed to be a combination of self-aldol products and diene degradation products.

The two major products, the cyclic hexadienes and the biaryl, shared similar R_f's under the screened chromatographic solvent mixtures making separation and isolation difficult by silica gel flash column chromatography.

John Murphy also performed an additive screen in order to try and limit the formation of the biaryl product. This screen identified 4-nitrobenzoic acid (4-NBA) as an additive that appeared to significantly reduce, but not completely inhibit, the formation of the biaryl product. With these refined reactions conditions John Murphy was then able to investigate the 1,6-conjugate addition of a number of aldehydic enamines to the phenyl substituted bis-cyano butadiene **41**. These results are shown in Table 3.1.[69]
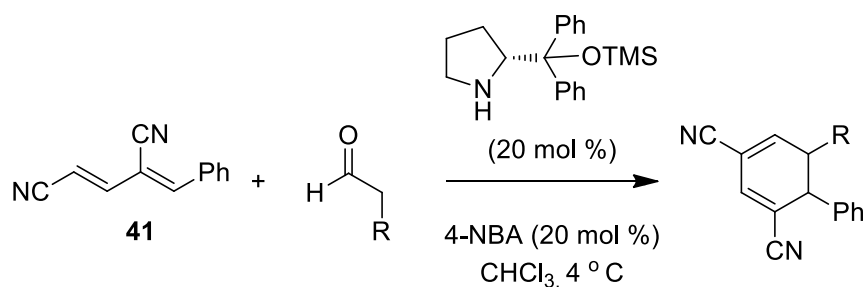
Table 3.1. 1,6-conjugate addition of aldehydic enamines to bis-cyano butadiene **41**.[69]

Entry	Cat.	Time (hr)	R	Yield	dr (*syn/anti*)	ee (%)
1	(*R*)	24	*n*Pr	72	1:99	99
2	(*R*)	68	*i*Pr	66	1:99	99
3	(*R*)	30	allyl	75	1:99	99
4	(*R*)	30	Ph	66	1:99	69
6[a]	(*S*)	38	Ph	75	1:99	-96

a - no acid additive used to reduce self-aldol chemistry.

As seen in Table 3.1, the cyclic hexadienes were obtained in moderate yields and with high stereocontrol. The diastereomeric ratio could also be observed by ^{1}H NMR spectroscopy and in each case the only diastereoisomer present was the *anti* diastereoisomer.

This chapter, in part, describes the continuation of these studies on the 1,6-conjugate addition to the phenyl substituted bis-cyano butadiene **41** and further explores the reactivity

of the extended family of bis-cyano butadienes as well as the cyano-ester and cyano-phenylsulfonyl butadienes.

3.2   Results and Discussion

3.2.1   Extended bis-cyano butadiene family

A number of the novel bis-cyano butadienes were applied to the 1,6-conjugate addition using the reaction conditions refined by John Murphy.[69] These efforts are summarised in Table 3.2. Despite increased reaction temperatures and extended reaction times the cyclic hexadiene products were not observed and instead a complex mixture resulted, including returned starting material.
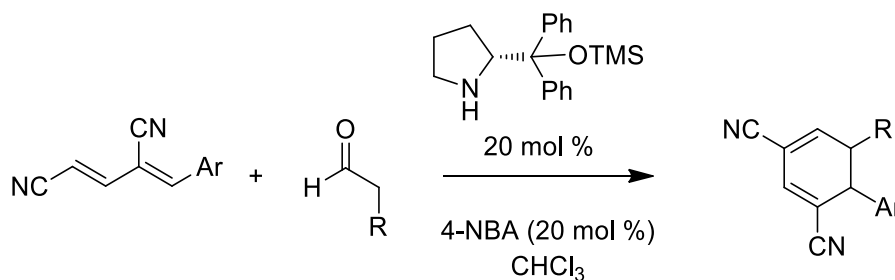
Table 3.2. 1,6-conjugate addition of aldehydic enamines to bis-cyano butadienes.

Entry	Cat.	Ar	Time (hr)	Temp (°C)	R	Observation
1	(*R*)	*p*-OMeC$_6$H$_5$	24	4	*n*Pr	Complex mixture
2	(*R*)	*p*-OMeC$_6$H$_5$	48	4	*n*Pr	Complex mixture
3	(*R*)	*p*-OMeC$_6$H$_5$	24	20	*n*Pr	Complex mixture
4	(*R*)	*p*-NMe$_2$C$_6$H$_5$	24	4	*n*Pr	Complex mixture
6	(*R*)	*p*-NMe$_2$C$_6$H$_5$	48	20	*n*Pr	Complex mixture

These results were disappointing as we had thought that the initial success with the phenyl bis-cyano butadiene **41** would carry through to the bis-cyano butadienes bearing

substituents on the aryl ring. The apparent lack of reactivity could be due to a mismatch in the nucleophilicity of the aldehydic enamine, derived from Jørgensen's catalyst, and the electrophilicity of the substituted diene scaffold. In each of the dienes investigated it could be argued that the electron-donating ability of the phenyl substituent is responsible for reduced electrophilicity at the δ-carbon of the diene arising from the mesomeric effect. This reduced electrophilicity in combination with additional steric constraints associated with the introduction of the substituent appear to have removed activity of the dienes towards enamine derived from Jørgensen's catalyst. The complex mixture that was obtained could be as a result of multiple self-aldol reactions involving the starting aldehyde.

3.2.2   Cyano-ester butadienes

Similarly, the cyano-ester butadienes were subjected to the previously developed reaction conditions that were utilized for the 1,6-conjugate addition of the aldehydic enamines to the bis-phenylsulfonyl and bis-ester butadienes. Again, disappointingly no evidence of the formation of the cyclic hexadiene products was observed and once more a complex mixture was obtained, including returned starting material. An increase in temperature and reaction time did not yield any observable product formation. These results are detailed in Table 3.3.
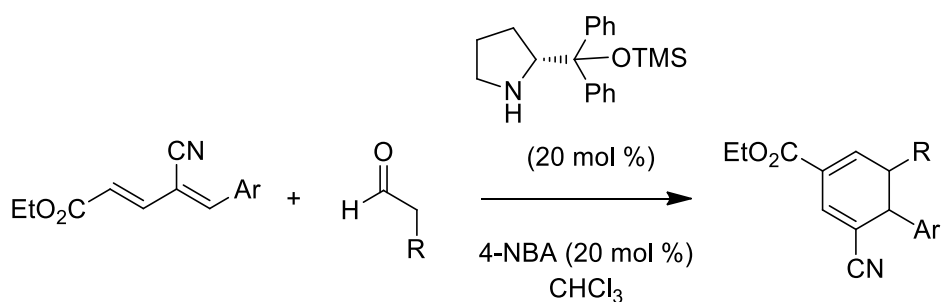
Table 3.3. 1,6-conjugate addition of aldehydic enamines to cyano-ester butadienes.

Entry	Cat.	Ar	Time (hr)	Temp (˚C)	R	Observation
1	(R)	C_6H_5 (**96**)	24	20	nPr	Complex mixture
2	(R)	p-NMe$_2$C$_6$H$_5$ (**102**)	24	20	nPr	Complex mixture
3	(R)	p-OMeC$_6$H$_5$ (**103**)	24	20	nPr	Complex mixture

3.2.3   Cyano-phenylsulfonyl butadienes

Similarly the cyano-phenylsulfonyl butadienes were subjected to the reaction conditions for the 1,6-conjugate addition of the aldehydic enamines and again none of the cyclic hexadiene products were observed. In this case complex mixtures resulted and some returned starting material, individual components of which could not be isolated by silica-gel column chromatography. These results are detailed in Table 3.4.
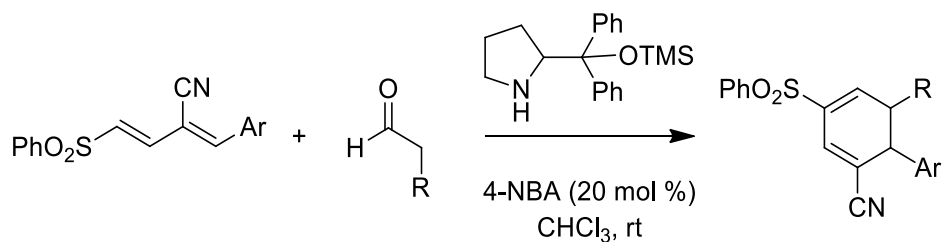
Table 3.4. 1,6-conjugate addition of aldehydic enamines to cyano-phenylsulfonyl butadienes.

Entry	Cat.	Ar	Time (hr)	R	Yield
1	(R)	C_6H_5 (**105**)	24	nPr	Complex mixture
2	(R)	p-FC_6H_5 (**110**)	24	nPr	Complex mixture
3	(R)	p-NO$_2C_6H_5$ (**111**)	24	nPr	Complex mixture

In contrast to the synthesis of the bis-phenylsulfonyl and bis-ester butadienes, the synthetic route to access the cyano-phenylsulfonyl butadienes allowed for the substitution of the terminal phenyl ring with electron-withdrawing substituents. The aim of this additional substitution was to increase the electrophilicity of the butadiene backbone arising from electron-withdrawal through inductive and mesomeric effects. Despite the use of the p-NO$_2$ substituent, an extremely inductively withdrawing substituent, the conjugate addition or cyclic hexadiene products were not observed by ^{1}H NMR spectroscopy. This could perhaps be due to steric clashes arising from the introduction of the NO$_2$ substituent on the phenyl ring.

3.2.4   Conclusion

The extended bis-cyano butadiene family, the cyano-ester butadienes and cyano-phenylsulfonyl butadienes were screened under the same reaction conditions and after 24 hr none of the cyclic hexadiene products were observable in the crude reaction mixtures. The previously reported bis-phenylsulfonyl and bis-ester butadienes differ in their reactivity with aldehydic enamines and so it may not be a complete surprise to find that the bis-cyano, cyano-ester and cyano-phenylsulfonyl butadienes also differ in their reactivity. In the case of the bis-phenylsulfonyl butadiene, complete conversion was observed after 24 hrs for all aldehydes tested, with the notable exception of the more sterically hindered isovaleraldehyde (40 hrs) and (*S*)-citronellal (144 hrs).[58] In contrast to the bis-phenylsulfonyl butadienes, the bis-ester butadienes were significantly less reactive. Some reactions of the bis-ester butadienes took up to 120 hrs for complete conversion (*n*-hexanal) and typically took 72 hrs to reach complete conversion.[59] The reactivity of the more electron-rich members of the bis-cyano butadiene family seem to suffer from a similar lack of reactivity with aldehydic enamines, this is perhaps due to the decreased electrophilicity at the 6-position of these butadienes. Similarly the cyano-ester and the cyano-phenylsulfonyl butadienes were also found to be unreactive under the reaction conditions screened for the 1,6-conjugate addition of aldehydic enamines.

Whilst the initial targets of the conjugate addition to the butadienes were the enantioenriched cyclic hexadienes, the aromatized biaryl products are also of synthetic interest and so further efforts were made to try to favour the exclusive formation of these interesting side-products.

3.3   Introduction to directed biaryl synthesis

The biaryl motif, and in particular the biphenyl motif, are privileged substructures within a number of pharmaceutically active compounds. The biphenyl motif has been noted as being a component of compounds found in many classes of therapeutic agents such as antifungal, antihypercholesteremic, antirheumatic, analgesic, anti-inflammatory agents.[100]   Biaryl compounds exhibiting axial chirality are also found in a number of pharmacologically active natural products (e.g. the antibacterial vancomycin), asymmetric ligands and asymmetric organocatalysts.[101,102]

A traditional method for the synthesis of symmetric biaryl scaffolds is the use of the Ullman reaction. First described by Ullman in 1901, the reaction consists of the copper catalyzed coupling of aryl halides (Figure 3.3).[103]
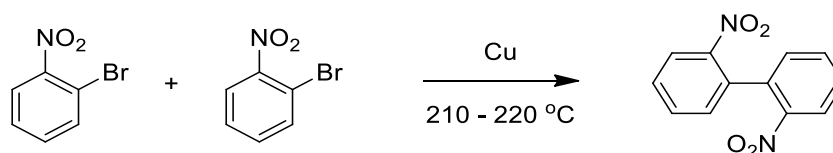
Figure 3.3. Copper catalyzed biaryl formation described by Ullman.[103]

The most generally accepted mechanism for the Ullman reactions describes the formation of an organo-cuprate intermediate **127** generated from aryl halide **126** which then reacts with a second equivalent of the aryl halide through oxidative addition to yield a second organo-cuprate intermediate **128**. Following reductive elimination the target biaryl **129** is formed (Figure 3.4).[104]

122
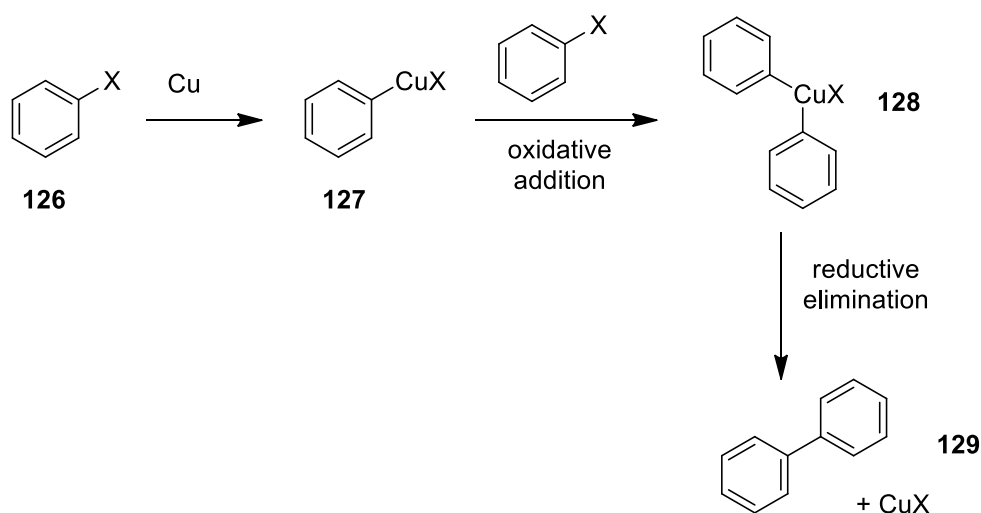
Figure 3.4. Generally accepted mechanism of the Ullman reaction.[104]

Whilst the Ullman reaction has been utilized extensively in the synthesis of biaryls[105], there are a number of limitations of this methodology. 1) Limited substrate scope, electron-withdrawing substituents activate the substrate towards coupling whilst electron-donating groups can greatly reduce the rate of reaction; 2) bulky substituents on the aryl ring also hamper reaction rates, this becomes an issue when highly substituted biaryl compounds are the desired targets; 3) the heterogeneous nature of the reaction mixture is also of concern as the reaction rates can be hindered if the starting materials are not mixed efficiently; 4) temperature sensitive substrates are also not compatible with the high temperatures required for the reaction to proceed; 5) the Ullman reaction is particularly useful in the synthesis of symmetric biaryls but has limitations in the synthesis of asymmetric biaryls due to the competing formation of the homocoupling products. For the reasons outlined above there has been significant interest in the development of novel methodologies for the synthesis of biaryl species, especially those with more challenging substitution patterns.

Many of the advances in the synthesis of biaryls have utilized transition metal mediated aryl C-C bond forming reactions, such as the Suzuki coupling (Pd catalyzed coupling of aryl halides/triflates/diazos and aryl boronic acids) and the Stille coupling (Pd catalyzed coupling of aryl halides/triflates and aryl trialkyl stannanes). These efforts, and others, have broadened the scope of accessible biaryl compounds. Transition metal mediated aryl-aryl bond formation in the synthesis of biaryl compounds has a number of benefits, such as, the use of low stoichiometric loadings of the transition metal catalysts, high turn-over numbers, as well as the availability of a variety of commercial substrates. This wide availability of

commercial coupling partners is due to the increase in the use of transition metal mediated reactions in the synthesis of medicinal chemistry compound libraries. A number of caveats also exist with the use of transition metal mediated methodologies, including the use of expensive catalysts, which can also produce undesired toxic metal waste products.[106] The prerequisite synthesis of non-commercially available coupling partners, for example those with challenging substitution patterns, can also hinder the use of transition metal mediated biaryl synthesis.

Whilst less common in the literature, a number of metal-free approaches to the synthesis of biaryl species have also been reported. One such report by Joshi *et al.* in 2015 describes the synthesis of biaryls from bis-substituted propenes and α,β-unsaturated aldehydes in the presence of DBU (Figure 3.5).[107] The authors postulate that the reaction takes place through the formation of the highly stabilized propene carbanion **130,** which then undergoes conjugate addition to the α,β-unsaturated aldehyde **131**. The resultant intermediate **132** then undergoes proton transfer to yield a new carbanion **133**. This carbanion can then undergo concomitant cyclization and elimination of water to yield the cyclic hexadiene **134** (Figure 3.5).[107] In their report the authors suggest that the final oxidation process is accelerated by oxygen to yield biaryl products of type **135**.
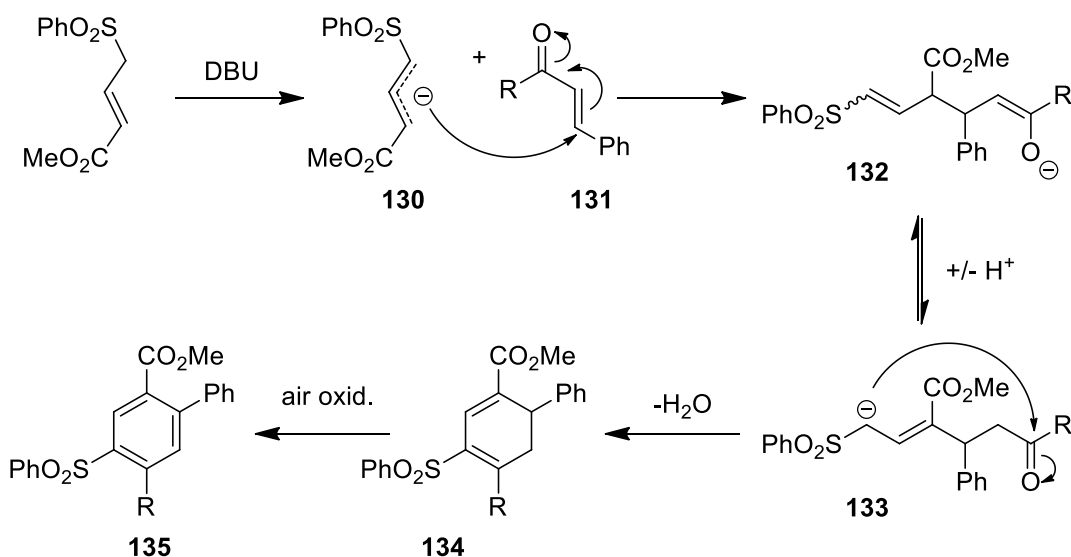
Figure 3.5. Conjugate addition of propene to α,β-unsaturated aldehydes followed by air oxidation to yield biaryl products reported by Joshi *et al.*[107]

Another 2015 report by Poudel *et al*. describes the metal-free synthesis of biaryls through a multi-component system (Figure 3.6).[108] Multi-component reactions (MCR) have garnered widespread attention in recent years due to their ability to generate molecular complexity in a low number of synthetic steps. The authors propose that the biaryl formation occurs through a domino Michael addition/intra- and inter-molecular aldol/[1,5]-hydrogen shift/tautomerization process and is an excellent example of the utility of MCR processes.

R^1 = OR, NHR or CH$_3$
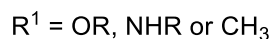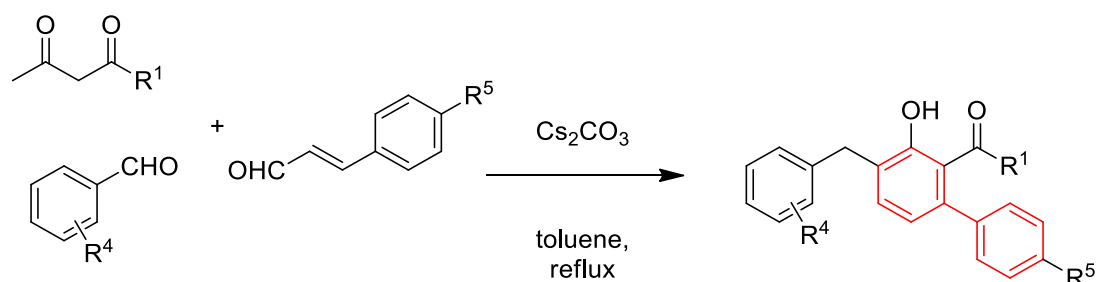
Figure 3.6. Biaryl synthesis through MCR reaction of diketones or β-keto esters/amides and substituted aryl aldehydes/cinnamaldehydes reported by Poudel *et al*.[108]

In both of the examples outlined above the scope of products available is dictated by the substitution patterns of the starting materials and as such novel methodologies which can access new substitution patterns is of synthetic interest.

The observation that the addition of aldehydic enamines to bis-cyano butadienes led to not only cyclic hexadienes but also to the formation of aromatized biaryl species **125** intrigued us as the products obtained are otherwise difficult to access through other methods. As such we devoted efforts to access the biaryl product exclusively.

3.3.1   Results and discussion

3.3.1.1   Reaction refinement

As we knew that the biaryl species **125** was produced as a side product during the formation of cyclic hexadienes from butadienes and aldehydic enamines (Figure 3.7) under the conditions previously optimized by John Murphy.[69] We now wished to investigate different means of favouring the biaryl product so as to produce it exclusively.
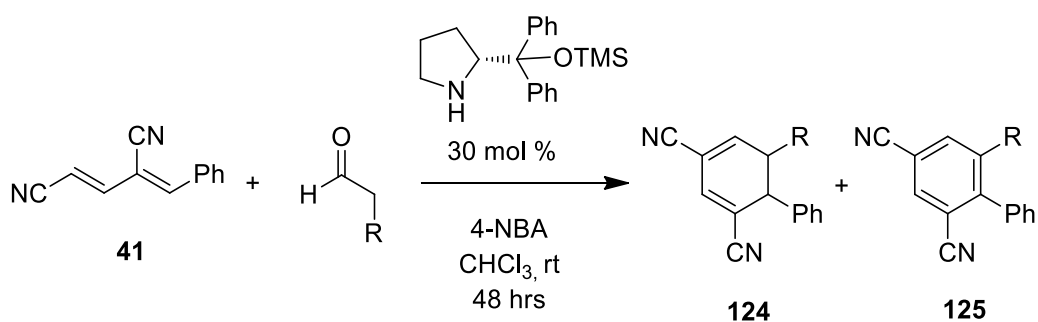
Figure 3.7. Synthesis of mixtures of cyclic hexadiene and biaryls.

1) To explore if the aromatization would occur under air oxidation as suggested by Joshi *et al.*, air was bubbled through the product mixture for 24 hrs.[107] No change in product ratio was observed indicating that O_2 was not responsible for the aromatization process. 2) The product mixture was allowed to stir, in the presence of Jørgensen's catalyst, for a further 48 h. This resulted in a slight increase in the amount of biaryl present, with the product ratio of hexadiene to biaryl going from 3.5:1 to 2.5:1. This result suggested to us that the aromatization process may be influenced by the presence of the amine base catalyst.

With the suggestion that the amine catalyst is responsible for generating the desired biaryl from the hexadiene, we now became interested in establishing a one pot synthesis of the biaryls from the acyclic diene and aldehyde. We anticipated that Jørgensen's chiral catalyst could be replaced by the achiral secondary amine piperidine and that piperidine could adopt the dual role of enamine formation, required for the conjugate addition step, and act as an amine base for the aromatisation step (Figure 3.8).
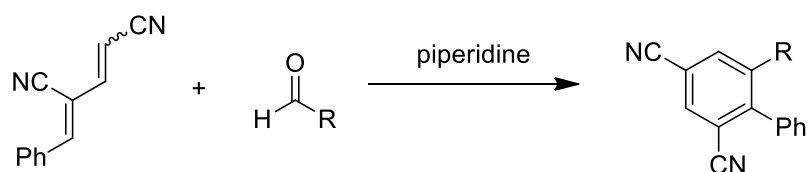
Figure 3.8. Synthesis of biaryls utilizing piperidine.

This indeed turned out to be the case and we subsequently found that the use of stoichiometric amounts of piperidine allowed us to consistently obtain conversion to the biaryl product within 16 h. Lower catalytic loadings resulted in incomplete aromatization of the cyclic hexadienes, which then resulted in difficult separation of the biaryl product from the reaction mixture.

A number of different aliphatic aldehydes were then used in the one pot synthesis of bis-cyano biphenyls. Similar yields were obtained in all cases, as shown in Table 3.5.
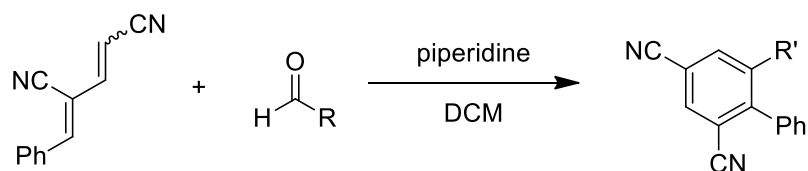
Table 3.5. Synthesis of biaryls from bis-cyano diene **X**

Entry	R	R'	Yield (%)
1	Et	Me (**136**)	49
2	Pr	Et (**137**)	52
3	*i*Pr	*i*Pr (**138**)	45
4	But	Pr (**125**)	55
5	Pent	But (**139**)	53

3.3.1.2 Spectroscopic characterization

The bis-cyano biphenyls were characterized through a combination of ^{1}H NMR and ^{13}C NMR experiments and the use of correlation experiments such as Heteronuclear Multiple Bond Correlation (HMBC) and Heteronuclear Single Quantum Correlation (HSQC) experiments was required in order to fully assign all of the NMR signals. Structural characterization and NMR signal assignment of bis-cyano biphenyl **125** shall be outlined below as an example.

The ^{1}H NMR spectrum of biphenyl **125** contains seven signals, the most characteristic of which are the more deshielded signals arising from the protons on the bis-cyano substituted phenyl ring, Figure 3.9.
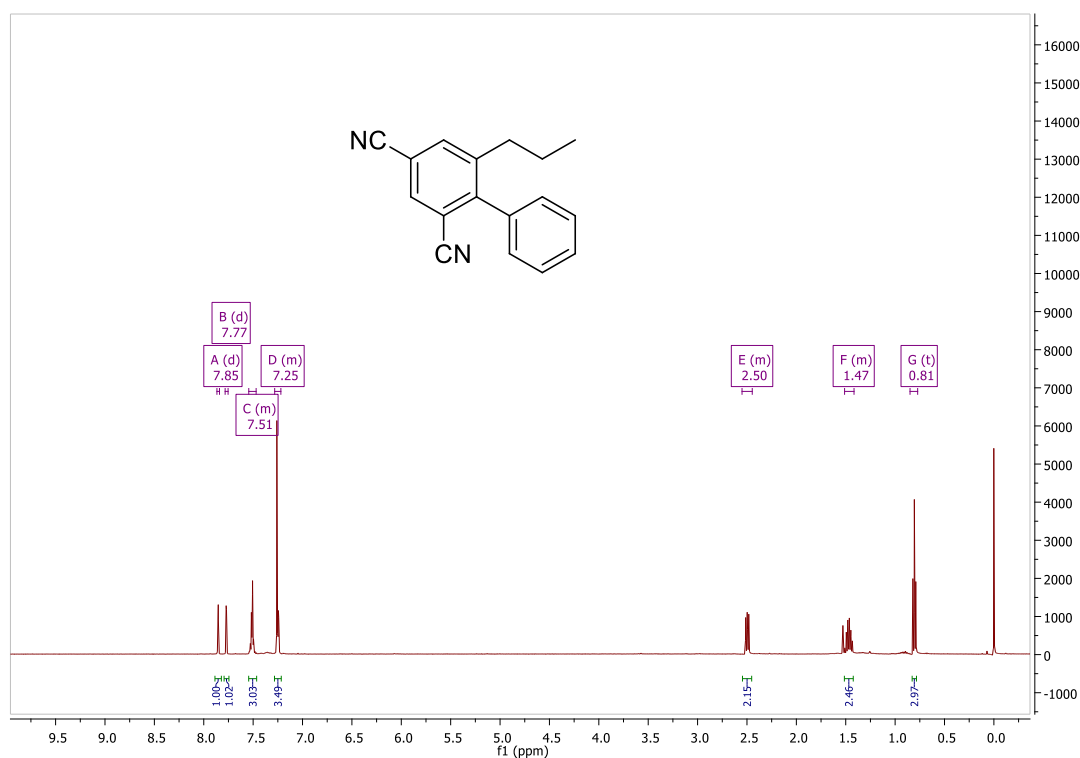
Figure 3.9. ^{1}H NMR spectrum of the aromatized product **125**.

The most deshielded signal at 7.85 ppm appears as a doublet with J = 1.6 Hz, this coupling constant arises from the long range ^4J *meta* coupling to the other aryl proton, this signal arises from the aryl proton alpha to both nitrile functional groups. The second most deshielded signal at 7.77 ppm appears as a doublet and has the reciprocal coupling constant of J = 1.6 Hz and arises from the other aryl proton alpha to only one nitrile functional group. The signals for the aryl protons on the unsubstituted phenyl ring appear in the aromatic region of the ^{1}H NMR spectrum. The signals arising from the alkyl chain appear in the

expected alkyl region of the ^{1}H NMR spectrum, the multiplicities of the two CH$_2$'s are more complicated than expected due to long range coupling into the aromatic ring, meaning that their assignments are that of multiplets. The ^{1}H NMR spectral assignment of the bis-cyano biphenyl **125** is summarized in Figure 3.10.
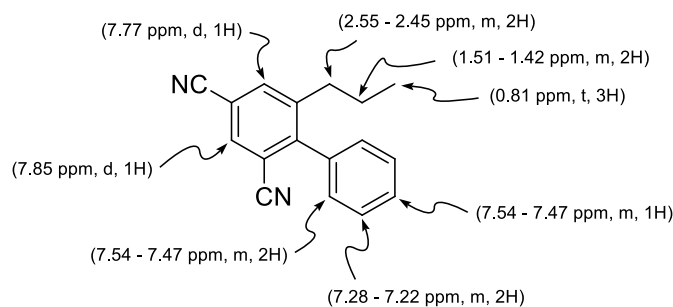
Figure 3.10. ^{1}H NMR spectral assignment of biaryl **125**.

The ^{13}C NMR spectrum of bis-cyano biphenyl **125** contains 15 unique signals, seven of which are quaternary in nature (Figure 3.11). These quaternary signals are the most difficult to assign in that they don't have a proton directly attached to them and so a 2D HSQC experiment is not of any assistance.
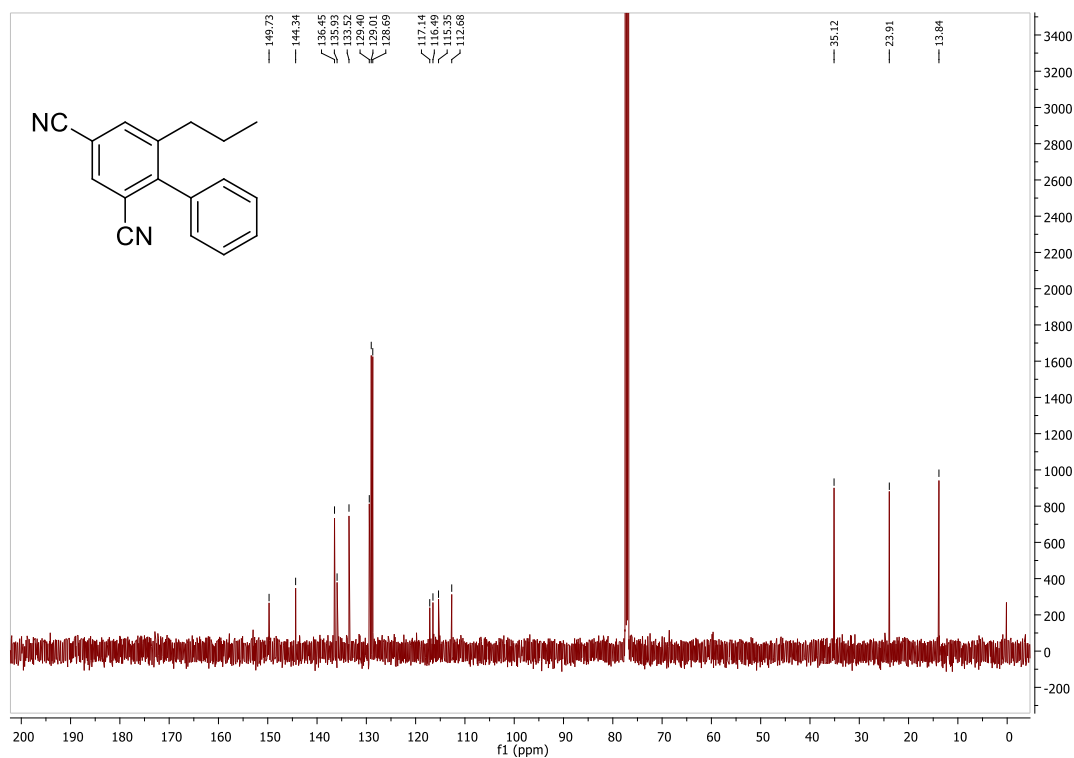
Figure 3.11. ^{13}C NMR spectrum of the aromatized product **125**.

The use of a HMBC experiment allowed for the assignment of these signals through careful analysis of the long range proton-carbon correlations, (Figure 3.12).
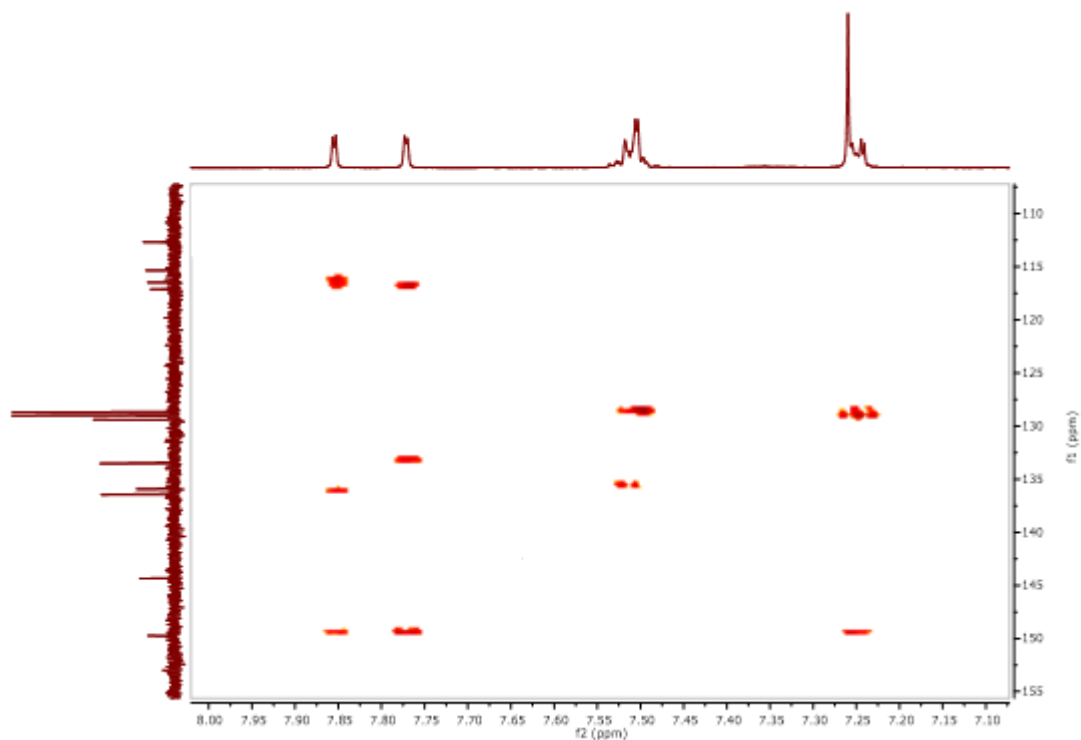
Figure 3.12. Selected region of the HMBC of aromatized product **125**.

The most useful of these correlations are summarized in Figure 3.13. Similar to the HMBC correlations observed in the bis-cyano butadienes, three bond correlations in HMBC experiments are typically more intense than that of two bond correlations due to a Karplus-type relationship. In Figure 3.13 a) the proton of interest shows correlation to the two nitrile quaternary carbons, the other aryl CH carbon and the quaternary carbon attached to the phenyl substituent. Comparison of these correlations to the correlations of Figure 3.13 b) allows one to distinguish between the two quaternary nitrile carbons as well as to identify the signal arising from quaternary aryl carbon attached to the phenyl substituent. Figure 3.13 a), b), c), and d) show correlation from protons on the alkyl chain, these correlations allow for the confirmation of the chemical shift for the signal arising from the quaternary aryl carbon attached to the alkyl chain. HSQC correlations could then be used to easily assign the ^{13}C NMR signals for carbons with hydrogens directly attached to them. The only remaining signals unaccounted for are the quaternary aryl carbons attached to each of the nitrile functional groups which appear at 115.4 and 112.7 ppm. Unfortunately, due to the peculiarity of HMBC experiments in that 2 bond correlations can appear weaker than that of

3 bond correlations, it was not possible to observe correlations which could aid in the assignment of these two signals. The quaternary aryl carbon *ortho* to the phenyl substituent was reasoned to be the signal appearing at 115.4 ppm and the quaternary aryl carbon *para* to the phenyl substituent was reasoned to be the signal appearing at 112.7 ppm.
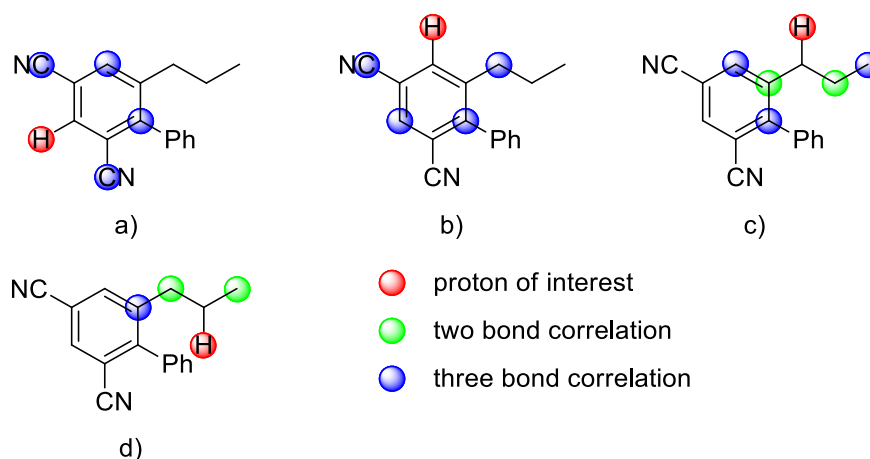
Figure 3.13. HMBC correlations of bis-cyano biaryl **125**.

The ^{13}C NMR spectral assignment of the bis-cyano biphenyl **125** is summarized in Figure 3.14.
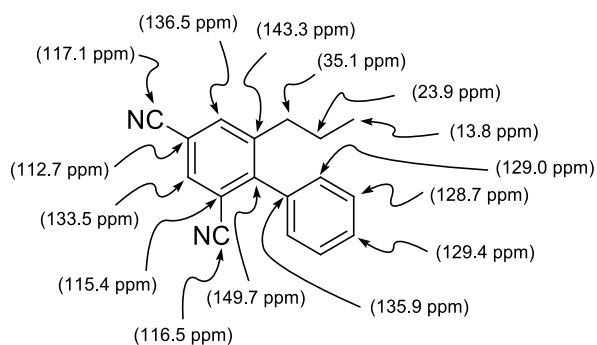
Figure 3.14. ^{13}C NMR spectral assignment of biaryl **125**.

A crystal structure of bis-cyano biphenyl **125** was ultimately obtained and this confirm the proposed structure.
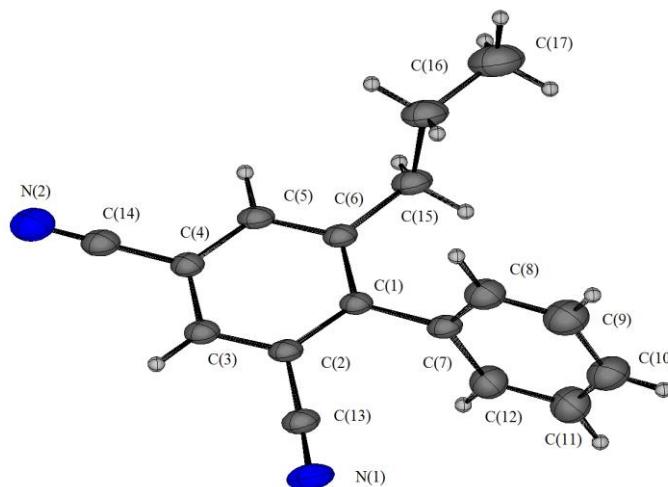
Figure 3.15. X-ray crystal structure of biphenyl **125**.

3.3.1.3   Reactions of cyano-ester dienes

The one pot synthesis of biaryls was also applied to the cyano-ester dienes. The same reaction conditions using stoichiometric amounts of piperidine was employed and a number of different aliphatic aldehydes were used. Similar yields of the expected biaryl were obtained in all cases expect for the reaction with *iso*valeraldehyde, entry 3, Table 3.6. We believe the lower yield is due to challenges in the isolation of the final biaryl product in this case, as opposed to a lack of consumption of starting material.
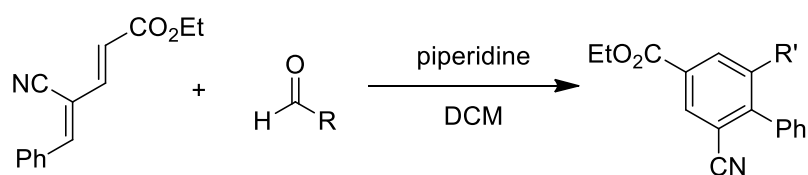
Table 3.6. Synthesis of biaryls from cyano-ester diene **X**

Entry	R	R'	Yield
1	Et	Me (**140**)	46
2	Pr	Et (**141**)	49
3	*i*Pr	*i*Pr (**142**)	35
4	Butyl	Pr (**143**)	64
5	Pentyl	Butyl (**144**)	56

3.3.1.3.1   Spectroscopic characterization

In order to fully assign all NMR signals for the cyano ester biphenyl **143**, a combination of ^{1}H NMR and ^{13}C NMR experiments and the use of correlation experiments such as Heteronuclear Multiple Bond Correlation (HMBC) and Heteronuclear Single Quantum Correlation (HSQC) experiments was again required. A summary of the resulting NMR signal assignments are given in Figure 3.14 and Figure 3.15 below.
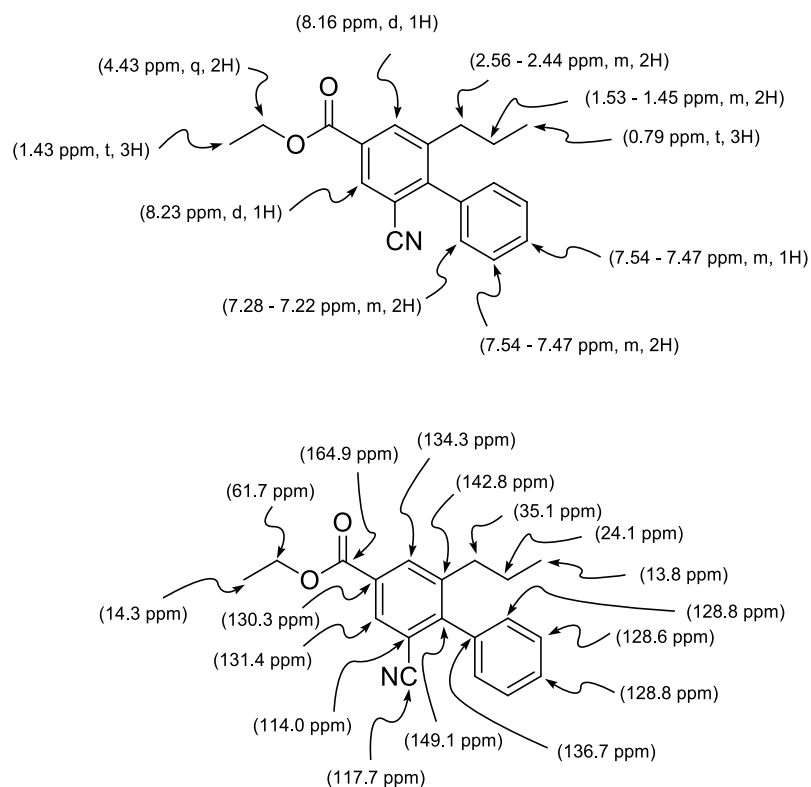
Figure 3.16. ^{1}H NMR and ^{13}C NMR spectral assignment of biaryl **143**.

3.3.1.4   Reactions of the cyano-phenylsulfonyl butadienes

Attempts to explore the synthesis of the biaryls to those containing both cyano and sulfonyl functionality did not prove fruitful. Multiple days at rt, under the same reaction conditions as used for the bis-cyano biaryls and cyano-ester biaryls did not result in any observable biaryl product (Figure 3.17).
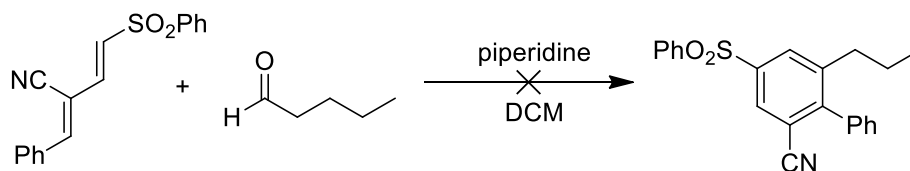
Figure 3.17. Attempted synthesis of cyano-phenylsulfonyl biaryl.

135

3.3.1.5   Study of aromatization of cyclic hexadiene 125

In order to develop an understanding of the aromatization process transforming the cyclic hexadiene **124** into the biaryl species **125**, an experiment was devised in which the formation of the biaryl could be monitored utilizing ^{1}H NMR spectroscopy. Integrals of corresponding starting material and product signals could be measured in order to glean some information on the reaction progress and perhaps identify solutions to improve yields of the biaryl products. The signals chosen in both the starting cyclic hexadiene **124** and the biaryl **125** are shown in Figure 3.18, these signals were chosen for their unique chemical shifts which were free from interfering signals allowing for easy integration.
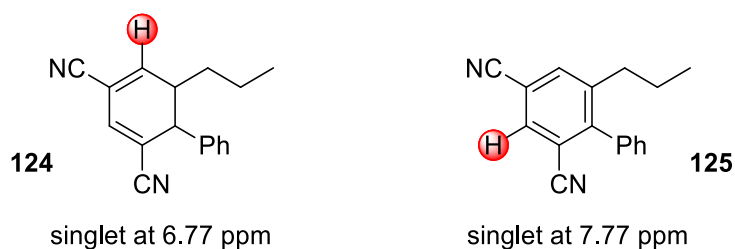
Figure 3.18. Signals of interest for the cyclic hexadiene **124** and the biaryl **125**.

Cyclic hexadiene **124** was dissolved in CDCl$_3$, 30 mol % of piperidine was added to the NMR tube and the reaction monitored every 30 mins. The resulting stacked ^{1}H NMR spectra illustrate the consumption of the cyclic hexadiene and the generation of the biaryl species.
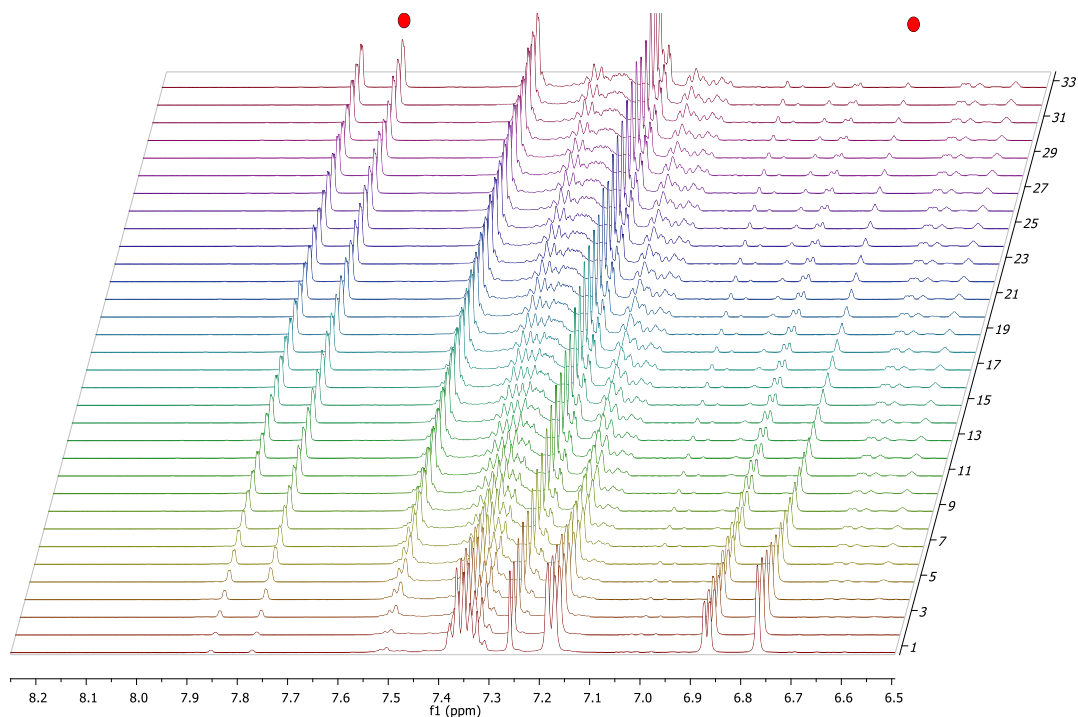
Figure 3.19. Stacked ^{1}H NMR spectra of the aromatization of the cyclic hexadiene **124** to the biaryl species **125**. The peak at 6.77 ppm arises from the cyclic hexadiene **124** and the peak at 7.77 ppm arises from the product biaryl **125**.

As can be seen in Figure 3.19 the starting cyclic hexadiene **124** is consumed throughout the reaction and biaryl **125** is produced. Whilst at first glance this may appear to be an equimolar conversion of one species to the other, plotting of the integrals for the signals of interest reveals a different story.

137

Plotting of the standardized integrals (using the initial integral of the starting cyclic hexadiene at 6.77 ppm) of the starting material and product yields the plot seen in Figure 3.20.
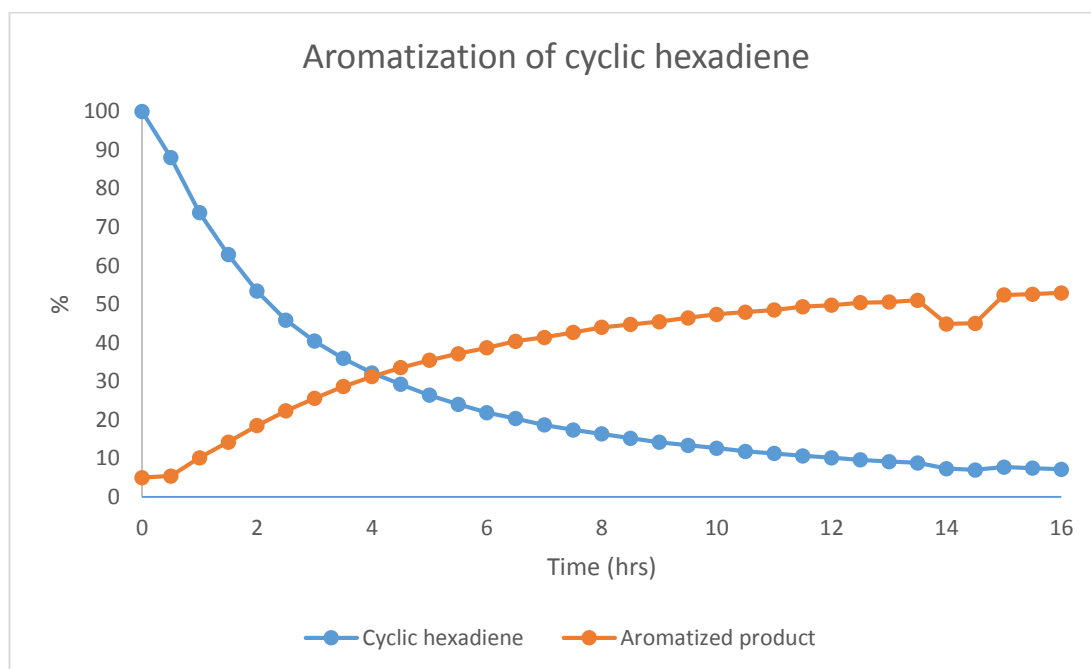
Figure 3.20. Graph showing the consumption of the starting cyclic hexadiene **124** and the formation of the aromatized biaryl **125** in the presence of 30 mol % piperidine. Reaction monitored every 30 mins by ^{1}H NMR spectroscopy. Integrals taken from starting material and product peaks corresponding to one proton each.

This plot clearly shows that there is not a 1:1 stoichiometric relationship between the consumption of the starting cyclic hexadiene **124** and the formation of the aromatized biaryl **125**. After 16 hrs, and near complete consumption of the cyclic hexadiene, there was only 53% of the biaryl species present. This result is in agreement with the typical yield seen for the formation of the biaryls. This result also indicates that there is a competing side reaction that is consuming the cyclic hexadiene before it can be converted to the biaryl, it is not clear based on ^{1}H NMR analysis what this side reaction could be however some discussion on potential side reactions and products will be outlined in Section 3.3.1.6.2.

3.3.1.6   Mechanistic discussion

There are two plausible reaction mechanisms which can describe the transformation from the butadienes to the biaryl species. **Mechanism 1)** A 1,6-conjugate addition followed by a concomitant cyclization and elimination of the catalyst to yield the cyclic hexadiene, which can then undergo aromatization to yield the biaryl species; **Mechanism 2)** an inverse-electron demand Diels-Alder cycloaddition followed by elimination of the catalyst to yield the cyclic hexadiene and subsequent aromatization giving the aromatized biaryl species. Both cases will be outlined in detail, including a discussion on the authors preference for the 1,6-conjugate addition mechanism.

In order to develop an understanding of the reaction mechanism it is helpful to first examine a case where the final product is chiral in nature, namely from that of addition to the bis-phenylsulfonyl butadiene.

Mechanism 1): A proposed mechanism for the 1,6-conjugate addition of an aldehydic enamine to the bis-phenylsulfonyl butadiene **145** followed by a concomitant cyclization and elimination of the organocatalyst **147** to yield the cyclic hexadiene **146** can be seen in Figure 3.21.[58,69]
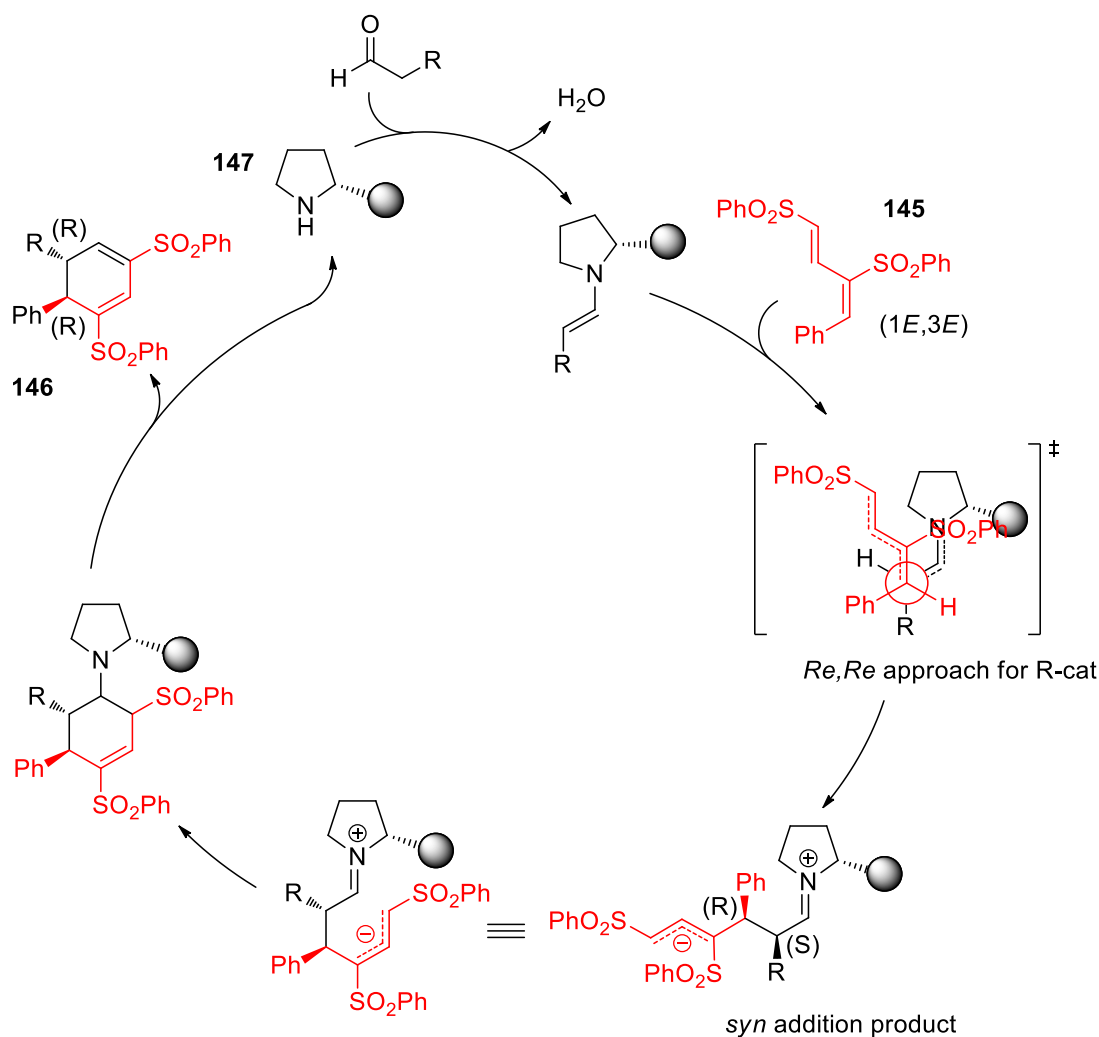
Figure 3.21. 1,6-conjugate addition/cyclization of aldehydic enamines and 1*E*,3*E* bis-phenylsulfonyl butadiene.[58,69]

The stereochemical outcome of the initial addition reaction can be described using the acyclic synclinal transition state model described by Seebach and Goliński.[109]

The favoured *anti-E*-enamine, generated from the *R* form of the catalyst **147**, approaches the diene in *Re,Re* fashion with the electron-withdrawing group on the diene (SO$_2$Ph) in close proximity to the approaching heteroatom of the enamine. This *Re,Re* approach leads to the generation of the two newly formed stereocentres in a 4*S*,5*R* fashion, when assigned by the Cahn-Ingold-Prelog rules.[39] The new stereocentres are formed in a *syn* configuration, rotation about the sigma bond then brings the anion and iminium reacting partners in close proximity. During the cyclization and elimination of the catalyst to yield the cyclic diene **146**, the priority of the substituents changes so that the absolute configuration now becomes 4*R*,5*R*. The same argument holds when the *S* hand of catalyst **147** is employed and it leads

to a *Si,Si* approach of the enamine, which after cyclization and elimination of the catalyst liberates the cyclic diene with an absolute configuration of 4*S*,5*S*.

In the case of the bis-phenylsulfonyl butadiene, crystal structure data for both the 4*R*,5*R* and the 4*S*,5*S* cyclic dienes, generated from the *R* and *S* forms of the catalyst respectively, have been obtained and confirms the absolute stereochemistry of the products (Figure 3.22).[58]
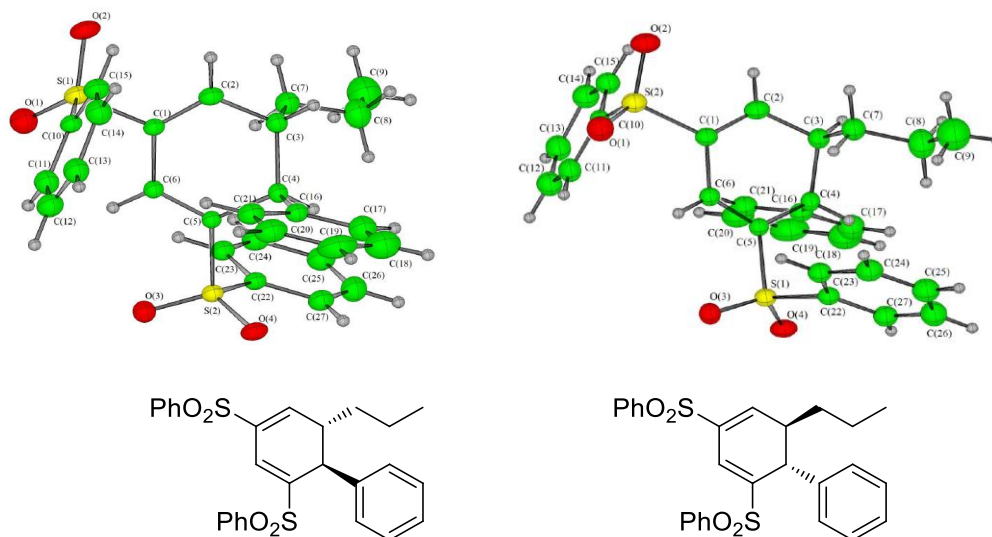
Figure 3.22. X-Ray crystal structures of the *S,S* and *R,R* enantiomers of the cyclic bis-phenylsulfonyl hexadienes **146** obtained by Murphy *et al*.[58]

When considering the addition of aldehydic enamines, derived from achiral piperidine, to bis-cyano and cyano-ester butadienes, the case becomes simplified as there is no stereocontrol originating from the organocatalyst to be accounted for (Figure 3.23). In this case, after condensation with the aldehyde, the piperidine derived enamine can approach the butadiene scaffold from either the *Re* and *Si* face with equal probability leading to a racemic mixture of the initial addition product **148**.
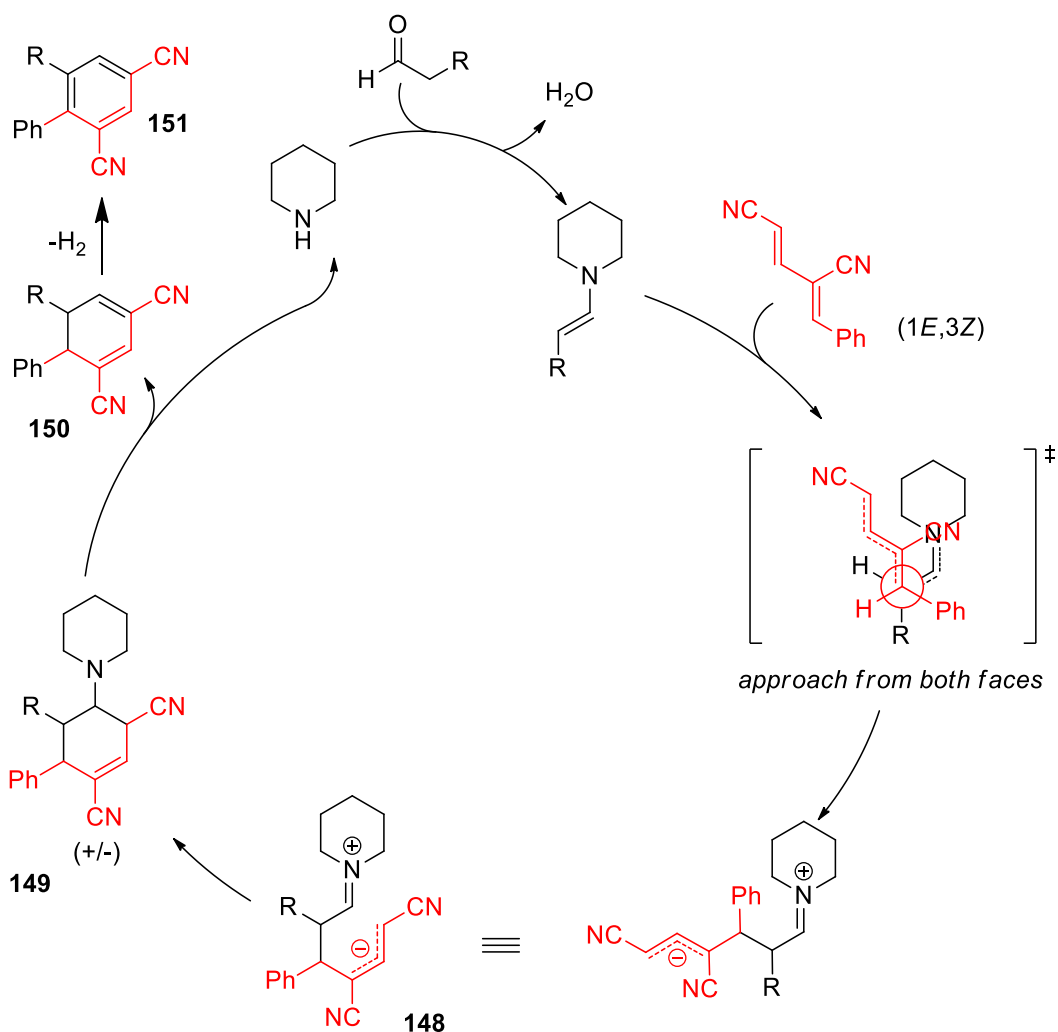
Figure 3.23. 1,6-conjugate addition/cyclization of aldehydic enamines and 1*E*,3*Z* bis-cyano butadiene **X** to yield biaryl species **X** catalyzed by piperidine.

Ring closure between the intermediate carbanion on the iminium leads to the racemic carbocycle **149**. In both cases, i.e. bis-phenylsulfonyl and the bis-cyano butadienes, this cyclization could occur in either a 6-*exo-trig* or 4-*exo-trig* fashion as allowed by Baldwin's rules.[110] The 4-*exo-trig* cyclization product was not observed in either case. This may be as a result of the decreased stability of the tertiary carbanion required for this cyclization in

comparison to the secondary carbanion required for the 6-*exo-trig* cyclization. This instability is due to the increased inductive donation of the alkyl groups at the tertiary carbanion versus that at the secondary carbanion (Figure 3.24). Elimination of the catalyst leads to the cyclic hexadiene **150** and, after formal elimination of hydrogen, the biaryl product **151** (Figure 3.23).
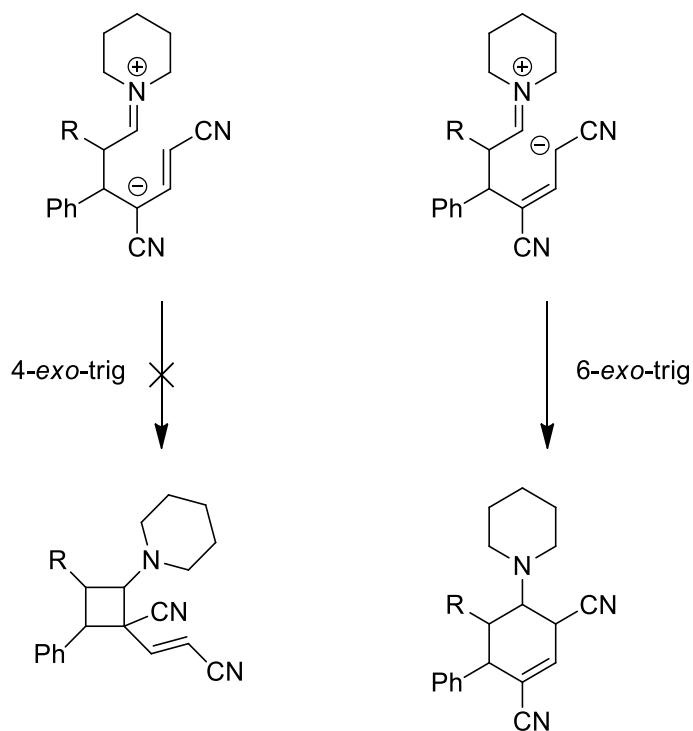
Figure 3.24. 4-*exo*-trig cyclization of the tertiary carbanion versus 6-*exo*-trig cyclization of the secondary carbanion.

Mechanism 2): Alternatively, one can consider an IEDDA cycloaddition mechanism to describe the transformation. The reaction is classified as inverse-electron demand as the diene component is electron-deficient while the dienophile is electron-rich. Within IEDDA cycloadditions there are four mechanisms which can be used to describe the transformation. These are depicted in **Figure 3.25** (pathway a-d).
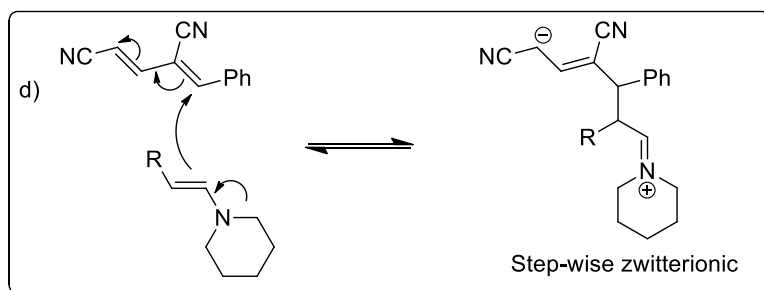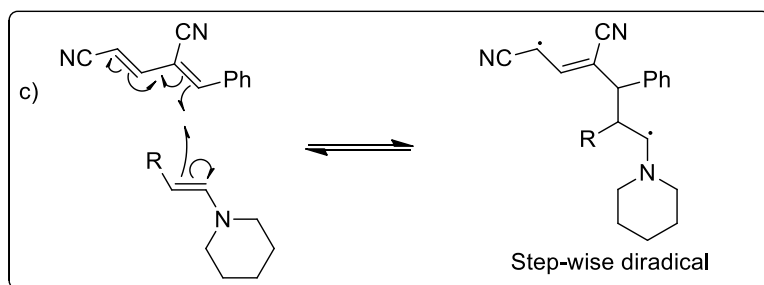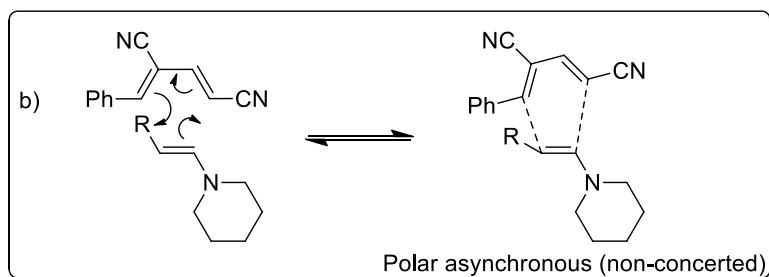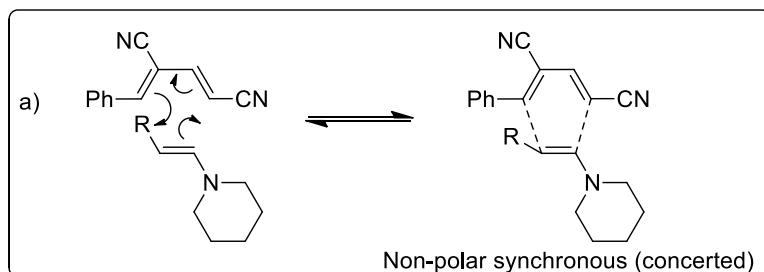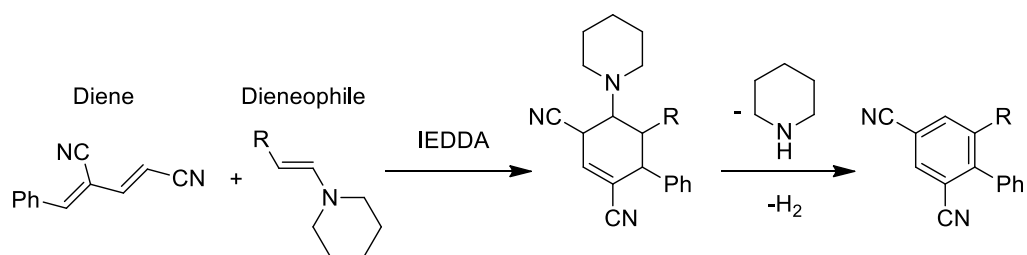
Figure 3.25. A number of plausible reaction pathways leading to cyclic hexadienes *via* a formal Diels-Alder reaction. Figure modified from a report by Linder *et al.*[111]

Pathway a) depicts the non-polar synchronous or concerted mechanism for a typical Diels-Alder cycloaddition and required the diene to be in the *s-cis* conformation. Whilst this is the most common description employed to explain the mechanism of a Diels-Alder reaction it has actually been found to be quite an uncommon occurrence, especially when there are non-H substituents present on either the diene of the dienophile.[111] In such cases the polar asynchronous pathway b) is often favoured.

Pathway b) depicts a polar asynchronous or non-concerted mechanism and also requires the diene to be in the *s-cis* conformation. In this pathway, polarization is developed across the olefins of the reacting partners, the negative pole of one partner will then be attracted to the positive pole of the other and bond formation will begin asynchronously. As the first bond is forming, further polarization will be developed throughout the reacting partners allowing for the final sigma bond to be formed. In short, in the polar asynchronous description the bonds are formed during separate bond-forming events in a non-concerted fashion.

Pathway c) depicts the cycloaddition occurring through a diradical intermediate. This pathway would require the formation of highly unstable diradical intermediates which are likely to be very short lived in solution and so this is not a favoured pathway.

Pathway d) depicts a step-wise zwitterionic reaction mechanism with nucleophilic attack of one reacting partner on the other (in this case the enamine attacking the butadiene). Generation of a formally charged intermediate results, which then undergoes cyclization to form a cyclic product. There is no formal difference between pathway d) and **Mechanism 1** (a step-wise conjugate addition cyclization).

A general pathway for the IEDDA cycloaddition (through either pathway a) or b), Figure 3.25) of aldehydic enamines and the bis-cyano butadiene is outlined in Figure 3.26. Similar to the reaction pathway for **Mechanism 1** outlined in Figure 3.23, the cyclohexene **149** is formed after which elimination of the piperidine catalyst leads to the cyclic hexadiene **150**. Once again formal loss of hydrogen leads to the biaryl species **151**.
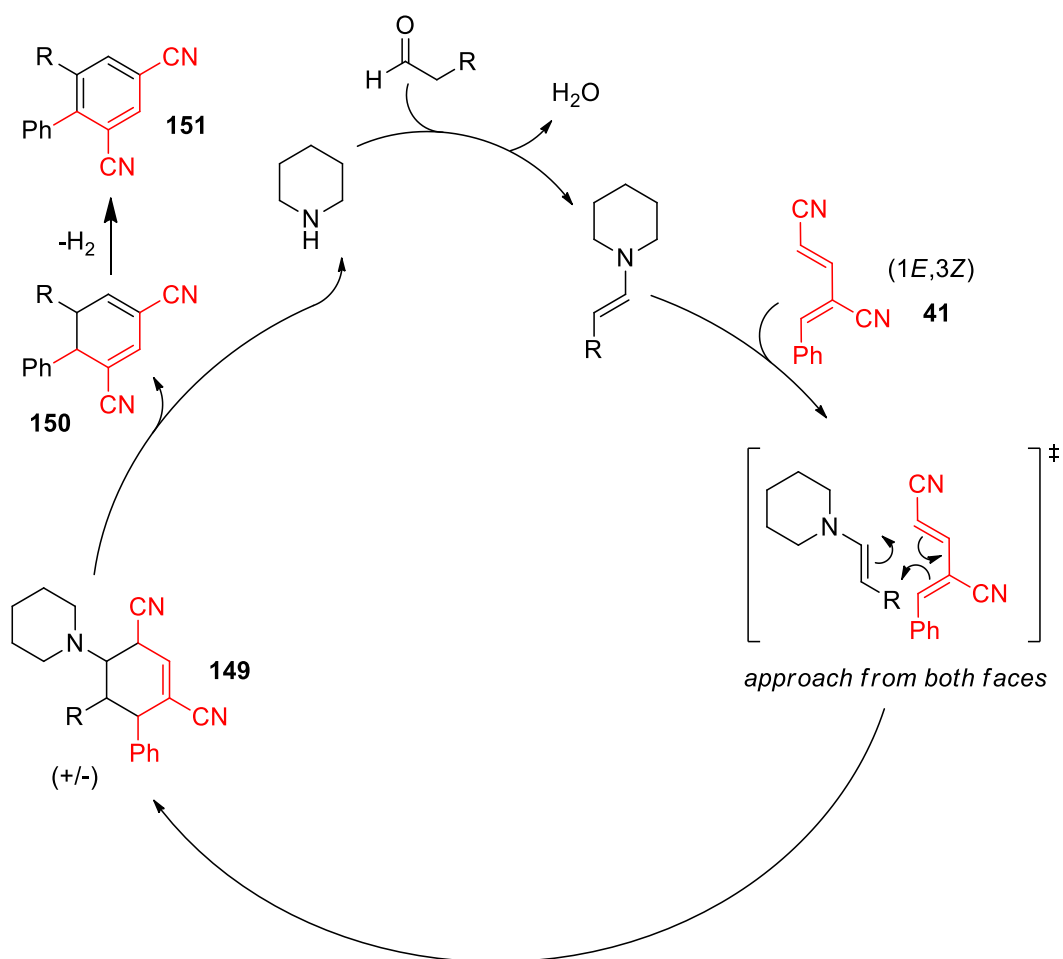
Figure 3.26. Proposed mechanism for the formation of the biaryl species through an IEDDA cycloaddition followed by formal loss of hydrogen.

3.3.1.6.1 Mechanism 1 vs Mechanism 2

In order to justify a preference for **Mechanism 1** over **Mechanism 2** it is helpful to apply the IEDDA cycloaddition mechanism (**Mechanism 2**) to an asymmetric variant of the cycloaddition to the *s-cis* 1*E,*3*E* bis-phenylsulfonyl butadiene. As [4+2] cycloadditions are stereospecific the consideration of the IEEDA allows us to use a stereochemical argument in conjunction with the fact that the only experimentally observed stereoisomer of the cyclic hexadiene product was the *anti R,R* isomer to justify a preference for **Mechanism 1**.

Taking the possible pathways outlined in Figure 3.25, applying either pathway **a)**, the synchronous concerted cycloaddition, or pathway **b)**, the asynchronous non-concerted cycloaddition, to the bis-phenylsulfonyl butadiene and the aldehydic enamine generates eight possible products (Figure 3.27). Experimentally the *anti R,R* isomer was the only isomer observed. The eight products are a result of the enamine approaching the butadiene in an *endo* or *exo* fashion, at the *Re* or *Si* faces of the butadiene, for two distinct regiochemical alignments of the reacting partners.
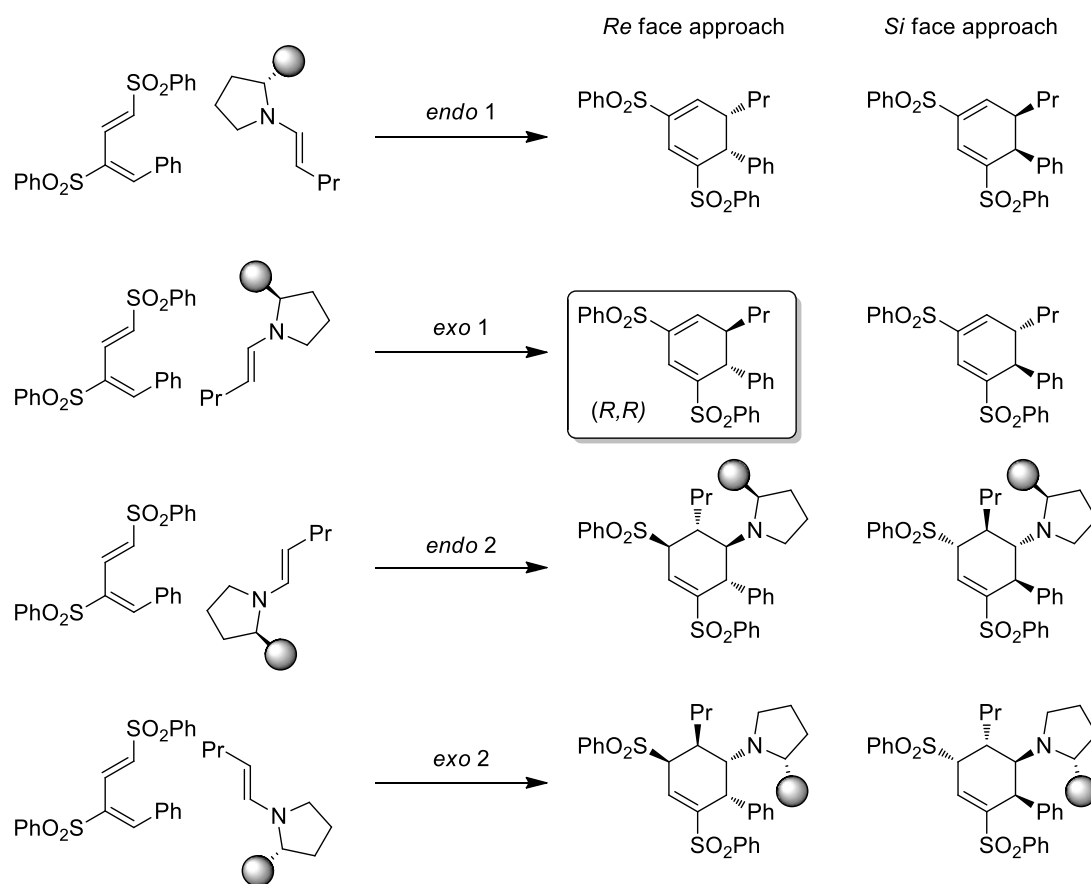
Figure 3.27. Possible IEDDA cycloadditions of aldehydic enamines and bis-phenylsulfonyl butadienes. The designation *Re* and *Si* refers to the geometry about the terminal olefin on the butadiene in each case. The *R* hand of the catalyst is used in each instance.

The first case *endo* 1, for both the *Re* and *Si* approach, leads to enantiomeric cyclohexadienes with the incorrect (*syn*) configuration of the product.

In the *exo* 1 *Re* approach, the predicted product has the correct configuration (*R,R*) when utilizing the *R* hand of the pyrrolidine catalyst. In the *exo* 1 *Si* approach, the resulting cycloadduct would have the incorrect absolute stereochemistry (*S,S*). This product is not observed and this could be as a result of the thermodynamically less favourable transition state for this approach, which would suffer from steric hindrance between the bulky substituent on the pyrrolidine catalyst and the butadiene when the enamine is approaching from the *Si* face of the butadiene.

Both the *endo* 2 and *exo* 2 cases lead to products that were not observed in any of the reaction mixtures. This is presumably due to the preference for the reacting partners to align in such a way that there sites of polarization are aligned accordingly (Figure 3.28).
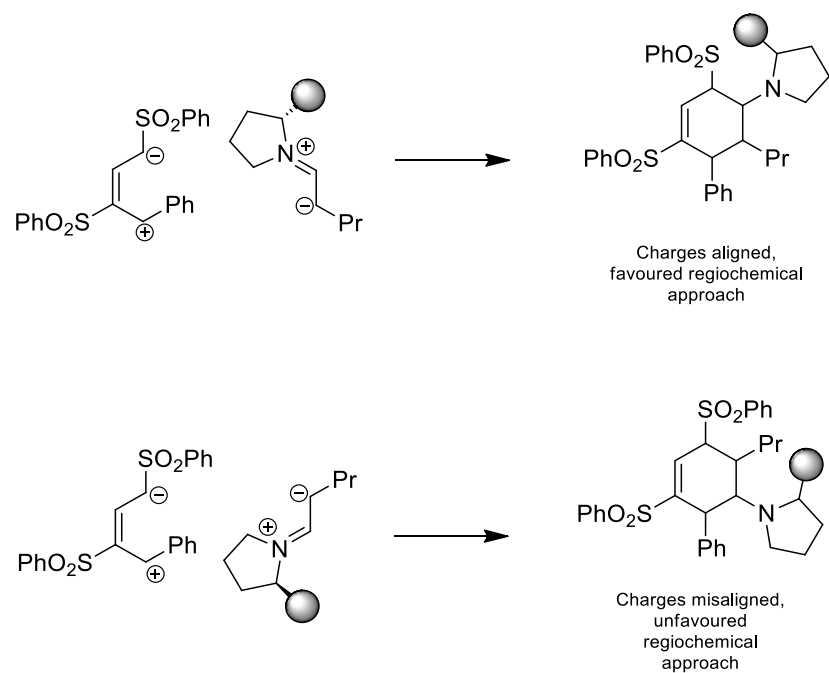
Figure 3.28. Alignment of charges for the two regiochemical approaches of the enamine on the butadiene.

The only approach that leads to the correct configuration of the product is that of *exo* 1 *Re* approach. Literature precedent shows a preference for *endo* selective cycloadditions of enamines, therefore we would favour the step-wise mechanism over an *exo* cycloaddition.[30]

If we consider the same four cases for the 1*E*,3*Z* *s-cis* bis-cyano butadiene we again are presented with eight possible products (Figure 3.29).
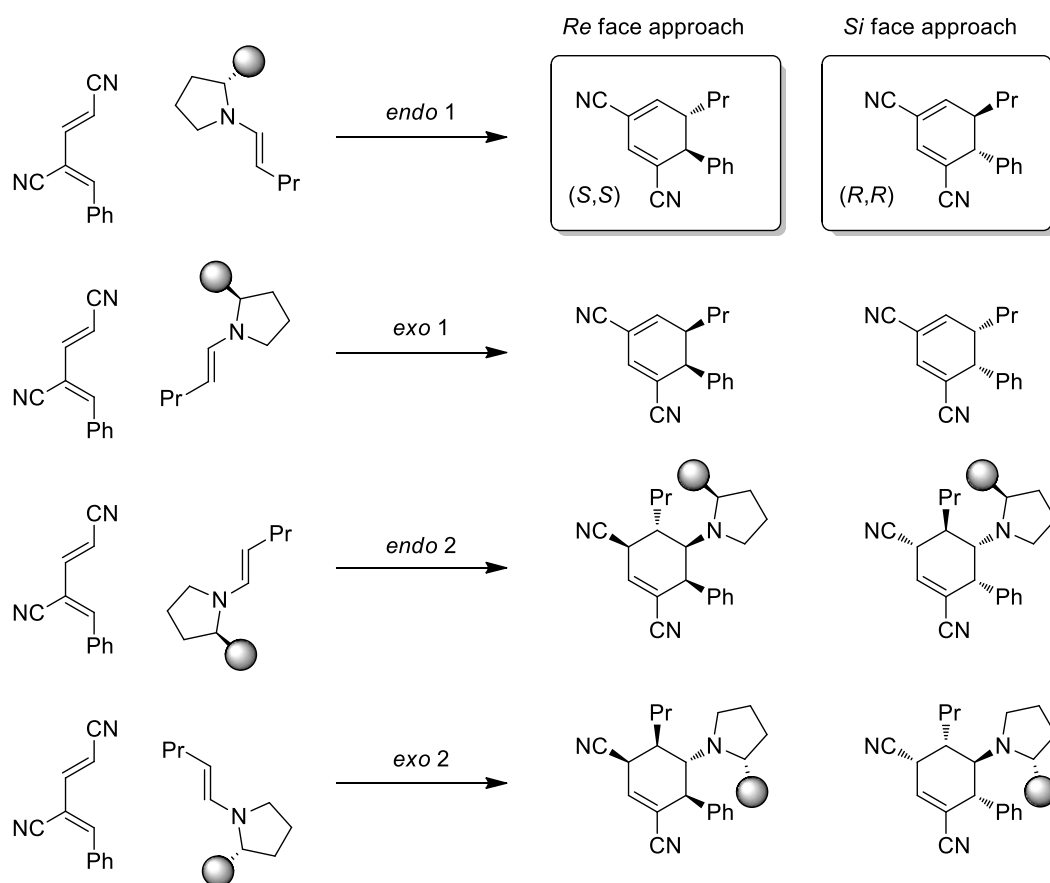
Figure 3.29. Possible IEDDA cycloadditions of aldehydic enamines and bis-cyano butadienes. In each case the cycloadducts result from approach of the enamine to the top face of the butadiene. The *R* hand of the catalyst is used in each instance.

This time, in contrast to the bis-phenylsulfonyl butadienes, the *endo* 1 approach leads to enantiomeric cyclic hexadienes with an *anti*-configuration. This is due to the change in geometry about the terminal olefin from *E*, in the bis-phenylsulfonyl butadienes, to *Z* in the bis-cyano butadienes. More insight on the mechanism could be obtained if the absolute stereochemistry of the product cyano cyclohexadiene could be confirmed by X-ray crystallography. In the case of *endo* 1 *Re* approach, the product would have a configuration of *S,S*. We predict, based on analogy to the bis-phenylsulfonyl butadienes, that this enantiomer would not be formed due to the steric clash between the bulky substituents on the pyrrolidine catalyst and the butadiene backbone. In the case of the *endo* 1 *Si* approach, the product would have an *R,R* configuration. Here we would predict that the *R,R* product would be the more thermodynamically favourable product due to the lack of steric clashing in the transition state in this approach.

In both the *Re* and *Si* approach of *exo* 1 we can see that the enantiomeric cyclohexadiene products would have a *syn*-configuration.

Similar to the bis-phenylsulfonyl butadienes, the *Re* and *Si* approaches for both the *endo 2* and *exo* 2 cases results in products that were not observed in any reaction mixtures. This is again presumably due to the unfavourable regiochemical alignment of the two reacting partners (Figure 3.28).

In conclusion, we have a general preference for the step-wise conjugate addition pathway (**Mechanism 1**) for the formation of the cyclic hexadienes from the reaction of butadienes and aldehydic enamines. Whilst not conclusive, this preference is supported by careful consideration of asymmetric variants of the transformation (the bis-phenylsulfonyl butadiene case), the products of which were amenable to X-ray crystallography.[58,69] In order to conclusively side with this mechanism, X-ray crystallography would also have to be performed on the cyclic hexadiene products resulting from the addition to both the bis-cyano and cyano-ester butadienes, something that to date has not been possible.

3.3.1.6.2   Aromatization step

At first look the final step of the reaction mechanism in the synthesis of biaryl species from bis-cyano butadienes, the formal loss of hydrogen, is not obvious (Figure 3.30).
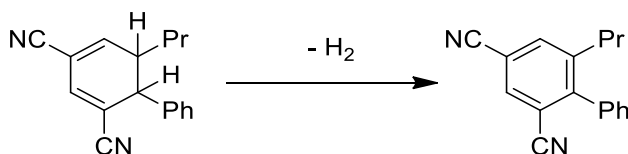
Figure 3.30. The formal loss of hydrogen from the cyclic hexadiene leading to the biaryl species.

A literature search revealed a single example wherein a base-induced hydride elimination was the proposed mechanism.[112] The authors used this proposition to explain the observed ability of a potassium fencholate-fenchone combination to act as dehydrogenation-aromatization agent. This report by Reetz *et al.* describes the dehydrogenation of dihydroarenes to arenes utilizing potassium fencholate **152** as a base and fenchone **154** as a hydride acceptor (**Figure 3.31**).[112] The authors noted that fenchone **154** was unable to undergo direct addition with the carbanion **153** due to steric restraints and could only undergo reduction by the hydride eliminated from the carbanion **153**.
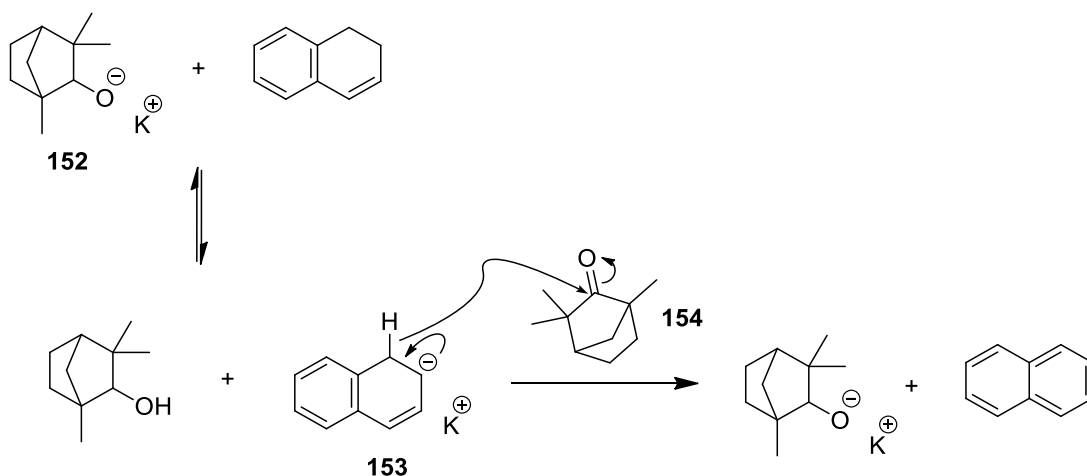
Figure 3.31. Reetz's potassium fencholate base induced aromatization.[112]

It could be proposed that the same process is happening to the cyclic hexadiene products through deprotonation of a highly acidic proton followed by hydride elimination to give the

biaryl species (Figure 3.32). Here, the intermediate is acting like a hydride transfer agent with the hydride immediately scavenged by an acceptor within the reaction mixture.
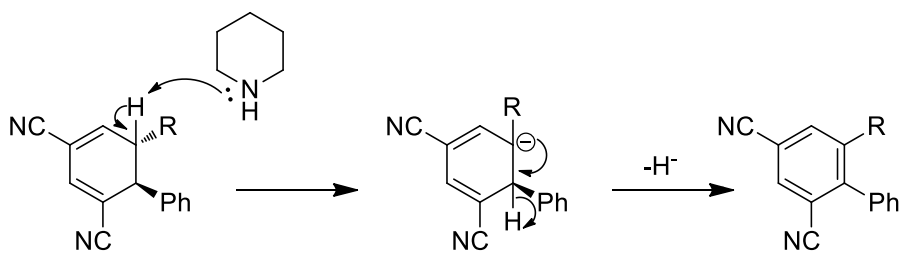
Figure 3.32. Deprotonation and hydride elimination to yield biaryl.

In our case there is no added sacrificial hydride acceptor present to accept the hydride that is eliminated. It is possible that the nitrile functionalities of the unreacted cyclic diene or the starting butadiene are acting as hydride acceptors in a similar fashion. This could account for product loss in the formation of the biaryls from butadienes.

A potential scenario whereby the eliminated hydride reduces the nitrile functionality of an already aromatized biaryl thereby reducing the isolated yield of the biaryl species is outlined in Figure 3.33.
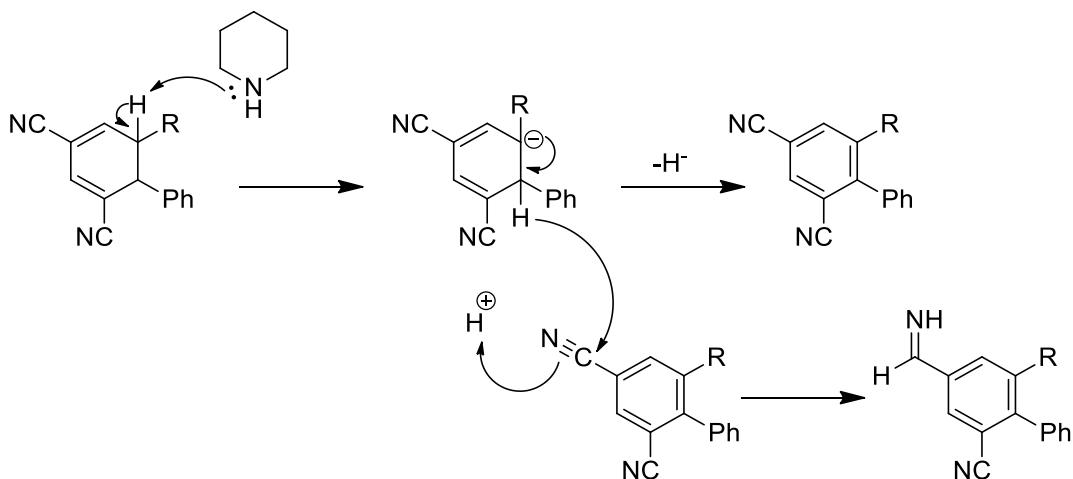
Figure 3.33. Deprotonation/hydride elimination with concomitant nitrile reduction leading to one of a number of potential products. This reduction can lead to a number of potential nitrile reduction products including a range of imines, amines and aldehydes.

This nitrile reduction could happen to either the biaryl species as outline above, to either of the nitriles present in the starting bis-cyano butadiene, or the cyclic hexadiene intermediate

leading to a large number of side-products. None of these products have to date been observed spectroscopically in order to confirm this hypothesis. There is however, a loss of material which cannot be accounted for. This leads us to believe that there is some parasitic side-reaction taking place which is effecting the yield of the process.

3.4 Other transformations

A number of other transformations, which we had hoped the bis-cyano butadienes may have been applicable to, were also explored throughout the course of this study. These transformations and their predicted products are detailed in

Figure 3.34. Unfortunately none of these transformations yielded any of the expected products and in many cases led to the decomposition of the bis-cyano butadiene.
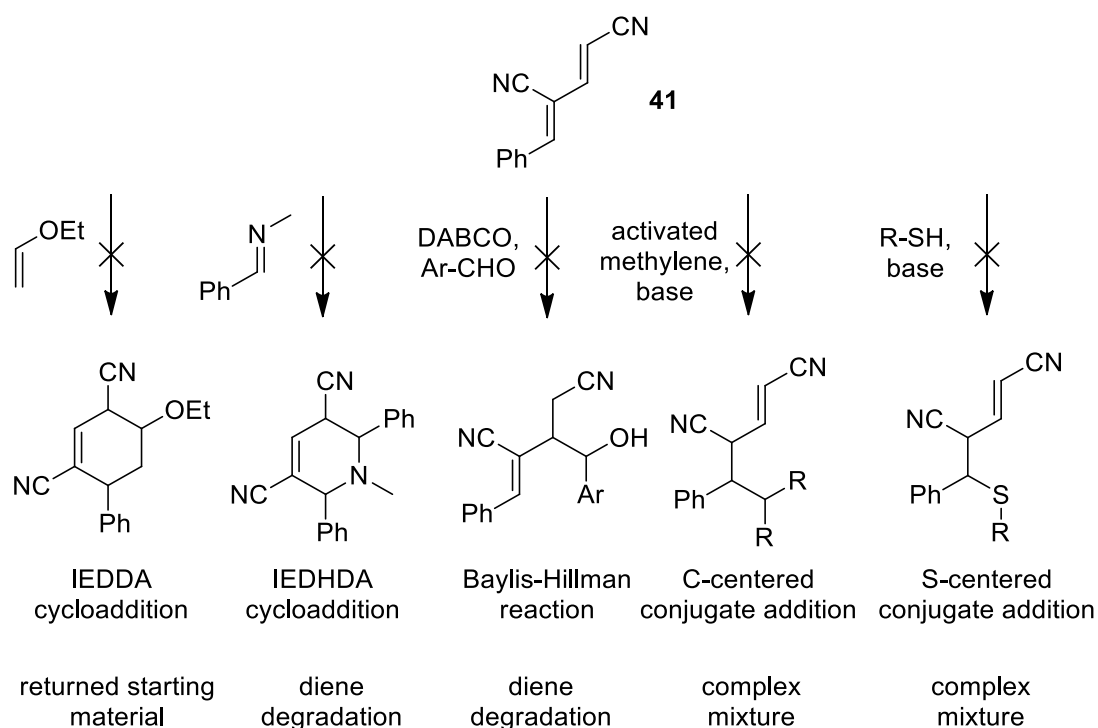
Figure 3.34. Additional reactions explored with the bis-cyano butadiene **41**.

3.5   Future work

The expansion of this methodology towards the synthesis of biaryls with substituted phenyl rings allows the exploration of some interesting new chemical space and potentially adds stereochemistry to the so far achiral biaryls. A brief description of the potential of these products is outlined below.

3.5.1   Introduction of axial chirality to biaryls

There is potential to introduce axial chirality into the biaryl products by utilizing butadienes with the appropriate substitution of the *o*-position on the aryl rings. Substitution of the *o*-positions on both aryl rings leads to a biaryl product with steric clashes (**Figure 3.35**). The net result of this sterically induced hindrance is the restricted rotation about the biaryl C-C sigma bond. If the steric hindrance is great enough, and therefore the energy barrier to rotation about the C-C sigma bond high enough at room temperature, then stereoisomerically pure axially chiral compounds could potentially be isolated.
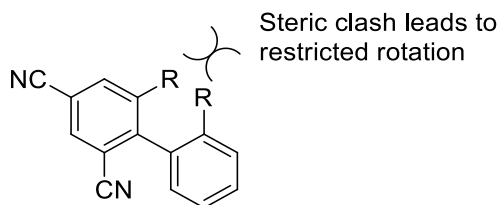
Figure 3.35. Sterically induced restricted rotation allows for the conservation of optical enrichment of biaryls.

Axial chirality should be present in biaryls with *ortho* substitution which are derived from butadienes with aryl groups that also contain *ortho* substitution. The restricted rotation resulting from the clashing substituents could be enough to lock the conformation of the biaryl in a fixed stereochemical arrangement.
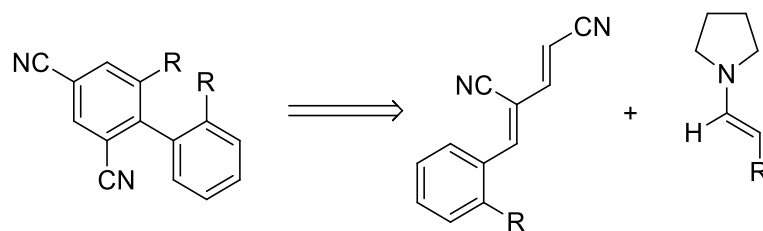
Figure 3.36. Synthesis of axially chiral biaryls from butadienes and aldehydic enamines. R = bulky substituent such as an alkyl group or large halogen.

Axial chirality is present in a number of importance pharmacologically relevant compounds such as the antibiotic vancomycin (Figure 3.37). Present also within vancomycin are a number of other forms of chirality such as the traditional stereogenic centres, observed at tetrahedral centres bearing four different substituents, as well as examples of planar chirality in the form of the diaryl ethers, which exhibit restricted rotation due to the *o*-Cl substituents.
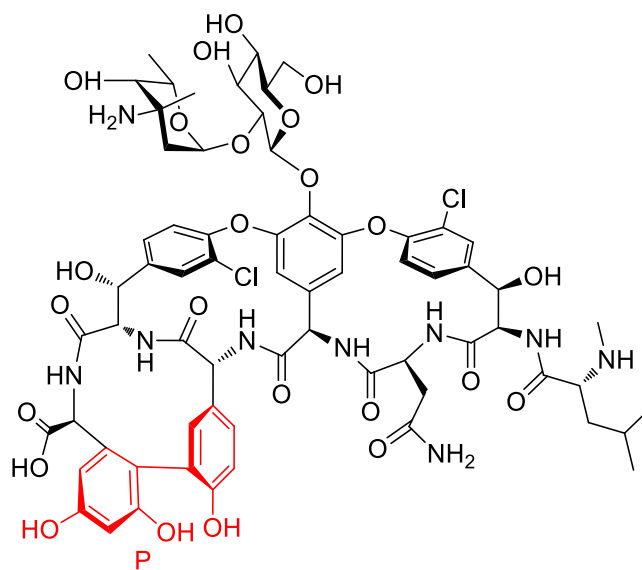
Figure 3.37. Vancomycin, axial chirality highlighted in red.

3.5.2   Palladium coupling reactions of bromo-derivatives

Biaryls adorned with a Br could potentially be applied to palladium coupling reactions with a number of commercially available coupling partners, e.g. boronic acids in the case of Suzuki coupling. An example of such a coupling can be seen in Figure 3.38, whereby an anthracene group could be added to the biaryl at the *-o,-m,* or *-p* position of the phenyl ring in order to

develop a family of fluorescent compounds. These compounds could also display axial chirality.
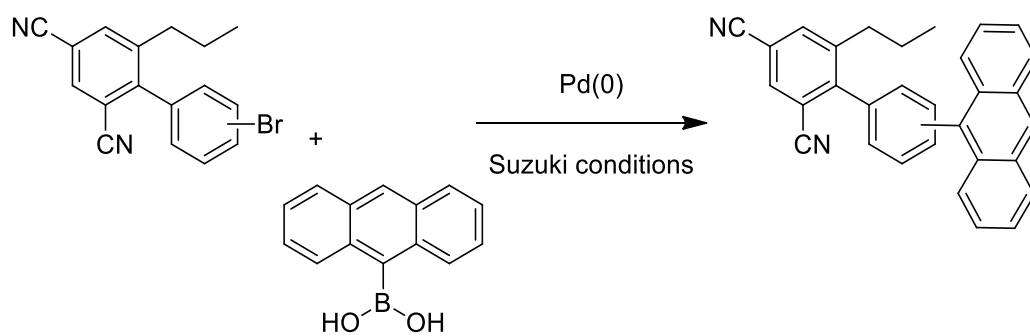
Figure 3.38. Suzuki coupling of bromo derivatized biaryls with boronic acids.

3.6   Conclusion

In conclusion we have developed a novel route to yield biaryl products through the conjugate addition/cyclization/hydride elimination of aldehydic enamines to 1,3-di-substituted butadienes (Figure 3.39).
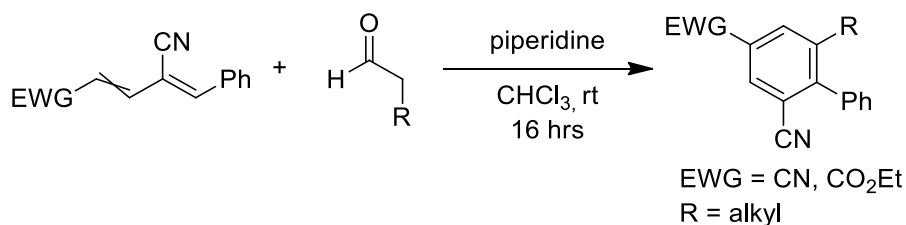
Figure 3.39. Synthesis of biaryls from the addition of aldehydic enamines to 1,3-disubstituted butadienes.

The substitution patterns accessible through this methodology are atypical of traditional biphenyl syntheses and so this methodology can be seen as a welcome addition to the synthetic chemist's toolbox towards the synthesis of biaryls. Whilst the exact mechanism of this transformation has not been definitively concluded, a stereochemical argument has been made towards rationalising a preference for a step-wise conjugate addition/cyclization followed by deprotonation/hydride elimination. The next rational step towards a deeper understanding of this transformation would be the synthesis of a crystalline cyclic hexadiene obtained in an enantioselective fashion.

4   Chapter 4: Pyran Synthesis

4.1   Introduction

Formyl acrylonitriles, whose syntheses are described in Chapter 2, were successfully employed in the synthesis of nitrile containing butadienes. During the course of those investigations an unexpected product was discovered that was the result of a conjugate addition/cyclization between a malononitrile anion and phenyl formyl acrylonitrile **57** (Section 2.2.10). As a result of this unexpected find it was considered pertinent to explore other potential reactivity patterns applicable to the formyl acrylonitriles. These considerations ultimately led to the use of formyl acrylonitriles in conjugate addition reactions and inverse electron-demand hetero-Diels-Alder cycloaddition reactions (IEDHDA), leading to the generation of 2-amino-4*H*-pyrans and 3,4-dihydro-2*H*-pyrans respectively.

4.1.1   Pyrans as valuable synthetic targets

The pyran motif (both the 2*H* and 4*H* isomers) and its related reduction products, dihydropyran and tetrahydropyran, are commonly found within the realm of pharmacologically active natural and non-natural products (**Figure 4.1**).

| 4*H*-pyran | 2*H*-pyran | 3,4-dihydro-2*H*-pyran | tetrahydro-2*H*-pyran |
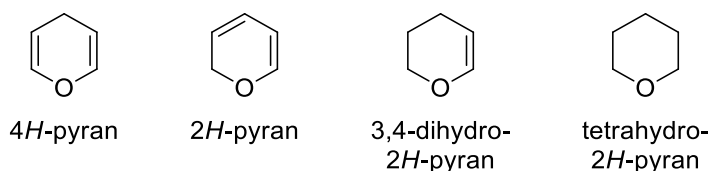
Figure 4.1. Pyran isomers and their reduction products.

Functionalized pyrans have been found to exhibit a broad range of biological activities including anticancer, cytotoxic, anti-retroviral, anti-inflammatory, antimalarial, and antidyslipidemic to name a few.[113,114]

4.1.1.1 Synthesis of 2-amino-4H-pyrans

Of particular importance is the 2-amino-4*H*-pyran motif which is found as part of numerous larger scaffolds that have exhibited therapeutic effects (Figure 4.2).
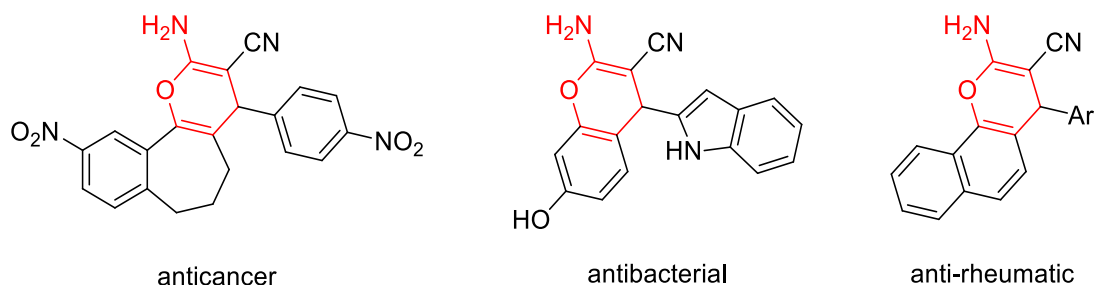
Figure 4.2. Examples of the presence of the 2-amino-4*H*-pyran motif present in a number of biologically active compounds.

2-Amino-4*H*-pyrans themselves have also been found to be of synthetic interest in the generation of other pharmacologically relevant compounds. An example of this is the amino-pyran **155** which was utilized as a synthetic intermediate in the synthesis of anticoagulant warfarin and related compounds by Wiener *et al.* (Figure 4.3).[115]
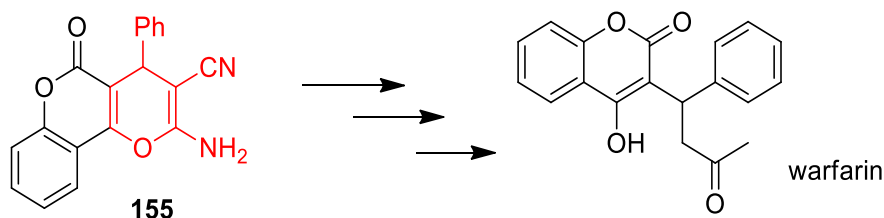
Figure 4.3. Synthesis of warfarin and related compounds described by Wiener *et al.* from a 2-amino-4*H*-pyran precursor.[115,116]

The majority of the literature reports detailing the synthesis of 2-amino-4*H*-pyrans utilize similar synthetic methods. Namely, the combination of either activated methylenes and unsaturated nitriles or from α,β-unsaturated carbonyl compounds and CH-acidic nitriles (Figure 4.4).[116] The distinction between either pathway essentially lies in whether or not the nitrile functionality is on the nucleophilic partner or the electrophilic partner. Both pathways presumably pass through a similar intermediate **156** before cyclization and tautomerization yield the final 2-amino-*4H*-pyran. A noteworthy point is in the literature such products are

typically substituted with R = >H at the 5 position, this may be of importance when discussing

the stability of 2-amino-*4H*-pyran where R = H at the 5-position.[116]
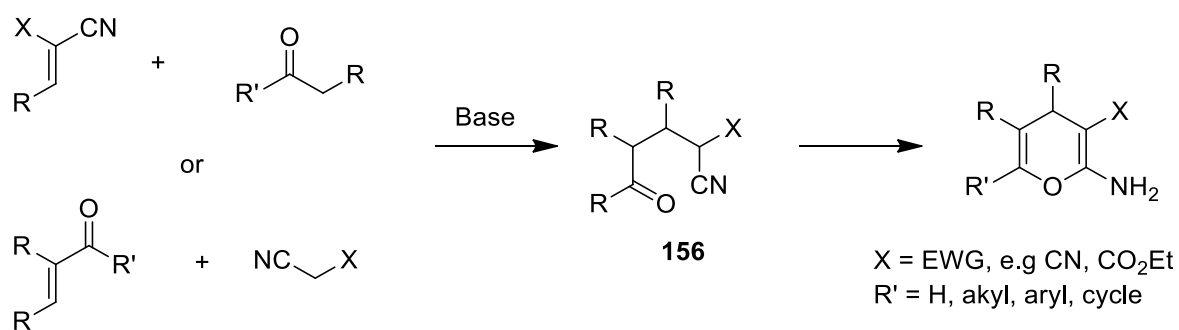
Figure 4.4. General synthesis of 2-amino-*4H*-pyrans from activated methylenes and unsaturated nitriles.[116]

4.1.1.2 Synthesis of 3,4-dihydro-2*H*-pyrans

The dihydropyran motif can be found within a number of natural products of pharmacological interest and includes carbohydrates. The term "glycal" is colloquially used to specifically describe saccharide subunits that are unsaturated between carbons 1 and 2 on their carbon backbone (Figure 4.5). Glycals can be generated from the formal elimination of the hemiacetal hydroxyl group and an adjacent hydrogen.
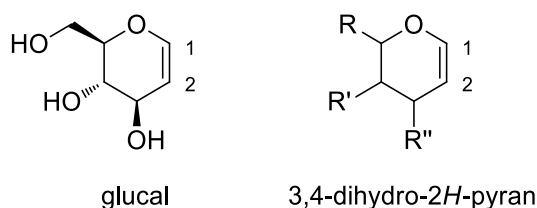
Figure 4.5. Glucal, the glycal of glucose, and the 3,4-dihydro-2*H*-pyran motif.

Glycals are well known for their ability to be utilized as both glycosylation donors and acceptors in the synthesis of oligosaccharide containing products.[117] As can be seen in Figure 4.5 glycals contain the 3,4-dihydro-2*H*-pyran motif at their core and the synthesis of functionalized dihydropyrans can lead to the generation of important synthetic intermediates. These intermediates can in turn be used in the generation of natural and unnatural glycals, which are used in a number of glycoconjugate therapeutics such as antibiotics and anti-tumour agents.

The dihydropyran motif is predominantly accessed through the use of Inverse Electron Demand Hetero Diels-Alder (IEDHDA) cycloaddition reactions. An advantage to the use of cycloaddition chemistry in the synthesis of these scaffolds is the quick and atom-economic access to polyfunctionalized mono-cyclic and poly-cyclic systems.

Evans *et al.* have reported the enantioselective synthesis of 3,4-dihydro-*2H*-pyran derivatives through IEDHDA cycloadditions of β,γ-unsaturated-α-ketoesters/phosphonates and electron rich olefins (Figure 4.6).[118] In order to reduce the activation energy barrier for these reactions Evans *et al.* employed a bis(oxazoline) Cu(II) chelating Lewis acid catalyst **157** and performed the reactions at cryogenic temperatures in order to obtain high stereoselectivity.
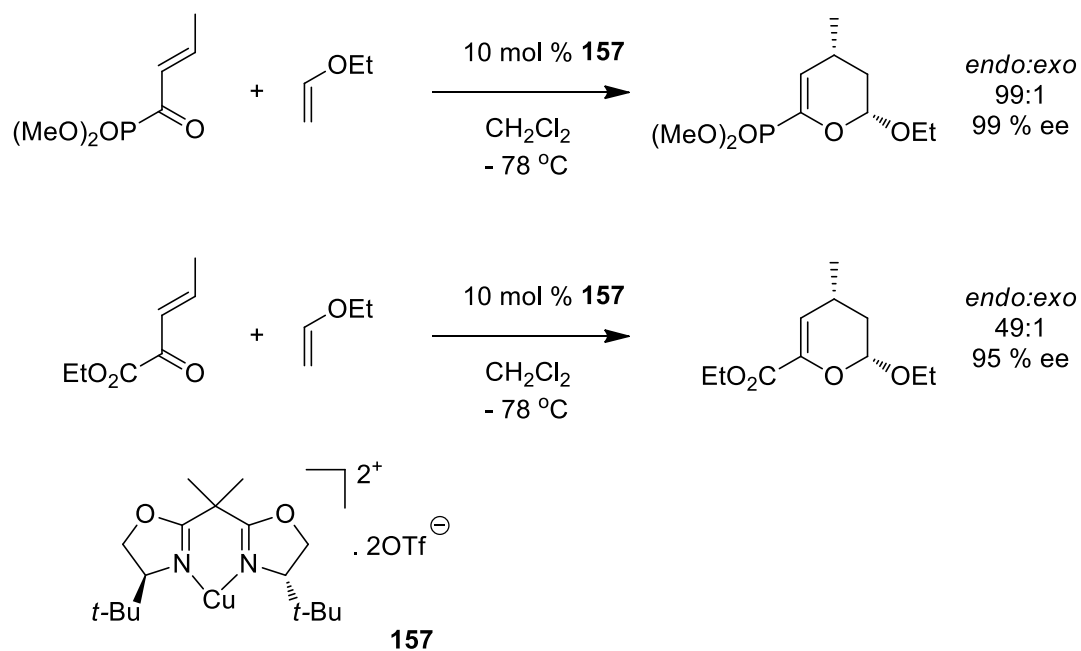
Figure 4.6. IEDHDA cycloadditions reported by Evans *et al.* yielding 2,4-dihydro-*2H*-pyrans.[118]

Jørgensen *et al.* have also reported an enantioselective organocatalytic variant of the IEDHDA reaction, utilizing aldehydic enamines and enones as the reacting partners to yield hemi-acetals containing the 3,4-dihydro-2*H*-pyran motif (Figure 4.7).[30] These hemi-acetals could then be further transformed into lactones.
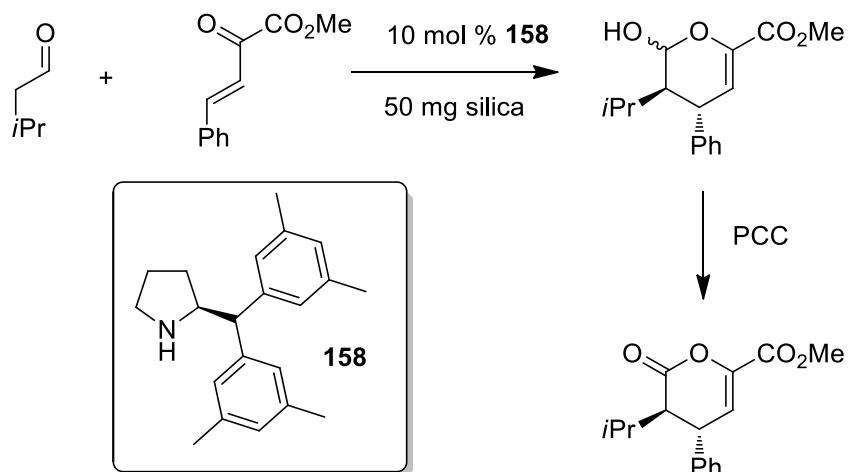
Figure 4.7. The organocatalytic IEDHDA cycloaddition reported by Jørgensen *et al.*[30]

4.2   Formyl acrylonitriles as Michael-type acceptors

The generic formyl acrylonitrile structure contains a number of electrophilic sites (Figure 4.8). During our investigations into the synthesis of nitrile containing butadienes, through the use of formyl acrylonitriles and base-free Wittig conditions, no additional products were observed and the butadienes were the sole isolated products. Further exploration of the reactivity patterns of formyl acrylonitriles would require careful consideration of the additional electrophilic positions on the formyl acrylonitrile structure. These sites are the nitrile carbon and the olefinic β-carbon (Figure 4.8).
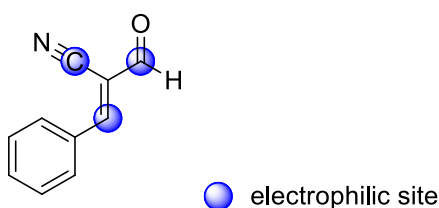
Figure 4.8. Electrophilic sites of the formyl acrylonitrile **57**.

One might expect a strong nucleophile to attack the carbonyl carbon in a direct fashion. The attack of a Grignard reagent on an aldehyde in the presence of a nitrile was utilized by Ho *et al.* in their synthesis of tacamonine (Figure 4.9).[119] Preferred attack at the carbonyl carbon is due to the more electrophilic nature of the carbonyl carbon in comparison to the nitrile carbon.
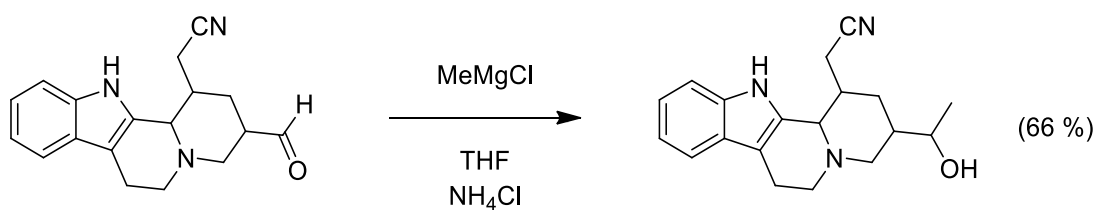
Figure 4.9. Addition of a Grignard reagent to an aldehyde, in the presence of a nitrile group, as performed by Ho *et al.*[119]

However, nitriles can also react in an electrophilic fashion. Wang *et al*. reported an example of the transformation of a nitrile to a ketone in their 2010 publication (Figure 4.10).[120]
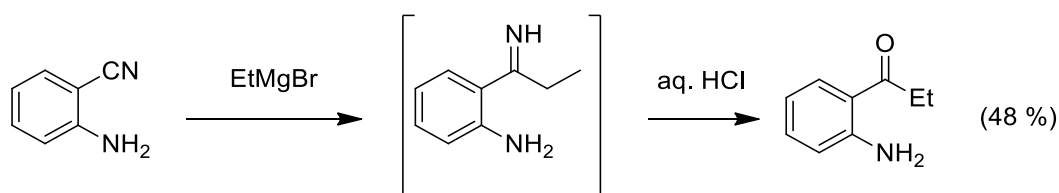
Figure 4.10. Conversion of a nitrile into a ketone as performed by Wang *et al*.[120]

The olefin of the formyl acrylonitrile motif is very electron deficient. This is due to the combined inductive withdrawal of both the nitrile and the aldehyde substituents on the alkene. Plausible resonance structures can also be generated showing the polarization of the terminal olefin carbon (Figure 4.11). This polarization makes the terminal carbon of the alkene susceptible to attack from suitable nucleophiles.
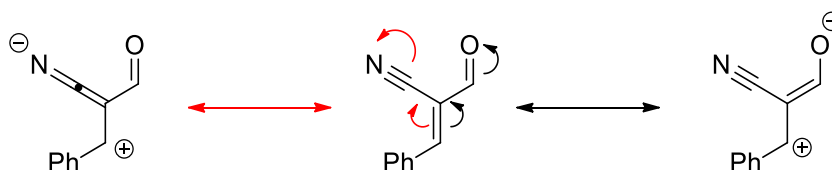
Figure 4.11. Possible resonance structures of the formyl acrylonitrile **57**.

Careful consideration of the reagents utilized must be undertaken when carrying out syntheses with substrates that contain multiple reactive functional groups. As exemplified by Kashima *et al.* in Figure 4.12, the choice of reagents dictates the chemoselectivity of the addition of the Grignard reagent.[121] The addition of CuI to the reaction mixture transmetallates the Grignard to yield a Gilman reagent, which reacts at the β-carbon of the unsaturated nitrile.
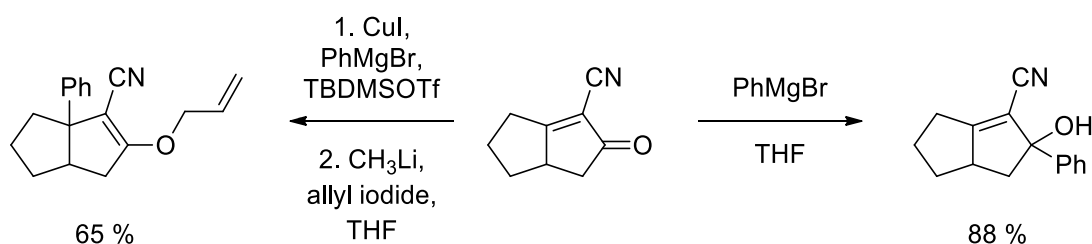
Figure 4.12. Selective attack of a Grignard at either the carbonyl carbon or the β-carbon performed by Kashima *et al*.[121]

In theory, the formyl acrylonitrile should be susceptible to the conjugate addition of suitable nucleophiles due to the increased electron-deficiency at the β-carbon. This reactivity however may be complicated due to the presence of the additional electrophilic sites as outlined above. In order to explore the utility of formyl acrylonitriles as Michael-type acceptors we devised experiments to determine their ability to undergo conjugate addition with a number of pronucleophilic activated methylenes.

4.2.1   Results and Discussion

As outlined previously in Section 2.2.10, the ability of the formyl acrylonitrile **57** to take part in conjugate addition chemistry was observed during our attempts to synthesize 1,1,3-tri-substituted butadienes. The retrosynthetic pathway to these tri-substituted butadienes can be seen in Figure 4.13. These tri-substituted butadienes should in theory be activated towards conjugate addition chemistry and were expected to make a welcome addition to the butadiene families described in Chapter 2. A simple Knoevenagel condensation of formyl acrylonitrile **57** and malononitrile was expected to generate the alpha olefin and yield the target butadiene **121**.
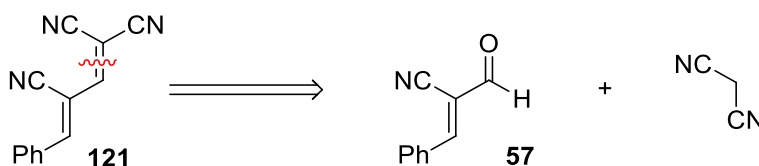
Figure 4.13. Retrosynthetic analysis of 1,1,3-trisubstituted butadiene **121**.

The use of malononitrile as a pro-nucleophile in Knoevenagel condensation chemistry has already been utilized by a number of groups in the synthesis of di-cyano substituted olefins. One particularly relevant report is that by Deshmukh *et al.*, which details the synthesis of methylenemalonitriles through the Knoevenagel condensation of aromatic aldehydes and malononitrile (Figure 4.14).[122] These species are particularly close in structure to our targeted tri-substituted butadienes.
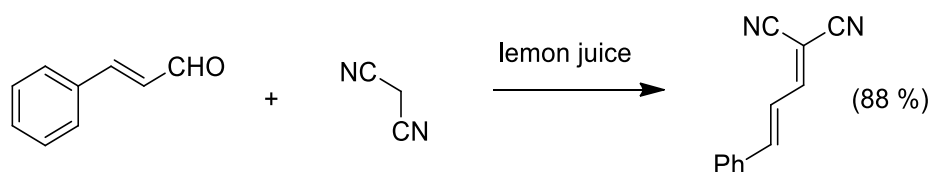
Figure 4.14. Synthesis of methylenemalonitriles by Deshmukh *et al.*[122]

When we attempted the forward reaction, instead of the expected butadiene product **121**, we observed the formation of a single unknown product in high yield. Detailed spectroscopic study, Section 4.2.1.1, allowed us to identify this product as the 4*H*-amino pyran **122** Figure 4.15.
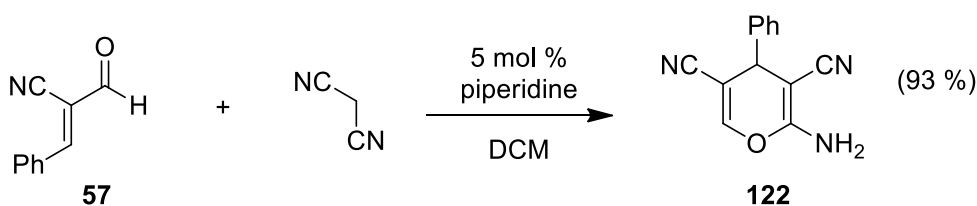
Figure 4.15. Synthesis of 4-H amino pyran **122**.

After the product had been identified, a return to the literature uncovered a report by Ciller *et al.* in 1985, which detailed the synthesis and spectral characterization of the amino-pyran **122** under similar conditions (Figure 4.19).[123] In this case the authors generated the formyl acrylonitrile **57** *in-situ* through the base induced ring-opening of isoxazole **159** to yield the oxopropanenitrile **160**. Condensation of **160** with benzaldehyde yielded the formyl acrylonitrile **57**. Reaction of the formyl acrylonitrile with malononitrile, in the presence of piperidine, gave the 2-amino-4*H*-pyran **122** in 61 % yield (Figure 4.16). This report focused predominately on the multiple uses of ring transformations of isoxazoles and as such the reaction scope explored was limited to two 2-amino-4H-pyran products.
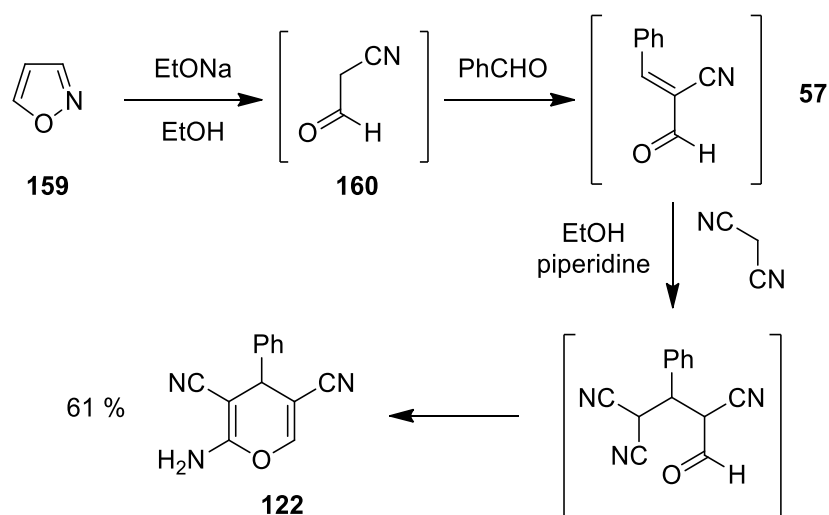
Figure 4.16. The synthesis of amino-pyran **122** as described by Ciller *et al.* The amino-pyran **122** product is the only isolated product from this reaction sequence.[123]

4.2.1.1   Spectroscopic characterization of 2-amino-4H-pyrans

The product 2-amino-4H-pyran **122** was identified initially using a combination of ^{1}H and ^{13}C NMR spectroscopic experiments (Figure 4.17 and Figure 4.18). The isolated product was essentially pure and only required washing with PE to obtain a pure sample. From the ^{1}H NMR spectrum, the absence of the aldehydic peak informed us that the starting material had been consumed. In place of the starting material ^{1}H NMR signals we now observed new sets of signals in the aromatic region indicating protons in deshielded environments. A new singlet integrating for 1 proton was also present at 4.32 ppm. In combination with the ^{13}C NMR and 2-D spectra the peaks at 7.73 ppm and 4.32 ppm were identified as the vinylic and proton at the 4-position of the pyran ring. The ^{13}C NMR also revealed the presence of two distinct quaternary nitrile carbons at 116.3 and 119.0 ppm.
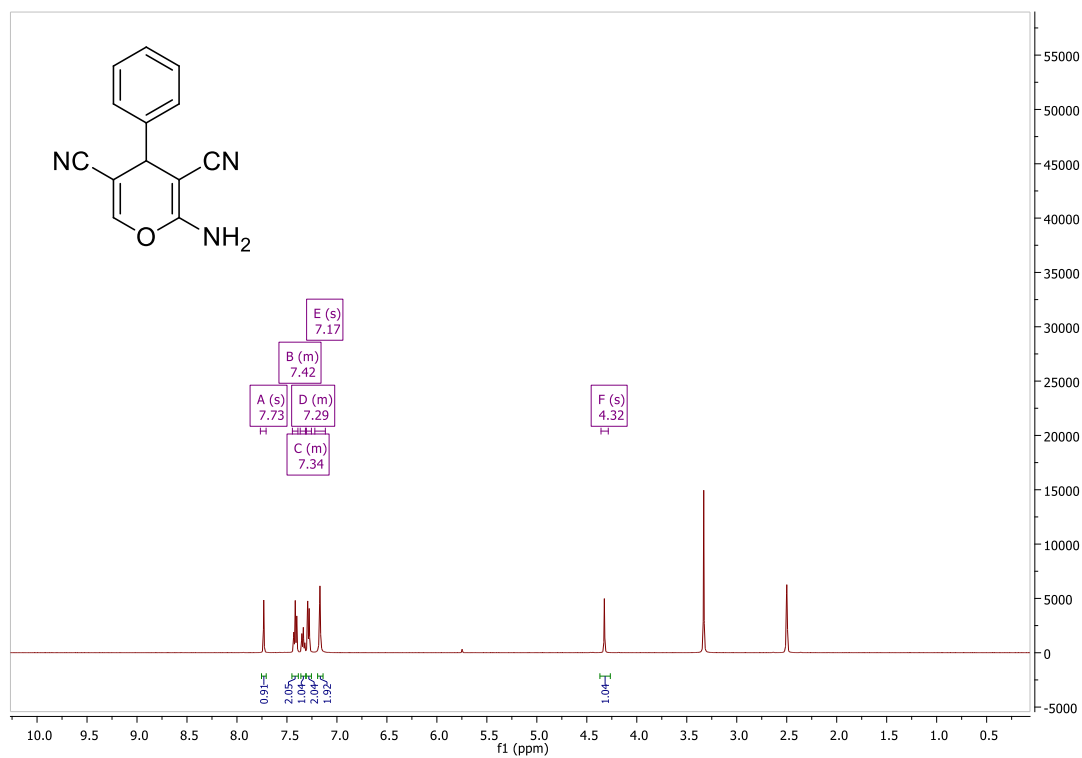
Figure 4.17. ^{1}H NMR of amino pyran **122**.
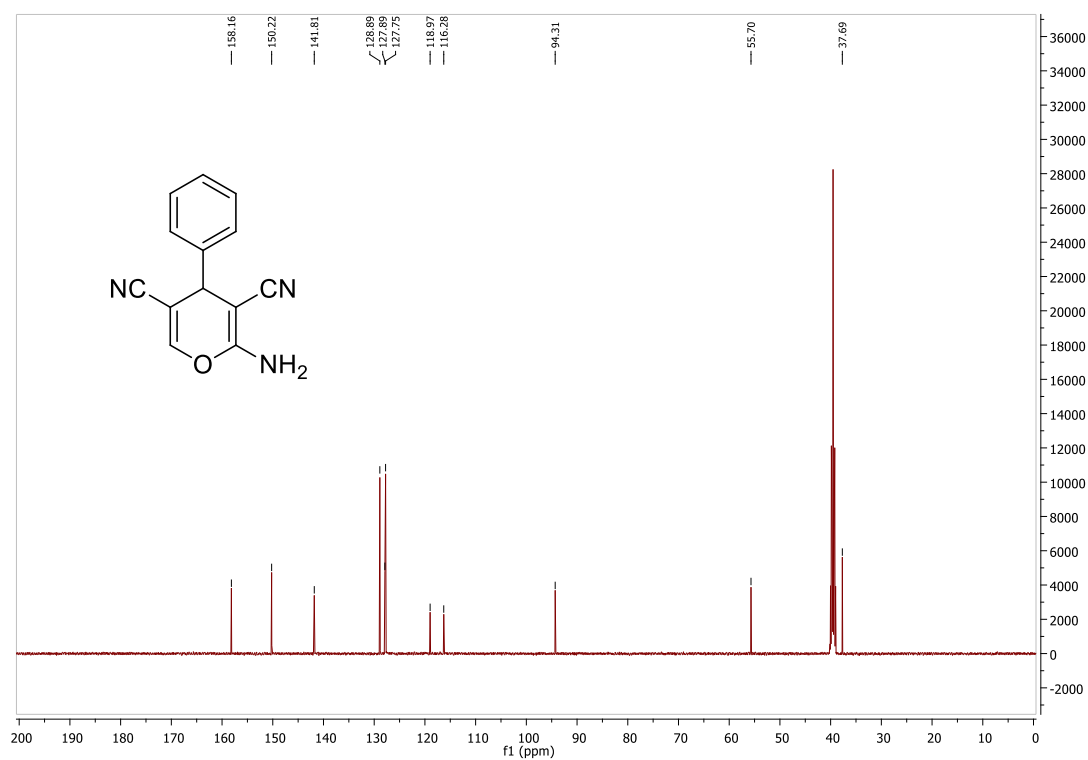
Figure 4.18. ^{13}C NMR spectrum of amino pyran **122**.

All of the above information in combination with the consideration of the malononitrile anion attacking in a conjugate fashion allowed us to elucidate the structure of the amino-pyran **122**. This was later supported by HRMS. A summary of the ^{1}H NMR and ^{13}C NMR spectral assignments are given in Figure 4.19.
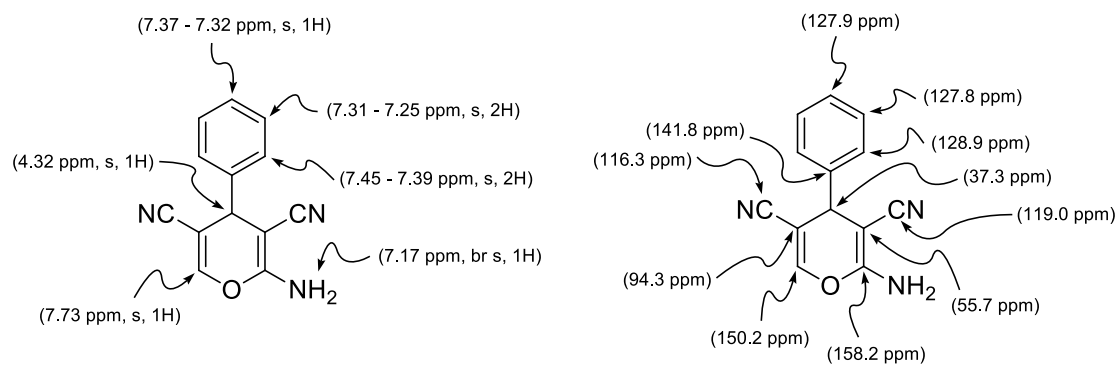
Figure 4.19. ^{1}H NMR and ^{13}C NMR spectral assignment for aminopyran **122**.

4.2.1.2   Substrate scope

A number of aryl substituted formyl acrylonitriles were explored as substrates for this reaction, Table 4.1. Aryl substituents containing strongly electron withdrawing groups were not explored as they could not be synthesised in our hands. The p-OMe, o-CH$_3$ and p-CH$_3$ formyl acrylonitriles did yield amino pyran products in good yields. Disappointingly however, when applied to formyl acrylonitriles bearing additional substituents on the phenyl ring, or a napthlene group, the reaction did not yield pure product. In each of those cases inseparable mixtures were obtained, when applied to silica gel chromatography none of the desired products could be isolated. This may be due to the instability of the amino pyrans.
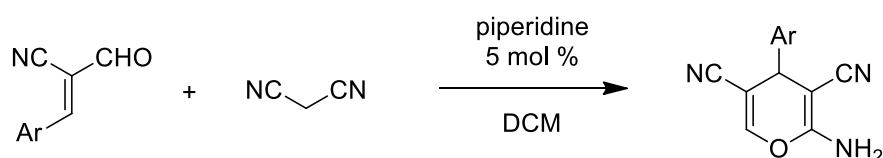
Table 4.1 Substrate scope

Entry	Ar	Yield (%)
1	p-OMe-C$_6$H$_5$ (**161**)	74
2	o-CH$_3$-C$_6$H$_5$ (**162**)	93
3	p-CH$_3$-C$_6$H$_5$ (**163**)	94
4	p-Cl-C$_6$H$_5$	Inseparable mixture
5	m-Cl-C$_6$H$_5$	Inseparable mixture
6	m-Br-C$_6$H$_5$	Inseparable mixture
7	p-NMe$_2$-C$_6$H$_5$	Inseparable mixture
8	Napthyl	Inseparable mixture

During the preparation of this manuscript a report by Reddy *et al.* described the synthesis of compounds **161-163** as well as a number of other amino pyrans bearing substitution on the phenyl ring under similar reaction conditions (10 mol % piperidine in EtOH) in good to moderate yields. These amino pyrans were also show to have moderate antifungal and anticancer properties with test *in vitro*.[124]

4.2.1.3   Reaction mechanism

A proposed mechanism for the conversion of formyl acrylonitriles to 2-amino-4*H*-pyrans is shown in Figure 4.20. Deprotonation of the α-proton of the activated methylene to **164**, followed by attack on the β-carbon of the formyl acrylonitrile **57** leads to the intermediate enolate **165**. The enolic oxygen then attacks the nitrile carbon leading to the imino-pyran **166**, which undergoes tautomerization to the amino-pyran product **122**.
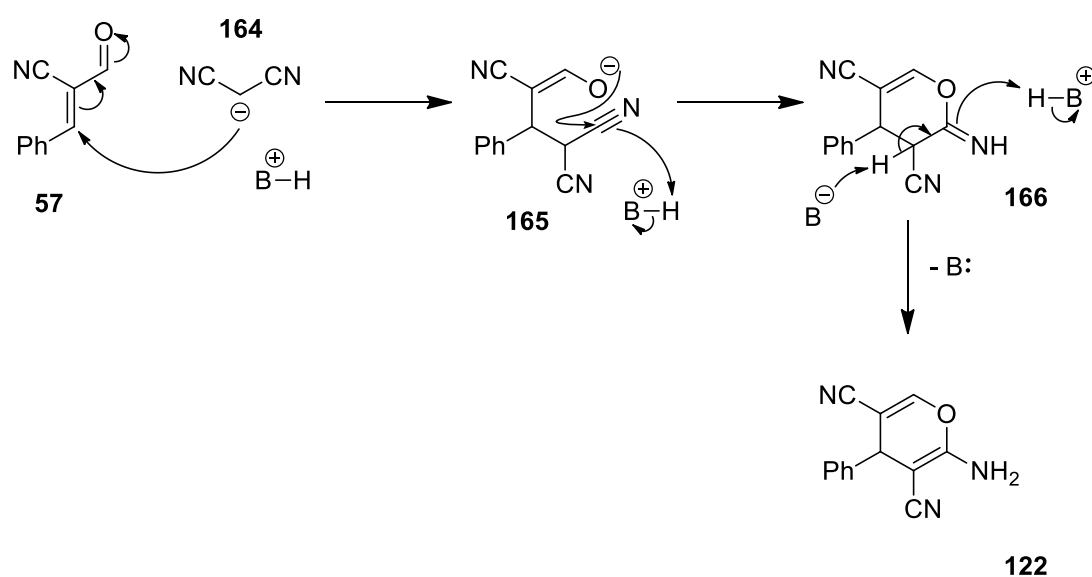
Figure 4.20. Proposed mechanism for the generation of 2-amino-4*H*-pyran **122** from malononitrile and formyl acrylonitrile **57**.

4.2.2   Attempted synthesis of optically enriched 4*H*-aminopyrans

The synthesis of optically pure 2-amino-4*H*-pyrans would also be of significant interest with regards to the potential biological activity of this class of compounds. As already outlined in Chapter 1, the biological activity of compounds bearing stereogenic centres can be dictated by their configuration, and in some cases different stereoisomers can have drastically different pharmacological effects.

There is some literature precedent for the synthesis of enantioenriched 2-amino-4*H*-pyrans through organocatalytic means. One such example is that of the report by Elnagdi *et al.* in which they describe the multicomponent reaction of aromatic aldehydes, malononitrile and activated methylenes in the presence of *L*-proline (Figure 4.21).[125]
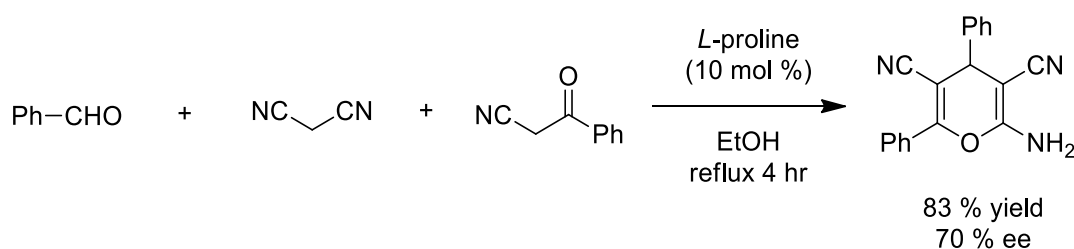
Figure 4.21. MCR reaction reported by Elnagdi *et al.* in the synthesis of chiral 2-amino-4*H*-pyrans.[125]

The authors do not suggest a mechanism for this particular transformation. However, it could be postulated that the proline first acts in a Brønsted acid/base fashion to catalyze the condensation of the propanenitrile **167** and the aromatic aldehyde to yield the α,β-unsaturated nitrile **168** (Figure 4.22). A competing reaction could be the deprotonation of the malononitrile and its subsequent condensation with the aromatic aldehyde. This does not occur and perhaps is due to the lower pKa of the α-hydrogen of the ketonitrile (10.2 in DMSO) compared to the α-hydrogen of malononitrile (11.1 in DMSO).[126,127] *L*-Proline could then act in a bifunctional manner to catalyze the Michael-type addition to the newly formed olefin of **168**. First, deprotonating malononitrile and second by forming hydrogen bonds with the α,β-unsaturated nitrile **168**. This preorganization could lead to control of the approach of the malononitrile carbanion and lead to enantiocontrol in the addition reaction (Figure 4.22). The addition product then undergoes concomitant cyclization where the enolic oxygen attacks the nitrile carbon. This leads to the 2-iminopyran intermediate **169**, which then tautomerizes to the 2-aminopyran product **170** (Figure 4.22).
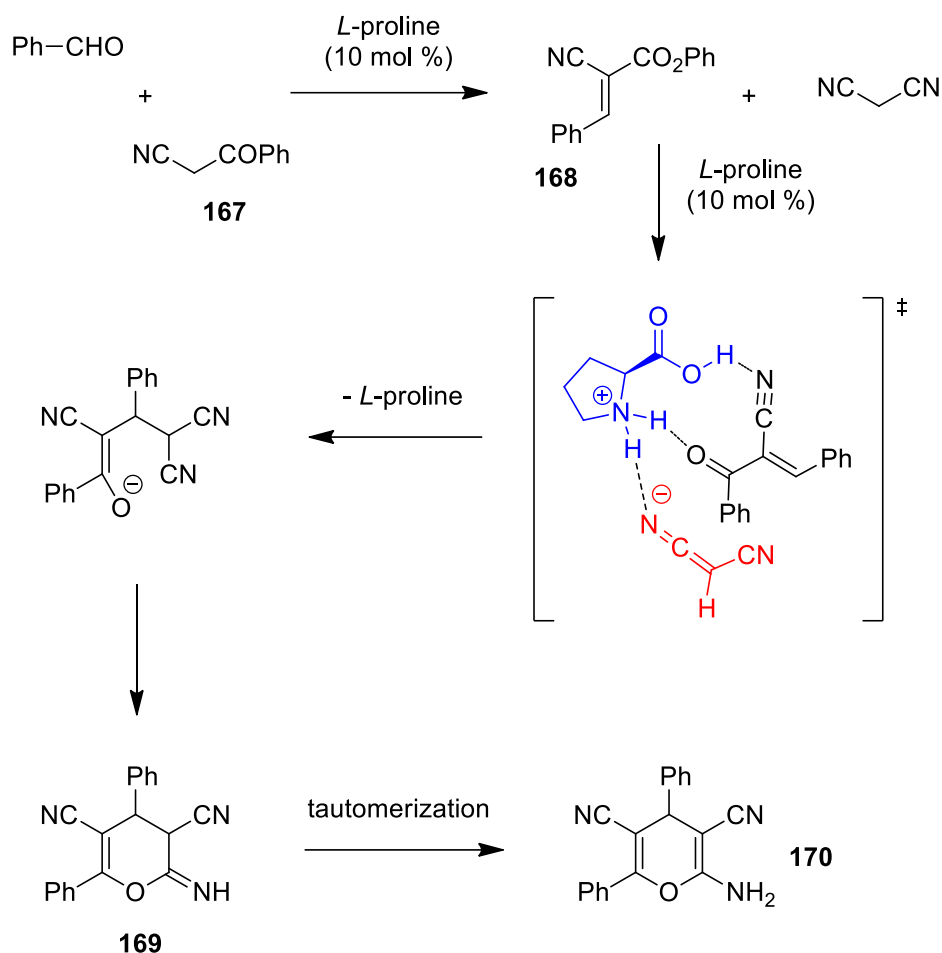
Figure 4.22. Postulated reaction sequence and transition state for the controlled addition of malononitrile to the α,β-unsaturated nitrile **168**.

Interestingly, in order to determine the ee of the reaction the authors utilized the chiral shift reagent europium tris[3-(heptafluoropropylhydroxymethylene)-(+)-camphorate]. After addition of a sufficient amount of the chiral shift reagent the ^{1}H NMR spectrum of **170** resolved into two distinct sets of signals. The distinct signals could then be integrated relative to one another in order to determine the ee.

Since the explosion of interest in organocatalyzed transformations in the early 2000's much effort has been given to the development of novel catalyst scaffolds. Inspired by the work of Elnagdi *et al*. we also chose to utilize a bifunctional catalyst to control the stereochemical outcome of the reaction.[125] For our study on the synthesis of optically enriched amino-pyrans we selected the bifunctional Takemoto's catalyst **171** (Figure 4.23).
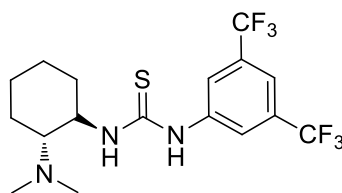
Figure 4.23. Takemoto's catalyst **171**.

Takemoto's catalyst contains a Brønsted basic dimethylamino group capable of activating pronucleophiles through deprotonation, as well as the thiourea motif capable of forming stabilizing hydrogen bonds with an incoming electrophile. We chose a thiourea based catalyst over a urea one as the thiourea hydrogens atoms are more effective hydrogen bond donors. This is due to the increased acidity of the –NH protons, which is a result of the increased stability of the deprotonated thiourea anion over the urea anion. A comparison of pKa values for representative urea and thiourea scaffolds also highlights the increased acidity of the thiourea variants. Diphenylurea **172** has a pKa value measured at 18.7 (in DMSO), while its sulfur analogue **173** has a pKa value measured at 13.4 (in DMSO) (Figure 4.24).[128] The acidity of the urea and thiourea protons can be modulated through alteration of the electronic nature of the substituents. As can been seen in Figure 4.24 the addition of the highly electron-withdrawing trifluoromethyl groups to the phenyl rings drastically lowers the pKa values of both the diphenyl urea and the diphenyl thiourea (13.8 and 8.5 respectively).[128] The pKa of Takemoto's catalyst **171** has been reported as 13.65 (in DMSO).[128]
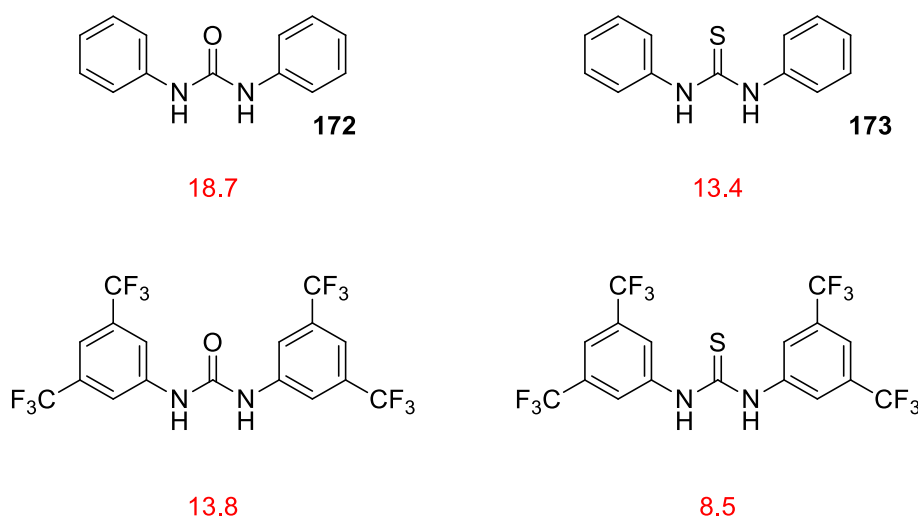
Figure 4.24. pKa values reported for a number of (thio)urea scaffolds. Values reported in DMSO.[128]

A tentative transition state for the initial Michael addition catalyzed by Takemoto's catalyst can be postulated (Figure 4.25). Preorganization of the malononitrile carbanion and the positively charged dimethylamino substituent may allow for the nucleophile to be preferentially guided to one face of the Michael acceptor. Hydrogen bonding of the thiourea motif with the electron-withdrawing carbonyl and nitrile substituents on the formyl acrylonitrile orientate may occur in such a way that the malononitrile carbanion approaches from the *Si* face. One could also envisage the formyl acrylonitrile orientated in such a way that the phenyl substituent is pointed towards the dimethylamino group and *Re* face approach of the nucleophile (Figure 4.25).

Si approach   Re approach
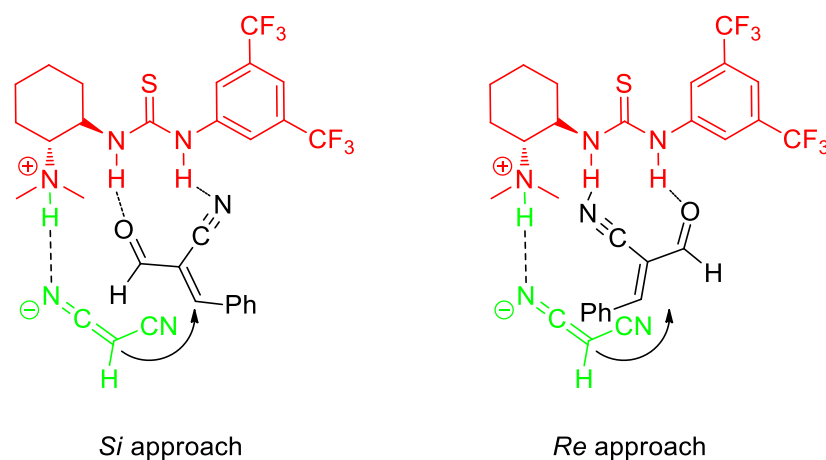
Figure 4.25. Proposed transition states leading to stereocontrolled approach of the malononitrile carbanion to the *Si* and *Re* faces of the formyl acrylonitrile **57**.

Steric repulsion between the phenyl and dimethylamino groups however could lead to a destabilising interaction between the catalyst and substrate and to a less likely transition state. Therefore the *Re* approach could be a less favoured approach. There is some literature precedent for the stereocontrol of a Michael-type addition in such a fashion. A report by Singh *et al*. describes the highly enantioselective conjugate addition of malononitrile to 2-enoylpyridines. Here Singh utilizes a urea based bifunctional catalyst to obtain the addition products in up to 95 % yield and in 97 % ee (Figure 4.26).[129]
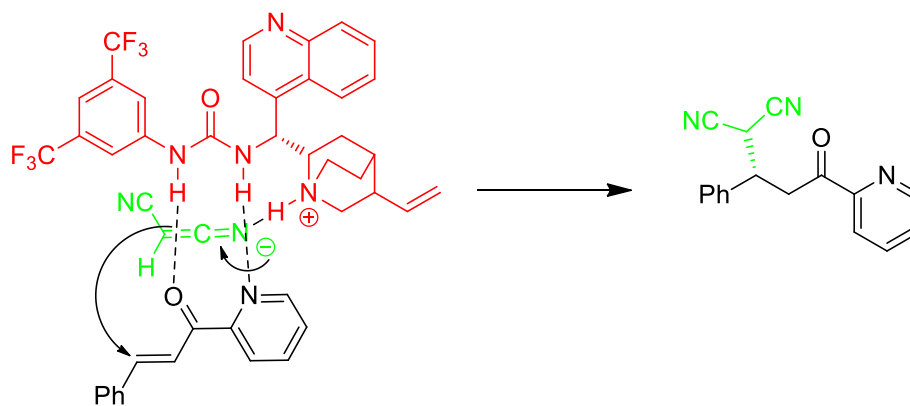
Figure 4.26. Proposed mechanism by Singh *et al.* for the conjugate addition of malononitrile to 2-enoylpyridines catalyzed by a urea based bifunctional catalyst.[129]

If the initial Michael addition is under stereocontrol and the subsequent ring closure occurs rapidly then it could be hoped that the newly forged stereogenic centre would be preserved during the ring closure step. The rapid ring closure and tautomerization of the imine to the amino form would then led to enantiomerically enriched amino-pyrans (Figure 4.27).
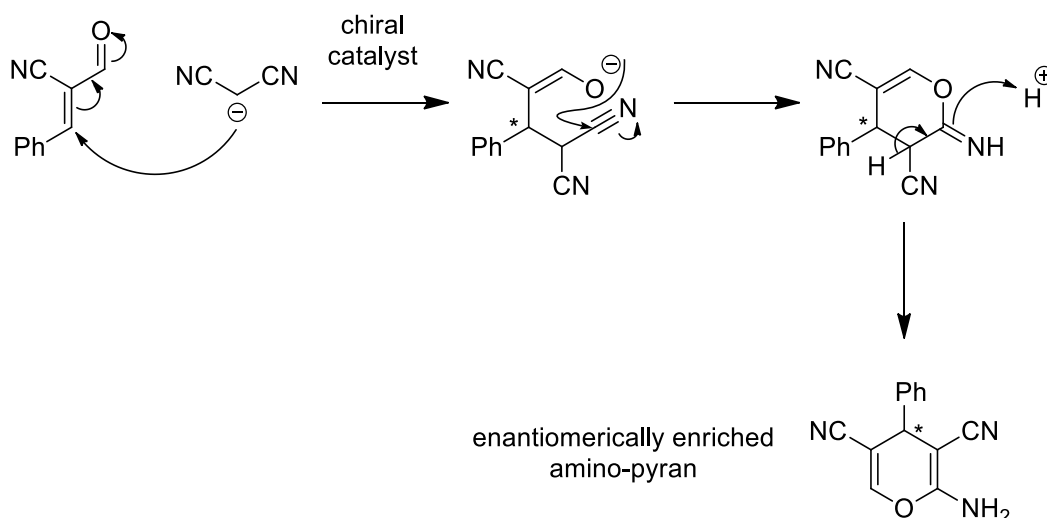
Figure 4.27. Proposed synthesis of enantiomerically pure amino-pyrans. * = stereogenic center.

Takemoto's catalyst **171** was able to catalyse the reaction of **57** with malononitrile to yield the dihydropyran **122** albeit in a lower yield of 45%. In order to investigate the level of stereocontrol exhibited by the chiral catalyst it was necessary to determine the ee of the amino-pyran product. Initially the chiral derivatizing agent (S)-(+)-α-methoxy-α-trifluoromethylphenylacetyl chloride **174** or Mosher's acyl chloride was employed in the hope of forming diastereoisomeric products that would be distinguishable by ¹H NMR

spectroscopy (Figure 4.28) . From the ratio of these two diastereoisomers it was hoped that we could determine the ee of the amino-pyran product. Unfortunately neither of the diastereoisomeric amides could be observed. This lack of reactivity could result from the reduced nucleophilicity of the amino group due to the electron-withdrawing effect of the conjugated nitrile functional group.
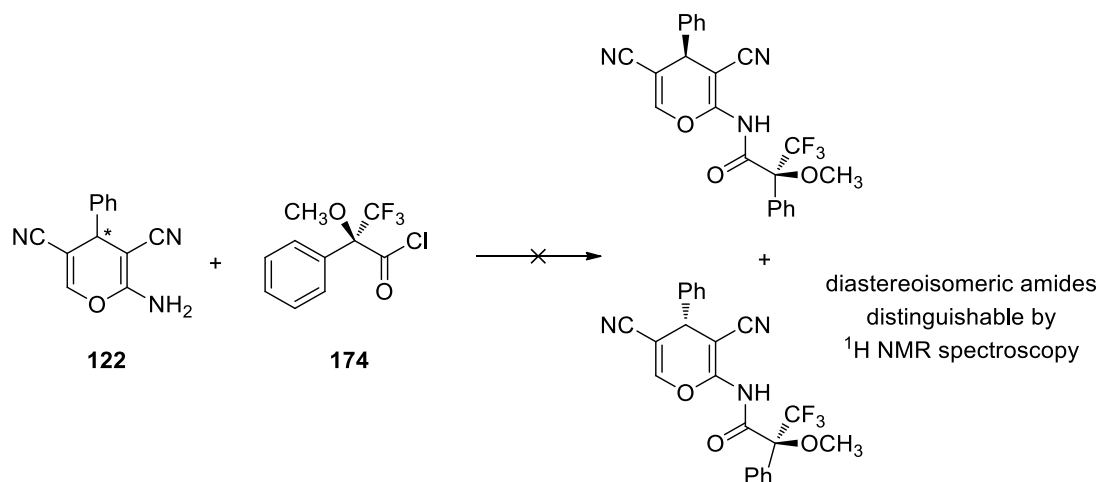
Figure 4.28. Proposed formation of diastereoisomeric amides utilizing the chiral derivatizing agent Mosher's acyl chloride **174**.

The next method employed in an attempt to determine the ee of the amino pyran products was chiral HPLC. The company Chiral Technologies Europe offers a chiral screening service in order to determine optimum separation conditions for scalemic mixtures. A racemic and a presumed enantioenriched sample were sent for screening on a number of chiral columns. Unfortunately, significant degradation to unknown products was observed in both cases and no further insight into the ee was obtained. To date, the determination of the ee of the amino pyran obtained using Takemoto's catalyst **171** has been unsuccessful.   In future work, the chiral shift reagent europium tris[3-(heptafluoropropylhydroxymethylene)-(+)-camphorate] could be investigated to obtain a measure of the ee in a manner similar to that reported by Elnagdi *et al.*[125]

4.2.3   Attempted addition of enamines to formyl acrylonitriles

In order to explore the potential addition of other C-centred nucleophiles to the formyl acrylonitriles we investigated the use of aldehydic enamines in organocatalytic conjugate addition reactions. Initial experiments did not yield any conversion of the formyl acrylonitrile to the desired conjugate addition product, Figure 4.29. The only products observed by ^{1}H NMR were believed to be as a result of self-aldol reactions. This could be due to the highly reversible nature of the initial conjugate addition step, which would be in part due to the acidity of the α-hydrogen between both the aldehyde and nitrile functionalities.
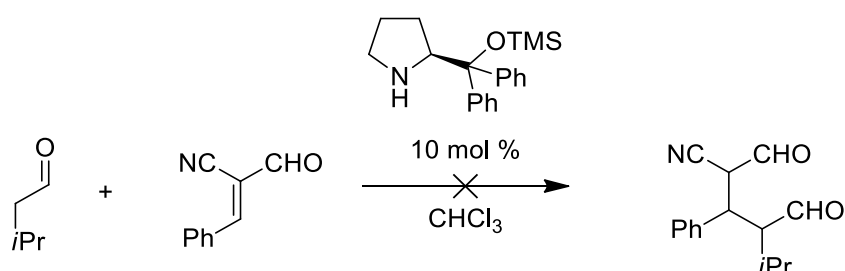
Figure 4.29. Attempted conjugate addition of aldehydic enamines to formyl acrylonitriles.

A potential side reaction that could have been anticipated to occur during the attempted conjugate addition of aldehydic enamines to formyl acrylonitriles would be that of an IEDDA reaction. Wherein, the formyl acrylonitriles acts as an electron-poor diene and the aldehydic enamine the electron-rich dieneophile (Figure 4.30). Without the subsequent release of the catalyst this side-reaction would have consumed the catalyst preventing any further reactivity. This potential side reaction would be analogous to the work carried out by Jørgensen *et al.,* discussed in Section 4.1.1.2 (Figure 4.7), in their IEDHDA reaction utilizing aldehydic enamines and enones as the reacting partners to yield hemi-acetals.[30]
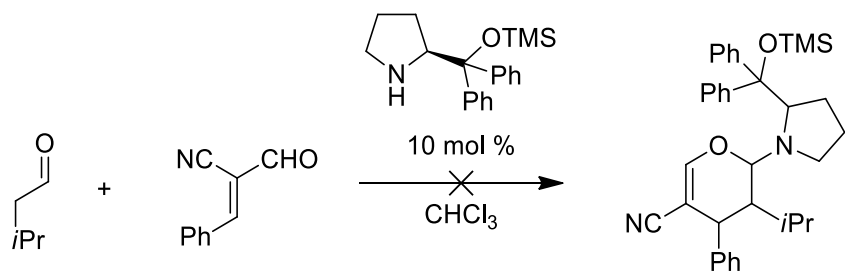
Figure 4.30. Potential IEDDA reaction of formyl acrylonitriles with aldehydic enamines.

Jørgensen *et al.* noted that the addition of 50 mg of silica to the reaction mixture (0.5 mmol scale) was sufficient to hydrolyse the cycloaddition product and thereby liberate the catalyst which could then re-enter the catalytic cycle.[30] We attempted this addition of silica to the reaction mixture whilst employing formyl acrylonitriles as the dienophiles however it still did not yield any cycloadducts. Despite the similar nature of these two reactions neither the conjugate addition or cycloaddition products were observed. This could be in part due to the bulky nature of the C-2 substituent on the organocatalyst.

4.3   Formyl acrylonitriles as electron-deficient dienes

At first, our interest in formyl acrylonitriles lay primarily in their use as intermediates in the synthesis of electron-deficient dienes. However, formyl acrylonitriles themselves can be viewed as electron-deficient heterodienes. As such, the possibility of formyl acrylonitriles acting as dienes in IEDDA cycloadditions was also considered.

Whilst investigating the use of formyl acrylonitriles as heterodienes in IEDDA cycloadditions a report by Lago-Santome *et al.* was found in the literature. This report described the utilization of the structurally related β-aryl-α-nitro-α,β-enals **175** as both heterodienes in IEDDA cycloadditions and as dienophiles in regular DA cycloaddition reactions (Figure 4.31).[130] As can be seen in Figure 4.31, formyl acrylonitriles and β-aryl-α-nitro-α,β-enals **175** are quite similar in structure, differing only in the nature of the electron-withdrawing substituent at the α-position.
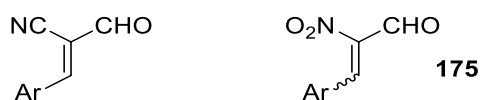
Figure 4.31. Structural similarities of formyl acrylonitriles and β-aryl-α-nitro-α,β-enals **175**.

In their report Alonso and co-workers describe the ambivalent nature of β-aryl-α-nitro-α,β-enals to undergo both inverse and regular demand Diels-Alder cycloaddition reactions. A selection of their results can be seen in Figure 4.32**.**
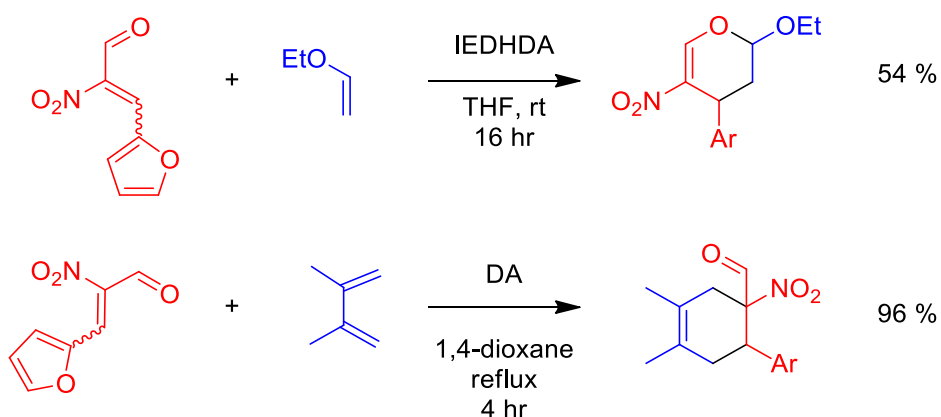
Figure 4.32. The ambivalent reactivity of β-aryl-α-nitro-α,β-enals exemplified in the participation in both DA and IEDHDA cycloaddition reactions reported by Lago-Santome *et al.*[130]

4.3.1   Results and Discussion

As mentioned, we anticipated that the formyl acrylonitriles could act as electron-poor heterodienes in a Diels Alder cycloaddition with a suitable electron rich dienophile. As a test reaction, the phenyl substituted formyl acrylonitrile **57** was selected along with ethyl vinyl ether as the electron rich dienophile, Figure 4.33. Both reactants were stirred together neat at rt and monitored by TLC. Full consumption of the starting formyl acrylonitrile was observed after 16 hrs, a DNP stain indicated complete consumption of the aldehyde. Simple evaporation of the ethyl vinyl ether and subsequent analysis of the crude product by NMR spectroscopy showed full conversion to the expected dihydropyrans **176**. The dihydropyran was isolated as a mixture of the *endo* and *exo* diastereoisomers in a 1:0.08 ratio, respectively. A full discussion on the mechanism and stereoselectivity of this reaction is given in Section 4.3.2. Details regarding the structural characterisation of the product pyran using ^{1}H and ^{13}C NMR spectroscopy is given in Section 4.3.1.3.
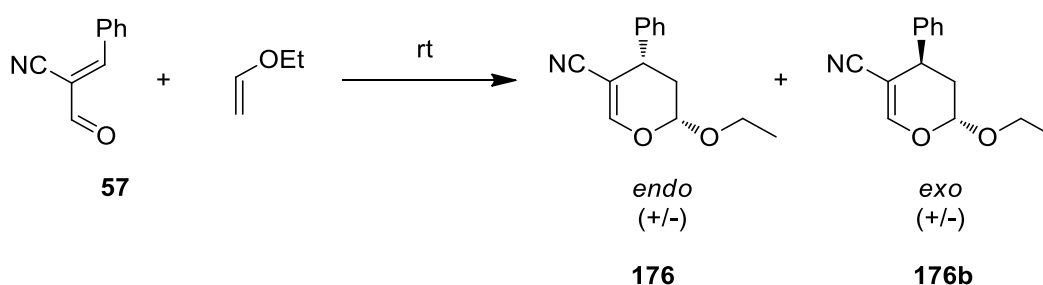
Figure 4.33. Test reaction of formyl acrylonitrile **57** and ethyl vinyl ether to yield 3,4-dihydro-*2H*-pyran **176**.

4.3.1.1   Reduction of equivalents

It was found that the number of equivalents of ethyl vinyl ether required for complete conversion could be reduced to four using CHCl$_3$ as the solvent in order to fully solubilize the formyl acrylonitriles.

4.3.1.2   Reaction scope

Several aryl formyl acrylonitriles were explored as substrates in the IEDHDA reaction with ethyl vinyl ether, Table 4.2. Quantitative yields were obtained in most cases but additional heating was required with some reactions. The *endo*:*exo* ratio was reasonably consistent for

all reactions, Table 4.2. Formyl acrylonitriles substituted with strongly electron withdrawing groups could not be investigated as their synthesis proved elusive in our hands. There appeared to be a reduced reactivity with the more electron-rich formyl acrylonitriles, with additional heating required to overcome the activation energy and achieve full conversion. This may be due to a higher energy LUMO of the electron-rich formyl acrylonitriles and hence a reduced susceptibility to attack from the HOMO of the dienophile, ethyl vinyl ether resulting in a requirement for additional heating.[131]
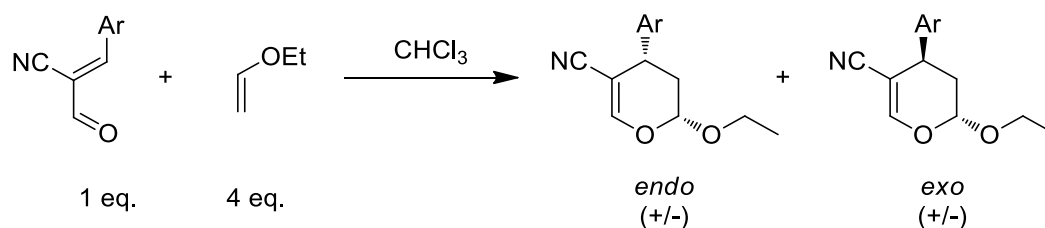
Table 4.2 IEDHDA of formyl acrylonitriles and ethyl vinyl ether.

Entry	Ar	Time (hr)	Temp (°C)	Yield (%)	Product	*endo:exo*
1	Ph	16	25	Quantitative[a]	(**176**)	1:0.08
2	o-CH$_3$C$_6$H$_5$	40	25	Quantitative[a]	(**177**)	1:0.18
3	m-CH$_3$C$_6$H$_5$	40	30	Quantitative[a]	(**178**)	1:0.11
4	p-CH$_3$C$_6$H$_5$	16	30	Quantitative[a]	(**179**)	1:0.11
5	m-ClC$_6$H$_5$	16	30	Quantitative[a]	(**180**)	1:0.11
6	p-BrC$_6$H$_5$	16	30	Quantitative[a]	(**181**)	1:0.13
7	m-FC$_6$H$_5$	16	25	Quantitative[a]	(**182**)	1:0.11
8	m-BrC$_6$H$_5$	40	25	Quantitative[a]	(**183**)	1:0.09
9	2-napthalenyl	24	30	No reaction	N/A	N/A
10	m-CF$_3$C$_6$H$_5$	16	25	Quantitative[a]	(**184**)	1:0.11
11	p-NMe$_2$C$_6$H$_5$	24	30	No reaction	N/A	N/A

[a] A quantitative yield was obtained due to residual solvent present from transfers.

4.3.1.3   Spectroscopic characterization of 3,4-dihydro-2H-pyrans

Through a combination of 1D and 2D ^{1}H and ^{13}C NMR experiments the following assignments were made for the chemical shifts observed in the ^{1}H and ^{13}C NMR spectra of dihydropyran **183**. The IUPAC numbering system utilized for assignment of proton and carbon signals is shown below in Figure 4.34.
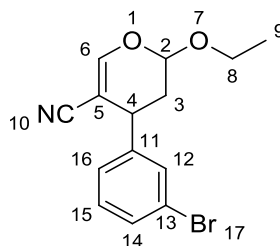
Figure 4.34. IUPAC numbering for 3,4-dihydro-*2H*-pyran **183**.

Characteristic signals in the ^{1}H NMR spectrum (Figure 4.35) include the acetal proton on C2, which appears as a doublet of doublets (dd). This splitting arises from coupling to the two diastereotopic protons. The acetal proton appears deshielded at 5.09 ppm due to the proximity of the two oxygen atoms. The protons on the methylene group C3 are diastereotopic due to the adjacent stereogenic centres. This diastereotopicity results in a doubling of the predicted signals, one for each of the non-equivalent protons. The two ddd are easily identified in the ^{1}H NMR spectrum and appear at 2.22 and 1.94 ppm. The CH_2 protons on C8 of the ethoxy group are also diastereotopic and again two signals appear for these non-equivalent protons. They appear as two distinct dq at 3.83 and 3.50 ppm and are deshielded due to the adjacent oxygen atom.
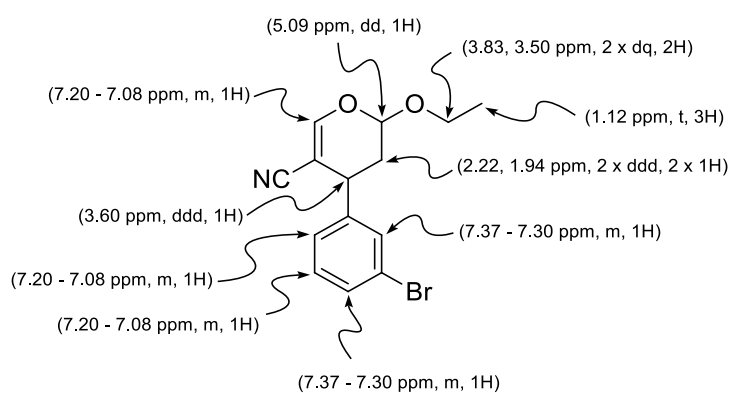
Figure 4.35. ^{1}H NMR spectral assignment for dihydropyran **183** (500 MHz, CDCl₃).

In the ^{13}C NMR spectrum (Figure 4.36) the characteristic signals (Figure 4.37) include the nitrile quaternary carbon C10 which appears at 118.0 ppm. HSQC and DEPT experiments allow for the identification of other characteristic signals. The olefinic carbon C6 signal occurs at 156.0 ppm, deshielded due to the conjugated nitrile functionality. The acetal carbon C2 at 99.0 ppm, is deshielded by the two adjacent oxygen atoms. The methylene carbon C3 at 35.6 ppm is easily identified through HSQC experiments due to the correlation of both ^{1}H NMR signal from the diastereotopic protons on C3 to the ^{13}C NMR signal of C3. The phenyl substituted carbon C4 at 37.4 ppm is also easily identified through HSQC experiments.
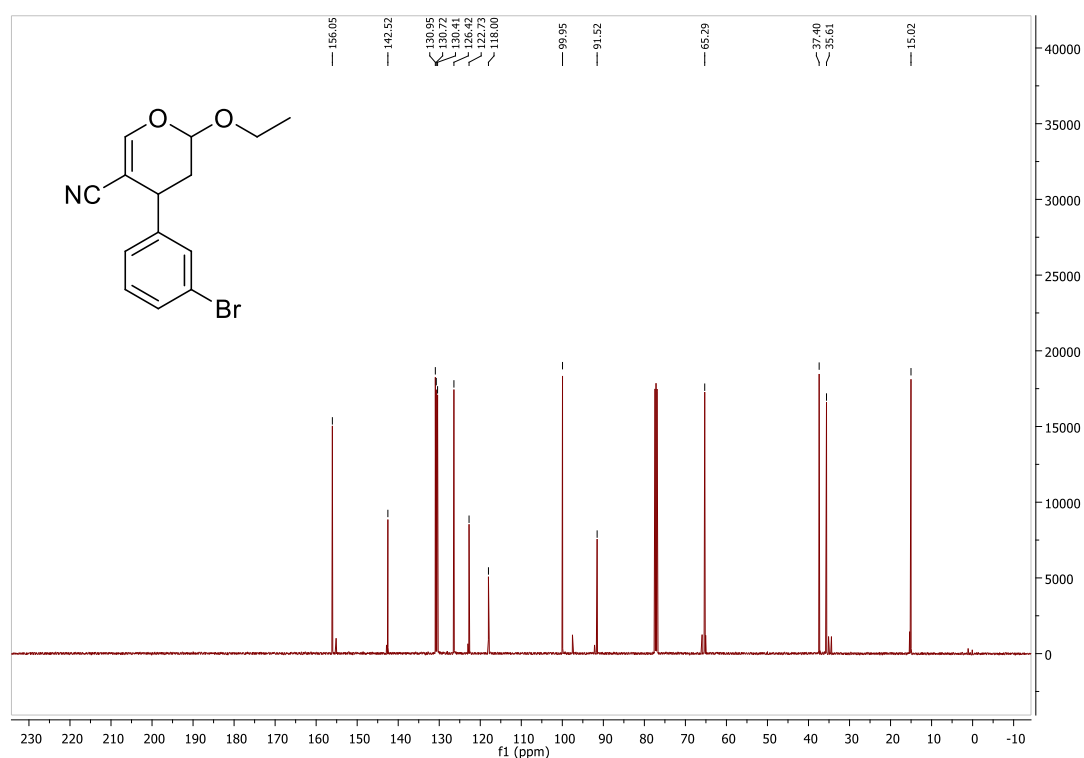
Figure 4.36. ^{13}C NMR of dihydropyran **183**.
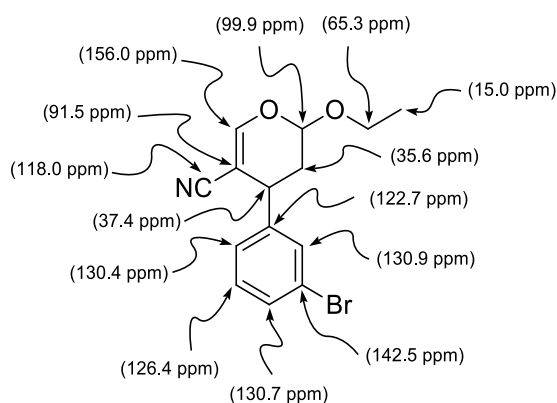
Figure 4.37. ^{13}C NMR spectral assignment for dihydropyran **183** (126 MHz, CDCl$_3$).

188

4.3.2   IEDHDA reaction detail

4.3.2.1   Woodward-Hoffmann rules on pericyclic reactions

The Diels-Alder cycloaddition between the formyl acrylonitriles and ethyl vinyl ether satisfy the Woodward-Hoffman rules. The Woodward-Hoffmann rules state that for thermal pericyclic reactions to be allowed the total number of $(4q+2)_s$ and $(4r)_a$ components must be odd, where 'q' and 'r' are integers and the subscripts 's' and 'a' stand for suprafacial and antarafacial respectively.

In the case of the Diels-Alder cycloaddition between formyl acrylonitriles and ethyl vinyl ether, there are six electrons moving suprafacially, considered as one $(4q+2)_s$ component, and no electrons moving antarafacially, i.e. no $(4r)_a$ component. Therefore the total number of $(4q+2)_s + (4r)_a$ components is equal to one, and therefore odd, and according to Woodward-Hoffmann rules is thermally allowed.

Kenichi Fukui developed Frontier Molecular Orbital (FMO) theory in order to explain the course of chemical reactions through the examination of the frontier molecular orbitals, namely the HOMO and LUMO of the reacting molecules. FMO theory is of particular use in conjunction with the Woodward-Hoffmann rules and can aid in the identification of suprafacial and antarafacial components of the diene and dieneophile in Diels-Alder cycloadditions. This can be seen in the Diels-Alder cycloaddition between the formyl acrylonitriles and ethyl vinyl ether where constructive suprafacial overlap occurs between the LUMO of the formyl acrylonitrile and the HOMO of the ethyl vinyl ether (Figure 4.38).

suprafacial overlap
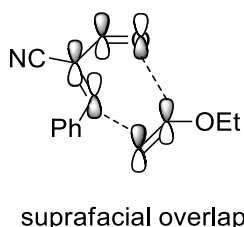
Figure 4.38. Identification of suprafacial orbital overlap through examination of FMO's.

4.3.2.2   Regioselectivity

Theoretically two regioisomeric products could be produced from the IEDHDA cycloaddition through differing approaches of the reactants to one another. One approach would lead to the 2,4,5-trisubstituted dihydropyran **176** and the other approach to the 3,4,5-trisubstituted dihydropyran **185** (Figure 4.39).
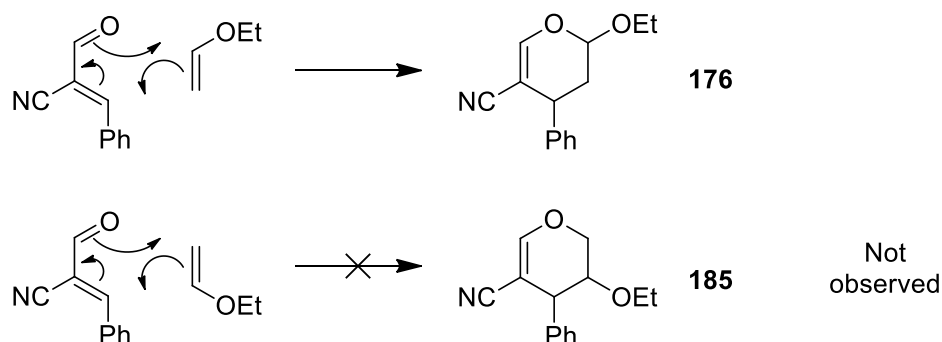
Figure 4.39. Plausible regioisomers from the cycloaddition of formyl acrylonitrile **57** and ethyl vinyl ether.

In each case, Table 4.2, only a single regioisomer was observed. This can be rationalized through the generation of resonance structures of the reactants and aligning the corresponding charges (Figure 4.40). From these resonance structures it can be seen that favourable interaction of the charges can only result from the approach of the reactants that leads to the 2,4,5-trisubstituted dihydropyrans (Figure 4.40).
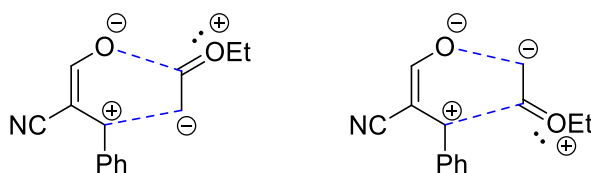
Figure 4.40. Resonance structures of formyl acrylonitrile **57** and ethyl vinyl ether showing favourable interaction of charges (left) and unfavourable interaction of charges (right).

4.3.2.3   Endo/Exo approach

In addition to the regiochemical concerns encountered with Diels-Alder cycloadditions one must also consider the *endo/exo* approach of the reacting partners. The *endo:exo* ratio of the cycloadducts can vary greatly depending on the electronic and steric nature of the

substituents on both reacting partners. As seen in Table 4.2 the *endo* product was identified as the major cycloadduct in each case investigated. Reasoning for this assignment will be outlined in Section 4.3.2.4.

The propensity for the *endo* cycloadduct to be the major product is often attributed to secondary orbital interactions. These secondary orbital interactions of nearby substituents can decrease transition state energies for the *endo* approach resulting in the *endo* isomer as the major product.

In the case of regular demand Diels-Alder cycloadditions, in which the HOMO of the diene and the LUMO of the dienophile interact, the terminal lobes of both the diene and dienophile are asymmetric and therefore can form constructive overlap in a suprafacial fashion (Figure 4.41). In the *endo* transition state the β and β' orbitals are also in phase and can overlap constructively thereby lowering the energy of the transition state leading to the *endo* cycloadduct. This constructive secondary orbital overlap is not present in the *exo* transition state due to the lack of proximity of the substituents on the dieneophile to the β carbon of the diene (Figure 4.41).
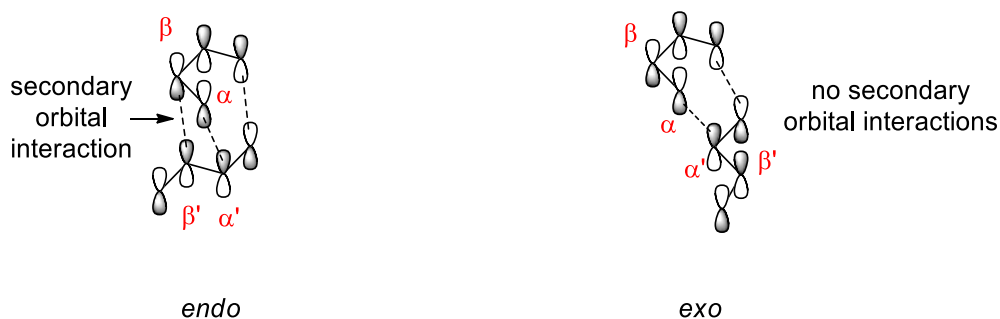
Figure 4.41. Regular demand Diels-Alder cycloaddition *endo*/*exo* transition states between the HOMO of the diene (top) and the LUMO of the dieneophile (bottom).

The inverse-electron demand hetero Diels-Alder cycloaddition, in which the electron-poor formyl acrylonitriles react with the electron-rich ethyl vinyl ether, occurs between the LUMO of the diene and the HOMO of the dienophile (Figure 4.42).
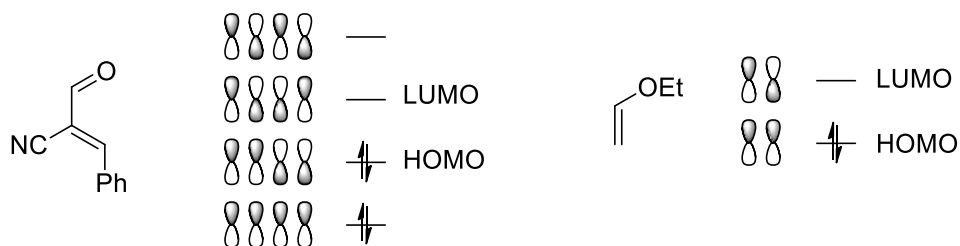
Figure 4.42. FMO diagrams for formyl acrylonitrile **57** and ethyl vinyl ether.

In this instance the terminal lobes of both the diene and dienophile are symmetrical and can react in a suprafacial fashion (Figure 4.43). Again in the *endo* transition state there is a possible constructive stabilizing interaction between the β and β' lobes that could lead to a lowering of the *endo* transition state energy when compared to the *exo* transition state. This stabilizing interaction is once again absent in the *exo* transition state due to the lack of proximity in the β and β' lobes.
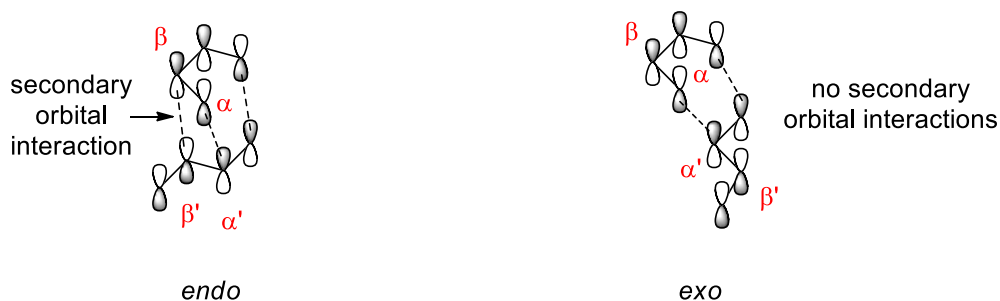
Figure 4.43. Inverse-electron demand Diels-Alder cycloaddition *endo*/*exo* transition states between the LUMO of the diene (top) and the HOMO of the dieneophile (bottom).

Steric interactions can also prevent the formation of stabilizing secondary orbital interactions and therefore also have an influence on the *endo*/*exo* ratio. The exact *endo*/*exo* ratio of each cycloaddition reaction is a result of these competing interactions. It appears that for the IEDDA cycloaddition between formyl acrylonitriles and ethyl vinyl ether the stabilizing secondary orbital interactions outweigh any destabilizing steric clashes as in each case the *endo* isomer was found to be the major isomer formed.

Due to the conservation of stereochemistry in Diels-Alder cycloadditions the *endo* approach leads to the formation of the *syn* cycloadduct (Figure 4.44).
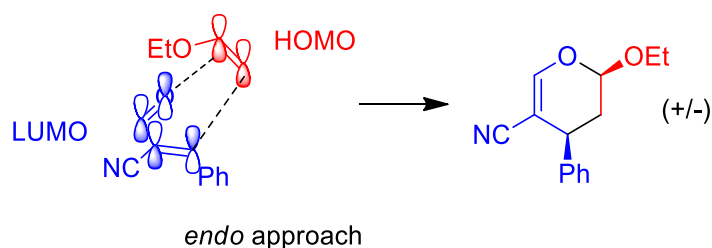
endo approach

Figure 4.44. Constructive overlap of the diene LUMO and dieneophile HOMO, *endo* approach.

Approach of the reactants in an *exo* fashion leads to the formation of the *anti* cycloadduct (Figure 4.45).
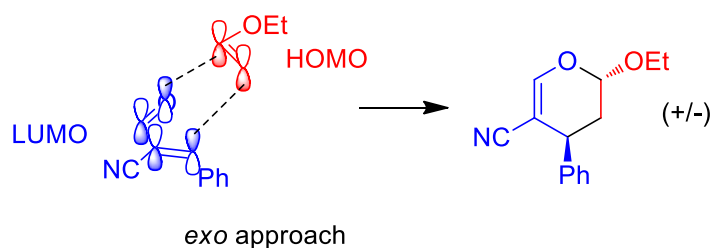
exo approach

Figure 4.45. Constructive overlap of the diene LUMO and dieneophile HOMO, *exo* approach.

In order to determine which cycloadduct was the major product, the *endo* (*syn*) or the *exo* (*anti*), one needs to investigate the relative stereochemistry of the ethoxy and phenyl substituents on the dihydropyran ring.

4.3.2.4   Relative stereochemistry of the ethoxy and phenyl substituents

The work on nitro-substituted dihydropyrans by Lago-Santome *et al.* suggested that the relative stereochemistry of substituents on dihydropyran rings could be elucidated through careful analysis of NOE experiments.[130] Dihydropyrans resulting from an *endo* approach could be expected to exhibit an NOE enhancement between the protons on C2 and C4 carbons due to the conformation of the cyclohexene ring (Figure 4.46).
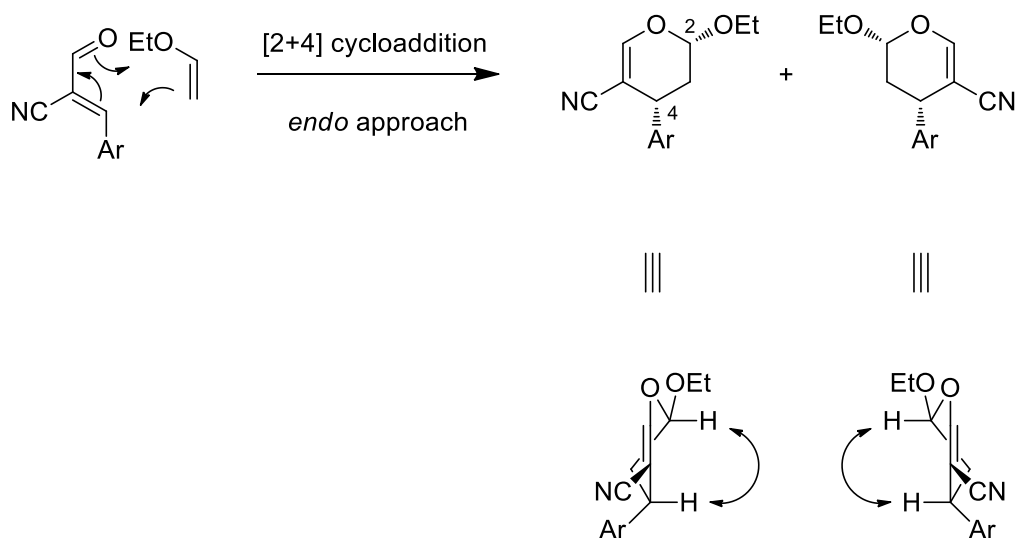
Figure 4.46. *Endo* approach of the dieneophile to the heterodiene leading to the two enantiomeric *endo* products, possible NOE shown.

This NOE enhancement should not appear between the protons on the C2 and C4 carbons in the *exo* cycloadduct, as these protons are no longer close to one another in space due to the cyclohexene conformation (Figure 4.47).
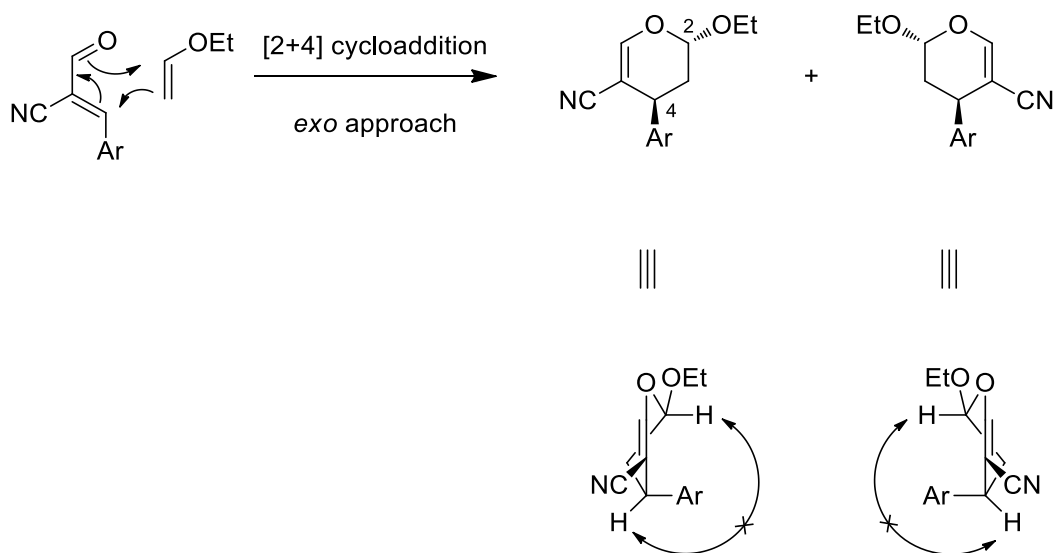
Figure 4.47. *Exo* approach of the dieneophile to the heterodiene leading to the two enantiomeric *exo* products.

The resulting spectrum from the NOESY experiment performed on dihydropyran **183** can be seen in Figure 4.48. A number of NOE's can be seen throughout the molecule, this is due to

the close proximity of a number of protons caused by the conformation of the cyclohexene ring.
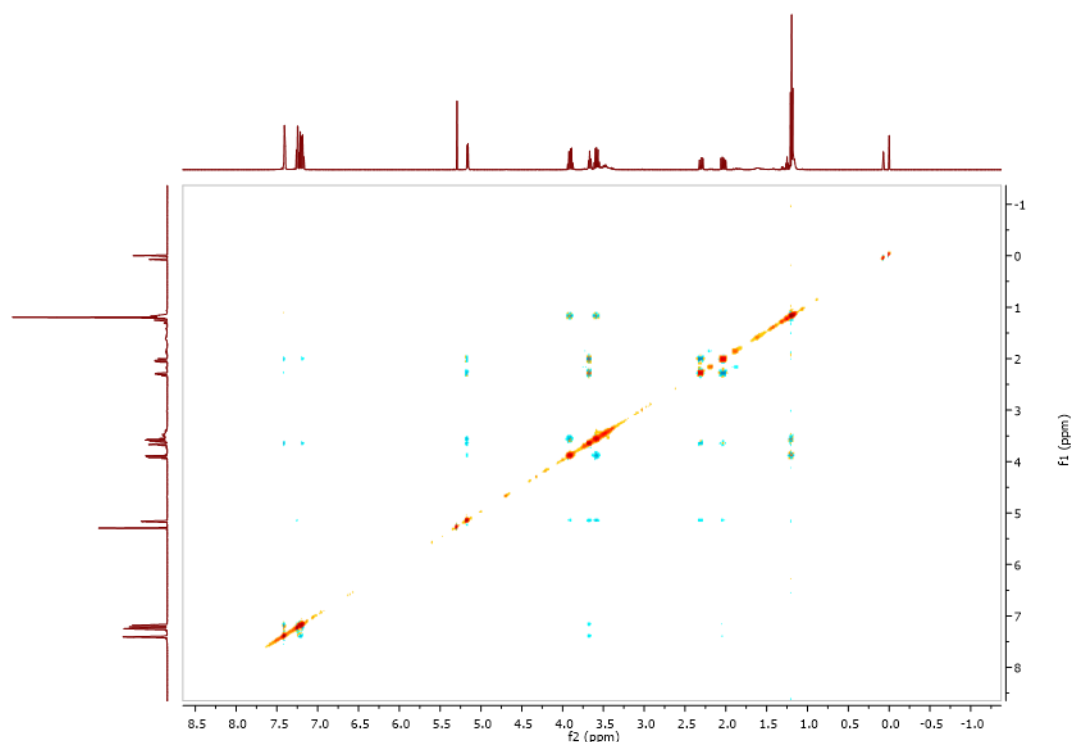
Figure 4.48. NOESY spectrum of dihydropyran **183**.

The NOE of interest for the purpose of determining the relative stereochemistry of the cycloadducts is that between the acetal proton on C2 and the proton on C4. An expansion of the relevant region of the NOESY spectrum does indeed reveal an NOE between these two protons (Figure 4.49). This result is in agreement with the expected NOE for the predicted conformation of the *endo* cycloadduct. Unfortunately, the *exo* product is not present in sufficient quantities to determine if there is an NOE between the protons on C2 and C4 in that cycloadduct.
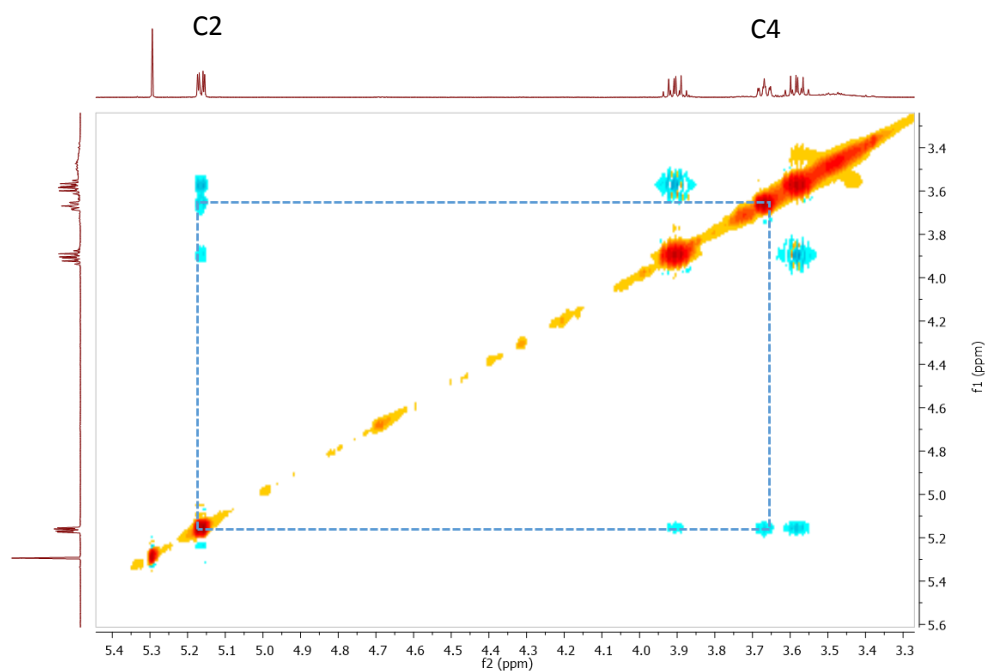
Figure 4.49. Expansion of the NOESY spectrum of dihydropyran **183** highlighting the NOE between the protons on C2 and C4.

In order to further support the assignment of the *endo* isomer as the major product in the cycloadditions of formyl acrylonitriles and ethyl vinyl ether it should be possible to determine the relative stereochemistry of the phenyl and ethoxy substituents through careful consideration of the coupling constants of key signals. The key coupling constants which should be investigated in order to determine the relative stereochemistry of the major product are those shared between the diastereotopic protons on C3 and the protons on C2 and C4. Consideration of the magnitude of these coupling constants with respect to a Karplus relationship should allow the relative stereochemistry of the ethoxy and phenyl substituents on C2 and C4 respectively to be determined. For ease, the IUPAC numbering of dihydropyran **183** is shown again in Figure 4.50.
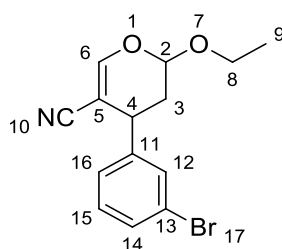
Figure 4.50. IUPAC numbering for 3,4-dihydro-*2H*-pyran **183**.

First the complete spectral assignment of the target molecule had to be elucidated (Section 4.3.1.3). The *m*-Br substituted dihydropyran **183**, was chosen for this study and the ^{1}H NMR spectrum of which can be seen in Figure 4.51. A number of key features of the molecule should be noted which can assist in the determination of the relative stereochemistry of the C2 and C4 substituents; 1) C2 and C4 are stereogenic centres; 2) as a result of the adjacent stereogenic centres the protons on C3 and C8 are diastereotopic; 3) the ^{1}H NMR signal for the acetal proton on C2 has a distinctive chemical shift (deshielded) and splitting pattern (doublet of doublets) and is easily identifiable and can be used as a tool to determine the relative stereochemistry of the C2 and C4 stereogenic centres.
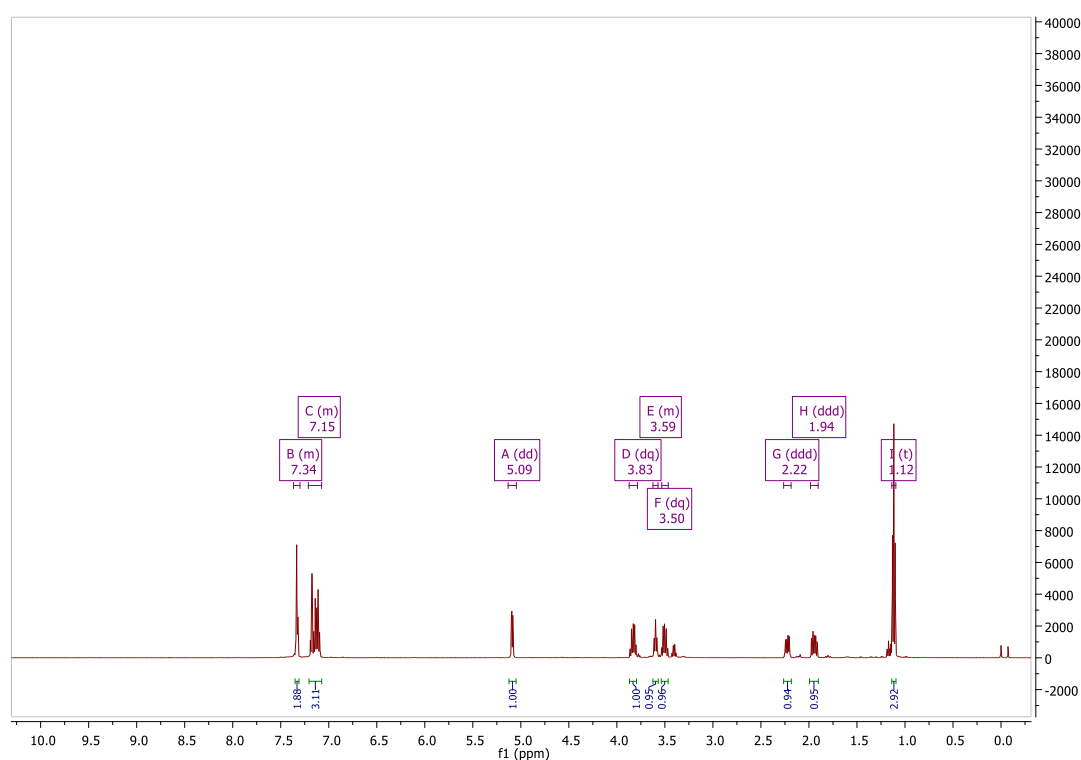
Figure 4.51. ^{1}H NMR spectrum of dihydropyran **183**.

The acetal proton on C2 has a distinct chemical shift of 5.09 ppm and a dd splitting pattern as can be seen in Figure 4.52. The dd pattern arises from two distinct couplings to each of the diastereotopic protons on C3. The magnitude of these couplings constants was measured as 7.2 Hz and 2.3 Hz.

197
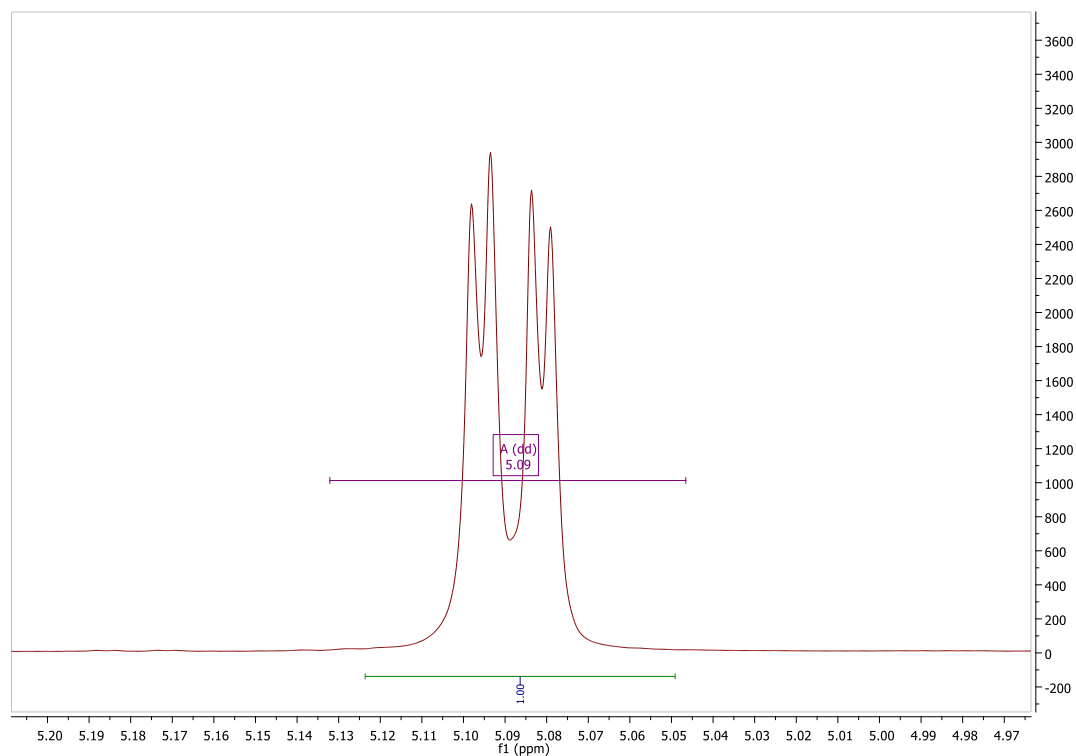
Figure 4.52. Acetal proton on C2 of dihydropyran **183**.

From the Karplus relationship the greater the overlap of the bonding orbitals the greater the coupling constant. This overlap is maximal when the H-C-C-H dihedral angle φ is 180° and the bonding orbitals are anti-periplanar and parallel. There is another maximum at 0° when the orbitals are periplanar but not parallel. The coupling is at a minimum (near 0 Hz) when the H-C-C-H dihedral angle φ is 90° and the bonding orbitals are perpendicular and orbital overlap is at a minimum (Figure 4.53).
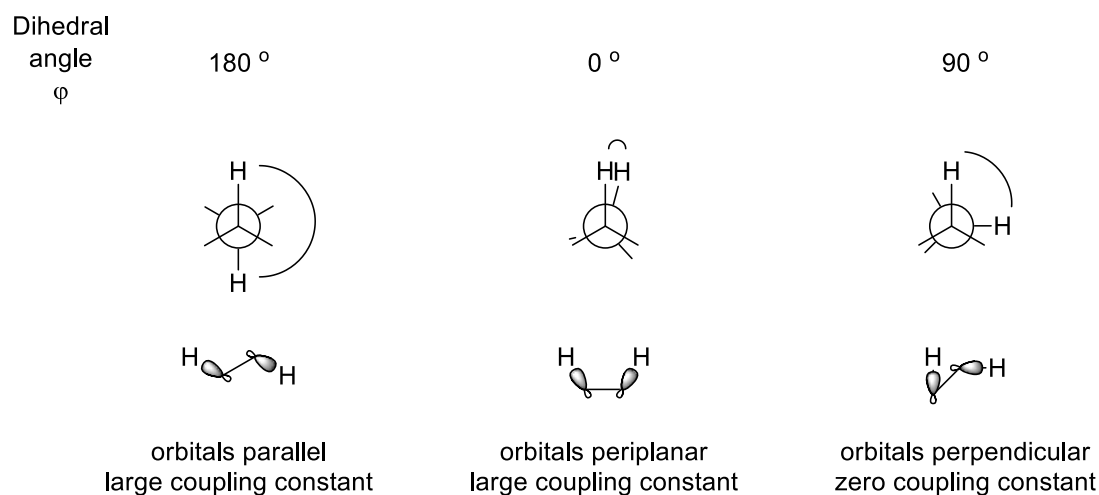
Figure 4.53. Dihedral angle to coupling constant relationship described by Karplus.

198

The magnitude of ^{3}J couplings can give an indication of dihedral angle φ and therefore give information on the relative stereochemistry of suitable molecules. This is the case with the dihydropyran family as will be outlined below.

The diastereotopic protons on C3 are non-equivalent and exhibit unique signals in the ^{1}H NMR spectrum of dihydropyran **183**. These two protons appear as ddd, a splitting pattern that arises from the coupling between the geminal diastereotopic proton on C3 and two separate vicinal couplings to the protons on C2 and C4. One of the diastereotopic protons on C3 has the following assignment 2.22 ppm (ddd, 14.0, 6.7, 2.3 Hz, 1H) and the other 1.94 ppm (ddd, 14.0, 8.2, 7.4 Hz, 1H). The largest coupling constant (14.0 Hz) in both signals arises from the geminal splitting of the other diastereotopic proton on C3. The two couplings to the acetal proton on C2 can be easily identified through the matching coupling constants of 7.4 Hz and 2.3 Hz of the acetal proton signal C2. From these coupling constants the pseudo-axial and pseudo-equatorial protons can be distinguished from one another. The magnitude of the coupling constant can be indicative of the dihedral angle φ and therefore the larger coupling constant of 7.4 Hz is thought to have a dihedral angle closest to 180˚ and the coupling constant of 2.3 Hz is thought to have more of an acute angle closer to 60˚. A representation of these coupling interactions and the postulated conformation of dihydropyran **183** can be seen in Figure 4.54.
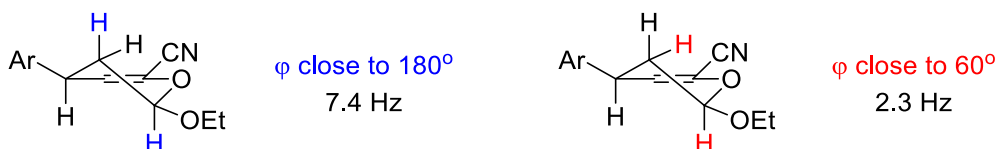
Figure 4.54. Vicinal couplings between the proton on C2 and the diastereotopic protons on C3.

Examining the coupling constants from the diastereotopic protons on C3 to the proton on C4 we are now presented with two new couplings constants of 8.2 Hz and 6.7 Hz, arising from the pseudo-axial and pseudo-equatorial protons on C3 respectively, as seen in Figure 4.55. Again the larger coupling constant of 8.2 Hz is indicative of a dihedral angle H-C-C-H φ close to 180˚ whilst the smaller coupling constant of 6.7 Hz is typical of a dihedral angle closer to 60˚.
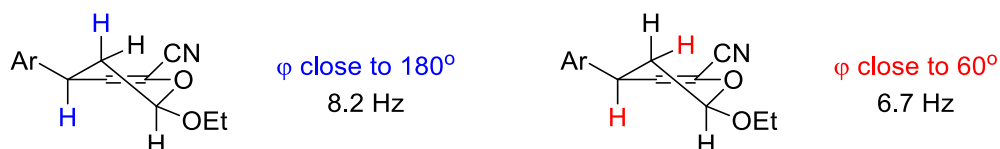
Figure 4.55. Vicinal couplings between the proton on C4 and the diastereotopic protons on C3.

This study of the coupling constants from C2 to C3 and through to C4 has allowed us to assign the relative stereochemistry of the ethoxy and phenyl substituents on C2 and C4 as *syn*. This assignment is in agreement with the presumption that the *endo* isomer would be the major product due to stabilizing secondary orbital interactions.

Whilst the majority of the signals from the *exo* cycloadduct are obscured due to overlapping signals with major *endo* cycloadduct, thankfully, the signals arising from the diastereotopic protons on C3 of the *exo* cycloadduct are clearly visible. This allows for some additional information to be gathered from the coupling constants of these signals. These signals appear, as expected, with the same ddd splitting pattern as their *endo* counterparts. The assignment for these signals is as follows; 2.11 ppm (ddd, 13.6, 5.8, 3.2 Hz, 1H) and 1.80 (13.6, 10.6, 2.5 Hz, 1H). Unlike the case of the *endo* cycloadduct we do not have data available for the signals arising from the acetal proton C2 and the proton on C4 to help in our elucidation.

However, looking at both sets of coupling constants we can see the large coupling constant of 13.6 Hz originates from the geminal coupling of the diastereotopic C3 protons. The signal at 1.80 ppm now has two remaining coupling constants of 10.6 Hz and 2.5 Hz, we postulate that the large coupling constant can only arise from a ^3J coupling of protons in a near anti-periplanar conformation. The remaining coupling constant for this proton of 2.5 Hz is therefore arising from the ^3J vicinal coupling of protons with a more acute dihedral angle φ

approaching 90˚. These coupling constants and the conformational relationships responsible for their magnitudes are visualized in Figure 4.56.
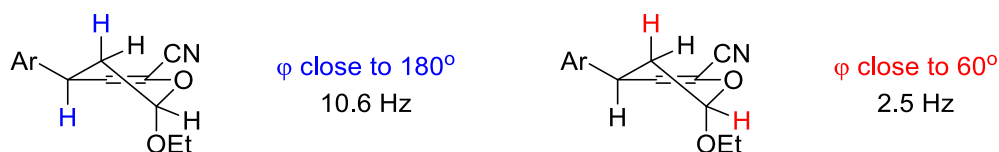
Figure 4.56. Vicinal coupling of the axial proton on C3 with the protons on C2 and C4.

The remaining signal at 2.11 ppm also has two remaining coupling constants to be accounted for of 5.8 Hz and 3.2 Hz. Both of these coupling constants are quite low indicating that neither are arising from protons nearing an anti-periplanar arrangement to one another. As can been seen in Figure 4.57 this would be the predicated case for both of these coupling constants. The larger of the two couplings constants (5.8 Hz) could arise from a dihedral angle φ nearing 60˚ whilst the smaller coupling constant (3.2 Hz) could arise from an even more acute dihedral angle φ.
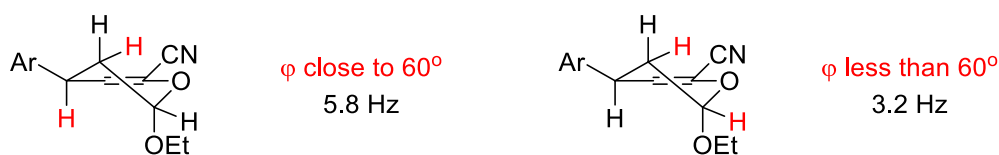
Figure 4.57. Vicinal coupling of the equatorial proton on C3 with the protons C2 and C4.

In the case of the *o*-CH$_3$ substituted dihydropyran **177** there is a larger *exo* component in the product distribution (*endo*:*exo* = 1:0.18) and therefore the *exo* signals are more visible in the ^{1}H NMR spectrum of **177**. In this instance the *exo* acetal signal of the proton on C2 is now visible in the ^{1}H NMR spectrum and its reciprocal coupling constants can be verified. Unlike the *m*-Br substituted dihydropyran **183** the proton on C4 in the case of the *o*-CH$_3$ substituted dihydropyran **177** can no longer be distinguished as it now overlaps with the diastereotopic protons on C8. Analysis of the coupling constants between the C2 and C3 protons of **177** and their comparison to *endo* and *exo* product conformations, as already performed on **183**, are in agreement with the assignment of the *endo* product as the major product.

Whilst not conclusive evidence that the major product of the IEDHDA cycloaddition between formyl acrylonitriles and ethyl vinyl ether is the *endo* cycloadduct, literature precedent,

NOESY experiments and configurational analysis through ^{1}H NMR spectroscopy strongly suggest that it is. Only X-Ray crystallographic data could be more conclusive and efforts to obtain crystals of some of the cycloadducts are underway.

4.4 Conclusion and future work

In conclusion we have developed methodologies for the synthesis of two interesting pyran derivatives, namely 2-amino-*4H*-pyrans and 3,4-dihydropyrans.

The amino-pyrans were accessed through an organocatalytic conjugate addition/cyclization reaction in racemic fashion (Figure 4.58). A screening of the substrate scope revealed the instability of the amino-pyrans which were noted to degrade over time and more rapidly if exposed to silica gel. Initial attempts at an asymmetric organocatalytic variant of this reaction also yielded the amino-pyran scaffold. However the determination of the enantiomeric ratio proved to be elusive due to the instability of the amino-pyrans. Future work on these interesting subtrates could include further modification of the scaffold in order to obtain a more stable final product.
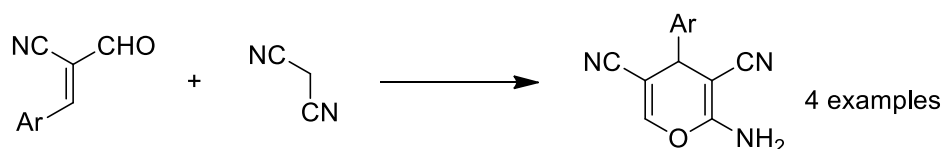
Figure 4.58. Synthesis of amino-pyrans

The 3,4-dihydropyrans were accessed through IEDHDA cycloadditions of formyl acrylonitriles and ethyl vinyl ether (Figure 4.59). A number of these reactions proceeded at 20 ˚C however particularly electron-rich formyl acrylonitriles required additional heating in order to go to completion. The IEDHDA reactions proceeded with high *endo* selectivity and in a regiospecific fashion. The assignment as *endo* selective was support by detailed NMR studies.
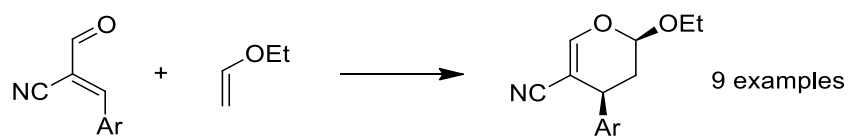
Figure 4.59. Synthesis of dihydropyrans.

4.5   General Conclusion

In conclusion, access to a number of members of three distinct 1,3-bis-substituted butadiene substrates was achieved, namely the bis-cyano, the cyano-ester, and the cyano phenylsulfonyl butadiene (Figure 4.60).
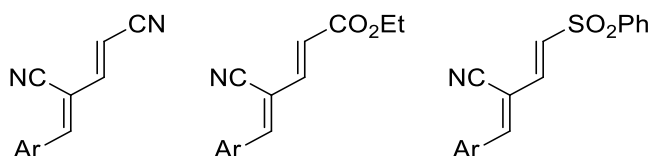
Figure 4.60. The 1,3-bis-substituted butadienes accessed.

Two of these families, the bis-cyano and the cyano-ester butadienes were particularly difficult to access due to the instability of the electron-poor butadiene products. A number of olefination reactions were screened before a base free Wittig methodology was developed, in conjunction with polymerization inhibitor 8-HQ, to allow access to these challenging substrates. This base free Wittig methodology represent a modular approach to diene synthesis through the combination of varied formyl acrylonitriles and stabilized ylides. The third family, the cyano-phenylsulfonyl butadienes were accessed through Knoevenagel chemistry already utilized by our group in the synthesis of butadienes.[58,59]

These butadienes were then screened in the already developed asymmetric organocatalytic 1,6-conjugate addition/cyclization utilized by our group in the synthesis of enantioenriched cyclic hexadienes. Whilst these substrates were hoped to react in a similar fashion to those already reported, none of the butadienes successfully generated the cyclic hexadienes under the reaction conditions screened. Two of the butadiene families, the bis-cyano and the cyano ester however did however give access to interesting novel highly functionalized biaryl species (Figure 4.61).
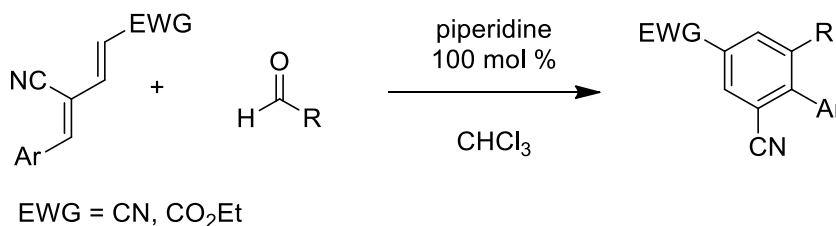
Figure 4.61. Synthesis of biaryl from 1,3-bis-substitured butadienes.

The butadienes substrates were studied by DFT in order to develop a better understanding of the conformations and configurations they adopt. It was found that these computational results are in agreement with experimentally observed trends.

The synthesis of 2-amino-*4H*-pyrans and 3,4-dihydro-*2H*-pyrans through conjugate addition and IEDHDA chemistry was also achieved (Figure 4.62).
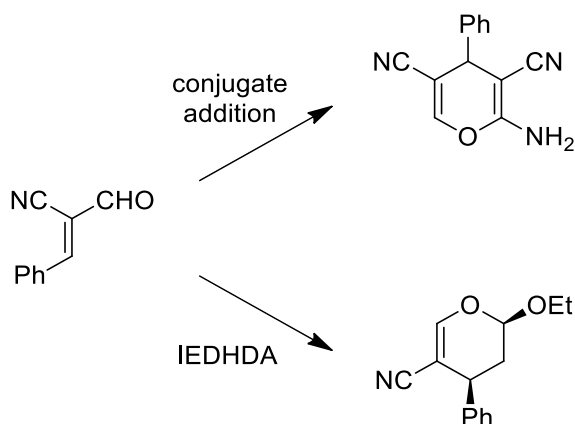
Figure 4.62. Synthesis of pyran derivatives from aryl formyl acrylonitriles.

Aryl formyl acrylonitriles were the key synthetic intermediates of many of the reactions detailed in this thesis allowing for access to six distinct compound classes. This highlight the remarkable reactivity of these before now little studied compounds.

5   Experimental

5.1   General Experimental

HPLC grade commercial solvents were used as is. Anhydrous THF was distilled under an atmosphere of argon over Na/benzophenone. Chemicals were purchased from the following suppliers Sigma-Aldrich, Acros-Organics, TCI and Alfa-Aesar and used as is. Yields refer to isolated compounds unless otherwise indicated. Thin Layer Chromatography was performed on Merck 0.25 mm silica gel plates (60F-254) using either UV lamp as a visualizing agent or through the use of chemical stains. Flash column chromatography was performed according to the method of Still et al. with Merck Silica Gel 60, using the elution system stated.[132]

All ^{1}H, ^{13}C, DEPT, COSY, HSQC and HMBC nuclear magnetic resonance spectra were recorded in CDCl3, on either a Bruker Avance spectrometer operating at 300 MHz for the ^{1}H nucleus, 75 MHz for the ^{13}C nucleus, 282 MHz for the ^{19}F nucleus and 121 MHz for the ^{31}P nucleus or a Bruker ASCEND 500 spectrometer operating at 500 MHz for the ^{1}H nucleus and 126 MHz for the ^{13}C nucleus. All chemical shifts are reported in ppm with respect to the residual solvent of the deuterated solvent utilized as described by Gottlieb *et al*.[133] Multiplicities are indicated as follows: s (singlet), d (doublet), t (triplet), q (quartet), quintet, hextet, m (multiplet), br s (broad singlet), dd (doublet of doublets), dq (doublet of quartets). Proton and carbon signals were assigned with the aid of 2D NMR experiments (COSY, HSQC or HMBC) and DEPT experiments. Coupling constants J are reported in Hz. Electrospray (ESI) mass spectra were collected on an Agilent Technologies 6410 Time of Flight LC/MS. Atmospheic Pressure Chemical Ionisation (APCI) mass spectra were collected on a Bruker micrOTOF III mass spectrometer. The interpretation of mass spectra was made with the help of the program "Agilent Masshunter Workstation Software". Infra-red spectra were obtained in the region 4000–400 cm−1 using a Perkin Elmer Spectrum 100 FTIR spectrometer. Samples were recorded using KBr disc, NaCl plate or Attenuated total refraction (ATR) as indicated.

Energy minimization and optimized structure calculations were performed using the Gaussian 03 software package with a B3LYP/6-31g(d) level of theory. Optimized structures were visualized using GaussView.

Note: Formyl acrylonitriles were found to be potent irritants and as such all operations involving their handling should be performed with the appropriate personal protective equipment.

5.2   Chapter 2

5.2.1   Synthesis of diethyl (2-amino-2-oxoethyl)phosphonate (64)
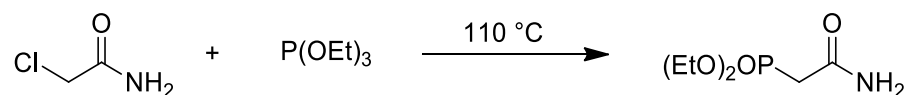
To neat triethyl phosphite 15.8 mL (92.1 mmol, 3 eq.) was added 2-chloroaceteamide 2.877 g (30.7 mmol, 1 eq.) and the resulting mixture heated to reflux at 110 °C for 16 hrs. The resulting clear pale yellow solution was allowed to cool to rt before being cooled to -20 °C. The resulting solid was filtered and washed with cold PE before being dissolved in minimal hot DCM. The hot solution of DCM was filtered and cold PE was added to the filtrate until precipitation ceased. The pale yellow crystalline solid was filtered to yield the product in 4.82 g (80 %).

^{1}H NMR (300 MHz, CDCl$_3$) δ 6.95 (s, 1H, N*H*), 6.27 (s, 1H, N*H*), 4.17 – 4.03 (m, 1H, OC*H$_2$*CH$_3$), 2.83 (d, *J* = 21.0 Hz, 1H, PC*H$_2$*), 1.29 (t, *J* = 7.0 Hz, 2H, OCH$_2$C*H$_3$*).

^{13}C NMR (75 MHz, CDCl$_3$) δ 166.8 (d, *J* = 3.8 Hz, *C*=O), 62.9 (d, *J* = 6.5 Hz, O*C*H$_2$CH$_3$), 35.0 (d, *J* = 130.8 Hz, P*C*H$_2$), 16.4 (d, *J* = 6.1 Hz, OCH$_2$*C*H$_3$).

m.p.: 76-78 °C (3:1 Toluene:PE)

Matches literature data.[83]

5.2.2   Synthesis of (2E,4Z)-4-cyano-5-phenylpenta-2,4-dienamide (63)
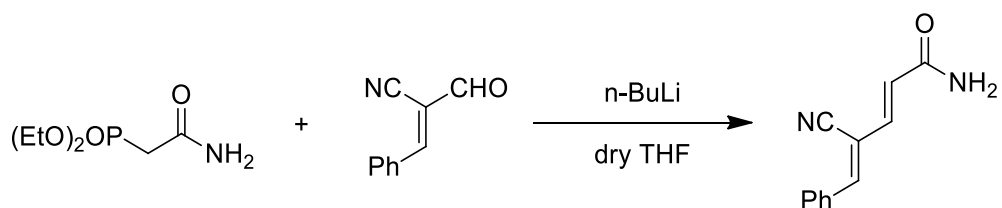
To a flame dried schlenk tube was added diethyl (2-amino-2-oxoethyl)phosphonate 0.390 g (2.00 mmol, 1 eq.), dry THF 20 mL was added and the resulting solution was cooled to -78 ˚C and stirred for 15 mins. n-BuLi 0.8 mL (2.00 mmol, 1 eq., 2.5 M in hexanes). To a separate flame dried schlenk tube was added α-cyano cinnamaldehyde **57** 0.314 g (2.00 mmol, 1 eq.) and 10 mL of dry THF was added before this solution was cooled to -78 ˚C. The aldehyde solution was then added dropwise *via* cannula to the phosphonate solution. The resulting solution was stirred at -78 ˚C for 2 hrs before being warmed to rt and stirred for a further 21 hrs. The now clear yellow solution was then carefully poured into 50 mL of distilled H_2O and extracted with 3 x 20 mL of DCM. The combined organics were washed with 30 mL of sat. brine solution and dried over Na_2SO_4. The dried solution was filtered and reduced *in vacuo* to yield a yellow solid. Slow recrystallization from DCM/PE yielded 0.096 g (24 %) of the product.

^{1}H NMR (300 MHz, CDCl$_3$) δ 7.91 – 7.80 (m, 2H), 7.52 – 7.43 (m, 3H), 7.41 (expected doublet overlapping with aromatics, 1H), 7.33 (br s, 1H), 6.44 (d, *J* = 15.0 Hz, 1H), 5.83 (s, 2H). **^{13}C NMR** (75 MHz, CDCl$_3$) δ 166.6, 149.7, 139.6, 132.9, 131.9, 130.0, 129.3, 123.9, 116.0, 108.6.

Mass: (APCI+) $C_{12}H_{11}N_2O$ Calc. (M+H$^+$) = 199.0866 found (M+H$^+$) = 199.0865 (0.4 ppm)

5.2.3   Synthesis of (E)-2-formyl-3-phenylacrylonitrile (57)
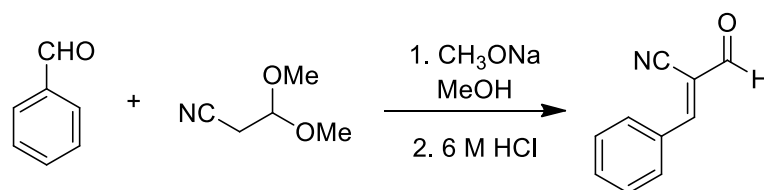
A mixture of benzaldehyde 2.18 mL (21.39 mmol, 1 eq.) and 3,3-dimethoxypropionitrile 2.4 mL (21.39 mmol, 1 eq.) was added dropwise to a neat solution of sodium methoxide 7.9 mL (20 mmol, 2 eq., 5.4 M in MeOH) and the resulting cloudy white solution was stirred at rt overnight. The reaction was reduced *in vacuo* to yield an off-white residue. To this was added 6 M HCl 30 mL and the reaction stirred at rt for 2 hrs. The white precipitate formed was collected by vacuum filtration and dissolved in 20 mL of DCM and dried over anhydrous Na_2SO_4, filtered and reduced *in vacuo*. The product was then precipitated from DCM/PE to yield a bright white solid 2.39 g (71 %).

¹H NMR (500 MHz, $CDCl_3$) δ 9.61 (s, 1H), 8.05 (d, *J* = 7.6 Hz, 2H), 7.91 (s, 1H), 7.68 − 7.59 (m, 1H), 7.59 − 7.52 (m, 2H) **¹³C NMR** (126 MHz, $CDCl_3$) δ = 186.8, 159.0, 134.5, 131.6, 131.4, 129.7, 114.3, 112.6. **IR:** (KBr Disc) 3066 (Ar-H), 2223 (Nitrile), 1691 (C=O), 1593 (C=C) cm^{-1}.

Matches literature data.[92]

5.2.4   Synthesis of (E)-2-formyl-3-(4-methoxyphenyl)acrylonitrile (61)
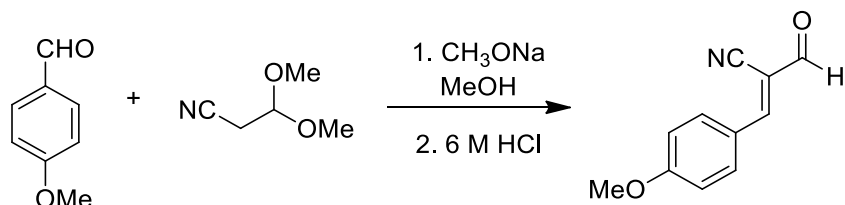
A mixture of benzaldehyde 2.5 mL (20.4 mmol, 1 eq.) and 3,3-dimethoxypropionitrile 2.3 mL (20.4 mmol, 1 eq.) was added dropwise to a neat solution of sodium methoxide 7.6 mL (41.0 mmol, 2 eq., 5.4 M in MeOH) and the resulting cloudy white solution was stirred at rt overnight. The reaction was reduced *in vacuo* to yield a pale yellow residue. To this was added 6 M HCl 20 mL and the reaction stirred at rt for 2 hrs. The pale yellow precipitate formed was collected by vacuum filtration and dissolved in 20 mL of DCM and dried over anhydrous Na_2SO_4, filtered and reduced *in vacuo*. The product was then precipitated from DCM/PE to yield a pale yellow solid 3.22 g (84 %).

¹H NMR (300 MHz, CDCl₃) δ 9.53 (s, 1H), 8.03 (d, *J* = 8.9 Hz, 2H), 7.82 (s, 1H), 7.02 (d, *J* = 8.9 Hz, 2H), 3.91 (s, 3H). **¹³C NMR** (75 MHz, CDCl₃) δ = 187.4, 164.8, 158.7, 134.2, 124.3, 115.2, 114.9, 109.2, 55.9. **IR:** (KBr Disc) 3021 (Ar-H), 2224 (Nitrile), 1677 (C=O), 1591 (C=C) cm⁻¹.

Matches literature data.[92]

5.2.5   Synthesis of (E)-3-(4-chlorophenyl)-2-formylacrylonitrile (80)
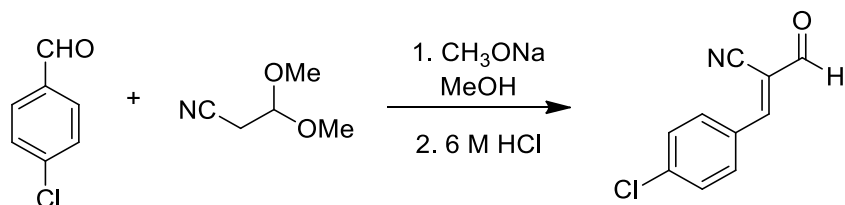
To neat sodium methoxide 6.35 mL (34.31 mmol, 5.4 M in MeOH, 2 eq.) was added dropwise a mixture of *p*-chlorobenzaldehyde 2.41 g (17.15 mmol, 1 eq.) and 3,3-dimethoxypropionitrile 1.92 mL (17.15 mmol, 1 eq.) dissolved in MeOH (5 mL). The resulting pale yellow opaque solution was stirred at rt for 16 hrs, after which time the reaction mixture was reduced *in vacuo* to yield a pale orange residue. To this was added 6 M HCl 30 mL and the reaction stirred at rt for 2 hrs. This resulting precipitate was collected by vacuum filtration and dissolved in 20 mL of DCM and dried over anhydrous Na_2SO_4, filtered and reduced *in vacuo*. The product was then precipitated from DCM/PE to yield a pale yellow solid 1.62 g (49 %).

^{1}H NMR (500 MHz, CDCl$_3$) δ 9.60 (s, 1H), 8.06 – 7.92 (m, 2H), 7.86 (s, 1H), 7.60 – 7.48 (m, 2H). **^{13}C NMR** (126 MHz, CDCl$_3$) δ = 186.4, 157.1, 141.0, 132.6, 130.2, 129.8, 114.1, 112.8. **IR:** (KBr Disc) 3088 (Ar-H), 2222 (Nitrile), 1693 (C=O), 1589 (C=C) cm^{-1}.

Matches literature data.[92]

5.2.6   Synthesis of (E)-2-formyl-3-(p-tolyl)acrylonitrile (81)
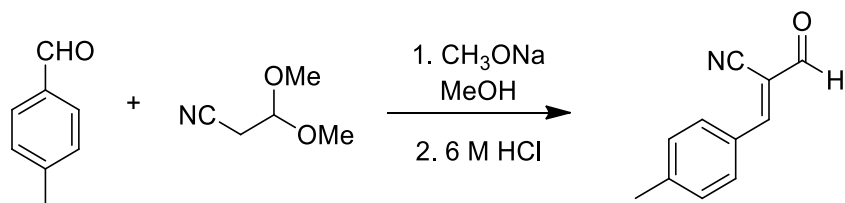
To neat sodium methoxide 6.35 mL (34.30 mmol, 2 eq.) was added dropwise a mixture of *p*-tolualdehyde 2 mL (17.15 mmol, 1 eq.) and 3,3-dimethoxypropionitrile 1.92 mL (17.15 mmol, 1 eq.), rinsing with MeOH 5 mL. The resulting cloudy white solution was stirred at rt for 16 hrs after which time it was reduced *in vacuo* to yield a pale white residue. To this was added 6 M HCl 30 mL and the reaction stirred at rt for 2 hrs. The resulting precipitate was collected by vacuum filtration and dissolved in 20 mL of DCM and dried over anhydrous Na_2SO_4, filtered and reduced *in vacuo*. The product was then precipitated from DCM/PE to yield a pale white solid 2.10 g (71 %).

^{1}H NMR (500 MHz, CDCl$_3$) δ 9.58 (s, 1H), 7.95 (d, *J* = 8.2 Hz, 2H), 7.86 (s, 1H), 7.36 (d, *J* = 8.1 Hz, 2H), 2.47 (s, 3H). **^{13}C NMR** (126 MHz, CDCl$_3$) δ = 187.0, 158.9, 146.2, 131.8, 130.5, 128.9, 114.6, 111.4, 22.2. **IR:** (ATR) 3025 (Ar-H), 2224 (Nitrile), 1691 (C=O), 1593 (C=C) cm^{-1}.

Matches literature data.[92]

5.2.7   Synthesis of (E)-3-(4-bromophenyl)-2-formylacrylonitrile (82)
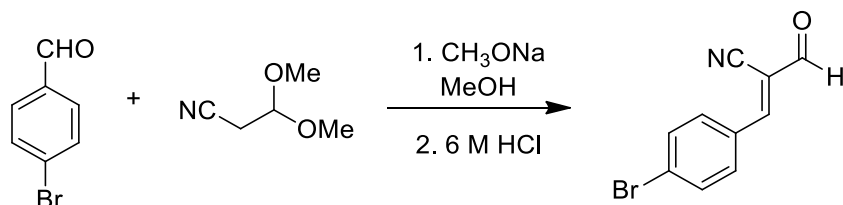
To neat sodium methoxide 8.25 mL (44.56 mmol, 2 eq.) was added dropwise a mixture of *p*-tolualdehyde 4.12 mL (22.28 mmol, 1 eq.) and 3,3-dimethoxypropionitrile 2.50 mL (22.28 mmol, 1 eq.), rinsing with MeOH 15 mL. The resulting cloudy white solution was stirred at rt for 16 hrs after which time it was reduced *in vacuo* to yield a pale yellow residue. To this was added 6 M HCl 30 mL and the reaction stirred at rt for 2 hrs. The resulting precipitate was collected by vacuum filtration and dissolved in 20 mL of DCM and dried over anhydrous Na_2SO_4, filtered and reduced *in vacuo*. The product was then precipitated from DCM/PE to yield a pale yellow solid 2.24 g (43 %).

^{1}H NMR (300 MHz, CDCl$_3$) δ 9.60 (s, 1H), 7.95 – 7.88 (m, 2H), 7.85 (s, 1H), 7.74 – 7.66 (m, 2H).

^{13}C NMR (75 MHz, CDCl$_3$) δ = 186.6, 157.4, 133.2, 132.6, 130.1, 129.8, 114.1, 112.9. **IR:** (ATR) 3091 (Ar-H), 2222 (Nitrile), 1690 (C=O), 1581 (C=C) cm^{-1}.

Matches literature data. [134]

5.2.8 Synthesis of (E)-3-(4-(dimethylamino)phenyl)-2-formylacrylonitrile (83)
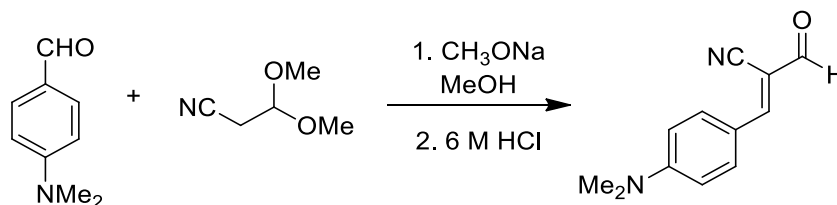
To neat sodium methoxide 8.25 mL (44.56 mmol, 2 eq.) was added dropwise a mixture of *p*-tolualdehyde 3.32 mL (22.28 mmol, 1 eq.) and 3,3-dimethoxypropionitrile 2.50 mL (22.28 mmol, 1 eq.), rinsing with MeOH 15 mL. The resulting cloudy yellow solution was stirred at rt for 16 hrs after which time it was reduced *in vacuo* to yield a bright yellow residue. To this was added 6 M HCl 30 mL and the reaction stirred at rt for 2 hrs. The resulting precipitate was collected by vacuum filtration and dissolved in 20 mL of DCM and dried over anhydrous Na_2SO_4, filtered and reduced *in vacuo*. The product was then precipitated from DCM/PE to yield a bright red solid 2.59 g (58 %). Note: Highly coloured material, stains easily.

^{1}H NMR (300 MHz, CDCl$_3$) δ 9.47 (s, 1H), 8.05 – 7.88 (m, 2H), 7.67 (s, 1H), 6.79 – 6.63 (m, 2H), 3.15 (s, 6H). **^{13}C NMR** (75 MHz, CDCl$_3$) δ = 187.7, 158.1, 154.5, 134.8, 119.5, 116.5, 111.9, 104.5, 40.3.

Matches literature data.[135]

5.2.9   Synthesis of (E)-2-formyl-3-(m-tolyl)acrylonitrile (84)
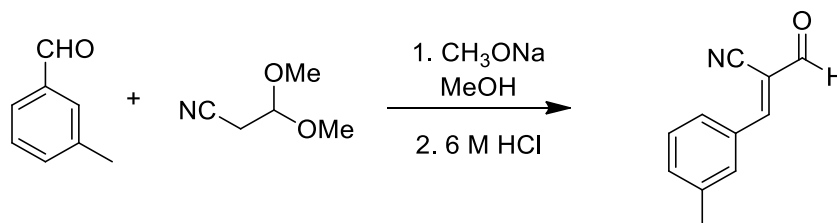
To neat sodium methoxide 3.30 mL (17.82 mmol, 2 eq.) was added dropwise a mixture of *m*-tolualdehyde 1.00 mL (8.9 mmol, 1 eq.) and 3,3-dimethoxypropionitrile 1.00 mL (8.9 mmol, 1 eq.), rinsing with MeOH 5 mL. The resulting cloudy white solution was stirred at rt for 16 hrs after which time it was reduced *in vacuo* to yield a pale white residue. To this was added 6 M HCl 30 mL and the reaction stirred at rt for 2 hrs. The resulting precipitate was collected by vacuum filtration and dissolved in 20 mL of DCM and dried over anhydrous Na_2SO_4, filtered and reduced *in vacuo*. The product was then precipitated from DCM/PE to yield a pale white solid 0.81 g (53 %).

^{1}H NMR (500 MHz, CDCl$_3$) δ 9.59 (s, 1H), 7.91 – 7.80 (m, 3H), 7.48 – 7.39 (m, 2H), 2.45 (s, 3H).
^{13}C NMR (126 MHz, CDCl$_3$) δ = 186.9, 159.2, 139.7, 135.5, 132.1, 131.4, 129.6, 128.8, 114.3, 112.3, 21.4. **IR:** (ATR) 3037 (Ar-H), 2230 (Nitrile), 1685 (C=O), 1611 (C=C) cm^{-1}.

R$_f$ 80:20 PE:EtOAc = 0.3 (Stains orange with DNP)

Matches literature data.[92]

5.2.10 Synthesis of (E)-2-formyl-3-(3-(trifluoromethyl)phenyl)acrylonitrile (85)
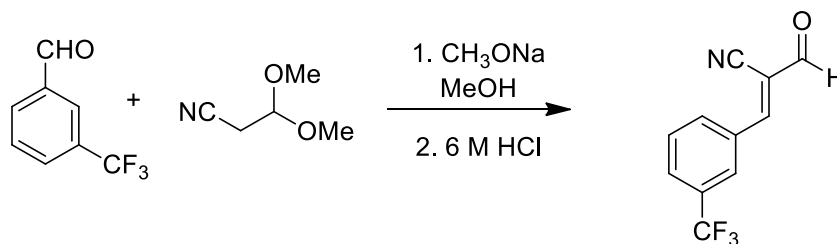
To neat sodium methoxide 3.30 mL (17.82 mmol, 2 eq.) was added dropwise a mixture of *m*-trifluorobenzaldehyde 1.20 mL (8.9 mmol, 1 eq.) and 3,3-dimethoxypropionitrile 1.00 mL (8.9 mmol, 1 eq.), rinsing with MeOH 5 mL. The resulting cloudy white solution was stirred at rt for 16 hrs after which time it was reduced *in vacuo* to yield a pale white residue. To this was added 6 M HCl 30 mL and the reaction stirred at rt for 2 hrs. The resulting precipitate was collected by vacuum filtration and dissolved in 20 mL of DCM and dried over anhydrous Na_2SO_4, filtered and reduced *in vacuo*. The product was then precipitated from DCM/PE to yield a pale white solid 0.67 g (34 %).

^{1}H NMR (500 MHz, CDCl$_3$) δ 9.63 (s, 1H), 8.35 (d, *J* = 7.5 Hz, 1H), 8.16 (s, 1H), 7.95 (s, 1H), 7.88 (d, *J* = 7.8 Hz, 1H), 7.73 (t, *J* = 7.9 Hz, 1H). **^{13}C NMR** (126 MHz, CDCl$_3$) δ 186.1, 156.5, 133.4, 132.4 (q, *J* = 33.3 Hz), 132.0, 130.5 (q, *J* = 3.6 Hz), 130.5, 128.5 (q, *J* = 3.8 Hz), 123.4 (q, *J* = 273.0 Hz), 114.4, 113.7. **^{19}F NMR** (471 MHz, CDCl$_3$) δ -63.11 (s). **IR:** (ATR) 3053 (Ar-H), 2228 (Nitrile), 1681 (C=O), 1612 (C=C) cm^{-1}.

R$_f$ 80:20 PE:EtOAc = 0.2 (Stains orange with DNP)

**5.2.11   Synthesis of (E)-3-(3-chlorophenyl)-2-formylacrylonitrile (86)**
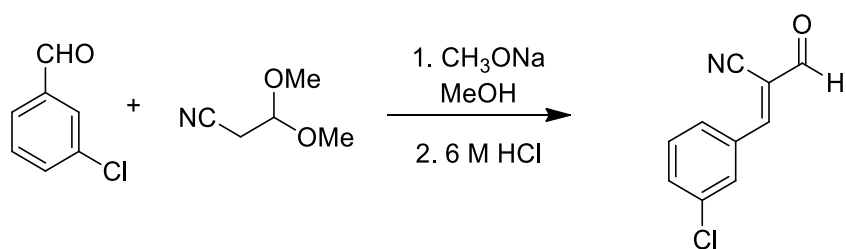
To neat sodium methoxide 6.35 mL (34.30 mmol, 2 eq.) was added dropwise a mixture of *m*-chlorobenzaldehyde 1.95 mL (17.15 mmol, 1 eq.) and 3,3-dimethoxypropionitrile 1.92 mL (17.15 mmol, 1 eq.), rinsing with MeOH 5 mL. The resulting cloudy white solution was stirred at rt for 16 hrs after which time it was reduced *in vacuo* to yield a pale white residue. To this was added 6 M HCl 30 mL and the reaction stirred at rt for 2 hrs. The resulting precipitate was collected by vacuum filtration and dissolved in 20 mL of DCM and dried over anhydrous Na_2SO_4, filtered and reduced *in vacuo*. The product was then precipitated from DCM/PE to yield a pale white solid 1.39 g (42 %).

^{1}H NMR (500 MHz, $CDCl_3$) δ 9.60 (s, 1H), 7.99 (d, *J* = 7.8 Hz, 1H), 7.96 (s, 1H), 7.84 (s, 1H), 7.60 (dd, *J* = 8.1, 0.9 Hz, 1H), 7.51 (t, *J* = 7.9 Hz, 1H). **^{13}C NMR** (126 MHz, $CDCl_3$) δ = 186.2, 156.8, 135.9, 134.2, 132.9, 131.3, 131.0, 129.1, 113.8. **IR:** (ATR) 3074 (Ar-H), 2222 (Nitrile), 1691 (C=O), 1612 (C=C) cm^{-1}.

Matches literature data.[92]

### 5.2.12   Synthesis of (E)-3-(3-fluorophenyl)-2-formylacrylonitrile (87)

To neat sodium methoxide 3.30 mL (17.82 mmol, 2 eq.) was added dropwise a mixture of *m*-fluorobenzaldehyde 0.94 mL (8.9 mmol, 1 eq.) and 3,3-dimethoxypropionitrile 1.00 mL (8.9 mmol, 1 eq.), rinsing with MeOH 5 mL. The resulting cloudy white solution was stirred at rt for 16 hrs after which time it was reduced *in vacuo* to yield a pale white residue. To this was added 6 M HCl 30 mL and the reaction stirred at rt for 2 hrs. The resulting precipitate was collected by vacuum filtration and dissolved in 20 mL of DCM and dried over anhydrous Na_2SO_4, filtered and reduced *in vacuo*. The product was then precipitated from DCM/PE to yield a pale white solid 0.75 g (48 %).

^{1}H NMR (500 MHz, $CDCl_3$) δ 9.61 (s, 1H), 7.87 (s, 1H), 7.84 – 7.80 (m, 1H), 7.79 – 7.74 (m, 1H), 7.55 (td, *J* = 8.1, 5.7 Hz, 1H), 7.34 (tdd, *J* = 8.3, 2.5, 0.9 Hz, 1H). **^{13}C NMR** (126 MHz, $CDCl_3$) δ 186.3, 163.0 (d, *J* = 249.7 Hz), 156.9 (d, *J* = 2.8 Hz), 133.2 (d, *J* = 7.8 Hz), 131.4 (d, *J* = 8.1 Hz), 127.4 (d, *J* = 3.1 Hz), 121.4 (d, *J* = 21.4 Hz), 117.6 (d, *J* = 22.8 Hz), 113.87, 113.78. **^{19}F NMR** (471 MHz, $CDCl_3$) δ -109.93 (s). **IR:** (ATR) 3066 (Ar-H), 2226 (Nitrile), 1689 (C=O), 1576 (C=C) cm^{-1}.

R$_f$ 80:20 PE:EtOAc = 0.2 (Stains orange with DNP)

5.2.13 Synthesis of (E)-3-(3-bromophenyl)-2-formylacrylonitrile (88)
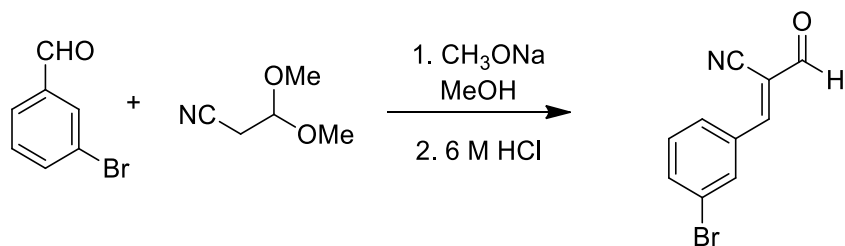
To neat sodium methoxide 6.35 mL (34.30 mmol, 2 eq.) was added dropwise a mixture of *m*-bromobenzaldehyde 2.00 mL (17.15 mmol, 1 eq.) and 3,3-dimethoxypropionitrile 1.92 mL (17.15 mmol, 1 eq.), rinsing with MeOH 5 mL. The resulting cloudy pale yellow solution was stirred at rt for 16 hrs after which time it was reduced *in vacuo* to yield a pale orange residue. To this was added 6 M HCl 30 mL and the reaction stirred at rt for 2 hrs. The resulting precipitate was collected by vacuum filtration and dissolved in 20 mL of DCM and dried over anhydrous Na_2SO_4, filtered and reduced *in vacuo*. The product was then precipitated from DCM/PE to yield a pale yellow solid 1.43 g (35 %).

¹H NMR (500 MHz, CDCl₃) δ 9.60 (s, 1H), 8.09 (t, *J* = 1.6 Hz, 1H), 8.05 (d, *J* = 7.9 Hz, 1H), 7.83 (s, 1H), 7.75 (dd, *J* = 8.0, 0.9 Hz, 1H), 7.45 (t, *J* = 8.0 Hz, 1H). **¹³C NMR** (126 MHz, CDCl₃) δ = 186.3, 156.8, 137.1, 134.3, 133.2, 131.2, 129.4, 123.7, 113.8. **IR:** (ATR) 3071 (Ar-H), 2222 (Nitrile), 1690 (C=O), 1610 (C=C) cm⁻¹.

Matches literature data.[92]

### 5.2.14   Synthesis of (E)-2-formyl-3-(o-tolyl)acrylonitrile (89)
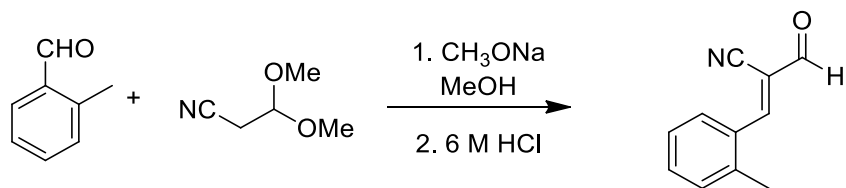
To neat sodium methoxide 3.30 mL (17.82 mmol, 2 eq.) was added dropwise a mixture of *m*-tolualdehyde 1.00 mL (8.9 mmol, 1 eq.) and 3,3-dimethoxypropionitrile 1.00 mL (8.9 mmol, 1 eq.), rinsing with MeOH 5 mL. The resulting cloudy white solution was stirred at rt for 16 hrs after which time it was reduced *in vacuo* to yield a pale white residue. To this was added 6 M HCl 30 mL and the reaction stirred at rt for 2 hrs. The resulting precipitate was collected by vacuum filtration and dissolved in 20 mL of DCM and dried over anhydrous Na_2SO_4, filtered and reduced *in vacuo*. The product was then precipitated from DCM/PE to yield a pale white solid 1.06 g (70 %).

^{1}H NMR (500 MHz, CDCl$_3$) δ 9.64 (s, 1H), 8.28 (d, *J* = 7.9 Hz, 1H), 8.25 (s, 1H), 7.52 − 7.46 (m, 1H), 7.41 − 7.32 (m, 2H), 2.52 (s, 3H). **^{13}C NMR** (126 MHz, CDCl$_3$) δ = 186.8, 156.4, 140.3, 134.1, 131.5, 130.3, 129.1, 127.3, 114.3, 113.7, 20.0. **IR:** (KBr Disc) 3033 (Ar-H), 2228 (Nitrile), 1685 (C=O), 1587 (C=C) cm^{-1}.

R$_f$ 80:20 PE:EtOAc = 0.3 (Stains orange with DNP)

Matches literature data.[92]

5.2.15 Synthesis of (E)-2-formyl-3-(naphthalen-1-yl)acrylonitrile (90)
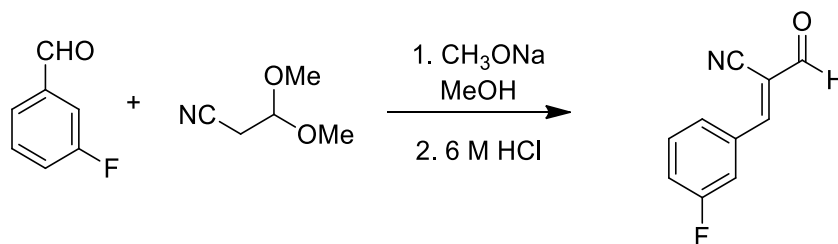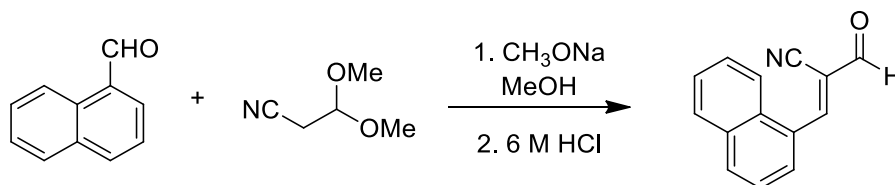

To neat sodium methoxide 4.80 mL (26.0 mmol, 2 eq.) was added dropwise a mixture of 1-napthaldehyde 1.80 mL (13.0 mmol, 1 eq.) and 3,3-dimethoxypropionitrile 1.50 mL (13.0 mmol, 1 eq.), rinsing with MeOH 10 mL. The resulting cloudy brown solution was stirred at rt for 16 hrs after which time it was reduced *in vacuo* to yield a brown residue. To this was added 6 M HCl 30 mL and the reaction stirred at rt for 2 hrs. The resulting yellow gum was collected by vacuum filtration and dissolved in 20 mL of DCM and dried over anhydrous Na_2SO_4, filtered and reduced *in vacuo*. The product was then precipitated from DCM/PE to yield a bright yellow solid 1.37 g (51 %).

^{1}H NMR (500 MHz, CDCl$_3$) δ 9.77 (s, 1H), 8.83 (s, 1H), 8.49 (d, *J* = 7.4 Hz, 1H), 8.11 (t, *J* = 8.8 Hz, 2H), 7.97 (d, *J* = 8.1 Hz, 1H), 7.75 − 7.58 (m, 3H). **^{13}C NMR** (126 MHz, CDCl$_3$) δ = 186.6, 155.5, 134.9, 133.8, 131.8, 129.6, 129.1, 128.5, 127.9, 127.2, 125.7, 122.4, 114.7, 114.5. **IR:** (KBr Disc) 3052 (Ar-H), 2221 (Nitrile), 1692 (C=O), 1568 (C=C) cm^{-1}.

Matches literature data. [79]

5.2.16 Synthesis of (E)-2-formyl-3-(thiophen-2-yl)acrylonitrile (91)
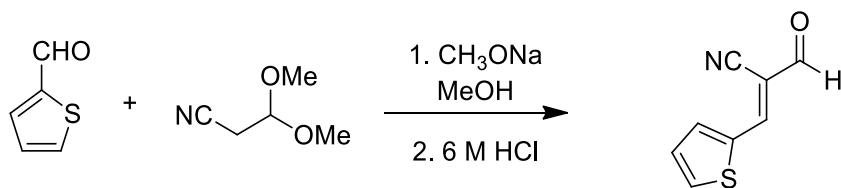
To neat sodium methoxide 6.6 mL (35.6 mmol, 2 eq.) was added dropwise a mixture of 2-thiophenecarboxaldehyde 1.66 mL (17.8 mmol, 1 eq.) and 3,3-dimethoxypropionitrile 2.00 mL (17.8 mmol, 1 eq.), rinsing with MeOH 5 mL. The resulting cloudy yellow solution was stirred at rt for 16 hrs after which time it was reduced *in vacuo* to yield a pale brown residue. This residue was suspended in 20 mL of 6 M HCl and heat to 100 ˚C for 1 hr during which time a yellow precipitate formed. This precipitate was collected by vacuum filtration and dissolved in the minimal DCM and precipitated with PE to give a golden yellow solid 1.54 g (60 %).

¹H NMR (300 MHz, CDCl₃) δ 9.55 (s, 1H), 8.04 (s, 1H), 7.94 – 7.89 (m, 2H), 7.29 (dd, *J* = 5.0, 3.9 Hz, 1H). **¹³C NMR** (126 MHz, CDCl₃) δ 186.1, 149.5, 138.2, 137.1, 136.2, 129.4, 114.6, 109.0. **IR:** (ATR) 3086 (Ar-H), 2219 (Nitrile), 1675 (C=O), 1591 (C=C) cm⁻¹.

5.2.17 Synthesis of 2-(triphenylphosphoranylidene)acetonitrile (71)
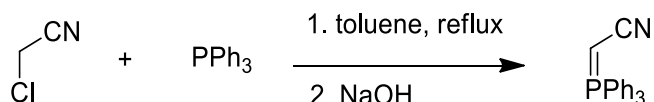
To triphenylphosphine 4.14 g (15.8 mmol, 1 eq.) was added toluene 20 mL and chloroacetonitrile 2.00 mL (31.3 mmol, 2 eq.) to yield a clear pale yellow solution which was refluxed at 120 °C for 16 hrs. A white precipitate was formed which was collected by vacuum filtration. The precipitate was then dissolved in 20 mL of DCM and transferred to a separating funnel and washed with 20 mL of 2 M NaOH. The organic layer was collected and the aqueous layer extracted with a further 3 x 20 mL of DCM. The combined organics were then dried over anhydrous Na_2SO_4, filtered and reduced *in vacuo* to yield a pale white solid which was precipitated by dissolving the solid in the minimal amount of DCM and adding PE until precipitation ceased. The resulting precipitate was collected by vacuum filtration to yield a bright white amorphous solid 4.43 g (93 %).

^{1}H NMR (500 MHz, CDCl$_3$) δ 7.66 – 7.55 (m, 9H), 7.55 – 7.45 (m, 6H), 1.58 (d, J_{PH} = 6.9 Hz, 1H). **^{13}C NMR** (126 MHz, CDCl$_3$) δ 132.87 (d, *J* = 10.1 Hz), 132.68 (d, *J* = 2.9 Hz), 129.18 (d, *J* = 12.3 Hz), 128.03 (d, *J* = 7.8 Hz), 127.49 (d, *J* = 91.8 Hz), -2.03 (d, *J* = 136.0 Hz). **^{31}P NMR** (202 MHz, CDCl$_3$) δ 23.16 (s). **IR:** (KBr) 3055 (Ar-H), 2139 (nitrile) cm^{-1}.

ESI-MS C$_{20}$H$_{17}$NP Calc. (M+H)$^+$ = 302.1093 found (M+H)$^+$ = 302.1105 (+4.09 ppm)

Matches literature data.[136]

5.2.18   Synthesis of (2E,4Z)-4-(4-methoxybenzylidene)pent-2-enedinitrile (62)
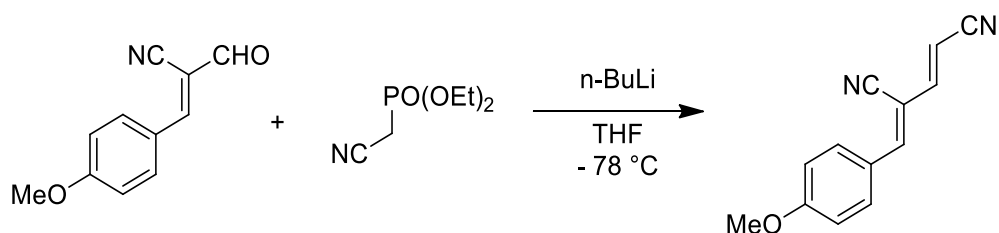
To a flame dried schlenk tube was added *p*-OMe α-cyano cinnamaldehyde 0.290 g (1.55 mmol, 1eq.) and dry THF 2 mL. The resulting pale yellow solution was brought to -78 ˚C and stirred at this temperature for 15 mins. In a separate flame-dried schlenk tube was added diethyl (cyanomethyl)phosphonate 0.5 mL (3.10 mmol, 2 eq.) and dry THF 20 mL, this solution was stirred until homogeneous and then cooled in an acetone/ice bath. To the resulting solution was added dropwise n–BuLi 1.24 mL (3.10 mmol, 2eq.). Upon completion of the addition the solution was allowed to warm to rt and stirred for 1hr before being cooled to -78 ˚C. The aldehyde solution was then added dropwise *via* cannula to the phosphonate solution, rinsing with an additional 4 mL of dry THF. The resulting bright yellow solution was stirred at -78 ˚C for 24 hrs. The reaction mixture was then quenched with sat. aq. NH$_4$Cl solution 20 mL and transferred to a 500 mL separating funnel. The mixture was diluted with 150 mL of distilled H$_2$O and then extracted with 3 x 50 mL of EtOAc. The combined organics were dried over anhydrous Na$_2$SO$_4$, filtered and reduced *in vacuo* to yield an orange/red solid. This solid was then dissolved in the minimal amount of hot DCM before being passed through a short silica plug rinsing with PE:EtOAc (65:35). The filtrate was reduced *in vacuo* to yield a yellow solid which was recrystallized from PE/EtOAc to yield 0.033 g (10 %) of a yellow solid.

^{1}H NMR (300 MHz, CDCl$_3$) δ 7.96 – 7.82 (m, 2H), 7.22 (s, 1H), 7.11 (d, *J* = 16.0 Hz, 1H), 7.03 – 6.93 (m, 2H), 5.81 (d, *J* = 16.0 Hz, 1H), 3.89 (s, 3H).**^{13}C NMR** (75 MHz, CDCl$_3$) δ = 163.4, 150.4, 147.6, 132.8, 125.1, 117.4, 115.3, 115.0, 104.8, 98.7, 55.8. **IR:** (ATR) 3049 (Ar-H), 2216 (nitrile), 1583 (C=C) cm^{-1}.

Mass: (APCI+) C$_{13}$H$_{11}$N$_2$O Calc. (M+H)$^+$ = 211.0866 found (M+H)$^+$ = 211.0863 (1.4 ppm)

5.2.19 Synthesis of (2E,4Z)-4-(4-methoxybenzylidene)pent-2-enedinitrile (62)
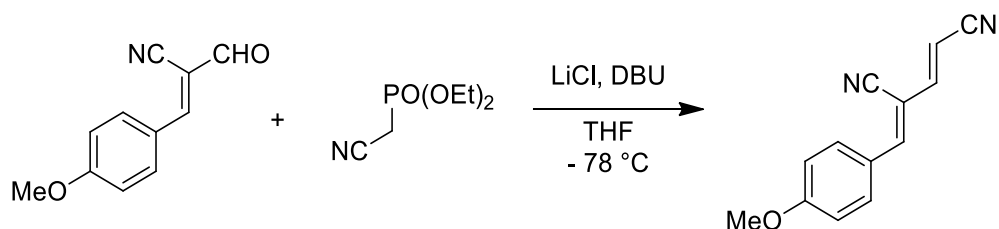
To a flame-dried schlenk tube was added *p*-OMe α-cyano cinnamaldehyde 0.374 g (2.0 mmol, 1 eq.) and LiCl 0.254 g (6 mmol, 3 eq., dried at 200 ˚C overnight) in THF 30 mL. To the resulting solution diethyl (cyanomethyl)phosphonate 0.33 mL (2.0 mmol, 1 eq.) was added and the solution cooled to 0 ˚C. To this was added DBU 0.3 mL (2 mmol, 1 eq.) dropwise, the reaction mixture turned cloudy white upon addition of the DBU. The reaction was stirred at 0 ˚C for 4 hrs after which time the reaction was quenched with sat. aq. NH_4Cl 5 mL. The reaction was then transferred to a separating funnel and diluted with distilled H_2O 20 mL and extracted with 3 x 50 mL of EtOAc. The combined organics were washed with sat. aq. brine 40 mL and dried over anhydrous Na_2SO_4, filtered and reduced *in vacuo* to yield a red/yellow solid. This solid was dissolved in the minimum DCM and passed through a short silica plug (4 cm (height) x 3.5 cm (diameter)) rinsing with PE:EtOAc (50:50). The filtrate was reduced *in vacuo* to yield 0.102 g (24 %) of a pale yellow solid.

¹H NMR (300 MHz, CDCl₃) δ 7.96 – 7.82 (m, 2H), 7.22 (s, 1H), 7.11 (d, *J* = 16.0 Hz, 1H), 7.03 – 6.93 (m, 2H), 5.81 (d, *J* = 16.0 Hz, 1H), 3.89 (s, 3H).**¹³C NMR** (75 MHz, CDCl₃) δ = 163.4, 150.4, 147.6, 132.8, 125.1, 117.4, 115.3, 115.0, 104.8, 98.7, 55.8. **IR:** (ATR) 3049 (Ar-H), 2216 (nitrile), 1583 (C=C) cm⁻¹.

5.2.20 Synthesis of (2E,4Z)-4-(4-methoxybenzylidene)pent-2-enedinitrile (62)
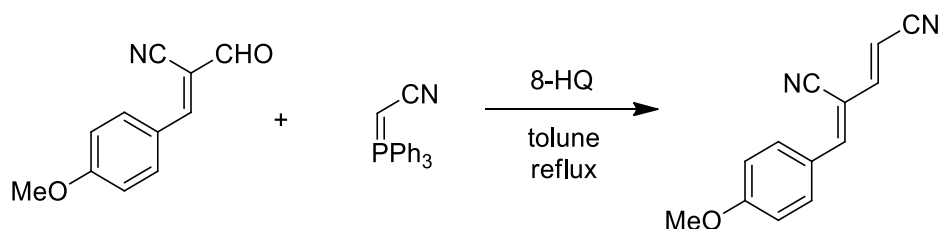
To a round bottom flask was added *p*-OMe α-cyano cinnamaldehyde 281 mg (1.5 mmol, 1 eq.), 2-(triphenylphosphoranylidene)acetonitrile 497 mg (1.65 mmol, 1.1 eq.) and 8-HQ 218 mg (1.5 mmol, 1 eq.). To this mixture was added 30 mL of toluene and the resulting yellow solution was refluxed for 2 hrs. After this time the reaction was allowed to cool to rt before it was passed through a short silica plug rinsing with 60:40 PE:EtOAc 500 mL to yield a pale yellow solution. This solution was reduced *in vacuo* to yield a bright yellow solid which was dissolved in a minimal amount of DCM and precipitated with PE to give a yield of 92 mg of a bright yellow solid (29 %).

^{1}H NMR (300 MHz, CDCl$_3$) δ 7.96 – 7.82 (m, 2H), 7.22 (s, 1H), 7.11 (d, *J* = 16.0 Hz, 1H), 7.03 – 6.93 (m, 2H), 5.81 (d, *J* = 16.0 Hz, 1H), 3.89 (s, 3H).**^{13}C NMR** (75 MHz, CDCl$_3$) δ = 163.4, 150.4, 147.6, 132.8, 125.1, 117.4, 115.3, 115.0, 104.8, 98.7, 55.8. **IR:** (ATR) 3049 (Ar-H), 2216 (nitrile), 1583 (C=C) cm^{-1}.

5.2.21 Synthesis of 2-(hydroxy(4-nitrophenyl)methyl)acrylonitrile (92)
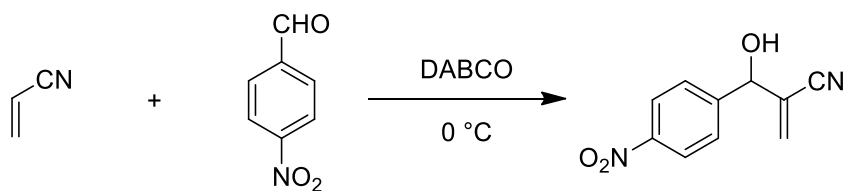
Acrylonitrile 2.6 mL (39.7 mmol, 6 eq.) and *p*-NO_2 benzaldehyde 1.0 g (6.6 mmol, 1 eq.) were mixed together neat and cooled to 0 ˚C. DABCO 0.743 g (6.62 mmol, 1 eq.) was added and the reaction stirred for 30 mins. Over this time the reaction mixture changed colour from deep red to a light orange suspension. The precipitate was collected by vacuum filtration to yield a yellow solid. This solid was dissolved in 10 mL of DCM and washed with 5 mL of 1M HCl followed by a wash with 10 mL of sat. $NaHCO_3$. The organic layer was collected, dried over Na_2SO_4, filtered and reduced *in vacuo* to yield a yellow solid 1.10 g (81 %).

^{1}H NMR (500 MHz, CDCl$_3$) δ 8.17 (d, *J* = 8.8 Hz, 1H), 7.63 − 7.49 (m, 1H), 6.15 (d, *J* = 1.2 Hz, 1H), 6.06 (d, *J* = 0.9 Hz, 1H), 5.42 (s, 1H), 3.73 (s, *J* = 87.0 Hz, 1H).

^{13}C NMR (126 MHz, CDCl$_3$) δ 147.9, 146.4, 131.4, 127.4, 125.4, 124.0, 116.5, 73.1.

Matches literature data.[137]

5.2.22 Synthesis of (2E,4Z)-4-benzylidenepent-2-enedinitrile (41)
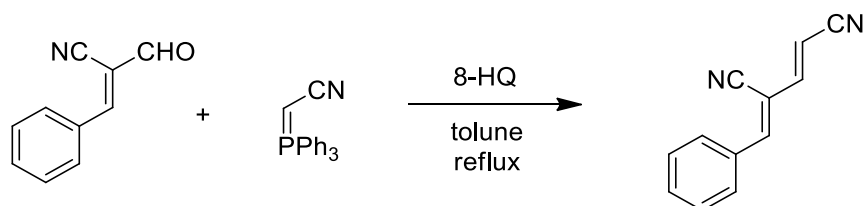
To a round bottom was added α-cyano cinnamaldehyde 157 mg (1.0 mmol, 1 eq.), 2-(triphenylphosphoranylidene)acetonitrile 331 mg (1.1 mmol, 1.1 eq.) and 8-HQ 145 mg (1.0 mmol, 1 eq.). To this mixture was added 20 mL of toluene and the resulting clear yellow solution was refluxed for 2 hrs. After this time the reaction was allowed to cool before it was passed through a short silica plug rinsing with 60:40 PE:EtOAc 500 mL to yield a pale yellow solution. This solution was reduced *in vacuo* to yield an off-white solid which was dissolved in a minimal amount of DCM and precipitated with PE at − 20 ˚C to give a yield of 89 mg (49 %) of a white solid.

^{1}H NMR (500 MHz, CDCl$_3$) δ 7.89 (d, *J* = 7.3 Hz, 2H), 7.57 − 7.47 (m, 3H), 7.32 (s, 1H, 2), 7.14 (d, *J* = 16.0 Hz, 1H, 3), 5.91 (d, *J* = 16.0 Hz, 1H, 4). **^{13}C NMR** (126 MHz, CDCl$_3$) δ = 150.8, 146.9, 132.8, 132.3, 130.4, 129.5, 117.0, 114.66, 108.1, 100.7. **IR:** (NaCl plate) 3047 (Ar-H), 2219 (nitrile), 1594 (C=C) cm^{-1}.

ESI-MS C$_{12}$H$_9$N$_2$ Calc. (M+H)$^+$ = 181.0760 found (M+H)$^+$ = 181.0769 (+4.93 ppm)

m.p: 108-112 ˚C (decomposition) (DCM/PE)

5.2.23 Synthesis of (2E,4Z)-4-benzylidenepent-2-enedinitrile (41) and (2Z,4Z)-4-benzylidenepent-2-enedinitrile (41b)
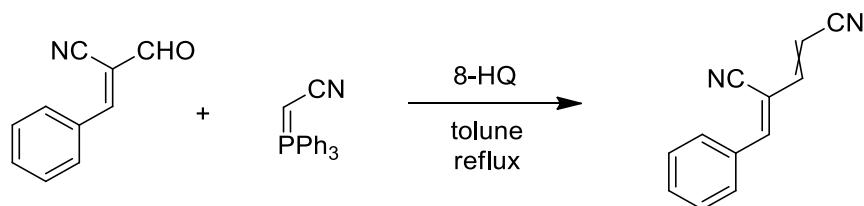
To a round bottom was added α-cyano cinnamaldehyde 236 mg (1.5 mmol, 1 eq.), 2-(triphenylphosphoranylidene)acetonitrile 497 mg (1.65 mmol, 1.1 eq.) and 8-HQ 218 mg (1.5 mmol, 1 eq.). To this mixture was added 30 mL of toluene and the resulting clear yellow solution was refluxed for 2 hrs. After this time the reaction was allowed to cool before it was passed through a short silica plug rinsing with two fractions of 60:40 PE:EtOAc, the first 300 mL and the second 200 mL to yield a pale yellow solutions. These solution were retained separately and reduced *in vacuo* to yield an off-white solids which were dissolved in a minimal amount of DCM and precipitated with PE at − 20 ˚C to give white solids. The first fraction yielded 109 mg (40 %) of the *E,Z* isomer and the second fraction yielded 99 mg (37 %) of the *Z,Z* isomer for a combined yield of 77 %.

^{1}H NMR (500 MHz, CDCl$_3$) δ 7.89 (d, *J* = 7.3 Hz, 2H), 7.57 − 7.47 (m, 3H), 7.32 (s, 1H, 2), 7.14 (d, *J* = 16.0 Hz, 1H, 3), 5.91 (d, *J* = 16.0 Hz, 1H, 4). **^{13}C NMR** (126 MHz, CDCl$_3$) δ = 150.8, 146.9, 132.8, 132.3, 130.4, 129.5, 117.0, 114.66, 108.1, 100.7. *E,Z* isomer

m.p: 108-112 ˚C (decomposition) (DCM/PE)

^{1}H NMR (300 MHz, CDCl$_3$) δ 7.92 (m, 2H), 7.60 − 7.42 (m, 4H), 6.75 (d, *J* = 11.9 Hz, 1H), 5.54 (d, *J* = 11.9 Hz, 1H). **^{13}C NMR** (75 MHz, CDCl$_3$) δ 151.9, 143.2, 132.8, 132.3, 130.5, 129.4, 115.1, 114.4, 106.5, 98.7. *Z,Z* isomer

ESI-MS: C$_{12}$H$_8$N$_2$ Calc. (M+Na)$^+$ = 203.0580 found (M+Na)$^+$ = 203.0571 (-4.09 ppm)

m.p: 124-128 ˚C (decomposition) (DCM/PE)

5.2.24 Synthesis of (2E,4Z)-4-(4-(dimethylamino)benzylidene)pent-2-enedinitrile (94)
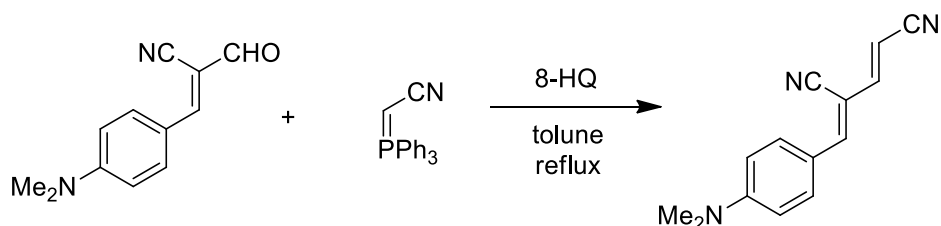
To a round bottom was added *p*-NMe$_2$ α-cyano cinnamaldehyde 600 mg (3.0 mmol, 1 eq.), 2-(triphenylphosphoranylidene)acetonitrile 994 mg (3.3 mmol, 1.1 eq.) and 8-HQ 435 mg (3.0 mmol, 1 eq.). To this mixture was added 30 mL of toluene and the resulting bright orange solution was refluxed for 2 hrs. After this time the reaction was allowed to cool before it was passed through a short silica plug rinsing with 60:40 PE:EtOAc 500 mL to yield a bright orange solution. This solution was reduced *in vacuo* to yield a bright red solid which was dissolved in a minimal amount of DCM and precipitated with PE at − 20 ˚C to give a yield of 357 mg of a bright red soild (53 %). Note: Highly coloured material, stains easily.

1H NMR (300 MHz, CDCl$_3$) δ 7.90 − 7.76 (m, 2H), 7.07 (asymmetric d, *J* = 15.5 Hz, 2H, Ar-C*H*C=C and C*H*=CHC≡N overlapped), 6.69 (m, 2H), 5.64 (d, *J* = 16.1 Hz, 1H), 3.11 (s, 6H).**13C NMR** (75 MHz, CDCl$_3$) δ = 153.2, 150.8, 148.6, 133.1, 120.1, 118.2, 116.4, 111.8, 100.2, 95.4, 40.2.

Mass: (APCI+) C$_{14}$H$_{13}$N$_3$ Calc. (M+H)$^+$ = 224.1182 found (M+H)$^+$ = 224.1186 (1.7 ppm)

5.2.25 Synthesis of (2E,4Z)-4-(thiophen-2-ylmethylene)pent-2-enedinitrile (95)
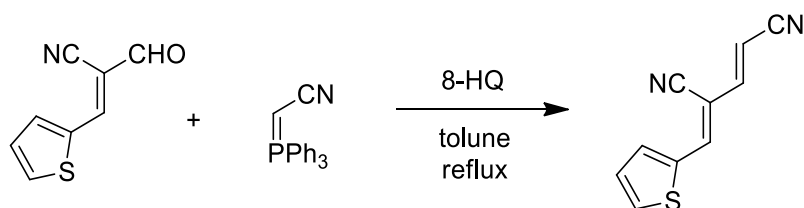
To a round bottom was added (E)-2-formyl-3-(thiophen-2-yl)acrylonitrile 218 mg (1.5 mmol, 1 eq.), 2-(triphenylphosphoranylidene)acetonitrile 497 mg (1.65 mmol, 1.1 eq.) and 8-HQ 218 mg (1.5 mmol, 1 eq.). To this mixture was added 30 mL of toluene and the resulting pale yellow solution was refluxed for 2 hrs. After this time the reaction was allowed to cool before it was passed through a short silica plug rinsing with 60:40 PE:EtOAc 500 mL to yield a pale yellow solution. This solution was reduced *in vacuo* to yield a pale yellow solid which was dissolved in a minimal amount of DCM and precipitated with PE at -20 °C to give a yield of 110 mg of a pale yellow solid (39 %).

Product contaminated with 11 % of *Z,Z* isomer, identified through the appearance of the olefinic proton signals which appear as follows in the ^{1}H NMR spectrum. **^{1}H NMR (300 MHz, CDCl$_3$) δ 6.68 (dd, *J* = 11.9, 0.6 Hz, 1H), 5.46 (d, *J* = 11.8 Hz, 1H).

^{1}H NMR (300 MHz, CDCl$_3$) δ 7.75 – 7.68 (m, 2H), 7.44 (br s, 1H), 7.20 (dd, *J* = 5.0, 3.9 Hz, 1H), 7.07 (dd, *J* = 16.0, 0.4 Hz, 1H), 5.80 (d, *J* = 16.0 Hz, 1H). *E,Z* isomer.

^{13}C NMR (75 MHz, CDCl$_3$) δ 146.4, 142.4, 136.8, 135.8, 134.1, 128.8, 117.2, 114.8, 104.9, 99.5. *E,Z* isomer.

5.2.26 Synthesis of ethyl 2-(triphenylphosphoranylidene)acetate (101)
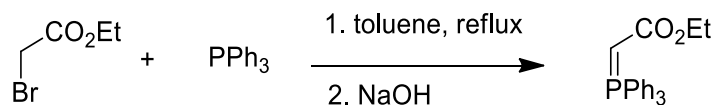
To triphenylphosphine 5.77 g (20.0 mmol, 1 eq.) was added toluene 40 mL and ethyl 2-bromoacetate 2.2 mL (22.0 mmol, 1.1 eq.) to yield a clear pale yellow solution which was refluxed at 120 ˚C overnight. A white precipitate was formed which was collected by vacuum filtration. The precipitate was then dissolved in 20 mL of DCM and transferred to a separating funnel and washed with 40 mL of 2 M NaOH. The organic layer was collected and the aqueous layer extracted with a further 3 x 30 mL of DCM. The combined organics were then dried over anhydrous Na_2SO_4, filtered and reduced *in vacuo* to yield a pale colourless solid which was precipitated by dissolving the solid in the minimal amount of DCM and adding PE until precipitation ceased. The resulting precipitate was collected by vacuum filtration to yield a colourless amorphous solid 5.206 g (75 %).

¹H NMR (300 MHz, $CDCl_3$) δ 7.70 – 7.60 (m, 6H), 7.59 – 7.50 (m, 3H), 7.49 – 7.40 (m, 6H), 3.97 (br s, 2H), 2.88 (br s, 1H), 1.18 (br s, 2H). Singlet signals very broad due to rotamerism.

¹³C NMR (75 MHz, $CDCl_3$) δ 133.07 (d, *J* = 10.0 Hz), 132.00 (d, *J* = 2.7 Hz), 128.79 (d, *J* = 12.2 Hz). Signals for the ylidic proton and the ethyl group not visible due to rotamerism.

³¹P NMR (202 MHz, $CDCl_3$) δ 17.81.

IR: (KBr) 3056 (Ar-H), 1605 (C=O) cm^{-1}

Matches literature data.[138]

5.2.27 Synthesis of (2E,4Z)-ethyl 4-cyano-5-phenylpenta-2,4-dienoate (96)
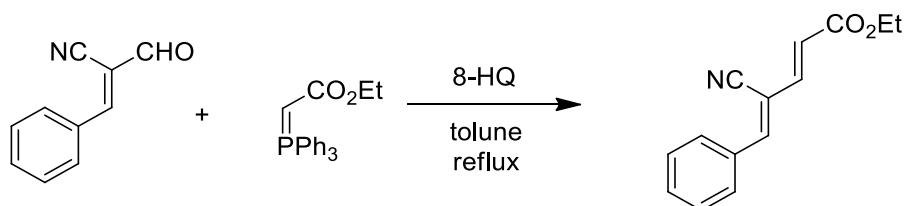
To a round bottom was added α-cyano cinnamaldehyde 236 mg (1.5 mmol, 1 eq.), ethyl 2-(triphenylphosphoranylidene)acetate 575 mg (1.65 mmol, 1.1 eq.) and 8-HQ 218 mg (1.5 mmol, 1 eq.). To this mixture was added 30 mL of toluene and the resulting yellow solution was refluxed for 2 hrs. After this time the reaction was allowed to cool before it was passed through a short silica plug rinsing with 60:40 PE:EtOAc 500 mL to yield a pale yellow solution. This solution was reduced *in vacuo* to yield a bright yellow solid which was dissolved in a minimal amount of DCM and precipitated with PE to give a yield of 250 mg (73 %) of a colourless solid.

^{1}H NMR (300 MHz, CDCl$_3$) δ 7.92 – 7.83 (m, 2H), 7.51 – 7.44 (m, 3H), 7.40 (dd, *J* = 15.4, 0.6 Hz, 1H), 7.32 (br s, 1H), 6.41 (d, *J* = 15.4 Hz, 1H), 4.26 (q, *J* = 7.1 Hz, 2H), 1.33 (t, *J* = 7.1 Hz, 3H). **^{13}C NMR** (75 MHz, CDCl$_3$) δ = 166.0, 149.8, 141.3, 132.9, 132.0, 130.0, 129.3, 122.8, 115.5, 108.8, 61.0, 14.4. **IR:** (ATR) 3033 (Ar-H), 2215 (nitrile), 1712 (C=O), 1626 (C=C) cm^{-1}.

ESI-MS C$_{14}$H$_{14}$NO$_2$ Calc. (M+H)$^+$ = 228.1019 found (M+H)$^+$ = 228.1011 (-3.43 ppm)

5.2.28 Synthesis of (2E,4Z)-ethyl 4-cyano-5-(4-(dimethylamino)phenyl)penta-2,4-dienoate (102)


To a round bottom was added *p*-NMe$_2$ α-cyano cinnamaldehyde 600 mg (3.0 mmol, 1 eq.), ethyl 2-(triphenylphosphoranylidene)acetate 1.15 g (3.3 mmol, 1.1 eq.) and 8-HQ 435 mg (3.0 mmol, 1 eq.). To this mixture was added 50 mL of toluene and the resulting yellow solution was refluxed for 2 hrs. After this time the reaction was allowed to cool before it was passed through a short silica plug rinsing with 60:40 PE:EtOAc 500 mL to yield a pale yellow solution. This solution was reduced *in vacuo* to yield a bright yellow solid which was dissolved in a minimal amount of DCM and precipitated with PE at − 20 ˚C to give a yield of 0.642 g (79 %) of a bright red solid.

^{1}H NMR (300 MHz, CDCl$_3$) δ 7.87 − 7.77 (m, 2H), 7.38 (dd, *J* = 15.4, 0.6 Hz, 1H), 7.14 (s, 1H), 6.74 − 6.65 (m, 2H), 6.23 (d, *J* = 15.4 Hz, 1H), 4.23 (q, *J* = 7.1 Hz, 2H), 3.08 (s, 6H), 1.32 (t, *J* = 7.1 Hz, 3H). **^{13}C NMR** (75 MHz, CDCl$_3$) δ = 166.8, 152.7, 150.2, 143.2, 132.6, 120.8, 118.6, 117.1, 111.8, 101.4, 60.6, 40.2, 14.4.

ESI-MS C$_{16}$H$_{19}$NO$_2$ Calc. (M+H)$^+$ = 271.1441 found (M+H)$^+$ = 271.1439 (-0.7 ppm)

5.2.29   Synthesis of (2E,4Z)-ethyl 4-cyano-5-(4-methoxyphenyl)penta-2,4-dienoate (103)
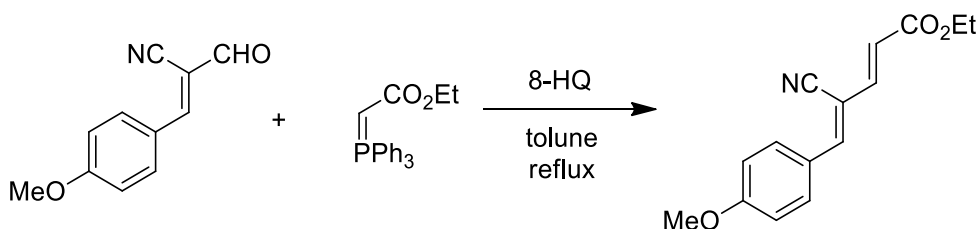
To a round bottom was added *p*-OMe α-cyano cinnamaldehyde 281 mg (1.5 mmol, 1 eq.), ethyl 2-(triphenylphosphoranylidene)acetate 575 mg (1.65 mmol, 1.1 eq.) and 8-HQ 218 mg (1.5 mmol, 1 eq.). To this mixture was added 30 mL of toluene and the resulting yellow solution was refluxed for 2 hrs. After this time the reaction was allowed to cool before it was passed through a short silica plug rinsing with 60:40 PE:EtOAc 500 mL to yield a pale yellow solution. This solution was reduced *in vacuo* to yield a bright yellow solid which was dissolved in a minimal amount of DCM and precipitated with PE to give a yield of 211 mg of a pale yellow solid (55 %).

1H NMR (300 MHz, CDCl$_3$) δ 7.87 (d, *J* = 8.9 Hz, 2H), 7.38 (d, *J* = 15.4 Hz, 1H), 7.24 (s, 1H), 6.96 (d, *J* = 8.9 Hz, 2H), 6.33 (d, *J* = 15.4 Hz, 1H), 4.24 (q, *J* = 7.1 Hz, 2H), 3.87 (s, 3H), 1.32 (t, *J* = 7.1 Hz, 3H). **13C NMR** (75 MHz, CDCl$_3$) δ = 166.4, 162.7, 149.5, 142.0, 132.3, 125.7, 121.2, 116.1, 114.8, 105.6, 60.9, 55.7, 14.4.

Mass: (APCI+) C$_{15}$H$_{16}$NO$_3$ Calc. (M+H)$^+$ = 258.1125 found (M+H)$^+$ = 258.1127 (1.0 ppm)

5.2.30 Synthesis of (2E,4Z)-ethyl 4-cyano-5-(thiophen-2-yl)penta-2,4-dienoate (104)
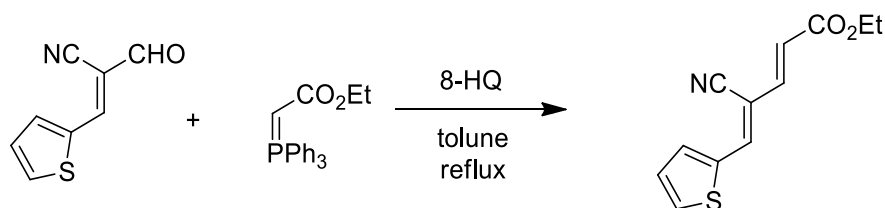
To a round bottom was added thiophenyl α-cyano cinnamaldehyde 217 mg (1.5 mmol, 1 eq.), ethyl 2-(triphenylphosphoranylidene)acetate 575 mg (1.65 mmol, 1.1 eq.) and 8-HQ 218 mg (1.5 mmol, 1 eq.). To this mixture was added 30 mL of toluene and the resulting yellow solution was refluxed for 2 hrs. After this time the reaction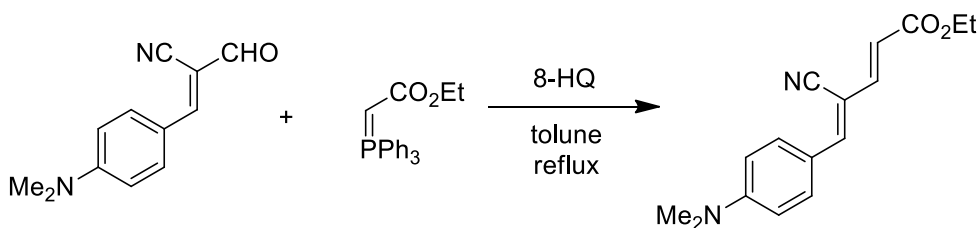 was allowed to cool before it was passed through a short silica plug rinsing with 60:40 PE:EtOAc 500 mL to yield a pale yellow solution. This solution was reduced *in vacuo* to yield a bright yellow solid which was dissolved in a minimal amount of DCM and precipitated with PE to give a yield of 157 mg of a bright yellow solid (49 %).

^{1}H NMR (300 MHz, CDCl$_3$) δ 7.73 – 7.60 (m, 2H), 7.44 (s, 1H), 7.35 (d, *J* = 15.4 Hz, 1H), 7.17 (dd, *J* = 5.0, 3.9 Hz, 1H), 6.35 (d, *J* = 15.4 Hz, 1H), 4.25 (q, *J* = 7.1 Hz, 2H), 1.32 (t, *J* = 7.1 Hz, 3H). **^{13}C NMR** (75 MHz, CDCl$_3$) δ = 166.2, 141.6, 140.8, 137.4, 134.6, 132.8, 128.5, 122.2, 115.7, 105.8, 61.0, 14.39.

IR: (ATR) 3045 (Ar-H), 2217 (nitrile), 1712 (C=O), 1624 (C=C) cm^{-1}.

Mass: (APCI+) C$_{12}$H$_{12}$NO$_2$S Calc. (M+H)$^+$ = 234.0583 found (M+H)$^+$ = 234.0587 (- 1.4 ppm)

5.2.31   Synthesis of 4-(phenylsulfonyl)but-2-enenitrile (109)
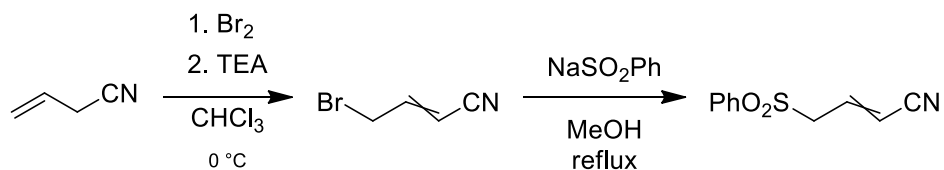
Allyl cyanide 1.6 mL (19.89 mmol, 1 eq.) was dissolved in 10 mL of $CHCl_3$ and cooled to 0° C. To this was added 1.2 mL of Br_2 (23.27 mmol, 1.2 eq.) dropwise, the resulting deep red solution was allowed to stir for 2 hrs whilst coming to rt. The solvent and excess Br_2 were removed *in vacuo* and the resulting pale yellow oil was suspended in 10 mL of $CHCl_3$. Triethylamine 5.5 mL (37.78 mmol, 2 eq.) was added dropwise (*caution - exothermic*). The resulting pale red suspension was diluted with 50 mL of H_2O and extracted 3 x 30 mL of DCM. The combined organics were dried over Na_2SO_4, filtered and reduced *in vacuo* to yield a dark brown oil. This brown oil was then diluted in 25 mL of MeOH. Benzenesulfinic acid sodium salt 6.53 g (39.78 mmol, 2 eq.) was then added and the resulting solution was refluxed at 80° C for 6 hrs. The solvent was reduced *in vacuo* to yield and black solid which was suspended in 30 mL H_2O and extracted 3 x 30 mL of DCM. The combined organics were dried over Na_2SO_4, filtered and reduced *in vacuo* to give a crude yield 1.171 g (28 %) of a foul smelling black oil. This crude material was used without further purification.

¹H NMR (300 MHz, CDCl₃) δ 7.94 – 7.84 (m, 4H), 7.78 – 7.68 (m, 2H), 7.66 – 7.54 (m, 4H), 6.63 – 6.49 (m, 2H), 5.61 (dt, *J* = 10.9, 0.9 Hz, 1H, *Z* isomer), 5.47 (dt, *J* = 16.3, 1.2 Hz, 1H, *E* isomer), 4.18 (dd, *J* = 7.9, 1.0 Hz, 2H, *Z* isomer), 3.98 (dd, *J* = 7.7, 1.2 Hz, 2H, *E* isomer).

5.2.32 Synthesis of (2Z,3E)-2-benzylidene-4-(phenylsulfonyl)but-3-enenitrile (105)
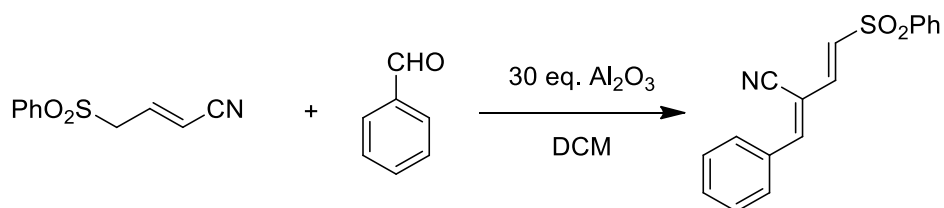
4-(phenylsulfonyl)but-2-enenitrile 2.06 g (9.94 mmol, 1.3 eq.) was dissolved in 100 mL of DCM. Dry basic aluminium oxide 23.38 g (229.32 mmol, 30 eq.) was added, followed by slow addition of benzaldehyde 0.78 mL (7.64 mmol, 1 eq.). The resulting dark brown suspension was stirred vigorously for 18 hr at rt. The reaction turned deep blue in colour overnight. The reaction mixture was filtered through a pad of celite and rinsed with 500 mL of DCM to yield a pale yellow filtrate. The filtrate was reduced *in vacuo* to yield and pale yellow solid which was dissolved in a minimal amount of hot DCM and precipitated with PE. The precipitate was collected by vacuum filtration, washed with cold PE and air dried to yield 0.914 g (41 %) of a fine yellow solid.

^{1}H NMR (300 MHz, CDCl$_3$) δ 7.97 – 7.90 (m, 2H), 7.90 – 7.83 (m, 2H), 7.72 – 7.62 (m, 1H), 7.62 – 7.52 (m, 2H), 7.51 – 7.39 (m, 5H), 6.85 (d, *J* = 14.9 Hz, 1H). **^{13}C NMR** (75 MHz, CDCl$_3$) δ = 152.2, 139.9, 139.1, 134.0, 132.7, 132.3, 131.3, 130.3, 129.6, 129.4, 127.9, 115.2, 106.5. **IR:** (ATR) 3048 (Ar-H), 2228 (nitrile), 1595 (C=C) cm^{-1}.

ESI-MS C$_{17}$H$_{14}$NO$_2$S Calc. (M+H)$^+$ = 296.074 found (M+H)$^+$ = 296.075 (+3.52 ppm)

m.p: 173 – 175 ˚C

5.2.33 Synthesis of (2Z,3E)-2-(4-fluorobenzylidene)-4-(phenylsulfonyl)but-3-enenitrile (110)
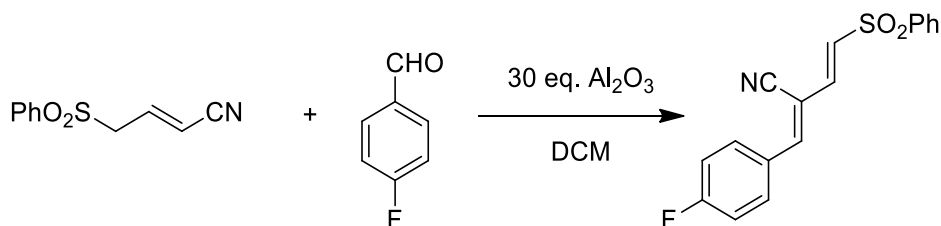
4-(phenylsulfonyl)but-2-enenitrile 2.578 g (12.44 mmol, 1.3 eq.) and *p*-fluorobenzaldehyde 1.03 mL (9.57 mmol, 1 eq.) were dissolved in 100 mL of DCM. To this solution was added aluminium oxide (basic, dried overnight at 200 ˚C) 29.27 g (287.1 mmol, 30 eq.) and the reaction stirred at rt overnight. The reaction mixture turned dark blue overnight. The reaction mixture was filtered through a pad of celite and rinsed with 500 mL of DCM to yield a pale yellow filtrate. The filtrate was reduced *in vacuo* to yield a yellow solid which was dissolved in a minimal amount of hot DCM and precipitated with PE. The precipitate was collected by vacuum filtration washed with cold PE and air dried to yield to yield 1.13 g (38 %) of a cream solid.

¹H NMR (300 MHz, CDCl₃) δ 7.98 – 7.83 (m, 4H), 7.71 – 7.63 (m, 1H), 7.63 – 7.53 (m, 2H), 7.43 (dd, *J* = 14.8, 0.5 Hz, 1H), 7.39 (s, 1H), 7.22 – 7.12 (m, 2H), 6.84 (d, *J* = 14.8 Hz, 1H). **¹³C NMR** (75 MHz, CDCl₃) δ = 166.75, 163.35, 150.54, 139.92, 138.90, 134.05, 132.77, 132.65, 131.53, 129.68, 128.80, 128.75, 127.98, 117.02, 116.72, 115.13, 106.30, 106.26. **¹⁹F NMR** (282 MHz, CDCl₃) δ = -104.02. **IR:** (ATR) 3083 (Ar-H), 2227 (nitrile), 1591 (C=C).

ESI-MS $C_{17}H_{13}FNO_2S$ Calc. (M+H)⁺ = 314.0646 found (M+H)⁺ = 314.0651 (1.66 ppm)

m.p: 188 – 191 ˚C (DCM/PE)

5.2.34 Synthesis of (2Z,3E)-2-(4-nitrobenzylidene)-4-(phenylsulfonyl)but-3-enenitrile (111)
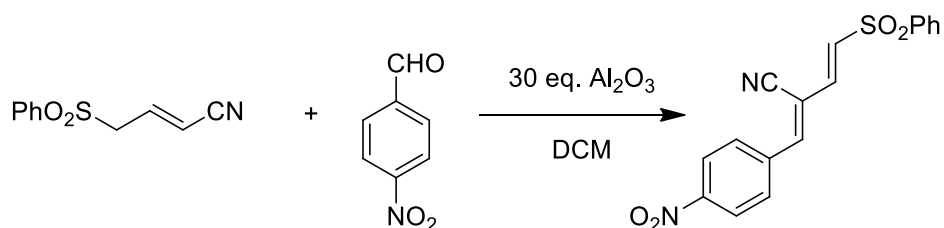
4-(phenylsulfonyl)but-2-enenitrile 1.679 g (8.10 mmol, 1.3 eq.) and *p*-nitrobenzaldehyde 0.941 g (6.23 mmol, 1 eq.) were dissolved in 100 mL of DCM. To this solution was added dry basic aluminium oxide 19.04 g (186.74 mmol, 30 eq.) and the reaction stirred at rt overnight. The dark brown reaction mixture turned dark blue overnight. The reaction mixture was filtered through a pad of celite and rinsed with 500 mL of DCM to yield a pale yellow filtrate. The filtrate was reduced *in vacuo* to yield a yellow solid which was dissolved in a minimal amount of hot DCM and precipitated with PE. The precipitate was collected by vacuum filtration, washed with cold PE and air dried to yield 0.721 g (38 %) of a yellow crystalline solid.

^{1}H NMR (300 MHz, CDCl$_3$) δ 8.37 – 8.28 (m, 2H), 8.06 – 7.98 (m, 2H), 7.98 – 7.90 (m, 2H), 7.74 – 7.64 (m, 1H), 7.64 – 7.56 (m, 2H), 7.50 (s, 1H), 7.46 (d, *J* = 14.9 Hz, 1H), 6.96 (d, *J* = 14.9 Hz, 1H). **^{13}C NMR** (75 MHz, CDCl$_3$) δ = 149.37, 148.46, 139.43, 137.91, 137.64, 134.34, 134.15, 130.84, 129.80, 128.12, 124.52, 114.37, 110.87. **IR:** (ATR) 3056 (Ar-H), 2223 (nitrile), 1518 (C=C), 1342 (NO$_2$), 1308 (NO$_2$) cm^{-1}.

ESI-MS C$_{17}$H$_{13}$N$_2$O$_4$S Calc. (M+H)$^+$ = 341.0591 found (M+H)$^+$ = 341.0601 (+3.02 ppm)

m.p: 154 – 158 ˚C (DCM/PE)

5.2.35   Synthesis of (Z)-(2-bromo-3,3-diethoxyprop-1-en-1-yl)benzene (114)
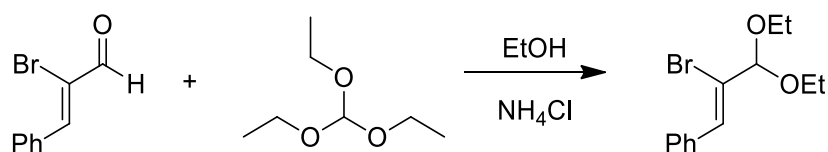
To a round bottom containing α-bromocinnamaldehyde 5.00 g (23.7 mmol, 1 eq.) was added ammonium chloride 0.1 g (1.8 mmol), triethylorthoformate 5.5 mL (33.1 mmol, 1.4 eq.) and 20 mL of EtOH. The resulting solution was refluxed at 100 ˚C for 1 hr. The reflux apparatus was then converted to a distillation apparatus and the lower boiling constituents were removed up to 170˚ C at atmospheric pressure. The resulting brown oil was diluted with 30 mL of H_2O and then extracted with 2 x 30 mL of DCM. The combined organics were then dried over Na_2SO_4, filtered and reduced in vacuo to yield 6.60 g (98 %) of a clear pale yellow oil.

¹H NMR (300 MHz, $CDCl_3$) δ 7.73 – 7.62 (m, 2H), 7.41 – 7.23 (m, 4H), 4.96 (d, *J* = 0.7 Hz, 1H), 3.69 (dq, *J* = 9.4, 7.1 Hz, 2H), 3.58 (dq, *J* = 9.4, 7.0 Hz, 2H), 1.27 (t, *J* = 7.1 Hz, 6H). **¹³C NMR** (75 MHz, $CDCl_3$) δ = 134.71, 129.91, 129.27, 128.38, 128.14, 122.74, 103.12, 61.91, 15.13.

Matches literature data.[139]

5.2.36 Synthesis of (Z)-2-bromo-3-phenylacrylaldehyde (115)
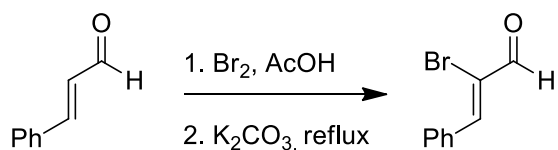
To a three-necked round bottomed flask was added 18.9 mL of cinnamaldehyde (0.15 mol) and AcOH 83.5 mL (1.46 mol, 9.7 eq.). The solution was cooled on ice and via Br_2 7.7 mL (0.15 mol) dropwise via dropping funnel. After the addition of Br_2 was complete the reaction was stirred for a further 15 mins. K_2CO_3 10.37 g (0.075 mol, 0.5 eq) was added in small portions whilst the reaction mixture was kept cold with ice. Note: Gas is evolved during the addition of the K_2CO_3. The reaction mixture was then refluxed at 120 ˚C for 30 mins and the resulting clear yellow solution was allowed to cool before being poured into a 500 mL round bottomed flask containing 220 mL of distilled H_2O. The flask was stoppered and the solution shaken vigorously until precipitation ceased. The yellow granular solid was filtered and then dissolved in 90 mL of hot EtOH, 25 mL of distilled H_2O was added, the solution became slightly opaque so it was heated until clear again before being allowed to slowly cool to rt. The resulting pale yellow solid was filtered to yield the product 24.21 g (76 %).

1H NMR (300 MHz, $CDCl_3$) δ 9.34 (s, 1H), 8.08 – 7.94 (m, 2H), 7.90 (s, 1H), 7.54 – 7.40 (m, 3H).
13C NMR (75 MHz, $CDCl_3$) δ = 187.17, 149.33, 132.99, 131.69, 131.04, 128.86, 124.33.

m.p – 68-70 ˚C (EtOH/H_2O)

Matches literature data.[140]

5.2.37 Synthesis of 2-(triphenylphosphoranylidene)acetaldehyde (120)
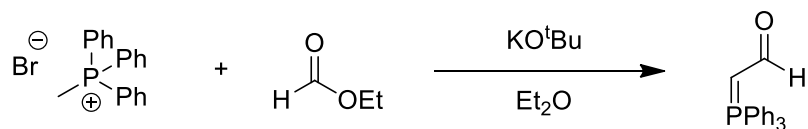
To a suspension of methyl triphenylphosphonium bromide 7.14 g (20 mmol, 1eq.) in dry DCM 50 mL was added KO^{t}Bu (24 mmol, 1.2 eq.) and the resulting bright yellow solution was stirred at rt for 1.5 hrs under a balloon of N_2.After this time the reaction mixture was transferred dropwise *via* a cannula to a separate round bottom flask containing ethyl formate 2.25 mL in dry DCM 15 mL. The reaction mixture turned cloudy white upon completion of this addition. The reaction mixture was stirred at rt for a further 1 hr after which time 0.1 M HCl 100 mL, followed by 1 M HCl 12 mL. The aqueous layer was collected with the aid of a separating funnel, the organic layer was further extracted with an additional 0.1 M HCl 3 x 20 mL. The combined aqueous layers were basified with 2 M NaOH to produce a cloudy white precipitate. 2 M NaOH was added until precipitation ceased. The resulting suspension was allowed to stand overnight before being filtered and washed with H_2O 5 mL and then Et_2O 5 mL to yield 4.19 g (69 %) of a cream solid.

^{1}H NMR (300 MHz, CDCl$_3$) δ 8.97 (dd, *J* = 38.2, 3.5 Hz, 1H$_{trans}$), 8.24 (dd, *J* = 10.8, 3.5 Hz, 1H$_{cis}$), 7.77 – 7.37 (m, 30H), 4.06 (dd, *J* = 19.3, 10.8 Hz, 1H$_{trans}$), 3.65 (dd, *J* = 24.6, 3.5 Hz, 1H$_{cis}$).

^{13}C NMR (126 MHz, CDCl$_3$) δ 181.7 (apparent t, overlapping doublets, *J* = 9.0 Hz), 133.3 (d, *J* = 10.2 Hz), 133.1 (d, *J* = 10.4 Hz), 132.9 (d, *J* = 2.9 Hz), 132.4 (d, *J* = 2.9 Hz), 129.2 (d, *J* = 12.3 Hz), 129.0 (d, *J* = 12.4 Hz), 126.5 (d, *J* = 90.3 Hz), 126.1 (d, *J* = 90.1 Hz), 56.6 (d, *J* = 110.3 Hz), 54.9 (d, *J* = 99.9 Hz).

^{31}P NMR (121 MHz, CDCl$_3$) δ 18.9, 14.9.

Matches literature data.[99]

5.2.38   Synthesis of (2Z,3E)-2-benzylidene-5-oxopent-3-enenitrile (119)
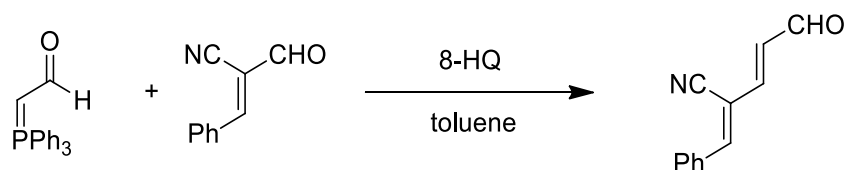
To a round bottom was added α-cyano cinnamaldehyde 157 mg (1.0 mmol, 1 eq.), 2-(triphenylphosphoranylidene)acetaldehyde 304 mg (1.0 mmol, 1.1 eq.) and 8-HQ 145 mg (1.0 mmol, 1 eq.). To this mixture was added 20 mL of toluene and the resulting yellow solution was refluxed for 2 hrs. After this time the reaction was allowed to cool before it was passed through a short silica plug rinsing with 60:40 PE:EtOAc 500 mL to yield a pale yellow solution. This solution was reduced *in vacuo* to yield a yellow orange solid which was dissolved in a minimal amount of DCM and precipitated with PE to give a yield of 66 mg (36 %) of a yellow solid.

^{1}H NMR (300 MHz, CDCl$_3$) δ 9.72 (d, *J* = 7.1 Hz, 1H), 7.97 – 7.88 (m, 2H), 7.57 – 7.45 (m, 3H), 7.43 (s, 1H), 7.22 (dd, *J* = 15.4, 0.6 Hz, 1H), 6.67 (dd, *J* = 15.4, 7.1 Hz, 1H). **^{13}C NMR** (75 MHz, CDCl$_3$) δ 191.9, 151.2, 147.8, 132.7, 132.7, 131.7, 130.4, 129.5, 115.2, 108.9. **IR:** (ATR) 3065 (Ar-H), 2222 (nitrile), 1669 (C=O), 1588 (C=C) cm^{-1}.

ESI-MS: C$_{12}$H$_{10}$NO Calc. (M+H)$^+$ = 184.0757 found (M+H)$^+$ = 184.0748 (-4.65 ppm)

5.2.39   Synthesis of (4E,6Z)-6-benzylidenehepta-2,4-dienedinitrile (118)
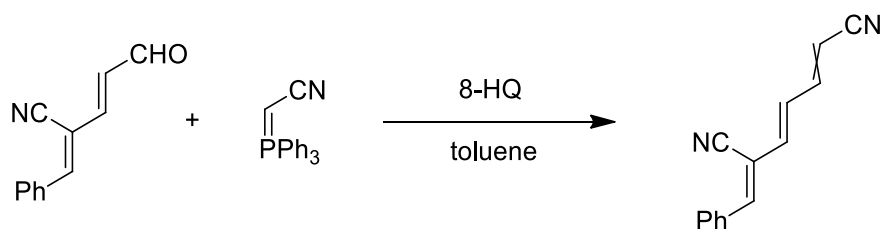
To a round bottom was added (2Z,3E)-2-benzylidene-5-oxopent-3-enenitrile 56 mg (0.30 mmol, 1 eq.), 2-(triphenylphosphoranylidene)acetonitrile 92 mg (0.3 mmol, 1 eq.) and 8-HQ 44 mg (1 mmol, 1 eq.). To this mixture was added 5 mL of toluene and the resulting yellow solution was refluxed for 2 hrs. After this time the reaction was allowed to cool before it was passed through a short silica plug rinsing with 60:40 PE:EtOAc 500 mL to yield a pale yellow solution. This solution was reduced *in vacuo* to yield a yellow oil which was dissolved in a minimal amount of DCM and precipitated with PE to give a yield of 19 mg (31 %) of a yellow solid

^{1}H NMR (300 MHz, CDCl$_3$) δ 7.92 – 7.79 (m, 4H), 7.48 (m, 6H), 7.26 (s, 1H), 7.16 – 7.02 (m, 2H), 6.95 – 6.60 (m, 5H), 5.54 (d, *J* = 15.8 Hz, 1H), 5.37 (d, *J* = 10.7 Hz, 1H).

^{13}C NMR (75 MHz, CDCl$_3$) δ = 148.3, 147.7, 147.6, 147.0, 138.1, 137.6, 133.2, 133.1, 131.8, 131.8, 129.9, 129.9, 129.8, 129.3, 129.3, 128.2, 117.9, 115.7, 109.9, 109.7, 101.3, 99.6.

E,E,Z:Z,E,E 1:0.5

IR: (ATR) 3060 (Ar-H), 2219 (nitrile), 1600 (C=C) cm^{-1}.

ESI-MS C$_{14}$H$_{11}$N$_2$ Calc. (M+H)$^+$ = 207.0917 found (M+H)$^+$ = 207.0920 (1.34 ppm)

5.3   Chapter 3

5.3.1   Synthesis of 6-butyl-1,6-dihydro-[1,1'-biphenyl]-2,4-dicarbonitrile (124)
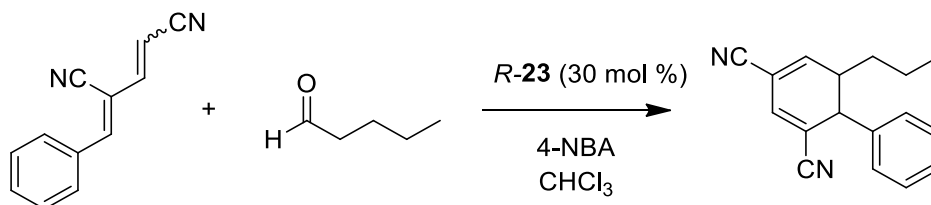
To a vial containing *R*-**23** 54.7 mg (0.17 mmol, 30 mol %) was added $CHCl_3$ 1.5 mL, 4-NBA 28.1 mg (0.17 mmol, 30 mol %) and valeraldehyde 66 μL (0.62 mmol, 1.1 eq.). The resulting solution was stirred at rt for 15 mins after which time bis-cyano butadiene **41** 100.0 mg (0.56 mmol, 1 eq., 0.7:1 *E,Z:Z,Z*) was added and the resulting solution was stirred at rt for 24 hrs. The resulting solution was passed through a short silica plug rinsing with 20 mL of Et_2O. To the filtrate was a small amount of silica gel and the solvent was reduced *in vacuo*. The resulting material was then dry loaded to the top of a silica column and purified by flash chromatography (98:2 PE:EtOAc). The fractions of interest were combined and reduced *in vacuo* to yield 83.7 mg (60 %) of a colourless oil.

¹H NMR (500 MHz, $CDCl_3$) δ 7.39 – 7.29 (m, 3H), 7.17 (m, 2H), 6.86 (m, 1H), 6.76 (br s, 1H), 3.54 (d, *J* = 5.5 Hz, 1H), 2.86 – 2.74 (m, 1H), 1.61 – 1.38 (m, 4H), 0.94 (t, *J* = 7.1 Hz, 3H).

¹³C NMR (126 MHz, $CDCl_3$) δ 150.1, 139.1, 132.7, 129.4, 128.5, 127.3, 117.5, 116.4, 114.6, 109.0, 44.5, 42.1, 35.5, 19.4, 13.9.

ESI-MS: $C_{17}H_{17}N_2$ Calc. $(M+H)^+$ = 249.1386 found $(M+H)^+$ = 249.1390 (1.64 ppm)

Matches literature data.[69]

5.3.2   Synthesis of 6-propyl-[1,1'-biphenyl]-2,4-dicarbonitrile (125)
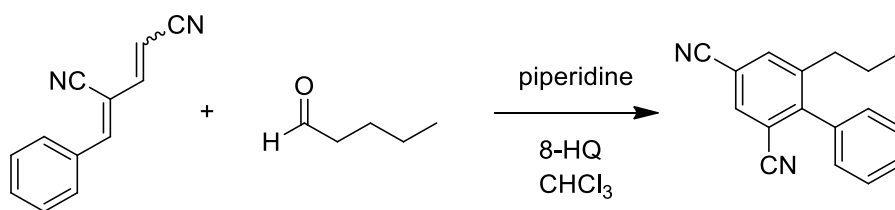
To a 10 mL vial was added bis-cyano diene **41** 100 mg (0.56 mmol, 1 eq., *Z,E:Z,Z,* 1:0.8), valeraldehyde 64.9 μL (0.61 mmol, 1.1 eq.), 8-HQ 81.2mg (0.56 mmol, 1 eq.) and CHCl$_3$ (3 mL). To the resulting pale yellow solution was added piperidine 55.3 μL (0.56 mmol, 1 eq.) and the reaction was stirred at rt for 16 hrs generating a pale red solution. The product was purified by column chromatography. A small amount of silica gel was added and the solvent removed *in vacuo* (at 30˚C) and dry loaded to the top of a silica column in 100 % PE. Upon loading a solvent system of 95:5 PE:Et$_2$O was employed until product elution. Column chromatography yielded 76.3 mg (55 %) of a pale yellow oil, which solidified on standing.

^{1}H NMR (500 MHz, CDCl$_3$) δ 7.85 (d, *J* = 1.6 Hz, 1H), 7.77 (d, *J* = 1.6 Hz, 1H), 7.54 – 7.47 (m, 3H), 7.28 – 7.22 (m, 2H), 2.55 – 2.45 (m, 2H), 1.51 – 1.42 (m, 2H), 0.81 (t, *J* = 7.3 Hz, 3H). **^{13}C NMR** (126 MHz, CDCl$_3$) δ = 149.7, 144.3, 136.5, 135.9, 133.5, 129.4, 129.0, 128.7, 117.1, 116.5, 115.4, 112.7, 35.1, 23.9, 13.8. **IR:** (KBr Disc) 3061 (Ar-H), 2235 (Nitrile), 1456-1453 (CH$_2$CH$_2$CH$_3$) cm^{-1}.

ESI-MS: C$_{17}$H$_{15}$N$_2$ Calc. (M+H)$^+$ = 247.1230 found (M+H)$^+$ = 247.1228 (-0.64 ppm)

R$_f$: 0.17 (90:10 PE:Et$_2$O)

5.3.3   Synthesis of 6-methyl-[1,1'-biphenyl]-2,4-dicarbonitrile (136)
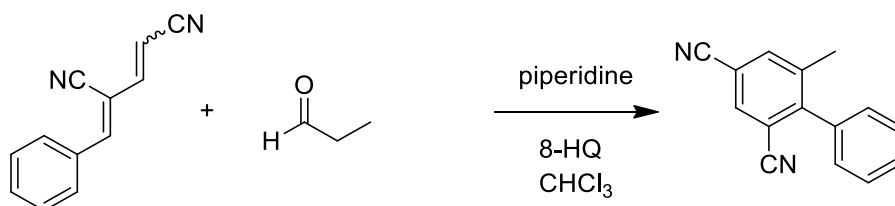
To a 10 mL vial was added bis-cyano diene **41** 100 mg (0.56 mmol, 1 eq., *Z,E:Z,Z,* 1:0.8), propionaldehyde 44.0 µL (0.61 mmol, 1.1 eq.), 8-HQ 81.2 mg (0.56 mmol, 1 eq.) and CHCl$_3$ (3 mL). To the resulting pale yellow solution was added piperidine 55.3 µL (0.56 mmol, 1 eq.) and the reaction was stirred at rt for 16 hrs generating a pale red solution. The product was purified by column chromatography. A small amount of silica gel was added and the solvent removed *in vacuo* (at 30˚C) and dry loaded to the top of a silica column in 100 % PE. Upon loading a solvent system of 95:5 PE:Et$_2$O was employed until product elution. Column chromatography yielded 60.4 mg (49%) of a yellow solid.

^{1}H NMR (500 MHz, CDCl$_3$) δ 7.87 (s, 1H), 7.77 (s, 1H), 7.56 – 7.46 (m, 3H), 7.31 – 7.21 (m, 2H), 2.24 (s, 3H). **^{13}C NMR** (126 MHz, CDCl$_3$) δ = 149.9, 139.8, 137.2, 136.0, 133.8, 129.5, 129.1, 128.6, 117.0, 116.5, 115.0, 112.5, 20.7. **IR:** (NaCl plate) 3062 (Ar-H), 2239 (Nitrile), 1469 (CH$_3$) cm^{-1}.

ESI-MS: C$_{15}$H$_{10}$N$_2$ Calc. (M+H)$^+$ = 219.0917 found (M+H)$^+$ = 219.0912 (-2.12 ppm)

R$_f$: 0.12 (90:10 PE:Et$_2$O)

5.3.4   Synthesis of 6-ethyl-[1,1'-biphenyl]-2,4-dicarbonitrile (137)

To a 10 mL vial was added bis-cyano diene **41** 100 mg (0.56 mmol, 1 eq., *Z,E:Z,Z,* 1:0.8), butyraldehyde 55.0 µL (0.61 mmol, 1.1 eq.), 8-HQ 81.2 mg (0.56 mmol, 1 eq.) and CHCl$_3$ (3 mL). To the resulting pale yellow solution was added piperidine 55.3 µL (0.56 mmol, 1 eq.) and the reaction was stirred at rt for 16 hrs generating a pale red solution. The product was purified by column chromatography. A small amount of silica gel was added and the solvent removed *in vacuo* (at 30˚C) and dry loaded to the top of a silica column in 100 % PE. Upon loading a solvent system of 95:5 PE:Et$_2$O was employed until product elution. Column chromatography yielded 67.3 mg (52 %) of a yellow solid.

^{1}H NMR (500 MHz, CDCl$_3$) δ 7.86 (d, *J* = 1.5 Hz, 1H), 7.79 (d, *J* = 1.3 Hz, 1H), 7.57 − 7.46 (m, 3H), 7.30 − 7.21 (m, 2H), 2.55 (q, *J* = 7.6 Hz, 2H), 1.10 (t, *J* = 7.6 Hz, 3H). **^{13}C NMR** (126 MHz, CDCl$_3$) δ = 149.6, 145.8, 135.9, 133.5, 129.4, 129.0, 128.6, 117.1, 116.5, 115.3, 112.9, 26.5, 14.9. **IR:** (NaCl plate) 3063 (Ar-H), 2237 (Nitrile), 1456 (CH$_3$) cm^{-1}.

ESI-MS: C$_{16}$H$_{12}$N$_2$ Calc. (M+H)$^+$ = 233.1073 found (M+H)$^+$ = 233.1071 (-0.77 ppm)

R$_f$: 0.15 (90:10 PE:Et$_2$O)

### 5.3.5   Synthesis of 6-isopropyl-[1,1'-biphenyl]-2,4-dicarbonitrile (138)
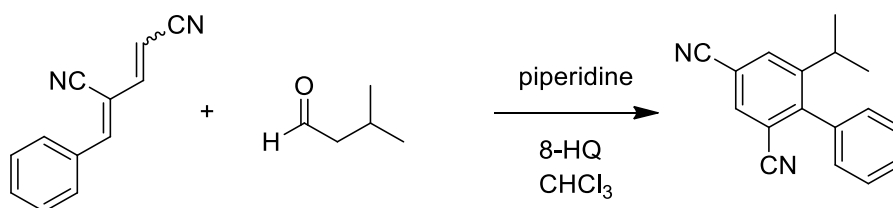
To a 10 mL vial was added bis-cyano diene **41** 100 mg (0.56 mmol, 1 eq., *Z,E:Z,Z,* 1:0.8), isovaleraldehyde 65.4 µL (0.61 mmol, 1.1 eq.), 8-HQ 81.2 mg (0.56 mmol, 1 eq.) and CHCl$_3$ (3 mL). To the resulting pale yellow solution was added piperidine 55.3 µL (0.56 mmol, 1 eq.) and the reaction was stirred at rt for 16 hrs generating a pale red solution. The product was purified by column chromatography. A small amount of silica gel was added and the solvent removed *in vacuo* (at 30˚C) and dry loaded to the top of a silica column in 100 % PE. Upon loading a solvent system of 95:5 PE:Et$_2$O was employed until product elution. Column chromatography yielded 62.6 mg (45 %) of a clear colourless oil, which solidified on standing.

^{1}H NMR (500 MHz, CDCl$_3$) δ 7.85 (d, *J* = 1.6 Hz, 1H), 7.84 (d, *J* = 1.6 Hz, 1H), 7.55 − 7.48 (m, 3H), 7.26 − 7.23 (m, 2H), 2.99 − 2.90 (m, 1H), 1.15 (s, 3H), 1.14 (s, 3H). **^{13}C NMR** (126 MHz, CDCl$_3$) δ = 150.6, 148.9, 135.9, 133.7, 133.2, 129.4, 129.0, 128.7, 117.3, 116.5, 115.3, 113.1, 30.2, 23.8. **IR:** (NaCl plate) 3063 (Ar-H), 2239 (Nitrile), 1465 (CH$_3$) cm^{-1}.

ESI-MS: C$_{17}$H$_{15}$N$_2$ Calc. (M+H)$^+$ = 247.1230 found (M+H)$^+$ = 247.1241 (4.65 ppm)

R$_f$: 0.17 (90:10 PE:Et$_2$O)

5.3.6   Synthesis of 6-butyl-[1,1'-biphenyl]-2,4-dicarbonitrile (139)
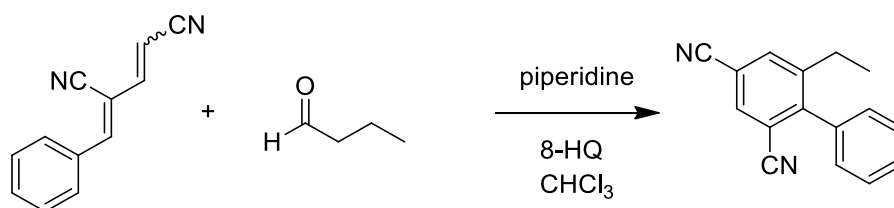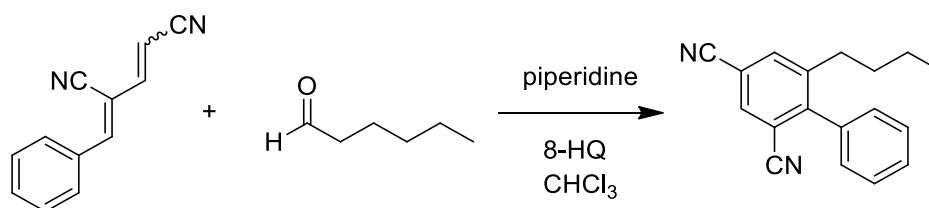

To a 10 mL vial was added bis-cyano diene **41** 100 mg (0.56 mmol, 1 eq., *Z,E:Z,Z,* 1:0.8), hexanal 75.0 μL (0.61 mmol, 1.1 eq.), 8-HQ 81.2 mg (0.56 mmol, 1 eq.) and $CHCl_3$ (3 mL). To the resulting pale yellow solution was added piperidine 55.3 μL (0.56 mmol, 1 eq.) and the reaction was stirred at rt for 16 hrs generating a pale red solution. The product was purified by column chromatography. A small amount of silica gel was added and the solvent removed *in vacuo* (at 30˚C) and dry loaded to the top of a silica column in 100 % PE. Upon loading a solvent system of 95:5 PE:Et_2O was employed until product elution. Column chromatography yielded 77.6 mg (53 %) of a pale yellow oil.

^{1}H NMR (500 MHz, $CDCl_3$) δ 7.85 (d, *J* = 1.6 Hz, 1H), 7.77 (d, *J* = 1.5 Hz, 1H), 7.56 − 7.46 (m, 3H), 7.28 − 7.23 (m, 2H), 2.62 − 2.41 (m, 2H), 1.46 − 1.36 (m, 2H), 1.22 − 1.14 (m, 2H), 0.78 (t, *J* = 7.3 Hz, 3H).

^{13}C NMR (126 MHz, $CDCl_3$) δ = 149.7, 144.6, 136.5, 135.9, 133.5, 129.4, 129.0, 128.7, 117.1, 116.5, 115.3, 112.7, 32.9, 32.8, 22.4, 13.7.

IR: (KBr disc) 3062 (Ar-H), 2234 (Nitrile), 1465-1443 ($CH_2CH_2CH_2CH_3$) cm^{-1}.

ESI-MS: $C_{18}H_{17}N_2$ Calc. $(M+H)^+$ = 261.1386 found $(M+H)^+$ = 261.1389 (0.98 ppm)

R_f: 0.19 (90:10 PE:Et_2O)

5.3.7   Synthesis of ethyl 2-cyano-6-methyl-[1,1'-biphenyl]-4-carboxylate (140)
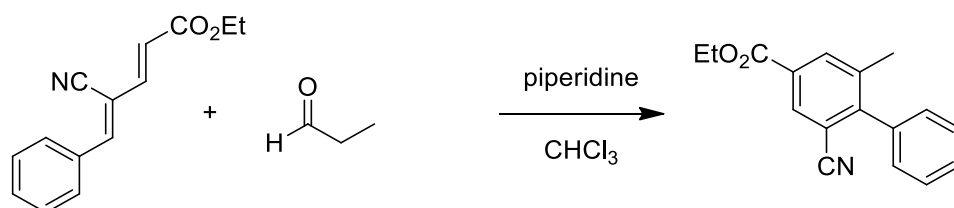
To a 10 mL vial was added cyano-ester diene **96** 100 mg (0.44 mmol, 1 eq.), propionaldehyde 35.0 µL (0.48 mmol, 1.1 eq.) and CHCl$_3$ (3 mL). To the resulting pale yellow solution was added piperidine 43.5 µL (0.44 mmol, 1 eq.) and the reaction was stirred at rt for 16 hrs. The product was purified by column chromatography. A small amount of silica gel was added and the solvent removed *in vacuo* (at 30˚C) and dry loaded to the top of a silica column in 100 % PE. Upon loading a solvent system of 95:5 PE:Et$_2$O was employed until product elution. Column chromatography yielded 53.8 mg (46 %) of a white solid.

^{1}H NMR (500 MHz, CDCl$_3$) δ 8.24 (s, 1H), 8.15 (s, 1H), 7.54 – 7.43 (m, 3H), 7.31 – 7.27 (m, 2H), 4.43 (q, *J* = 7.1 Hz, 2H), 2.24 (s, 3H), 1.43 (t, *J* = 7.1 Hz, 3H). **^{13}C NMR** (126 MHz, CDCl$_3$) δ = 165.0, 149.4, 138.3, 137.0, 135.2, 131.8, 130.3, 129.0, 128.9, 128.8, 117.8, 113.9, 61.8, 20.7, 14.4. **IR:** (KBr disc) 3058 (Ar-H), 2230 (Nitrile), 1711 (C=O), 1445 (CH$_3$) cm^{-1}.

ESI-MS: C$_{17}$H$_{16}$NO$_2$ Calc. (M+H)$^+$ = 266.1176 found (M+H)$^+$ = 266.1165 (-3.99 ppm)

R$_f$: 90:10 PE:EtOAc = 0.43

5.3.8   Synthesis of ethyl 2-cyano-6-ethyl-[1,1'-biphenyl]-4-carboxylate (141)

To a 10 mL vial was added cyano-ester diene **96** 100 mg (0.44 mmol, 1 eq.), butyraldehyde 43.6 μL (0.48 mmol, 1.1 eq.) and $CHCl_3$ (3 mL). To the resulting pale yellow solution was added piperidine 43.5 μL (0.44 mmol, 1 eq.) and the reaction was stirred at rt for 16 hrs. The product was purified by column chromatography. A small amount of silica gel was added and the solvent removed *in vacuo* (at 30˚C) and dry loaded to the top of a silica column in 100 % PE. Upon loading a solvent system of 95:5 PE:Et$_2$O was employed until product elution. Column chromatography yielded 60.7 mg (49 %) of a colourless oil.

1H NMR (500 MHz, CDCl$_3$) δ 8.24 (d, *J* = 1.7 Hz, 1H), 8.18 (d, *J* = 1.7 Hz, 1H), 7.53 − 7.44 (m, 3H), 7.30 − 7.26 (m, 2H), 4.44 (q, *J* = 7.1 Hz, 2H), 2.55 (q, *J* = 7.6 Hz, 2H), 1.43 (t, *J* = 7.1 Hz, 3H), 1.09 (t, *J* = 7.6 Hz, 3H). **13C NMR** (126 MHz, CDCl$_3$) δ = 165.0, 149.0, 144.4, 136.8, 133.8, 131.5, 130.6, 128.9, 128.9, 128.8, 117.8, 114.1, 61.8, 26.6, 15.3, 14.5. **IR:** (ATR) 3069 (Ar-H), 2231 (Nitrile), 1720 (C=O), 1445 (CH$_3$) cm^{-1}.

ESI-MS: $C_{18}H_{17}NO_2$ Calc. $(M+H)^+$ = 280.1332 found $(M+H)^+$ = 280.1323 (-3.25 ppm)

R$_f$: 90:10 PE:EtOAc = 0.34

5.3.9   Synthesis of ethyl 2-cyano-6-isopropyl-[1,1'-biphenyl]-4-carboxylate (142)
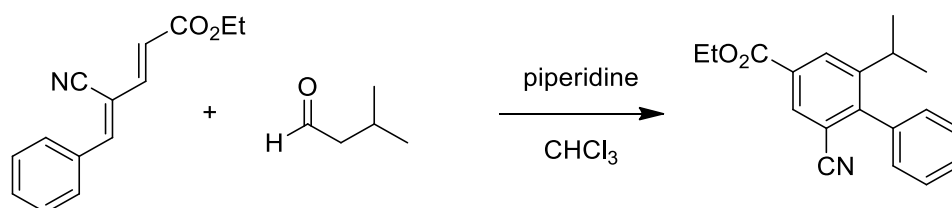
To a 10 mL vial was added cyano-ester diene **96** 100 mg (0.44 mmol, 1 eq.), isovaleraldehyde 51.5 µL (0.48 mmol, 1.1 eq.) and $CHCl_3$ (3 mL). To the resulting pale yellow solution was added piperidine 43.5 µL (0.44 mmol, 1 eq.) and the reaction was stirred at rt for 16 hrs. The product was purified by column chromatography. A small amount of silica gel was added and the solvent removed *in vacuo* (at 30˚C) and dry loaded to the top of a silica column in 100 % PE. Upon loading a solvent system of 95:5 PE:Et$_2$O was employed until product elution. Column chromatography yielded 45.3 mg (35 %) of a white solid.

^{1}H NMR (500 MHz, CDCl$_3$) δ 8.26 (d, *J* = 1.7 Hz, 1H), 8.22 (d, *J* = 1.7 Hz, 1H), 7.54 − 7.45 (m, 3H), 7.29 − 7.23 (m, 2H), 4.44 (q, *J* = 7.1 Hz, 2H), 2.93 (sept, 1H, *J* = 6.9 Hz), 1.44 (t, *J* = 7.1 Hz, 3H), 1.16 (d, *J* = 6.9 Hz, 6H). **^{13}C NMR** (126 MHz, CDCl$_3$) δ = 165.1, 149.2, 148.4, 136.9, 131.3, 130.8, 128.9, 128.9, 128.8, 117.8, 114.0, 61.8, 30.1, 23.9, 14.5. **IR:** (KBr disc) 3073 (Ar-H), 2233 (Nitrile), 1712 (C=O), 1464 (CH$_3$) cm^{-1}.

ESI-MS: $C_{19}H_{20}NO_2$ Calc. (M+H)$^+$ = 294.1489 found (M+H)$^+$ = 294.1474 (-4.9 ppm)

R$_f$ 90:10 PE:EtOAc = 0.49

5.3.10 Synthesis of ethyl 2-cyano-6-propyl-[1,1'-biphenyl]-4-carboxylate (143)
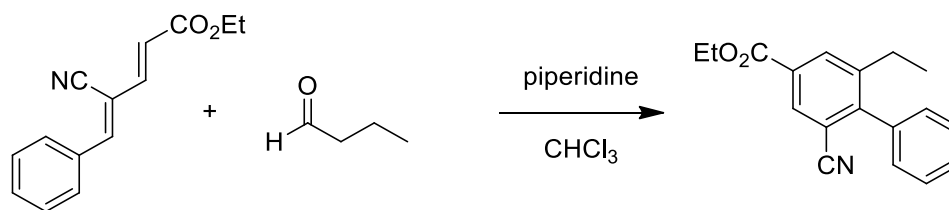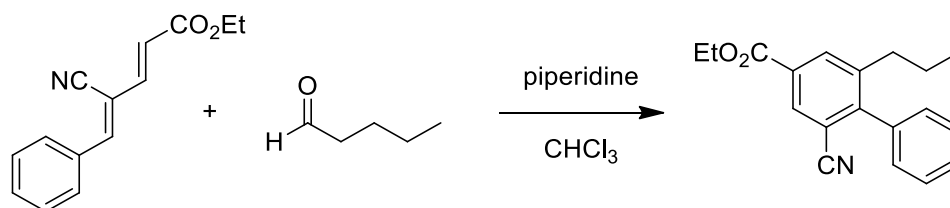

To a 10 mL vial was added cyano-ester diene **96** 100 mg (0.44 mmol, 1 eq.), valeraldehyde 51.0 μL (0.48 mmol, 1.1 eq.) and $CHCl_3$ (3 mL). To the resulting pale yellow solution was added piperidine 43.5 μL (0.44 mmol, 1 eq.) and the reaction was stirred at rt for 16 hrs. The product was purified by column chromatography. A small amount of silica gel was added and the solvent removed *in vacuo* (at 30°C) and dry loaded to the top of a silica column in 100 % PE. Upon loading a solvent system of 95:5 PE:Et_2O was employed until product elution. Column chromatography yielded 83.1 mg (64 %) of a colourless oil.

^{1}H NMR (500 MHz, $CDCl_3$) δ 8.23 (d, *J* = 1.7 Hz, 1H), 8.16 (d, *J* = 1.7 Hz, 1H), 7.53 − 7.43 (m, 3H), 7.29 − 7.25 (m, 2H), 4.43 (q, *J* = 7.1 Hz, 2H), 2.56 − 2.44 (m, 2H), 1.53 − 1.45 (m, 2H), 1.43 (t, *J* = 7.1 Hz, 3H), 0.79 (t, *J* = 7.3 Hz, 3H). **^{13}C NMR** (126 MHz, $CDCl_3$) δ = 164.9, 149.1, 142.8, 136.7, 134.3, 131.4, 130.3, 128.8, 128.8, 128.6, 117.7, 114.0, 61.7, 35.1, 24.1, 14.3, 13.8. **IR:** (ATR) 3064 (Ar-H), 2230 (Nitrile), 1720 (C=O), 1445 (CH_3) cm^{-1}.

ESI-MS: $C_{19}H_{20}NO_2$ Calc. (M+H)$^+$ = 294.1489 found (M+H)$^+$ = 294.1508 (3.21 ppm)

R$_f$ 90:10 PE:EtOAc = 0.51

5.3.11 Synthesis of ethyl 2-butyl-6-cyano-[1,1'-biphenyl]-4-carboxylate (144)
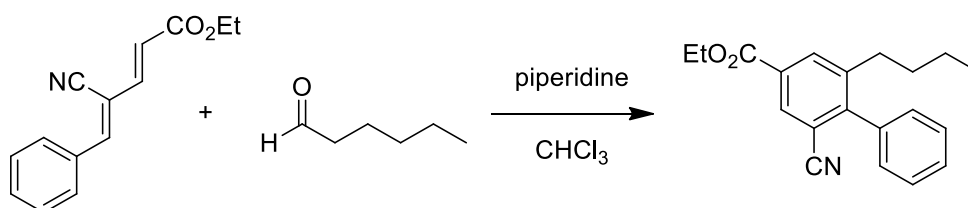
To a 10 mL vial was added cyano-ester diene **96** 100 mg (0.44 mmol, 1 eq.), hexanal 58.9 μL (0.48 mmol, 1.1 eq.) and $CHCl_3$ (3 mL). To the resulting pale yellow solution was added piperidine 43.5 μL (0.44 mmol, 1 eq.) and the reaction was stirred at rt for 16 hrs. The product was purified by column chromatography. A small amount of silica gel was added and the solvent removed *in vacuo* (at 30˚C) and dry loaded to the top of a silica column in 100 % PE. Upon loading a solvent system of 95:5 PE:Et_2O was employed until product elution. Column chromatography yielded 76.0 mg (56 %) of a colourless oil.

^{1}H NMR (500 MHz, $CDCl_3$) δ 7.85 (d, *J* = 1.6 Hz, 1H), 7.77 (d, *J* = 1.5 Hz, 1H), 7.56 − 7.46 (m, 3H), 7.28 − 7.23 (m, 2H), 2.62 − 2.41 (m, 2H), 1.46 − 1.36 (m, 2H), 1.22 − 1.14 (m, 2H), 0.78 (t, *J* = 7.3 Hz, 3H). **^{13}C NMR** (126 MHz, $CDCl_3$) δ = 149.7, 144.6, 136.5, 135.9, 133.5, 129.4, 129.0, 128.7, 117.1, 116.5, 115.3, 112.7, 32.9, 32.8, 22.4, 13.7. **IR:** (ATR) 3064 (Ar-H), 2231 (Nitrile), 1721 (C=O), 1466-1445 ($CH_2CH_2CH_2CH_3$) cm^{-1}.

ESI-MS: $C_{20}H_{22}NO_2$ Calc. $(M+H)^+$ = 308.1645 found $(M+H)^+$ = 308.1660 (4.72 ppm)

R_f: 90:10 PE:EtOAc = 0.30

5.4   Chapter 4

5.4.1   Synthesis of 2-amino-4-phenyl-4H-pyran-3,5-dicarbonitrile (122)
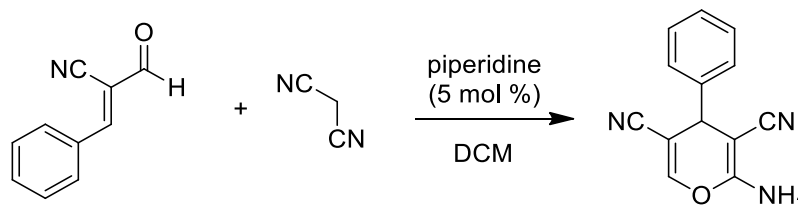
To a 10 ml vial containing α-cyano cinnamaldehyde 157.0 mg (1.0 mmol, 1 eq.) and malononitrile 73.0 mg (1.1 mmol, 1.1 eq.) was added 1 mL of DCM to yield a pale yellow solution. To this solution piperidine 4.94 µL (0.05 mmol, 5 mol %) and the reaction was stirred for 20 mins. The resulting white precipitate was collected by vacuum filtration and washed with cold PE to yield 0.207 g (93 %) of a white solid which turned dark red over time.

^{1}H NMR (500 MHz, DMSO) δ 7.73 (s, 1H), 7.45 – 7.39 (m, 2H), 7.37 – 7.31 (m, 1H), 7.31 – 7.25 (m, 2H), 7.17 (br s, 2H), 4.32 (s, 1H).**^{13}C NMR** (126 MHz, DMSO) δ = 158.2 (O*C*NH$_2$, 4), 150.2 (*C*H, vinylic, 2), 141.8 (QAr*C*,7), 128.9 (Ar*C*), 127.9 (Ar*C*), 127.8 (Ar*C*), 119.0 (C≡N, 13), 116.3 (C≡N, 14), 94.3 (Q*C*,1), 55.7 (Q*C*,5), 37.7 (*C*H, 6).**IR:**

Mass: (APCI+) C$_{14}$H$_{16}$NO$_2$ Calc. (M+H)$^+$ = 230.1176 found (M+H)$^+$ = 230.1175 (-0.1 ppm)

Matches literature data.[123]

5.4.2   Synthesis of 2-amino-4-phenyl-4H-pyran-3,5-dicarbonitrile (122)
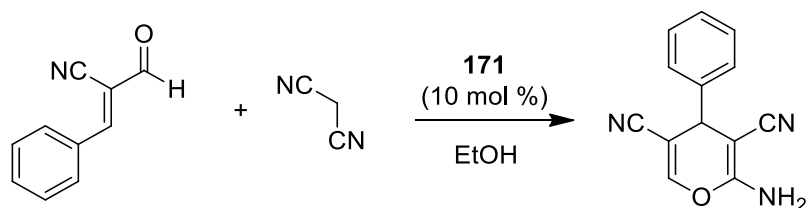
To a vial containing α-cyano cinnamaldehyde 79.0 mg (0.5 mmol, 1eq.) was added EtOH 1 mL followed by the addition of 36.0 mg (0.55 mmol) of malononitrile and 20.7 mg of catalyst **171** (0.05 mmol, 10 mol %). The reaction mixture solubilized upon addition of the catalyst and was stirred at rt for 20 mins during which time a white precipitate formed. The reaction was allowed to stir at rt overnight. The resulting suspension was reduced *in vacuo* to yield pale red solid which was recrystallized from EtOH/PE to yield 50 mg (45 %) of a pale yellow solid which turned dark red over time.

Spectral data is in agreement with alternative synthesis and literature report.[123]

5.4.3   Synthesis of 2-amino-4-(4-methoxyphenyl)-4H-pyran-3,5-dicarbonitrile (161)
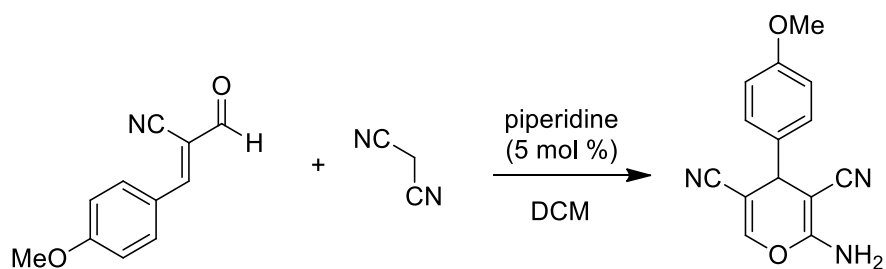
To a 10 ml vial containing *p*-OMe α-cyano cinnamaldehyde 120.0 mg (0.64 mmol, 1 eq.) and malononitrile 47.0 mg (0.70 mmol, 1.1 eq.) was added 1 mL of DCM to yield a pale yellow solution. To this solution piperidine 3.20 μL (0.03 mmol, 5 mol %) and the reaction was stirred for 20 mins. The resulting white precipitate was collected by vacuum filtration and washed with cold PE to yield 119.0 mg (74 %) of a pale yellow solid which turned dark red over time.

¹H NMR (500 MHz, DMSO) δ 7.69 (s, 1H), 7.19 (d, *J* = 8.4 Hz, 2H), 7.12 (s, 2H), 6.96 (d, *J* = 8.4 Hz, 2H), 4.26 (s, 1H), 3.77 (s, 3H).**¹³C NMR** (126 MHz, DMSO) δ 159.3, 158.5, 150.4, 134.4, 129.4, 119.5, 116.9, 114.7, 95.1, 56.5, 55.6, 37.4.

m.p: 119-121 ˚C

Matches literature data.[124]

5.4.4   Synthesis of 2-amino-4-(o-tolyl)-4H-pyran-3,5-dicarbonitrile (162)
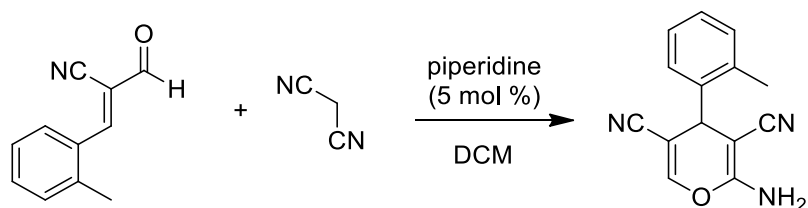
To a 10 ml vial containing α-cyano cinnamaldehyde 85.6 mg (0.5 mmol, 1 eq.) and malononitrile 36.0 mg (0.55 mmol, 1.1 eq.) was added 1 mL of DCM to yield a pale yellow solution. To this solution piperidine 4.94 µL (0.05 mmol, 5 mol %) and the reaction was stirred for 20 mins. The resulting white precipitate was collected by vacuum filtration and washed with cold PE to yield 0.207 g (93 %) of a white solid.

^{1}**H NMR** (500 MHz, DMSO) δ 7.73 (s, 1H), 7.30 − 7.24 (m, 1H), 7.23 − 7.18 (m, 3H), 7.14 (s, 2H), 4.64 (s, 1H), 2.37 (s, 3H).^{13}**C NMR** (126 MHz, DMSO) δ 158.2, 150.3, 139.7, 135.5, 130.7, 128.8, 127.6, 126.9, 119.0, 116.3, 94.1, 55.6, 34.1, 18.8.

Mass: (APCI-) $C_{14}H_{11}N_3O$ Calc. (M$^-$) = 237.0907 found (M$^-$) = 237.0900 (3.1 ppm)

m.p: 138-140 ˚C

Matches literature data.[124]

5.4.5   Synthesis of 2-amino-4-(p-tolyl)-4H-pyran-3,5-dicarbonitrile (163)
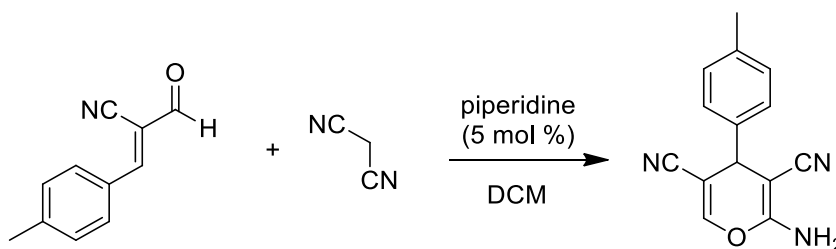
To a 10 ml vial containing p-CH$_3$ α-cyano cinnamaldehyde 85.6 mg (0.5 mmol, 1 eq.) and malononitrile 36.0 mg (0.55 mmol, 1.1 eq.) was added 1 mL of DCM to yield a pale yellow solution. To this solution piperidine 4.94 μL (0.05 mmol, 5 mol %) and the reaction was stirred for 20 mins. The resulting pale yellow precipitate was collected by vacuum filtration and washed with cold PE to yield 114.4 g (94 %) of a pale yellow solid which darkened over time to a pale red solid.

^{1}H NMR (500 MHz, DMSO) δ 7.71 (d, *J* = 1.0 Hz, 1H), 7.24 – 7.11 (m, 6H), 4.26 (d, *J* = 1.0 Hz, 1H), 2.31 (s, 3H).

^{13}C NMR (126 MHz, DMSO) δ 158.1, 150.0, 138.9, 137.1, 129.4, 127.6, 119.0, 116.3, 94.5, 55.8, 37.3, 20.7.

Mass: (APCI-) C$_{14}$H$_{10}$N$_3$O Calc. (M-H$^+$) = 236.0829 found (M-H$^+$) = 236.0826 (1.5 ppm)

5.4.6   Synthesis of 2-ethoxy-4-phenyl-3,4-dihydro-2H-pyran-5-carbonitrile (176)

To a vial containing α-cyano cinnamaldehyde 39.3 mg (0.25 mmol, 1 eq.) was added 0.2 mL of DCM and ethyl vinyl ether 95.8 µL (1.00 mmol, 4 eq.). The resulting clear colourless solution was stirred at 25 ˚C for 16 hrs after which time the volatiles were reduced *in vacuo* to yield a clear colourless oil in a quantitative yield. *Endo:Exo* 1:0.08.

¹H NMR (500 MHz, CDCl₃) δ 7.38 – 7.31 (m, 2H), 7.30 – 7.20 (m, 4H), 5.15 (dd, *J* = 8.4, 2.2 Hz, 1H, 5), 3.93 (dq, *J* = 9.5, 7.1 Hz, 1H, 10), 3.71 (ddd, *J* = 9.9, 6.4, 1.7 Hz, 1H, 3), 3.61 (dq, *J* = 9.5, 7.1 Hz, 1H, 10), 2.31 (ddd, *J* = 13.9, 6.4, 2.2 Hz, 1H, 4), 2.02 (ddd, *J* = 13.9, 9.9, 8.4 Hz, 1H, 4), 1.21 (t, *J* = 7.1 Hz, 3H, C*H*₃, 11). *Endo* isomer.

¹³C NMR (126 MHz, CDCl₃) δ = 155.8 (C=*C*H, 1), 140.0 (QAr*C*, 8), 128.9 (Ar*C*H, 12), 127.7 (Ar*C*H, 14), 127.6 (Ar*C*H, 13), 118.1 (*C*≡N, 7), 100.7 (O*C*HO, 5), 92.5 (Q*C*C≡N, 2), 65.3 (*C*H₂CH₃, 10), 38.4 (*C*H-Ph, 3), 36.4 (*C*H₂, 4), 15.0 (CH₂*C*H₃, 11). *Endo* isomer.

IR: (NaCl plate) 3064 (Ar-H), 2213 (nitrile), 1621 (C=C), 1455 (CH₃), 1148 (C-O-C)

Mass: (APCI+) C₁₄H₁₆NO₂ Calc. (M+H)⁺ = 230.1176 found (M+H)⁺ = 230.1178 (+1.23 ppm)

R_f: 80:20 PE:EtOAc = 0.49

5.4.7   Synthesis of 2-ethoxy-4-(o-tolyl)-3,4-dihydro-2H-pyran-5-carbonitrile (177)
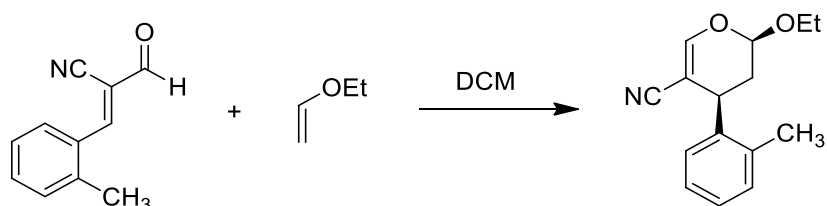
To a vial containing *o*-CH$_3$ α-cyano cinnamaldehyde 42.8 mg (0.25 mmol, 1 eq.) was added 0.4 mL of DCM and ethyl vinyl ether 95.8 μL (1.00 mmol, 4 eq.). The resulting clear colourless solution was stirred at 25 ˚C for 40 hrs after which time the volatiles were reduced *in vacuo* to yield a clear colourless oil, which solidified on standing, in a quantitative yield. *Endo:Exo* 1:0.18.

^{1}H NMR (500 MHz, CDCl$_3$) δ 7.25 (d, *J* = 1.4 Hz, 1H), 7.24 − 7.14 (m, 5H), 5.16 (dd, *J* = 8.4, 2.2 Hz, 1H), 4.01 − 3.91 (m, 2H), 3.62 (dq, *J* = 9.4, 7.1 Hz, 1H), 2.35 (s, 3H), 2.28 (ddd, *J* = 13.9, 6.4, 2.2 Hz, 1H), 1.94 (ddd, *J* = 13.9, 9.7, 8.5 Hz, 1H), 1.22 (t, *J* = 7.1 Hz, 3H). *Endo* isomer.

^{13}C NMR (126 MHz, CDCl$_3$) δ 155.9, 137.7, 135.4, 130.8, 127.4, 127.0, 126.7, 118.1, 100.7, 97.7, 92.7, 65.3, 34.8, 19.3, 15.0. *Endo* isomer.

IR: (NaCl plate) 3065 (Ar-H), 2213 (nitrile), 1622 (C=C), 1492 (CH$_3$), 1147 (C-O-C)

Mass: (APCI+) C$_{15}$H$_{18}$NO$_2$ Calc. (M+H)$^+$ = 224.1332 found (M+H)$^+$ = 224.1337 (2.0 ppm)

R$_f$: 80:20 PE:EtOAc = 0.47

5.4.8   Synthesis of 2-ethoxy-4-(m-tolyl)-3,4-dihydro-2H-pyran-5-carbonitrile (178)
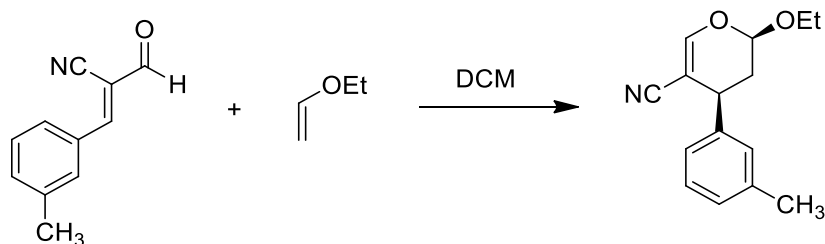
To a vial containing *m*-CH$_3$ α-cyano cinnamaldehyde 42.8 mg (0.25 mmol, 1 eq.) was added 0.4 mL of DCM and ethyl vinyl ether 95.8 μL (1.00 mmol, 4 eq.). The resulting clear colourless solution was stirred at 30 ˚C for 40 hrs after which time the volatiles were reduced *in vacuo* to yield an off white solid in a quantitative yield. *Endo*:*Exo* 1:0.11.

^{1}H NMR (500 MHz, CDCl$_3$) δ 7.27 – 7.16 (m, 2H), 7.13 – 6.99 (m, 3H), 5.14 (dd, *J* = 8.5, 2.1 Hz, 1H), 3.94 (dq, *J* = 9.4, 7.1 Hz, 1H), 3.69 – 3.65 (m, 1H), 3.64 – 3.57 (m, 1H), 2.34 (s, 3H), 2.30 (ddd, *J* = 13.9, 6.4, 2.0 Hz, 1H), 2.01 (ddd, *J* = 13.9, 9.9, 8.7 Hz, 1H), 1.22 (t, *J* = 7.1 Hz, 3H). *Endo* isomer.

^{13}C NMR (126 MHz, CDCl$_3$) δ 155.7, 139.9, 138.6, 128.9, 128.5, 128.4, 124.7, 118.2, 100.8, 92.8, 65.4, 38.5, 36.5, 21.6, 15.1. *Endo* isomer.

IR: (NaCl plate) 3059 (Ar-H), 2213 (nitrile), 1622 (C=C), 1489 (CH$_3$), 1144 (C-O-C)

Mass: (APCI+) C$_{15}$H$_{18}$NO$_2$ Calc. (M+H)$^+$ = 224.1332 found (M+H)$^+$ = 224.1332 (- 0.2 ppm)

R$_f$: 80:20 PE:EtOAc = 0.51

5.4.9   Synthesis of 2-ethoxy-4-(p-tolyl)-3,4-dihydro-2H-pyran-5-carbonitrile (179)
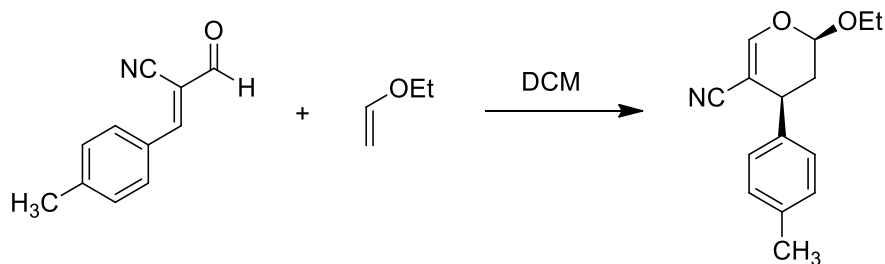
To a vial containing *p*-CH$_3$ α-cyano cinnamaldehyde 42.8 mg (0.25 mmol, 1 eq.) was added 0.4 mL of DCM and ethyl vinyl ether 95.8 µL (1.00 mmol, 4 eq.). The resulting clear colourless solution was stirred at 30 ˚C for 16 hrs after which time the volatiles were reduced *in vacuo* to yield an off white solid in a quantitative yield. *Endo*:*Exo* 1:0.11.

^{1}H NMR (500 MHz, CDCl$_3$) δ 7.20 (d, *J* = 1.9 Hz, 1H), 7.18 – 7.09 (m, 4H), 5.15 (dd, *J* = 8.6, 2.1 Hz, 1H), 3.95 (dq, *J* = 9.5, 7.1 Hz, 1H), 3.68 (ddd, *J* = 10.2, 6.4, 1.9 Hz, 1H), 3.63 (dq, *J* = 9.5, 7.1 Hz, 1H), 2.33 (s, 3H), 2.30 (ddd, *J* = 13.9, 6.4, 2.1 Hz, 1H), 2.01 (ddd, *J* = 13.9, 10.2, 8.6 Hz, 1H), 1.23 (t, *J* = 7.1 Hz, 3H). *Endo* isomer.

^{13}C NMR (126 MHz, CDCl$_3$) δ 155.5, 137.3, 136.8, 129.6, 127.4, 118.1, 100.8, 92.8, 65.3, 38.1, 36.4, 21.1, 15.0. *Endo* isomer.

IR: (NaCl plate) 3054 (Ar-H), 2213 (nitrile), 1621 (C=C), 1441 (CH$_3$), 1148 (C-O-C)

Mass: (APCI+) C$_{15}$H$_{18}$NO$_2$ Calc. (M+H)$^+$ = 244.1332 found (M+H)$^+$ = 244.1339 (1.7 ppm)

R$_f$: 80:20 PE:EtOAc = 0.61

5.4.10 Synthesis of 4-(3-chlorophenyl)-2-ethoxy-3,4-dihydro-2H-pyran-5-carbonitrile (180)
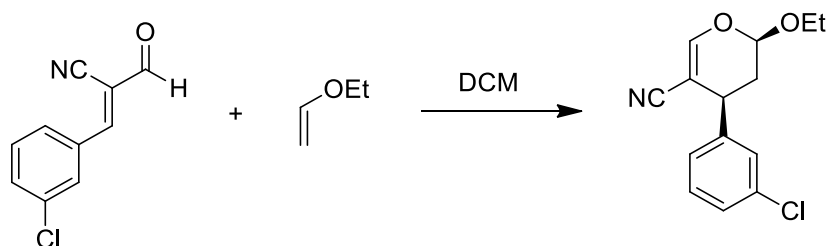
To a vial containing *m*-Cl α-cyano cinnamaldehyde 47.9 mg (0.25 mmol, 1 eq.) was added 0.4 mL of DCM and ethyl vinyl ether 95.8 µL (1.00 mmol, 4 eq.). The resulting clear colourless solution was stirred at 30 ˚C for 16 hrs after which time the volatiles were reduced *in vacuo* to yield an off white solid in a quantitative yield. *Endo*:*Exo* 1:0.11.

^{1}H NMR (500 MHz, CDCl$_3$) δ 7.29 – 7.23 (m, 4H), 7.13 (dt, *J* = 7.1, 1.6 Hz, 1H), 5.16 (dd, *J* = 7.3, 2.3 Hz, 1H), 3.91 (dq, *J* = 9.4, 7.1 Hz, 1H), 3.68 (ddd, *J* = 8.4, 6.7, 1.6 Hz, 1H), 3.58 (dq, *J* = 9.4, 7.1 Hz, 1H), 2.30 (ddd, *J* = 14.0, 6.7, 2.3 Hz, 1H), 2.03 (ddd, *J* = 14.0, 8.4, 7.3 Hz, 1H), 1.19 (t, *J* = 7.1 Hz, 3H). *Endo* isomer.

^{13}C NMR (126 MHz, CDCl$_3$) δ 156.0, 142.3, 134.6, 130.2, 128.1, 127.9, 126.0, 118.0 (s), 100.0, 91.7, 65.3, 37.6, 35.7, 15.0. *Endo* isomer.

IR: (NaCl plate) 3065 (Ar-H), 2214 (nitrile), 1622 (C=C), 1476 (CH$_3$), 1148 (C-O-C)

Mass: (APCI+) C$_{14}$H$_{15}$ClNO$_2$ Calc. (M+H)$^+$ = 264.0786 found (M+H)$^+$ = 264.0785 (-0.5 ppm)

R$_f$: 80:20 PE:EtOAc = 0.55

5.4.11 Synthesis of 4-(4-bromophenyl)-2-ethoxy-3,4-dihydro-2H-pyran-5-carbonitrile (181)
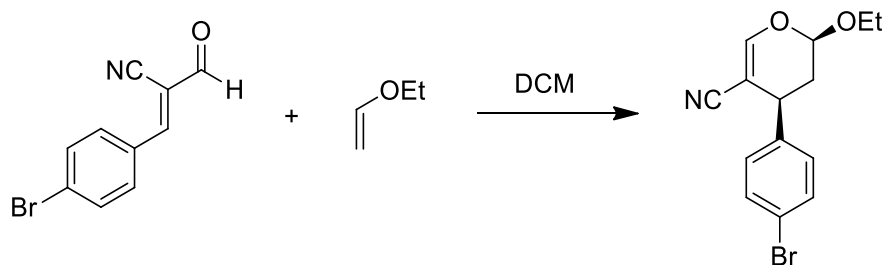
To a vial containing *p*-Br α-cyano cinnamaldehyde 59.0 mg (0.25 mmol, 1 eq.) was added 0.4 mL of DCM and ethyl vinyl ether 95.8 μL (1.00 mmol, 4 eq.). The resulting clear colourless solution was stirred at 30 ˚C for 16 hrs after which time the volatiles were reduced *in vacuo* to yield an off white solid in a quantitative yield. *Endo*:*Exo* 1:0.13

^{1}H NMR (500 MHz, CDCl$_3$) δ 7.49 − 7.45 (m, 2H), 7.23 (d, *J* = 1.8 Hz, 1H), 7.15 − 7.10 (m, 2H), 5.16 (dd, *J* = 7.7, 2.3 Hz, 1H), 3.92 (dq, *J* = 9.4, 7.1 Hz, 1H), 3.70 − 3.66 (m, 1H), 3.60 (dq, *J* = 9.4, 7.1 Hz, 1H), 2.30 (ddd, *J* = 14.0, 6.6, 2.3 Hz, 1H), 2.00 (ddd, *J* = 14.0, 9.1, 7.7 Hz, 1H), 1.20 (t, *J* = 7.1 Hz, 3H). *Endo* isomer.

^{13}C NMR (126 MHz, CDCl$_3$) δ 156.0, 139.2, 132.1, 129.5, 121.6, 118.0, 100.3, 91.9, 65.4, 37.6, 36.0, 15.1. *Endo* isomer.

IR: (NaCl plate) 3064 (Ar-H), 2213 (nitrile), 1621 (C=C), 1489 (CH$_3$), 1149 (C-O-C)

Mass: (APCI+) C$_{14}$H$_{15}$BrNO$_2$ Calc. (M+H)$^+$ = 308.0281 found (M+H)$^+$ = 308.0275 (1.9 ppm)

R$_f$: 80:20 PE:EtOAc = 0.50

5.4.12   Synthesis of 2-ethoxy-4-(3-fluorophenyl)-3,4-dihydro-2H-pyran-5-carbonitrile

   (182)
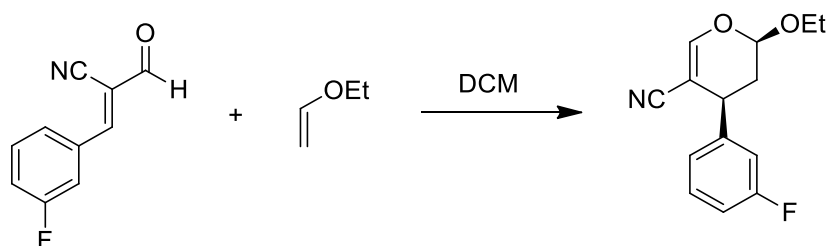
To a vial containing *m*-F α-cyano cinnamaldehyde 43.8 mg (0.25 mmol, 1 eq.) was added 0.4 mL of DCM and ethyl vinyl ether 95.8 μL (1.00 mmol, 4 eq.). The resulting clear colourless solution was stirred at 25 ˚C for 16 hrs after which time the volatiles were reduced *in vacuo* to yield a clear colourless oil in a quantitative yield. *Endo*:*Exo* 1:0.11.

¹H NMR (500 MHz, CDCl₃) δ 7.35 − 7.28 (m, 1H), 7.24 (d, *J* = 1.6 Hz, 1H), 7.06 − 6.92 (m, 3H), 5.16 (dd, *J* = 7.6, 2.3 Hz, 1H), 3.92 (dq, *J* = 9.4, 7.1 Hz, 1H), 3.74 − 3.68 (m, 1H), 3.59 (dq, *J* = 9.4, 7.1 Hz, 1H), 2.31 (ddd, *J* = 14.0, 6.6, 2.3 Hz, 1H), 2.03 (ddd, *J* = 14.0, 8.7, 7.8 Hz, 1H), 1.20 (t, *J* = 7.1 Hz, 3H). *Endo* isomer.

¹³C NMR (126 MHz, CDCl₃) δ 163.1 (d, *J* = 246.3 Hz), 156.0, 142.7 (d, *J* = 7.1 Hz), 130.4 (d, *J* = 8.3 Hz), 123.4 (d, *J* = 2.9 Hz), 118.0, 114.8 (d, *J* = 22.1 Hz), 114.7 (d, *J* = 21.1 Hz), 100.2, 91.9, 65.4, 37.8 (d, *J* = 1.8 Hz), 35.9, 15.0. *Endo* isomer.

¹⁹F NMR (471 MHz, CDCl₃) δ -112.57.

IR: (NaCl plate) 3065 (Ar-H), 2214 (nitrile), 1622 (C=C), 1487 (CH₃), 1169 (C-O-C)

Mass: (APCI+) $C_{14}H_{14}FNO_2$ Calc. (M+H)⁺ = 248.1081 found (M+H)⁺ = 248.1076 (-2.14 ppm)

R_f: 80:20 PE:EtOAc = 0.46

5.4.13   Synthesis of 4-(3-bromophenyl)-2-ethoxy-3,4-dihydro-2H-pyran-5-carbonitrile

(183)
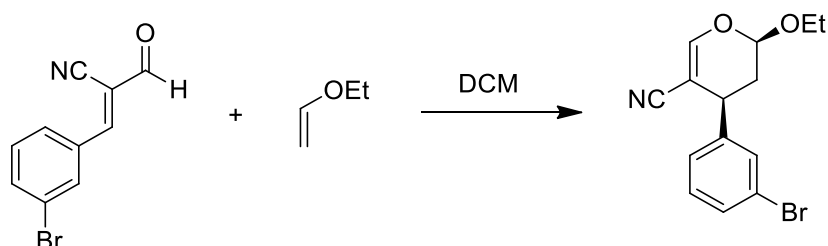
To a vial containing *m*-Br α-cyano cinnamaldehyde 59.0 mg (0.25 mmol, 1 eq.) was added 0.4 mL of DCM and ethyl vinyl ether 95.8 µL (1.00 mmol, 4 eq.). The resulting clear colourless solution was stirred at 25 ˚C for 40 hrs after which time the volatiles were reduced *in vacuo* to yield a pale orange oil in a quantitative yield. *Endo*:*Exo* 1:0.09.

^{1}H NMR (500 MHz, CDCl$_3$) δ 7.37 – 7.30 (m, 2H), 7.20 – 7.08 (m, 3H), 5.09 (dd, *J* = 7.4, 2.3 Hz, 1H), 3.83 (dq, *J* = 9.3, 7.1 Hz, 1H), 3.63 – 3.57 (m, 1H), 3.50 (dq, *J* = 9.3, 7.1 Hz, 1H), 2.22 (ddd, *J* = 14.0, 6.7, 2.3 Hz, 1H), 1.94 (ddd, *J* = 14.0, 8.2, 7.4 Hz, 1H), 1.12 (t, *J* = 7.1 Hz, 3H).

^{13}C NMR (126 MHz, CDCl$_3$) δ = 156.0, 142.5, 130.9, 130.7, 130.4, 126.4, 122.7, 118.0, 99.9, 91.5, 65.3, 37.4, 35.6, 15.00.

IR: (NaCl plate) 3062 (Ar-H), 2213 (nitrile), 1622 (C=C), 1474 (CH$_3$), 1148 (C-O-C)

Mass: (APCI+) C$_{14}$H$_{15}$BrNO$_2$ Calc. (M+H)$^{+}$ = 308.0281 found (M+H)$^{+}$ = 308.0269 (3.8 ppm)

R$_f$: 80:20 PE:EtOAc = 0.42

5.4.14 Synthesis of 2-ethoxy-4-(3-(trifluoromethyl)phenyl)-3,4-dihydro-2H-pyran-5-carbonitrile (184)
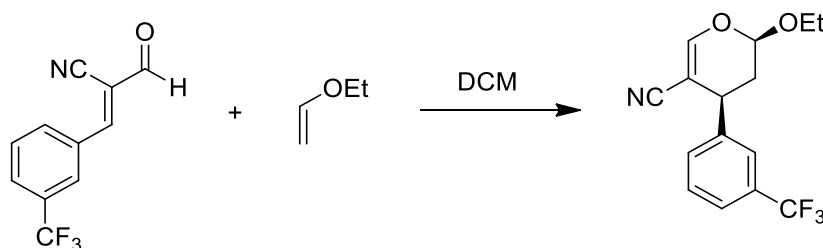
To a vial containing *m*-CF$_3$ α-cyano cinnamaldehyde 56.3 mg (0.25 mmol, 1 eq.) was added 0.4 mL of DCM and ethyl vinyl ether 95.8 µL (1.00 mmol, 4 eq.). The resulting clear colourless solution was stirred at 25 ˚C for 16 hrs after which time the volatiles were reduced *in vacuo* to yield a pale red oil in a quantitative yield. *Endo:Exo*

^{1}H NMR (500 MHz, CDCl$_3$) δ 7.57 − 7.42 (m, 4H), 7.28 (s, 1H), 5.19 (dd, *J* = 6.5, 2.2 Hz, 1H), 3.90 (dq, *J* = 14.2, 7.1 Hz, 1H), 3.77 (m, 1H), 3.57 (dq, *J* = 14.2, 7.1 Hz, 1H), 2.34 (ddd, *J* = 14.0, 6.9, 2.2 Hz, 1H), 2.08 (m, 1H), 1.16 (t, *J* = 7.1 Hz, 3H). *Endo* isomer.

^{13}C NMR (126 MHz, CDCl$_3$) δ 156.2, 141.4, 131.3, 131.2 (q, *J* = 32.3 Hz), 129.4, 124.8 (q, *J* = 3.8 Hz), 124.5 (q, *J* = 3.7 Hz), 124.2 (q, *J* = 272.4 Hz), 118.0, 99.8, 91.4, 65.4, 37.4, 35.5, 15.0. *Endo* isomer.

^{19}F NMR (471 MHz, CDCl$_3$) δ -62.61 (s).

IR: (NaCl plate) 3071 (Ar-H), 2215 (nitrile), 1624 (C=C), 1452 (CH$_3$), 1126 (C-O-C)

Mass: (APCI+) C$_{15}$H$_{15}$F$_3$NO$_2$ Calc. (M+H)$^+$ = 298.1049 found (M+H)$^+$ = 298.1055 (- 1.8 ppm)

R$_f$: 80:20 PE:EtOAc = 0.51

6   Appendix

6.1 Optimized structures

6.1.1 Bis-cyano butadiene (41) *s-trans*

From left to right, *E,E, E,Z, Z,E, Z,Z.*
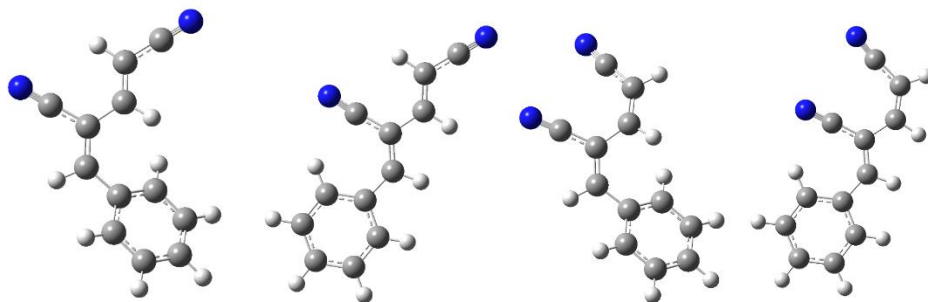
6.1.2 Bis-cyano butadiene (41) *s-cis*

From left to right, *E,E, E,Z, Z,E, Z,Z.*
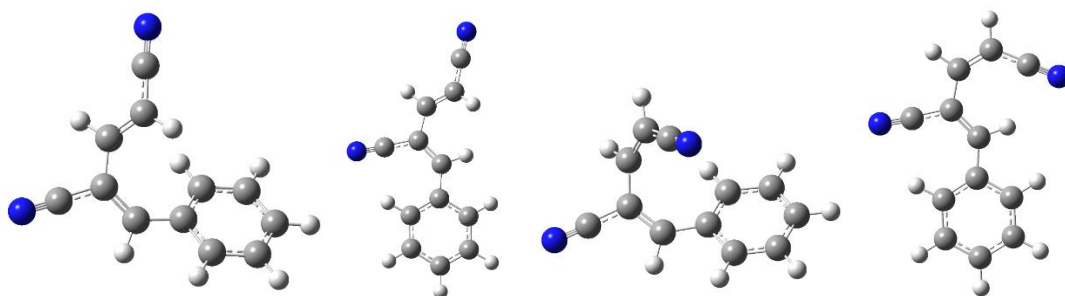
6.1.3 Cyano ester butadiene (96) *s-trans*

From left to right, *E,E, E,Z, Z,E, Z,Z.*
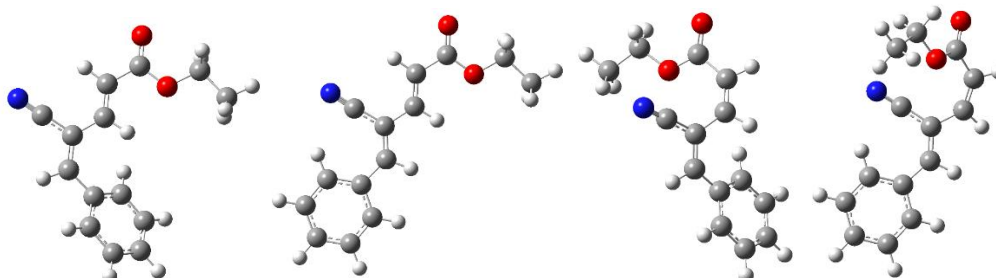
6.1.4 Cyano ester butadiene (96) *s-cis*

From left to right, *E,E, E,Z, Z,E, Z,Z.*
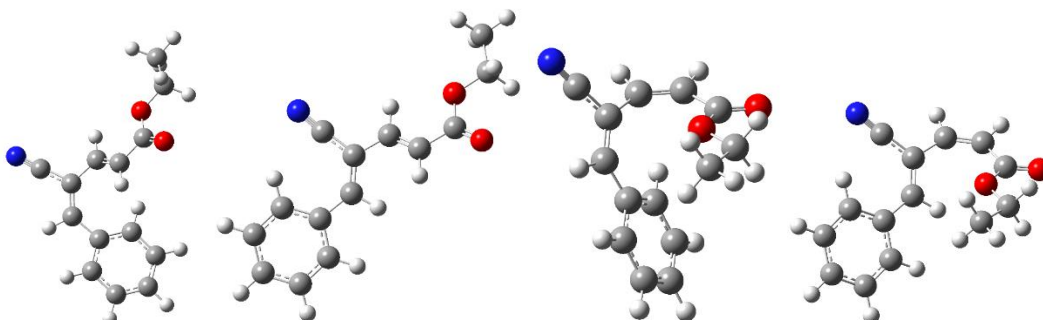
6.1.5   Cyano phenylsulfonyl butadiene (105) *s-trans*

From left to right, *E,E, E,Z, Z,E, Z,Z*.
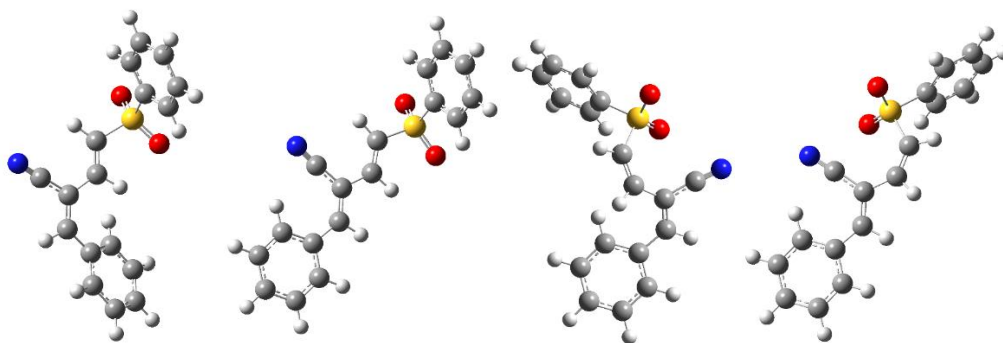
6.1.6   Cyano phenylsulfonyl butadiene (105) *s-cis*

From left to right, *E,E, E,Z, Z,Z*. A lowest computed energy ground state was not found for the *Z,E* butadiene in this case.
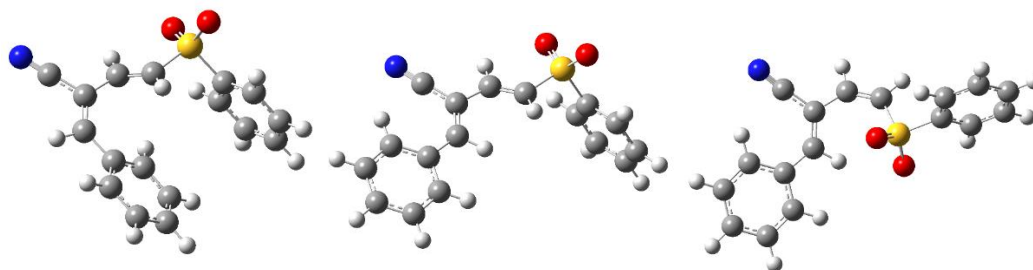
6.1.7   Bisphenylsulfonyl butadiene (123) *s-trans*

From top left to bottom right, *E,E, E,Z, Z,Z*.
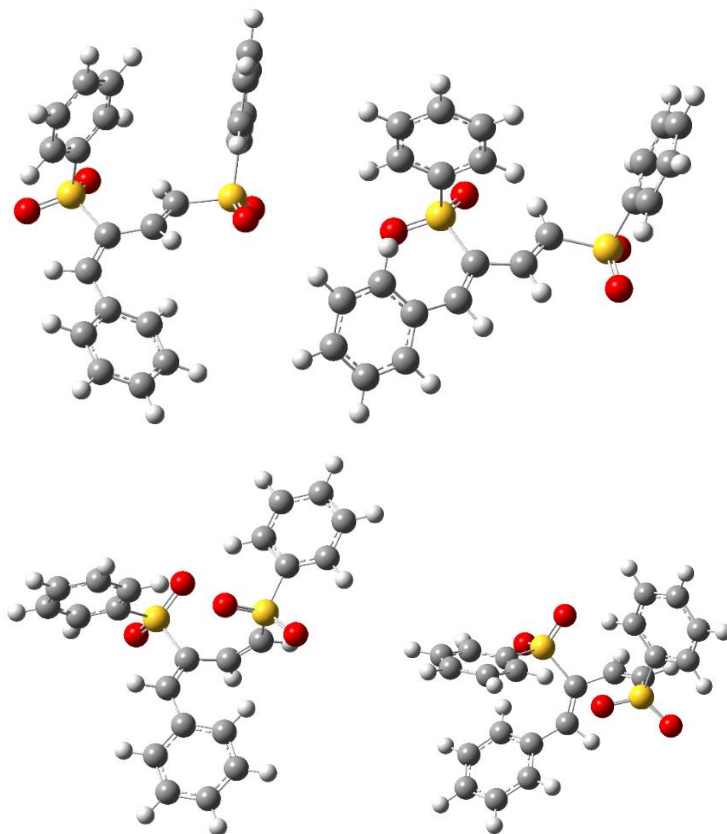
6.1.8   Bisphenylsulfonyl butadiene (123) *s-cis*

From top left to bottom right, *E,E, E,Z, Z,Z.*
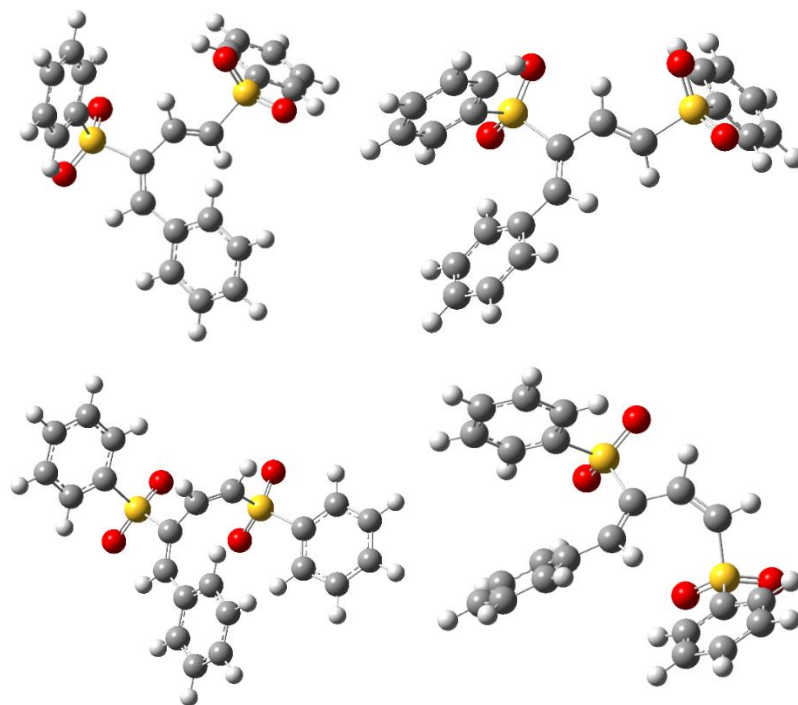
6.2   X-Ray structure data

6.2.1   Crystal structure data for (2Z,3E)-2-benzylidene-4-(phenylsulfonyl)but-3-enenitrile (105)

Table 1. Crystal data and structure refinement for **105**.

Identification code	**105**
Empirical formula	C17 H13 N O2 S
Formula weight	295.34
Temperature	298(2) K
Wavelength	0.7107 Å
Crystal system	Triclinic
Space group	P-1
Unit cell dimensions	a = 5.9304(9)Å α = 100.605(11)°
	b = 10.8423(15)Å β = 97.036(12)°
	c = 11.8426(14)Å γ = 103.199(13)°
Volume	717.84(17) Å^3
Z	2
Density (calculated)	1.366 Mg/m^3
Absorption coefficient	0.229 mm^{-1}
F(000)	308
Crystal size	0.55 x 0.50 x 0.35 mm
Theta range for data collection	2.93 to 29.3402 °.
Index ranges	-7<=h<=7; -13<=k<=12; -8<=l<=15
Reflections collected	5583
Independent reflections	2624 [R_{int} = 0.0225]
Reflections observed (>2σ)	2058
Data Completeness	0.998
Absorption correction	Semi-empirical from equivalents
Max. and min. transmission	1.00000 and 0.95924
Refinement method	Full-matrix least-squares on F^2
Data / restraints / parameters	2624 / 0 / 190
Goodness-of-fit on F^2	1.037
Final R indices [I>2σ(I)]	R_1 = 0.0434 wR_2 = 0.0922
R indices (all data)	R_1 = 0.0608 wR_2 = 0.1068
Largest diff. peak and hole	0.222 and -0.265 e.Å^{-3}

[a]$R_1 = \Sigma||F_o| - |F_c||/\Sigma|F_o|$. [b]$wR_2 = |\Sigma w(|Fo|^2 - |Fc|^2)/\Sigma|w(F_o)^2|^{1/2}$, w = $1/[\sigma^2(Fo^2) + (.0373P)^2 + .2713P]$. P = $(F_o^2 + 2Fc^2)/3$.

Table 2. Atomic coordinates (x 10^4) and equivalent isotropic
displacement parameters (Å^2 x 10^3) for **105**.U(eq) is defined
as one third of the trace of the orthogonalized Uij tensor.

Atom	x	y	z	U(eq)
S(1)	2416(1)	794(1)	3039(1)	38(1)
O(1)	3488(3)	−259(2)	2795(2)	52(1)
O(2)	264(3)	571(2)	3494(2)	53(1)
N(1)	7641(4)	5199(2)	5827(2)	53(1)
C(1)	4437(4)	2096(2)	3995(2)	36(1)
C(2)	6414(4)	1930(2)	4504(2)	36(1)
C(3)	8206(4)	2888(2)	5387(2)	34(1)
C(4)	10027(4)	2533(2)	5910(2)	35(1)
C(5)	7908(4)	4181(2)	5649(2)	36(1)
C(6)	12016(4)	3247(2)	6815(2)	35(1)
C(7)	12414(4)	4537(2)	7407(2)	51(1)
C(8)	14368(5)	5108(3)	8249(3)	59(1)
C(9)	15969(5)	4429(3)	8523(2)	52(1)
C(10)	15627(4)	3168(2)	7951(2)	46(1)
C(11)	13670(4)	2579(2)	7106(2)	39(1)
C(12)	1886(4)	1350(2)	1755(2)	36(1)
C(13)	3099(4)	1063(2)	868(2)	46(1)
C(14)	2630(5)	1458(3)	−156(2)	55(1)
C(15)	965(5)	2138(3)	−286(3)	57(1)
C(16)	−222(5)	2435(3)	603(3)	57(1)
C(17)	218(4)	2037(2)	1632(2)	47(1)

Table 3.   Bond lengths [Å] and angles [°] for **105**.

S(1)-O(1)	1.4311(17)	S(1)-O(2)	1.4331(17)
S(1)-C(1)	1.737(2)	S(1)-C(12)	1.756(2)
N(1)-C(5)	1.135(3)	C(1)-C(2)	1.316(3)
C(2)-C(3)	1.458(3)	C(3)-C(4)	1.346(3)
C(3)-C(5)	1.435(3)	C(4)-C(6)	1.452(3)
C(6)-C(11)	1.393(3)	C(6)-C(7)	1.397(3)
C(7)-C(8)	1.372(4)	C(8)-C(9)	1.371(4)
C(9)-C(10)	1.366(4)	C(10)-C(11)	1.377(3)
C(12)-C(13)	1.373(3)	C(12)-C(17)	1.377(3)
C(13)-C(14)	1.376(3)	C(14)-C(15)	1.371(4)
C(15)-C(16)	1.367(4)	C(16)-C(17)	1.380(3)
O(1)-S(1)-O(2)	118.40(11)	O(1)-S(1)-C(1)	108.80(10)
O(2)-S(1)-C(1)	108.13(11)	O(1)-S(1)-C(12)	108.57(11)
O(2)-S(1)-C(12)	107.36(11)	C(1)-S(1)-C(12)	104.74(10)
C(2)-C(1)-S(1)	119.78(18)	C(1)-C(2)-C(3)	126.7(2)
C(4)-C(3)-C(5)	123.5(2)	C(4)-C(3)-C(2)	119.6(2)
C(5)-C(3)-C(2)	116.93(19)	C(3)-C(4)-C(6)	132.0(2)
N(1)-C(5)-C(3)	178.2(3)	C(11)-C(6)-C(7)	117.7(2)
C(11)-C(6)-C(4)	116.5(2)	C(7)-C(6)-C(4)	125.8(2)
C(8)-C(7)-C(6)	120.4(2)	C(9)-C(8)-C(7)	120.8(2)
C(10)-C(9)-C(8)	119.9(2)	C(9)-C(10)-C(11)	120.1(2)
C(10)-C(11)-C(6)	121.2(2)	C(13)-C(12)-C(17)	120.6(2)
C(13)-C(12)-S(1)	119.44(19)	C(17)-C(12)-S(1)	119.9(2)
C(12)-C(13)-C(14)	119.6(2)	C(15)-C(14)-C(13)	120.1(3)
C(16)-C(15)-C(14)	120.2(3)	C(15)-C(16)-C(17)	120.4(3)
C(12)-C(17)-C(16)	119.1(3)		

280

Table 4.   Anisotropic displacement parameters ($Å^2$ x 10^3) for **105.** The anisotropic displacement factor exponent takes the form: $-2\pi^2[h^2a*^2$ U11 +... +2hka*b*U

Atom	U11	U22	U33	U23	U13	U12
S(1)	40(1)	31(1)	41(1)	4(1)	1(1)	10(1)
O(1)	61(1)	32(1)	60(1)	1(1)	−5(1)	21(1)
O(2)	44(1)	55(1)	56(1)	13(1)	13(1)	5(1)
N(1)	56(1)	39(1)	66(2)	9(1)	5(1)	20(1)
C(1)	40(1)	31(1)	38(1)	5(1)	2(1)	12(1)
C(2)	38(1)	31(1)	38(1)	5(1)	5(1)	11(1)
C(3)	38(1)	30(1)	34(1)	7(1)	7(1)	12(1)
C(4)	40(1)	30(1)	37(1)	6(1)	6(1)	11(1)
C(5)	33(1)	38(1)	37(1)	8(1)	1(1)	10(1)
C(6)	38(1)	34(1)	34(1)	7(1)	4(1)	10(1)
C(7)	54(2)	39(1)	56(2)	0(1)	−6(1)	20(1)
C(8)	62(2)	43(2)	60(2)	−9(1)	−10(1)	13(1)
C(9)	45(1)	54(2)	47(2)	4(1)	−8(1)	6(1)
C(10)	39(1)	53(2)	48(2)	16(1)	0(1)	14(1)
C(11)	42(1)	36(1)	39(1)	8(1)	5(1)	11(1)
C(12)	34(1)	30(1)	38(1)	2(1)	−2(1)	6(1)
C(13)	46(1)	42(1)	50(2)	6(1)	9(1)	14(1)
C(14)	64(2)	53(2)	45(2)	9(1)	15(1)	11(1)
C(15)	60(2)	58(2)	46(2)	15(1)	−7(1)	7(1)
C(16)	49(2)	59(2)	63(2)	16(2)	−6(1)	21(1)
C(17)	42(1)	51(2)	46(2)	6(1)	4(1)	18(1)

Table 5. Hydrogen coordinates (x 10^4) and isotropic displacement
parameters (Å^2 x 10^3) for **105.**

Atom	x	y	z	U(eq)
H(1)	4123	2907	4147	47
H(2)	6696	1119	4277	47
H(4)	10008	1668	5640	46
H(7)	11347	5011	7230	66
H(8)	14610	5967	8640	77
H(9)	17286	4826	9096	68
H(10)	16715	2708	8132	60
H(11)	13450	1720	6724	51
H(13)	4231	603	958	60
H(14)	3443	1263	-760	71
H(15)	644	2398	-981	74
H(16)	-1333	2908	514	74
H(17)	-601	2231	2234	61

6.2.2 Crystal structure data for 6-propyl-[1,1'-biphenyl]-2,4-dicarbonitrile (125)

Table 1. Crystal data and structure refinement for **125**.

Identification code	**125**
Empirical formula	C17 H14 N2
Formula weight	246.30
Temperature	300.4(2) K
Wavelength	0.71073 Å
Crystal system	Triclinic
Space group	P-1
Unit cell dimensions	a = 8.6538(10) Å α= 66.365(10)°.
	b = 9.4897(11) Å β= 68.105(10)°.
	c = 10.2268(10) Å γ = 86.609(9)°.
Volume	709.86(15) Å^3
Z	2
Density (calculated)	1.152 Mg/m^3
Absorption coefficient	0.069 mm^{-1}
F(000)	260
Crystal size	0.50 x 0.40 x 0.20 mm^3
Theta range for data collection	3.954 to 29.473°.
Index ranges	-11<=h<=8, -13<=k<=12, -13<=l<=12
Reflections collected	5810
Independent reflections	3290 [R(int) = 0.0196]
Completeness to theta = 25.242°	99.7 %
Absorption correction	Semi-empirical from equivalents
Max. and min. transmission	1.00000 and 0.90444
Refinement method	Full-matrix least-squares on F^2
Data / restraints / parameters	3290 / 0 / 173
Goodness-of-fit on F^2	1.014
Final R indices [I>2sigma(I)]	R1 = 0.0635, wR2 = 0.1529
R indices (all data)	R1 = 0.1188, wR2 = 0.1959
Extinction coefficient	n/a
Largest diff. peak and hole	0.145 and -0.232 e.Å^{-3}

Table 2. Atomic coordinates (x 10^4) and equivalent isotropic displacement parameters (Å^{2}x 10^3) for **125**. U(eq) is defined as one third of the trace of the orthogonalized U^{ij} tensor.

	x	y	z	U(eq)
N(1)	9965(3)	5848(2)	1285(3)	85(1)
N(2)	3420(3)	1760(3)	1753(3)	92(1)
C(1)	5766(2)	6565(2)	2217(2)	48(1)
C(2)	6831(2)	5514(2)	1800(2)	50(1)
C(3)	6263(3)	4271(2)	1670(2)	55(1)
C(4)	4594(3)	4067(2)	1946(2)	52(1)
C(5)	3519(3)	5107(2)	2328(2)	55(1)
C(6)	4078(2)	6355(2)	2462(2)	52(1)
C(7)	6455(2)	7879(2)	2334(2)	51(1)
C(8)	6293(3)	7833(3)	3744(3)	76(1)
C(9)	6966(4)	9043(3)	3834(4)	91(1)
C(10)	7812(4)	10308(3)	2534(4)	88(1)
C(11)	7961(4)	10380(3)	1150(4)	98(1)
C(12)	7295(4)	9169(3)	1039(3)	81(1)
C(13)	8583(3)	5724(2)	1510(3)	61(1)
C(14)	3948(3)	2777(3)	1831(2)	65(1)
C(15)	2850(3)	7443(3)	2885(3)	67(1)
C(16)	1882(3)	6868(3)	4624(3)	85(1)
C(17)	676(4)	7942(4)	5057(4)	121(1)

284

Table 3. Bond lengths [Å] and angles [°] for **125**.

_____

N(1)-C(13)	1.134(3)
N(2)-C(14)	1.135(3)
C(1)-C(6)	1.400(3)
C(1)-C(2)	1.402(3)
C(1)-C(7)	1.479(3)
C(2)-C(3)	1.375(3)
C(2)-C(13)	1.442(3)
C(3)-C(4)	1.374(3)
C(3)-H(3)	0.9300
C(4)-C(5)	1.386(3)
C(4)-C(14)	1.439(3)
C(5)-C(6)	1.379(3)
C(5)-H(5)	0.9300
C(6)-C(15)	1.506(3)
C(7)-C(12)	1.367(3)
C(7)-C(8)	1.379(3)
C(8)-C(9)	1.367(3)
C(8)-H(8)	0.9300
C(9)-C(10)	1.358(4)
C(9)-H(9)	0.9300
C(10)-C(11)	1.346(4)
C(10)-H(10)	0.9300
C(11)-C(12)	1.377(3)
C(11)-H(11)	0.9300
C(12)-H(12)	0.9300
C(15)-C(16)	1.525(3)
C(15)-H(15A)	0.9700
C(15)-H(15B)	0.9700
C(16)-C(17)	1.489(3)
C(16)-H(16A)	0.9700
C(16)-H(16B)	0.9700
C(17)-H(17A)	0.9600
C(17)-H(17B)	0.9600
C(17)-H(17C)	0.9600
C(6)-C(1)-C(2)	118.22(17)

C(6)-C(1)-C(7)	122.00(16)
C(2)-C(1)-C(7)	119.75(17)
C(3)-C(2)-C(1)	122.33(18)
C(3)-C(2)-C(13)	118.47(17)
C(1)-C(2)-C(13)	119.20(17)
C(4)-C(3)-C(2)	118.62(17)
C(4)-C(3)-H(3)	120.7
C(2)-C(3)-H(3)	120.7
C(3)-C(4)-C(5)	120.28(18)
C(3)-C(4)-C(14)	120.31(17)
C(5)-C(4)-C(14)	119.40(19)
C(6)-C(5)-C(4)	121.51(18)
C(6)-C(5)-H(5)	119.2
C(4)-C(5)-H(5)	119.2
C(5)-C(6)-C(1)	119.02(17)
C(5)-C(6)-C(15)	119.07(18)
C(1)-C(6)-C(15)	121.90(18)
C(12)-C(7)-C(8)	118.1(2)
C(12)-C(7)-C(1)	120.70(18)
C(8)-C(7)-C(1)	121.23(19)
C(9)-C(8)-C(7)	120.6(2)
C(9)-C(8)-H(8)	119.7
C(7)-C(8)-H(8)	119.7
C(10)-C(9)-C(8)	120.5(2)
C(10)-C(9)-H(9)	119.8
C(8)-C(9)-H(9)	119.8
C(11)-C(10)-C(9)	119.6(2)
C(11)-C(10)-H(10)	120.2
C(9)-C(10)-H(10)	120.2
C(10)-C(11)-C(12)	120.6(3)
C(10)-C(11)-H(11)	119.7
C(12)-C(11)-H(11)	119.7
C(7)-C(12)-C(11)	120.6(2)
C(7)-C(12)-H(12)	119.7
C(11)-C(12)-H(12)	119.7
N(1)-C(13)-C(2)	178.0(2)
N(2)-C(14)-C(4)	179.1(3)
C(6)-C(15)-C(16)	112.53(18)

C(6)-C(15)-H(15A)	109.1
C(16)-C(15)-H(15A)	109.1
C(6)-C(15)-H(15B)	109.1
C(16)-C(15)-H(15B)	109.1
H(15A)-C(15)-H(15B)	107.8
C(17)-C(16)-C(15)	113.0(2)
C(17)-C(16)-H(16A)	109.0
C(15)-C(16)-H(16A)	109.0
C(17)-C(16)-H(16B)	109.0
C(15)-C(16)-H(16B)	109.0
H(16A)-C(16)-H(16B)	107.8
C(16)-C(17)-H(17A)	109.5
C(16)-C(17)-H(17B)	109.5
H(17A)-C(17)-H(17B)	109.5
C(16)-C(17)-H(17C)	109.5
H(17A)-C(17)-H(17C)	109.5
H(17B)-C(17)-H(17C)	109.5

_____

Symmetry transformations used to generate equivalent atoms:

Table 4. Anisotropic displacement parameters (Å^2x 10^3) for **125**. The anisotropic displacement factor exponent takes the form: $-2\pi^2[\,h^2\,a^{*2}U^{11} + ... + 2\,h\,k\,a^*\,b^*\,U^{12}\,]$

	U^{11}	U^{22}	U^{33}	U^{23}	U^{13}	U^{12}
N(1)	55(1)	85(1)	118(2)	-43(1)	-33(1)	5(1)
N(2)	110(2)	77(1)	91(2)	-38(1)	-31(1)	-23(1)
C(1)	50(1)	45(1)	42(1)	-12(1)	-17(1)	-1(1)
C(2)	49(1)	49(1)	50(1)	-17(1)	-18(1)	1(1)
C(3)	56(1)	51(1)	52(1)	-21(1)	-15(1)	3(1)
C(4)	60(1)	47(1)	45(1)	-15(1)	-17(1)	-7(1)
C(5)	48(1)	59(1)	52(1)	-17(1)	-18(1)	-6(1)
C(6)	52(1)	49(1)	48(1)	-15(1)	-19(1)	1(1)
C(7)	53(1)	50(1)	55(1)	-22(1)	-23(1)	4(1)
C(8)	96(2)	70(2)	65(2)	-20(1)	-38(1)	-11(1)
C(9)	126(2)	85(2)	90(2)	-40(2)	-63(2)	-1(2)
C(10)	110(2)	64(2)	121(2)	-42(2)	-69(2)	4(2)
C(11)	137(3)	60(2)	88(2)	-17(1)	-43(2)	-25(2)
C(12)	115(2)	58(1)	63(2)	-17(1)	-30(1)	-20(1)
C(13)	57(1)	55(1)	72(1)	-27(1)	-24(1)	5(1)
C(14)	70(2)	64(1)	54(1)	-22(1)	-18(1)	-9(1)
C(15)	58(1)	64(1)	84(2)	-32(1)	-30(1)	10(1)
C(16)	70(2)	92(2)	87(2)	-42(2)	-16(1)	11(2)
C(17)	91(2)	128(3)	138(3)	-78(2)	-14(2)	20(2)

Table 5.   Hydrogen coordinates (x 10^4) and isotropic displacement parameters (Å^{2}x 10 ^{3}) for **125**.

	x	y	z	U(eq)
H(3)	6993	3584	1401	71
H(5)	2396	4960	2498	71
H(8)	5720	6971	4643	99
H(9)	6845	8999	4793	119
H(10)	8285	11121	2599	115
H(11)	8519	11255	260	127
H(12)	7419	9229	74	105
H(15A)	2063	7568	2385	87
H(15B)	3450	8449	2502	87
H(16A)	1275	5866	5004	111
H(16B)	2671	6731	5124	111
H(17A)	1275	8920	4735	157
H(17B)	79	7509	6157	157
H(17C)	-103	8091	4560	157

6.3   Selected spectra

125

125

292
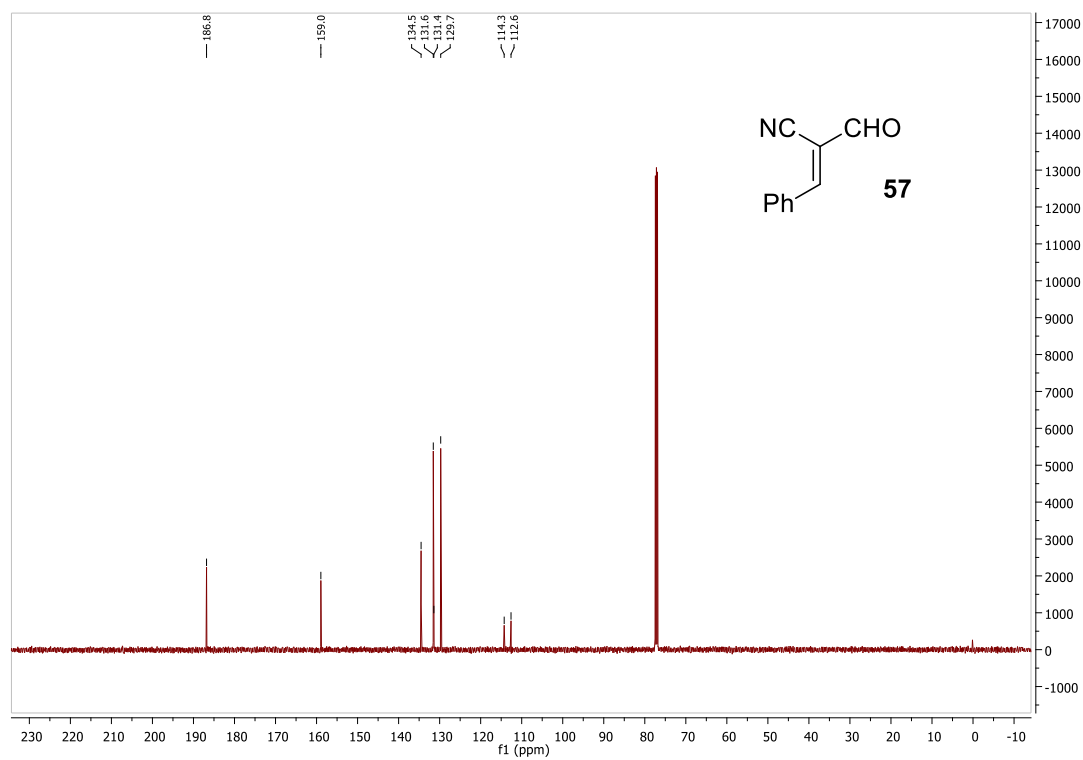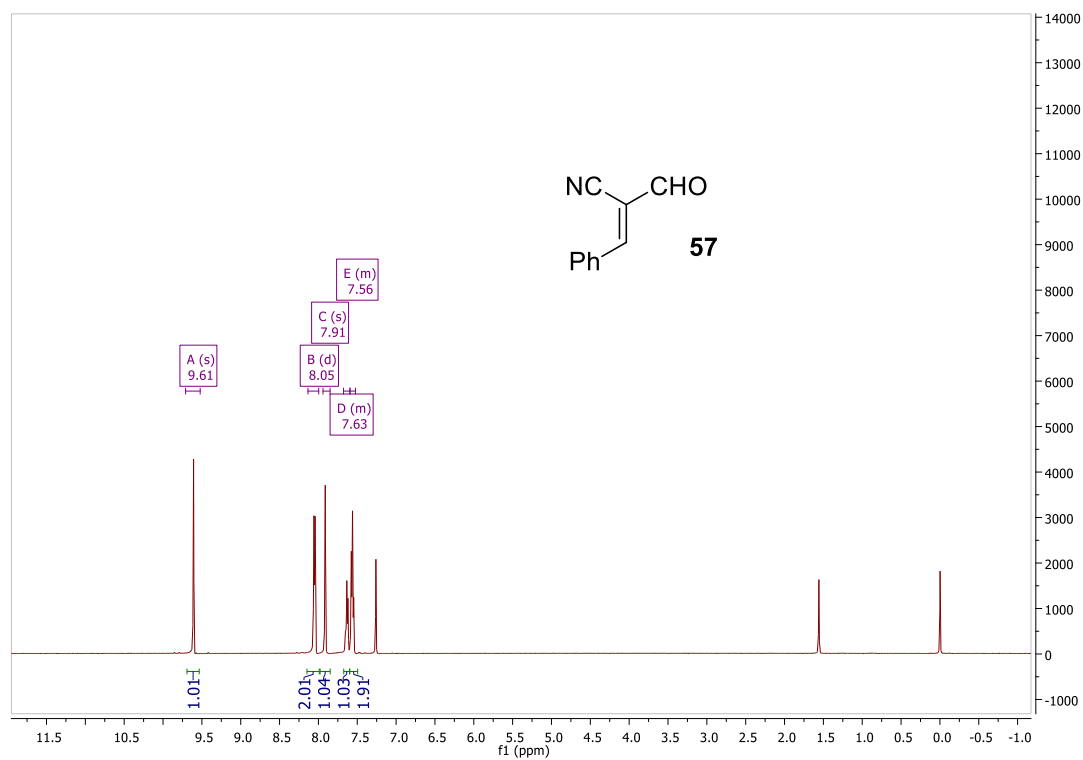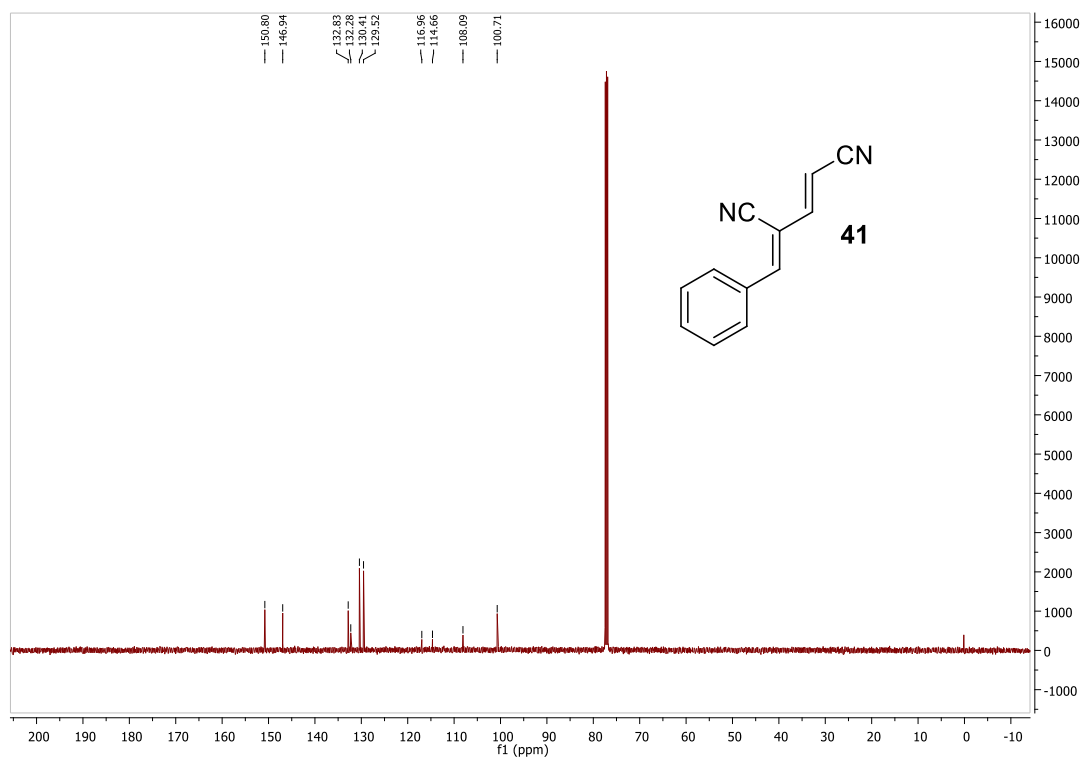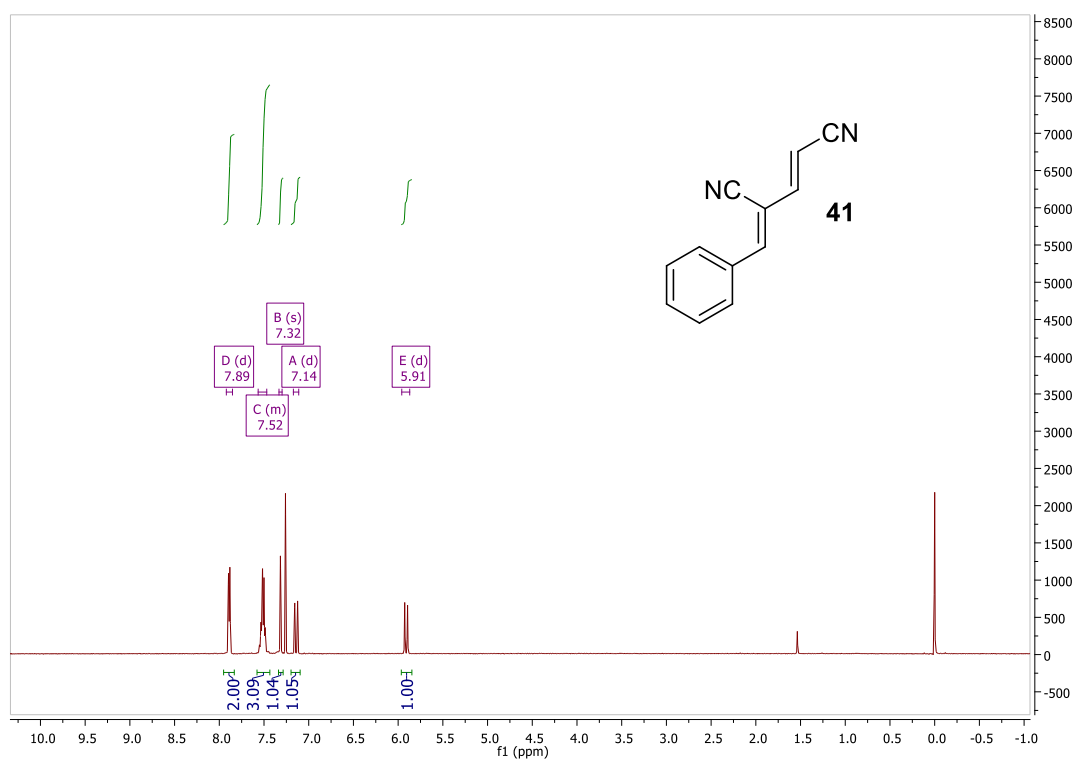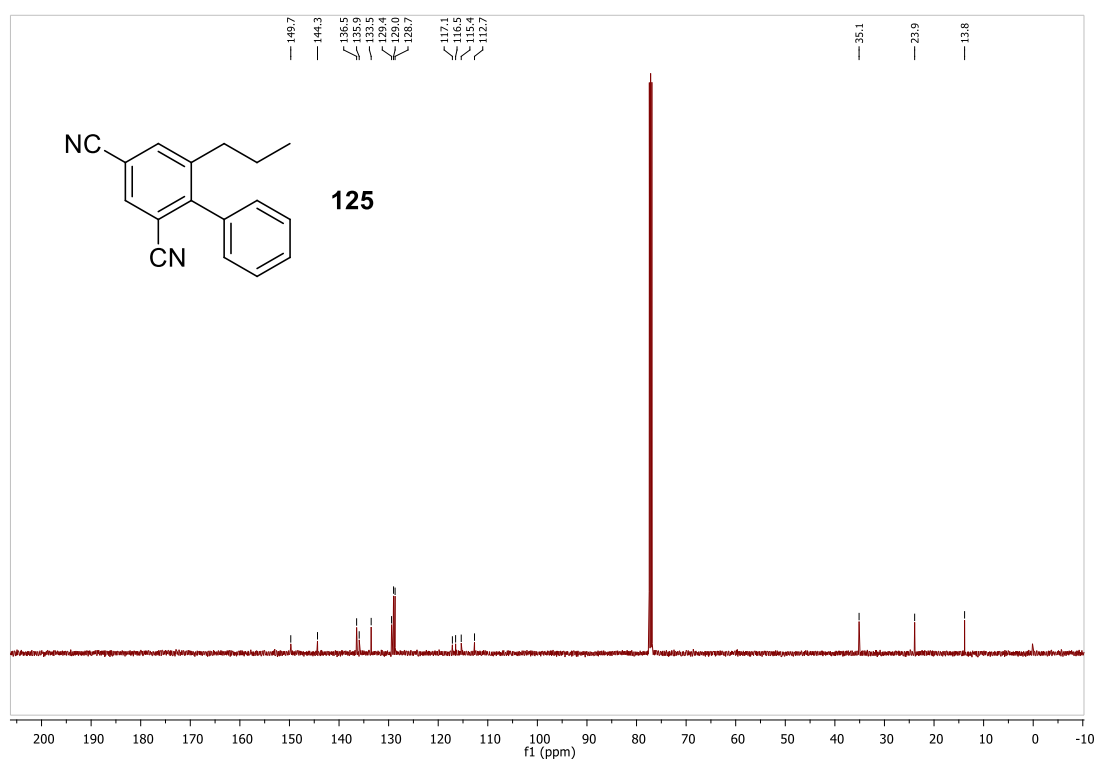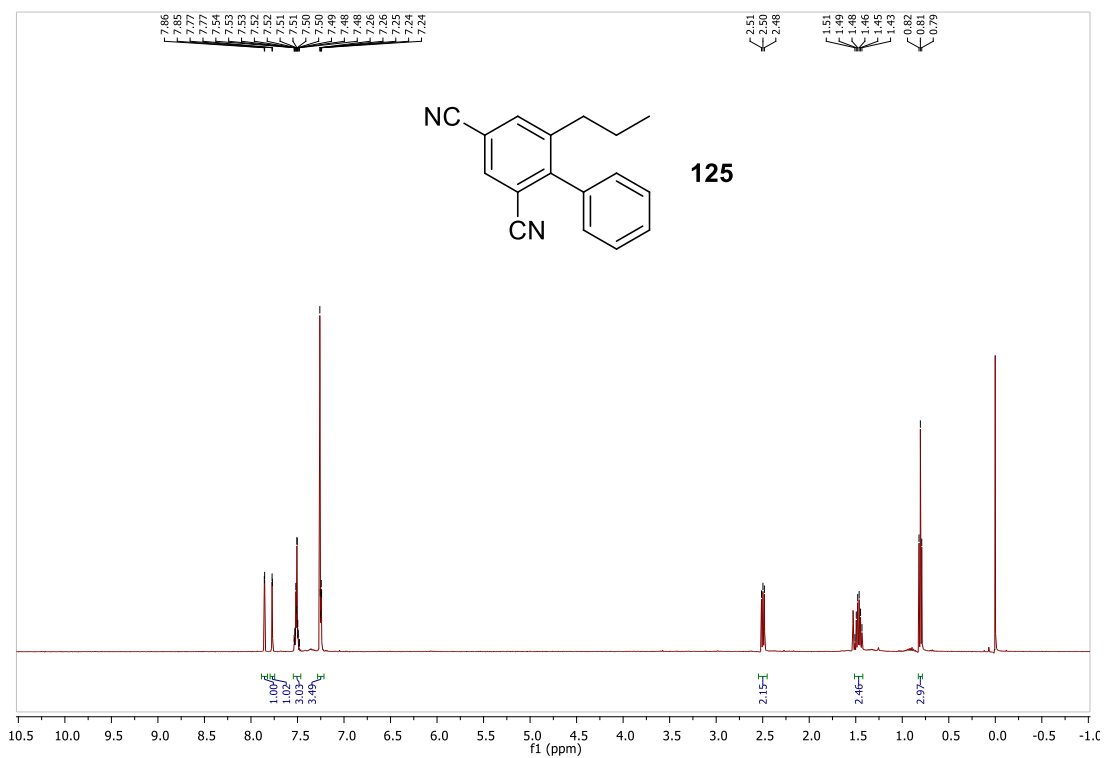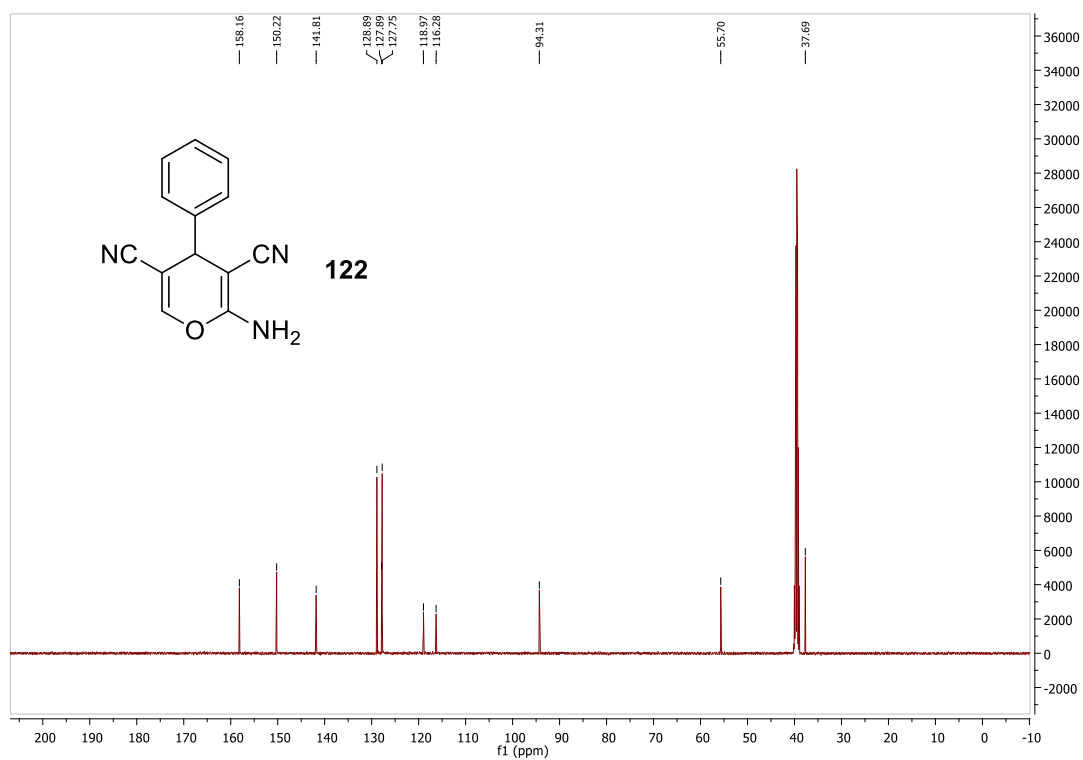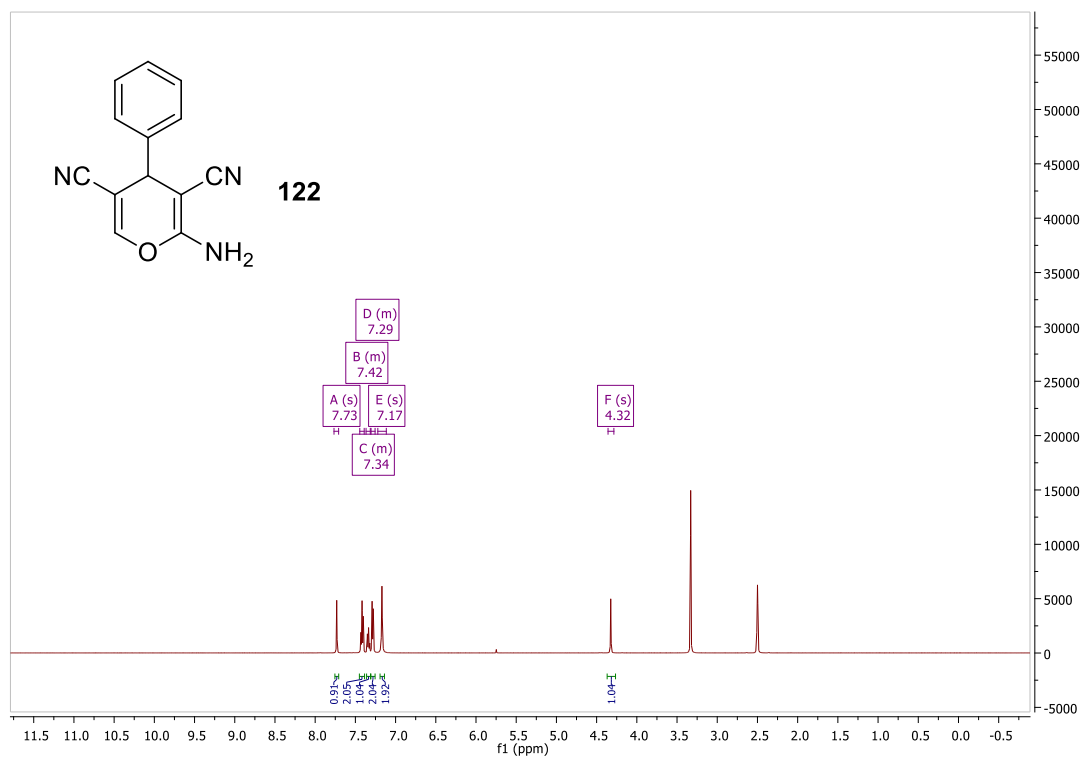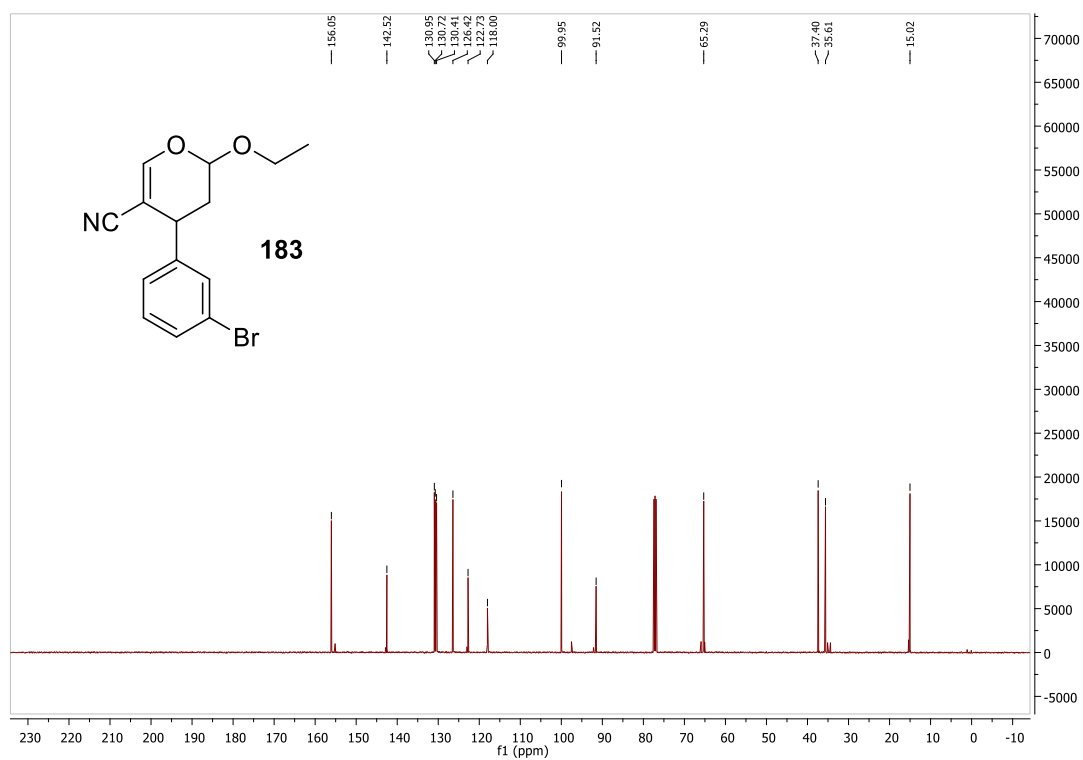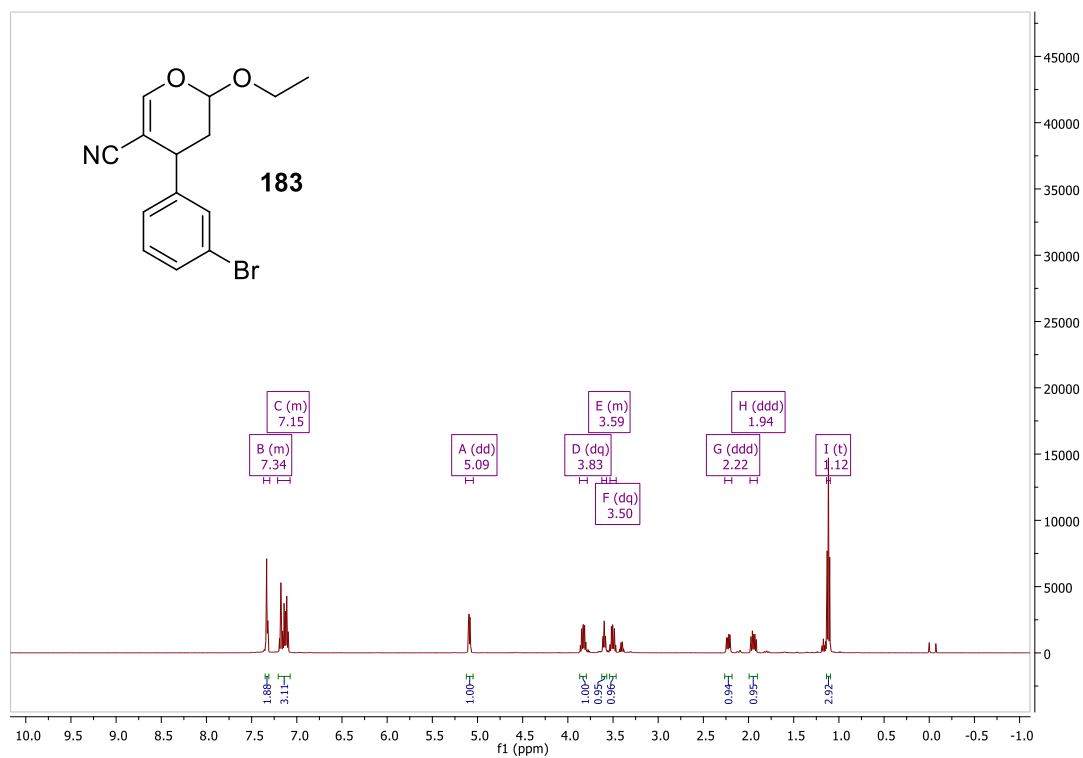
7. Bibliography

(1)   Blackmond, D. G. *Phil. Trans. R. Soc. B* **2011**, *366*, 2878.

(2)   Wei, J.; Lv, X.; Lü, Y.; Yang, G.; Fu, L.; Yang, L.; Wang, J.; Gao, J.; Cheng, S.; Duan, Q.; Jin, C.; Li, X. *Eur. J. Org. Chem.* **2013**, *2013*, 2414.

(3)   Verbiest, T.; Rodriguez, V. *Opt. Mater. Express.* **2011**, *1*, 3.

(4)   George, B. K.; Robin, D. M. *J. Chem. Ed.* **1975**, *52*, 777.

(5)   Sariaslani, F. S.; Rosazza, J. P. N. *Enzyme Microb. Technol.* **1984**, *6*, 242.

(6)   Marckwald, W. *Chem. Ber.* **1904**, *37*, 349.

(7)   Koskinen, A. M. P. *Asymmetric Synthesis of Natural Products*; John Wiley & Sons, Ltd: Chichester, UK, 2012.

(8)   Wang, Z. *Comprehensive Organic Name Reactions and Reagents*; John Wiley & Sons Inc.: Hoboken, NJ, 2009.

(9)   Bredig, G. F., P.S. *Biochem. Z.* **1913**, *46*, 7.

(10)   Nozaki, H.; Moriuti, S.; Takaya, H.; Noyori, R. *Tetrahedron Lett.* **1966**, *7*, 5239.

(11)   Picquet, M. *Platinum Met. Rev.* **2013**, *57*, 272.

(12)   Colacot, T. J. *Platinum Met. Rev.* **2002**, *46*, 82.

(13)   Pracejus, H. *Justus Liebigs Ann. Chem.* **1960**, *634*, 9.

(14)   Wynberg, H.; Helder, R. *Tetrahedron Lett.* **1975**, *16*, 4057.

(15)   Hajos, Z. G.; Parrish, D. R. *J. Org. Chem.* **1974**, *39*, 1615.

(16)   Eder, U.; Sauer, G.; Weichert, R. *Angew Chem Int Ed Engl* **1971**, *10*, 496.

(17)   Zhong, G.; Hoffmann, T.; Lerner, R. A.; Danishefsky, S.; Barbas, C. F. *J. Am. Chem. Soc.* **1997**, *119*, 8131.

(18)   Bradshaw, B.; Bonjoch, J. *Synlett* **2012**, *23*, 337.

(19)   List, B.; Lerner, R. A.; Barbas, C. F. *J. Am. Chem. Soc.* **2000**, *122*, 2395.

(20)   Berkessel, A.; Gröger, H. *Asymmetric Organocatalysis*; Wiley-VCH Verlag GmbH & Co. KGaA: Weinheim, 2005.

(21)   Ahrendt, K. A.; Borths, C. J.; David, W. C. *J. Am. Chem. Soc.* **2000**, *122*, 4243.

(22)   Wittig, G.; Blumenthal, H. *Chem. Ber.* **1927**, *60*, 1085.

(23)   Mannich, C.; Davidsen, H. *Ber. Dtsch. Che. Ges.* **1936**, *69B*, 2106.

(24)   Stork, G.; Terrell, R.; Szmuszkovicz, J. *J. Am. Chem. Soc.* **1954**, *76*, 2029.

(25)   Stork, G.; Landesman, H. K. *J. Am. Chem. Soc.* **1956**, *78*, 5128.

(26)   Bøgevig, A.; Juhl, K.; Kumaragurubaran, N.; Zhuang, W.; Jørgensen, K. A. *Angew Chem Int Ed Engl* **2002**, *41*, 1790.

(27)   List, B. *J. Am. Chem. Soc.* **2000**, *122*, 9336.

(28)   List, B.; Pojarliev, P.; Martin, H. J. *Org. Lett.* **2001**, *3*, 2423.

(29)   Zhong, G. *Angew. Chem. Int. Ed.* **2003**, *42*, 4247.

(30)   Juhl, K.; Jørgensen, K. A. *Angewandte Chemie - International Edition* **2003**, *42*, 1498.

(31)   Wagner, J.; Lerner, R. A.; Barbas III, C. F. *Science* **1995**, *270*, 1797.

(32)   Franzén, J.; Marigo, M.; Fielenbach, D.; Wabnitz, T. C.; Kjærsgaard, A.; Jørgensen, K. A. *J. Am. Chem. Soc.* **2005**, *127*, 18296.

(33)   Hayashi, Y.; Gotoh, H.; Hayashi, T.; Shoji, M. *Angew. Chem. Int. Ed.* **2005**, *44*, 4212.

(34)   Kempf, B.; Hampel, N.; Ofial, A. R.; Mayr, H. *Chemistry* **2003**, *9*, 2209.

(35) List, B. *Asymmetric Organocatalysis (Topics in Current Chemistry)*; Springer 2009.

(36) Diner, P.; Kjaersgaard, A.; Lie, M. A.; Jørgensen, K. A. *Chem-Eur J* **2008**, *14*, 122.

(37) Seebach, D.; Grošelj, U.; Badine, D. M.; Schweizer, W. B.; Beck, A. K. *Helv. Chim. Acta* **2008**, *91*, 1999.

(38) Schmid, M. B.; Zeitler, K.; Gschwind, R. M. *Angewandte Chemie (International ed. in English)* **2010**, *49*, 4997.

(39) Cahn, R. S.; Ingold, C.; Prelog, V. *Angew Chem Int Edit* **1966**, *5*, 385.

(40) Marigo, M.; Fielenbach, D.; Braunton, A.; Kjaersgaard, A.; Jørgensen, K. A. *Angew Chem Int Ed Engl* **2005**, *44*, 3703.

(41) Marigo, M.; Wabnitz, T. C.; Fielenbach, D.; Jørgensen, K. A. *Angewandte Chemie (International ed. in English)* **2005**, *44*, 794.

(42) Agami, C.; Levisalles, J.; Puchot, C. *J. Chem. Soc., Chem. Commun.* **1985**, *1*, 441.

(43) Puchot, C.; Samuel, O.; Dunach, E.; Zhao, S.; Agami, C.; Kagan, H. B. *J. Am. Chem. Soc.* **1986**, *108*, 2353.

(44) Hoang, L.; Bahmanyar, S.; Houk, K. N.; List, B. *J. Am. Chem. Soc.* **2003**, *125*, 16.

(45) Bahmanyar, S.; Houk, K. N.; Martin, H. J.; List, B. *J. Am. Chem. Soc.* **2003**, *125*, 2475.

(46) Zimmerman, H. E.; Traxler, M. D. *J. Am. Chem. Soc.* **1957**, *79*, 1920.

(47) Michael, A. *Journal für Praktische Chemie* **1887**, *35*, 349.

(48) Alexakis, A.; Andrey, O. *Org. Lett.* **2002**, *4*, 3611.

(49) Melchiorre, P.; Jørgensen, K. A. *J. Org. Chem.* **2003**, *68*, 4151.

(50) Sulzer-Mosse, S.; Alexakis, A. *Chem Commun (Camb)* **2007**, 3123.

(51) Sulzer-Mossé, S.; Tissot, M.; Alexakis, A. *Org. Lett.* **2007**, *9*, 3749.

(52) Fuson, R. C. *Chem. Rev.* **1935**, *16*, 1.

(53) Almasi, D.; Alonso, D. A.; Najera, C. *Tetrahedron: Asymmetry* **2007**, *18*, 299.

(54) Tsogoeva, S. B. *Eur. J. Org. Chem.* **2007**, 1701.

(55) Silva, E.; Silva, A. *Synthesis* **2012**, *44*, 3109.

(56) Ralls, J. W. *Chem. Rev.* **1959**, *59*, 329.

(57) Bernardi, L.; López-Cantarero, J.; Niess, B.; Jørgensen, K. A. *J. Am. Chem. Soc.* **2007**, *129*, 5772.

(58) Murphy, J. J.; Quintard, A.; McArdle, P.; Alexakis, A.; Stephens, J. C. *Angew. Chem. Int. Ed.* **2011**, *50*, 5095.

(59) Pezzati, B.; Chellat, M. F.; Murphy, J. J.; Besnard, C.; Reginato, G.; Stephens, J. C.; Alexakis, A. *Org. Lett.* **2013**, *15*, 2950.

(60) Caruana, L.; Kniep, F.; Johansen, T. K.; Poulsen, P. H.; Jørgensen, K. A. *J. Am. Chem. Soc.* **2014**, *136*, 15929.

(61) Richter, D.; Hampel, N.; Singer, T.; Ofial, A. R.; Mayr, H. *Eur. J. Org. Chem.* **2009**, *2009*, 3203.

(62) Feng, X.; Zhou, Z.; Yin, X.; Li, R.; Chen, Y.-C. *Eur. J. Org. Chem.* **2014**, *2014*, 5906.

(63) Lear, M. J.; Hayashi, Y. *ChemCatChem* **2013**, *5*, 3499.

(64) Tian, X.; Liu, Y.; Melchiorre, P. *Angew. Chem. Int. Ed.* **2012**, *51*, 6439.

(65) Dell'Amico, L.; Albrecht, Ł.; Naicker, T.; Poulsen, P. H.; Jørgensen, K. A. *J. Am. Chem. Soc.* **2013**, *135*, 8063.

(66)   Jones, S. B.; Simmons, B.; Mastracchio, A.; MacMillan, D. W. C. *Nature* **2011**, *475*, 183.

(67)   Belot, S.; Massaro, A.; Tenti, A.; Mordini, A.; Alexakis, A. *Org. Lett.* **2008**, *10*, 4557.

(68)   Baschieri, A.; Bernardi, L.; Ricci, A.; Suresh, S.; Adamo, M. F. *Angew. Chem. Int. Ed.* **2009**, *48*, 9342.

(69)   Murphy, J. J. *PhD Thesis, National University of Ireland Maynooth* **2012**.

(70)   Ahn, K.-D.; Hall, H. K. *J. Polym. Sci. Polym. Chem. Ed.* **1981**, *19*, 629.

(71)   McNab, H. *Contemp. Org. Synth.* **1996**, *3*, 373.

(72)   Banciu, M. D.; Brown, R. F. C.; Coulston, K. J.; Eastwood, F. W.; Macrae, T. *Aust. J. Chem.* **1998**, *51*, 695.

(73)   Masuyama, Y.; Sato, H.; Kurusu, Y. *Tetrahedron Lett.* **1985**, *26*, 67.

(74)   Padwa, A.; Gareau, Y.; Harrison, B.; Norman, B. H. *J. Org. Chem.* **1991**, *56*, 2713.

(75)   Fleming, F. F.; Wang, Q. *Chem. Rev.* **2003**, *103*, 2035.

(76)   House, H. O.; Umen, M. J. *J. Org. Chem.* **1973**, *38*, 3893.

(77)   Rappoport, Z. *Patai's Chemistry of Functional Groups: The Cyano Group*; John Wiley & Sons Ltd.: London, 1970.

(78)   Wasserman, H. H.; Suryanarayana, B.; Grassetti, D. D. *J. Am. Chem. Soc.* **1956**, *78*, 2808.

(79)   Elliott, A. J.; Morris, P. E., Jr.; Petty, S. L.; Williams, C. H. *J Org Chem* **1997**, *62*, 8071.

(80)   Gabbutt, C. D.; Heron, B. M.; Hursthouse, M. B.; Malik, K. M. A. *Phosphorus Sulfur* **2000**, *166*, 99.

(81)   Blanchette, M. A.; Choy, W.; Davis, J. T.; Essenfeld, A. P.; Masamune, S.; Roush, W. R.; Sakai, T. *Tetrahedron Lett.* **1984**, *25*, 2183.

(82)   Maetz, P.; Rodriguez, M. *Tetrahedron Lett.* **1997**, *38*, 4221.

(83)   Zhang, J.; Polishchuk, E. A.; Chen, J.; Ciufolini, M. A. *J Org Chem* **2009**, *74*, 9140.

(84)   Takeda, T. In *Modern Carbonyl Olefination*; Wiley-VCH Verlag GmbH & Co. KGaA: Weinheim, FRG, 2005.

(85)   Couvillon, L. J.; US41910054A, Monsanto, Chemicals: United States, 1956.

(86)   Wittig, G.; Geissler, G. *Liebigs Ann Chem* **1953**, *580*, 44.

(87)   Wittig, G.; Schöllkopf, U. *Chem. Ber.* **1954**, *87*, 1318.

(88)   Wittig, G.; Haag, A. *Chem. Ber.* **1963**, *96*, 1535.

(89)   Robiette, R.; Richardson, J.; Aggarwal, V. K.; Harvey, J. N. *J. Am. Chem. Soc.* **2006**, *128*, 2394.

(90)   Byrne, P. a.; Gilheany, D. G. *Chem. Soc. Rev.* **2013**, *42*, 6670.

(91)   Vedejs, E.; Snoble, K. a. J. *J. Am. Chem. Soc.* **1973**, *95*, 5778.

(92)   Maeda, S.; Horikawa, N.; Obora, Y.; Ishii, Y. *J Org Chem* **2009**, *74*, 9558.

(93)   Yadav, L. D. S.; Srivastava, V. P.; Patel, R. *Tetrahedron Lett.* **2008**, *49*, 3142.

(94)   Sandes, J. M.; Borges, A. R.; Junior, C. G.; Silva, F. P.; Carvalho, G. A.; Rocha, G. B.; Vasconcellos, M. L.; Figueiredo, R. C. *Bioorg Chem* **2010**, *38*, 190.

(95)   Masuyama, Y.; Yamazaki, H.; Toyoda, Y.; Kurusu, Y. *Synthesis* **1985**, *1985*, 964.

(96)   Hartog, T. d.; Huang, Y.; Fañanás-Mastral, M.; Meuwese, A.; Rudolph, A.; Pérez, M.; Minnaard, A. J.; Feringa, B. L. *ACS Catalysis* **2015**, *5*, 560.

(97)   Krause, N. *J. Org. Chem.* **1992**, *57*, 3509.

(98)   Krause, N.; Thorand, S. *Inorg. Chim. Acta* **1999**, *296*, 1.

(99)   Schmidt, A.; Hilt, G. *Org. Lett.* **2013**, *15*, 2708.

(100)   Bemis, G. W.; Murcko, M. A. *J. Med. Chem.* **1996**, *39*, 2887.

(101)   Horton, D. a.; Bourne, G. T.; Smythe, M. L. *Cancer Research* **2003**, *103*, 893.

(102)   Hajduk, P. J.; Bures, M.; Praestgaard, J.; Fesik, S. W. *J. Med. Chem.* **2000**, *43*, 3443.

(103)   Ullmann, F.; Bielecki, J. *Ber. Dtsch. Chem. Ges.* **1901**, *34*, 2174.

(104)   Sambiagio, C.; Marsden, S. P.; Blacker, A. J.; McGowan, P. C. *Chem Soc Rev* **2014**, *43*, 3525.

(105)   Hassan, J.; Sévignon, M.; Gozzi, C.; Schulz, E.; Lemaire, M. *Chem. Rev.* **2002**, *102*, 1359.

(106)   Roopan, S. M.; Palaniraja, J. *Res. Chem. Intermed.* **2015**, *41*, 8111.

(107)   Joshi, P. R.; Undeela, S.; Reddy, D. D.; Singarapu, K. K.; Menon, R. S. *Org. Lett.* **2015**, *17*, 1449.

(108)   Poudel, T. N.; Lee, Y. R. *Org. Lett.* **2015**, *17*, 2050.

(109)   Seebach, D.; Goliński, J. *Helv. Chim. Acta* **1981**, *64*, 1413.

(110)   Baldwin, J. E. *J. Chem. Soc., Chem. Commun.* **1976**, 734.

(111)   Linder, M.; Brinck, T. *J. Org. Chem.* **2012**, *77*, 6563.

(112)   Reetz, M. T.; Eibach, F. *Angew. Chem. Int. Ed.* **1978**, *17*, 278.

(113)   Brahmachari, G. *Green Synthetic Approaches for Biologically Relevant Heterocycles: An Overview*; Elsevier Inc., 2014.

(114)   Mandha, S. R.; Siliveri, S.; Alla, M.; Bommena, V. R.; Bommineni, M. R.; Balasubramanian, S. *Bioorg. Med. Chem. Lett.* **2012**, *22*, 5272.

(115)   Wiener, C.; Schroeder, C. H.; West, B. D.; Link, K. P. *J. Org. Chem* **1962**, *27*, 3086.

(116)   Litvinov, Y. M.; Shestopalov, A. M. *Adv. Heterocycl. Chem.* **2011**, *103*, 175.

(117)   Danishefsky, S. J.; Bilodeau, M. T. *Angew Chem Int Ed Engl* **1996**, *35*, 1380.

(118)   Evans, D. A.; Johnson, J. S.; Olhava, E. J. *J. Am. Chem. Soc.* **2000**, *122*, 1635.

(119)   Ho, T.-L.; Gorobets, E. *Tetrahedron* **2002**, *58*, 4969.

(120)   Zhang, J.; Zhu, D.; Yu, C.; Wan, C.; Wang, Z. *Org. Lett.* **2010**, *12*, 2841.

(121)   Kashima, H.; Kawashima, T.; Wakasugi, D.; Satoh, T. *Tetrahedron* **2007**, *63*, 3953.

(122)   Deshmukh, M. B.; Patil, S. S.; Jadhav, S. D.; Pawar, P. B. *Synth. Commun.* **2012**, *42*, 1177.

(123)   Ciller, J. A.; Martin, N.; Seoane, C.; Soto, J. L. *J Chem Soc Perk T 1* **1985**, 2581.

(124)   Reddy, T. N.; Ravinder, M.; Bikshapathi, R.; Sujitha, P.; Kumar, C. G.; Rao, V. J. *Med. Chem. Res.* **2017**, 1.

(125)   Hilmy Elnagdi, N. M.; Al-Hokbany, N. S. *Molecules* **2012**, *17*, 4300.

(126)   Matthews, W. S.; Bares, J. E.; Bartmess, J. E.; Bordwell, F. G.; Cornforth, F. J.; Drucker, G. E.; Margolin, Z.; McCallum, R. J.; McCollum, G. J.; Vanier, N. R. *J. Am. Chem. Soc.* **1975**, *97*, 7006.

(127)   Bordwell, F. G.; Van der Puy, M.; Vanier, N. R. *J. Org. Chem* **1976**, *41*, 1883.

(128)   Jakab, G.; Tancon, C.; Zhang, Z.; Lippert, K. M.; Schreiner, P. R. *Org. Lett.* **2012**, *14*, 1724.

(129)   Molleti, N.; Rana, N. K.; Singh, V. K. *Org. Lett.* **2012**, *14*, 4322.

(130)   Lago-Santome, H.; Martinez-Bescos, P.; Fernandez-Gonzalez, M.; Ozores-Viturro, L.; Cagide-Fagin, F.; Alonso, R. *J. Org. Chem* **2014**, *79*, 8645.

(131)   Pałasz, A. *Top. Curr. Chem.* **2016**, *374*, 24.

(132)   Still, W. C.; Kahn, M.; Mitra, A. *The Journal of Organic Chemistry* **1978**, *43*, 2923.

(133)   Gottlieb, H. E.; Kotlyar, V. *The Journal of organic* **1997**, *62*, 7512.

(134)   Reddy, T. N.; Ravinder, M.; Bagul, P.; Ravikanti, K.; Bagul, C.; Nanubolu, J. B.; Srinivas, K.; Banerjee, S. K.; Rao, V. J. *Eur J Med Chem* **2014**, *71*, 53.

(135)   Goehring, W. 2005.

(136)   Burling, S.; Paine, B. M.; Nama, D.; Brown, V. S.; Mahon, M. F.; Prior, T. J.; Pregosin, P. S.; Whittlesey, M. K.; Williams, J. M. *J Am Chem Soc* **2007**, *129*, 1987.

(137)   Zhao, S.; He, M.; Guo, Z.; Zhou, N.; Wang, D.; Li, J.; Zhang, L. *RSC Adv.* **2015**, *5*, 32839.

(138)   Mao, Y.; Mathey, F. *Org. Lett.* **2012**, *14*, 1162.

(139)   Gilley, C. B.; Buller, M. J.; Kobayashi, Y. *Org. Lett.* **2007**, *9*, 3631.

(140)   *Org. Synth.* **1945**, *25*, 92.